LECTURE NOTES

EE275: Electric Motor and Motion Control (2025)

Jiahao Chen[a]

[a]SIST 1D#206, ShanghaiTech University, China

ARTICLE HISTORY
Compiled June 11, 2025

ABSTRACT
The course is arranged in a manner of "from theory to engineering". This is one essential core course to cover the four major courses, including electric machinery (steady state behaviors, winding design), ac machine transient analysis (winding function, mathematical modeling, numerical simulation), machine design (complex number star of slots plot, multi-phase machine theory, maxwell stress tensor), and motor control (with an emphasis on engineering practices, e.g., system identification, commissioning, controller tuning, disturbance observer, inverter modeling).

Contents

CONTACT Jiahao by email: chenjh2@shanghaitech.edu.cn

1. Chapter 1: Modeling of Electric Machine

Electric machine is governed by both electrical dynamics and mechanical dynamics, and its mathematical modeling therefore stems from physics. In particular, this course will use the math-intensive approach.

1.1. Review on Newton's Second Law of Motion

It all begins with the concept of motion (i.e., momentum) of a particle:

$$\vec{p} = m\vec{v} \tag{1}$$

Here, $\vec{p}$ is momentum, m is the mass of the particle, and $\vec{v}$ is the derivative of the particle's position with respect to time t.

The Newton's second law of motion states that *"the change of motion of an object is proportional to the force impressed; and is made in the direction of the straight line in which the force is impressed."*[1] The first half of the sentence defines the size of the force, and second half defines the direction of the force. That is,

$$\frac{\mathrm{d}}{\mathrm{d}t}\vec{p} = m\frac{\mathrm{d}}{\mathrm{d}t}\vec{v} = \vec{F} \tag{2}$$

The assumption of a particle (a point mass) is convenient such that the force vector $\vec{F}$ is applied where the point mass locates.

*1.1.1. Circular Motion and Centripetal Force**

Let's take a brief detour to motivate why later we are interested in circular motion or rotation.

The circular motion is an important test you can do to measure the inertial mass of an object if one day you are teleported to some unknown planet (of which you don't know the gravity) by some evil aliens.[2] The mass m can be calculated using the formula for centripetal force:

$$F = m\frac{v^2}{r} = mr\omega^2 \tag{3}$$

where ω is the angular speed and r denotes the radius of the circular motion. This formula can be derived using geometry relation[3], but is centripetal force really an actual force and where is it from?

The equation of motion (EOM) (2) can describe any motion including translational motion and circular motion, but have you ever attempted to use it to describe the circular motion? Here is an tentative example that rewrites (2) into the component-

[1] Quoted from Wikipedia: https : //en.wikipedia.org/wiki/Newton%27s_laws_of_motion#Second

[2] "How hard it is to get it going is one thing, and how much it weighs is something else." -Quote from https://www.feynmanlectures.caltech.edu/I_09.html

[3] https://en.wikipedia.org/wiki/Centripetal_force

wise form, and it only considers circular motion in the xy plane (assuming $v_z \equiv 0$):

$$\begin{aligned} &\begin{bmatrix} F_x \\ F_y \end{bmatrix} = m\frac{\mathrm{d}}{\mathrm{d}t}\begin{bmatrix} v_x \\ v_y \end{bmatrix} \\ &\text{s.t. } \sqrt{v_x^2 + v_y^2} = r\omega = \text{Const.} \\ &\text{and } (v_x, v_y) \cdot (F_x, F_y) = v_x F_x + v_y F_y = 0 \end{aligned} \tag{4}$$

Using this model, can you easily show that $\sqrt{F_x^2 + F_y^2} = mr\omega^2 = \text{Const.}$?

Instead, we often adopt a different approach to change the frame of reference.

*1.1.2. Vector Derivative in a Rotating Reference Frame**

One implied assumption for the equation of motion (EOM) (2) to hold is that the vectors are referred to an inertial frame of reference.

If the adopted reference frame is accelerating with respect to an inertial frame, then the force vector $\vec{F}$ needs to be corrected to include the so-called "inertial forces" to make Newton's second law stay valid in this non-inertial frame. Inertial forces include gravity (translational acceleration), Coriolis force, **centripetal force**, and Euler force [3, section 12.6]. This explains where the centripetal force (3) comes from. Let's derive it!

First, we need to understand how taking time derivative works for a position vector:

$$\frac{\mathrm{d}}{\mathrm{d}t}\vec{r} = \frac{\mathrm{d}}{\mathrm{d}t}\left(r_x\hat{x} + r_y\hat{y} + r_z\hat{z}\right) = \left(\dot{r}_x\hat{x} + \dot{r}_y\hat{y} + \dot{r}_z\hat{z}\right) + 0 \tag{5}$$

where we use a dot $\dot{}$ to denote the time derivative of a variable, and note we have, for the default Cartesian xyz frame, $\frac{\mathrm{d}}{\mathrm{d}t}\hat{x} = \frac{\mathrm{d}}{\mathrm{d}t}\hat{y} = \frac{\mathrm{d}}{\mathrm{d}t}\hat{z} = 0$, meaning that the unit vectors $\hat{x}, \hat{y}, \hat{z}$ are not moving.

Now consider a rotating frame with angular speed vector $\vec{\omega}$,[4] and the same position vector $\vec{r}$ can as well be represented using the new unit vectors $\hat{d}, \hat{q}, \hat{n}$:

$$\vec{r} = r_d\hat{d} + r_q\hat{q} + r_n\hat{n} = r_x\hat{x} + r_y\hat{y} + r_z\hat{z} \tag{6}$$

[4]Angular speed vector $\vec{\omega}$ is in fact a pseudo vector with its vector direction denoting the rotation axis.

of which taking time derivative yields[5]

$$\begin{aligned}\frac{\mathrm{d}}{\mathrm{d}t}\vec{r} &= \frac{\mathrm{d}}{\mathrm{d}t}\left(r_d\hat{d} + r_q\hat{q} + r_n\hat{n}\right)\\ &= \left(\dot{r}_d\hat{d} + \dot{r}_q\hat{q} + \dot{r}_n\hat{n}\right) + \left(r_d\frac{\mathrm{d}}{\mathrm{d}t}\hat{d} + r_q\frac{\mathrm{d}}{\mathrm{d}t}\hat{q} + r_n\frac{\mathrm{d}}{\mathrm{d}t}\hat{n}\right)\\ &= \left(\dot{r}_d\hat{d} + \dot{r}_q\hat{q} + \dot{r}_n\hat{n}\right) + \left(r_d\vec{\omega}\times\hat{d} + r_q\vec{\omega}\times\hat{q} + r_n\vec{\omega}\times\hat{n}\right)\\ &= (\dot{r}_d, \dot{r}_q, \dot{r}_n)_{\hat{d}\hat{q}\hat{n}} + \vec{\omega}\times(r_d, r_q, r_n)_{\hat{d}\hat{q}\hat{n}}\\ &= \left(\frac{\mathrm{d}}{\mathrm{d}t}\vec{r}\right)_{\hat{d}\hat{q}\hat{n}} + \vec{\omega}\times(\vec{r})_{\hat{d}\hat{q}\hat{n}} = \left(\frac{\mathrm{d}}{\mathrm{d}t}\vec{r}\right)_{\hat{x}\hat{y}\hat{z}}\end{aligned} \tag{7}$$

This last row is useful because we have avoided taking time derivative of the moving unit vectors $\hat{d}, \hat{q}, \hat{n}$. **We use the subscripts to indicate that those subscripted unit vectors in $\vec{r}$ need not be differentiated.**

This relation is also true for other physics variables, e.g., the flux linkage vector has the following relation between its dqn frame derivative and $\alpha\beta\gamma$ frame derivative :

$$\left(\frac{\mathrm{d}}{\mathrm{d}t}\boldsymbol{\psi}\right)_{\hat{d}\hat{q}\hat{n}} + \vec{\omega}_{\text{syn}}\times(\boldsymbol{\psi})_{\hat{d}\hat{q}\hat{n}} = \left(\frac{\mathrm{d}}{\mathrm{d}t}\boldsymbol{\psi}\right)_{\hat{\alpha}\hat{\beta}\hat{\gamma}} \tag{8}$$

where though the voltage term $\omega_{\text{syn}}\times(\boldsymbol{\psi})_{\hat{d}\hat{q}\hat{n}}$ does not exist in reality, it is famous and goes by the name of **rotational back emf** in the motor control textbook.

*1.1.3. Derivation of Inertial Forces (Centripetal Force)**

In the EOM (2), we need to take twice-differentiation on the position vector, which gives rise to the inertial forces in a rotating frame of reference dqn:

$$\frac{\mathrm{d}}{\mathrm{d}t}\frac{\mathrm{d}}{\mathrm{d}t}(\vec{r})_{\hat{x}\hat{y}\hat{z}} = \left(\left(\frac{\mathrm{d}}{\mathrm{d}t} + \vec{\omega}\times\right)\left(\frac{\mathrm{d}}{\mathrm{d}t} + \vec{\omega}\times\right)\vec{r}\right)_{\hat{d}\hat{q}\hat{n}} = \frac{\vec{F}}{m} \tag{9}$$

which leads to[6]

$$m\left(\frac{\mathrm{d}^2}{\mathrm{d}t^2}\vec{r}\right)_{\hat{d}\hat{q}\hat{n}} = m\left(\frac{\mathrm{d}^2}{\mathrm{d}t^2}\vec{r}\right)_{\hat{x}\hat{y}\hat{z}} \underbrace{-2m\vec{\omega}\times(\vec{v})_{\hat{d}\hat{q}\hat{n}}}_{\text{Coriolis force}} \underbrace{-m\vec{\omega}\times(\vec{\omega}\times\vec{r})}_{\text{Centrifugal force}} \underbrace{-m\left(\frac{\mathrm{d}\vec{\omega}}{\mathrm{d}t}\right)_{\hat{d}\hat{q}\hat{n}}\times\vec{r}}_{\text{Euler force}} \tag{10}$$

from which we realize it is now safe for us to assume all time derivatives are only applied to vector components and we can assume time derivatives always ignore unit vectors. As a result, we can omit all unit vector subscripts to write down the Newton's

[5]The following holds for unit vector $\hat{n}$ that spins with angular speed $\vec{\omega}$:

$$\frac{\mathrm{d}}{\mathrm{d}t}\hat{n} = \frac{\omega\mathrm{d}t\sin\theta}{\mathrm{d}t} = \vec{\omega}\times\hat{n}, \text{ with } \theta = \langle\vec{\omega}, \hat{n}\rangle$$

[6]Watch video by Ben Yelverton `https://www.youtube.com/watch?v=NBnRe2LNjTc` for detailed process.

second law of motion in a non-inertial frame of reference dqn:

$$\begin{aligned}(10) \Leftrightarrow & m\frac{\mathrm{d}^2}{\mathrm{d}t^2}\vec{r} = \vec{F} + \vec{F}_{\text{Cori}} + \vec{F}_{\text{Cent}} + \vec{F}_{\text{Euler}} \\ & m\frac{\mathrm{d}^2}{\mathrm{d}t^2}\vec{r} = \vec{F} - 2m\vec{\omega}\times\vec{v} \ - m\vec{\omega}\times(\vec{\omega}\times\vec{r}) - m\frac{\mathrm{d}\vec{\omega}}{\mathrm{d}t}\times\vec{r}\end{aligned} \tag{11}$$

Let's pick a proper constant angular speed vector $\vec{\omega}$ such that the particle m in circular motion is at still in the dqn frame, i.e., $m\frac{\mathrm{d}^2}{\mathrm{d}t^2}(\vec{r})_{\hat{d}\hat{q}\hat{n}} = 0$, so it leads to the centripetal force formula we learn in high school:

$$\begin{aligned}&\vec{v} = 0 \Rightarrow \vec{F}_{\text{Cori}} = 0 \\ &\frac{\mathrm{d}\vec{\omega}}{\mathrm{d}t} = 0 \Rightarrow \vec{F}_{\text{Euler}} = 0 \\ &F = -\vec{F}_{\text{Cent}} = |m\vec{\omega}\times(\vec{\omega}\times\vec{r})| = m\omega^2 r = m\frac{v^2}{r}\end{aligned} \tag{12}$$

where the last row assumes the orthogonality between $\vec{\omega}$ and $\vec{r}$ such that $|\vec{\omega}\times\vec{r}| = \omega r$.

It is safe to skip this subsection for now because we don't really study circular motion of a free particle, but this subsection is worth a re-read after you have learned Park transformation.

1.2. Rotational Version of Newton's Second Law

Instead of a free point mass or particle, we are interested in describing the motion of a rigid body inside which a point remains fixed, that is, a self-spinning solid mass. In other terms, basically you can think what we are going to study is the motion of a lever.[7] The main difference of a rotating rigid body from a free moving particle is the existence of **constraint forces**.

According to Euler's rotation theorem,[8] we shall put the origin of our Cartesian coordinate system to that fixed point of the rigid body, and derive the rotational version of (2).

The fixed point of the rigid body implies that any force attempting to change the distance between fixed point and another point of the rigid body has no effect. The "effective force" applied at $\vec{r}$ that is able to change the **angular motion** of the rigid body about the fixed point or origin is orthogonal to the position vector $\vec{r}$, which is known as torque, formally defined using a cross product:

$$\vec{T} = \vec{r}\times\vec{F} \tag{13}$$

where $\vec{r}$ is a vector starts at origin and points to the action point of the force vector $\vec{F}$. Therefore, the EOM (2) can be rewritten in terms of torque to a point mass m

[7] "Lever is a movable bar that pivots on a fulcrum attached to a fixed point." –Quoted from the Wiki of lever.
[8] https://en.wikipedia.org/wiki/Euler%27s_rotation_theorem

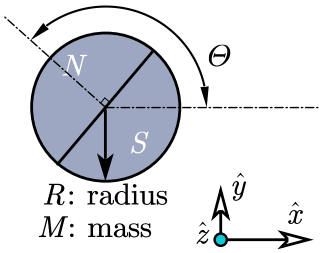

Figure 1. The cross section of a cylinder with mass M and radius R, and it is made of permanent magnet.

that constitutes the rigid body:

$$\begin{aligned}
&m\vec{r}\times\frac{\mathrm{d}}{\mathrm{d}t}\vec{v}=\vec{r}\times\vec{F}\\
&\Rightarrow\vec{r}\times\frac{\mathrm{d}}{\mathrm{d}t}\vec{v}+\left(\frac{\mathrm{d}}{\mathrm{d}t}\vec{r}\right)\times\vec{v}-\left(\frac{\mathrm{d}}{\mathrm{d}t}\vec{r}\right)\times\vec{v}=\frac{\vec{r}\times\vec{F}}{m}\\
&\Rightarrow\frac{\mathrm{d}}{\mathrm{d}t}\left(\vec{r}\times\vec{v}\right)-\left(\frac{\mathrm{d}}{\mathrm{d}t}\vec{r}\right)\times\vec{v}=\frac{\vec{r}\times\vec{F}}{m}\\
&\Rightarrow m\left|\vec{r}\right|^2\frac{\mathrm{d}}{\mathrm{d}t}\vec{\Omega}=\vec{r}\times\vec{F}\\
&\Rightarrow J\frac{\mathrm{d}}{\mathrm{d}t}\vec{\Omega}=\vec{T}\Leftrightarrow J\frac{\mathrm{d}}{\mathrm{d}t}\Omega\hat{z}=T\hat{z}
\end{aligned}\tag{14}$$

where note the speed of the particle $\vec{v}=\left(\frac{\mathrm{d}}{\mathrm{d}t}\vec{r}\right)$ is the line speed, and also note line speed equals to the cross product of radius and angular speed: $\vec{v}=\vec{\Omega}\times\vec{r}$, the moment of inertia of a point mass is derived as $J=mr^2$. We can assume the axis of rotation of $\vec{\Omega}$ aligns with the z-axis of the reference frame, so we can remove the unit vector $\hat{z}$ from both sides of the EOM to reach the following one degree of freedom EOM:

$$J\frac{\mathrm{d}}{\mathrm{d}t}\Omega=T\tag{15}$$

1.3. Mechanical Dynamics of an Electric Machine

To our interest, let's derive the motion dynamics of a solid cylinder (with mass M and radius R) that rotates about its center axis parallel to $\hat{z}$. Basically, we need to apply the rotational version law (15) to every particle that makes up the cylinder:

$$\left(\Sigma J\right)\frac{\mathrm{d}}{\mathrm{d}t}\Omega=\left(\Sigma T\right)\tag{16}$$

where note all particles share the same angular speed of Ω [rad/s], and the sum of the rotational inertia can be calculated by integrating the mass of the infinitesimally thin rings from radius 0 to radius R (see example permanent magnet solid rotor in Fig. 1)

$$\left(\Sigma J\right)=\int_0^R\rho\left(2\pi r\mathrm{d}r\right)r^2=\frac{M}{\pi R^2}\left(2\pi\frac{1}{4}R^4\right)=\frac{1}{2}MR^2=J_s\tag{17}$$

where the area density of the cylinder is $\rho = \frac{M}{\pi R^2}$ [kg/m^2] and J_s denotes the shaft's moment of inertia. The practical meaning of this result is to allow us to estimate the inertia of a rotor shaft by measuring its radius and mass.

Based on the sources of the torque, we can decompose the torque sum into an unknown load torque T_L and an electromagnetic torque T_{em} that is controllable:

$$(\Sigma T) = T_{\text{em}} - T_L \tag{18}$$

Plug the new variables defined in (17) and (18) into (16), and the mechanical dynamics governing the angular motion of the rotor shaft around z-axis are derived as

$$J_s \frac{\mathrm{d}}{\mathrm{d}t} \Omega = T_{\text{em}} - T_L \tag{19}$$

where Ω is defined as the change rate of the angular location Θ of the solid cylinder:

$$\Omega = \frac{\mathrm{d}}{\mathrm{d}t} \Theta \tag{20}$$

and the rotational kinetic energy of the mechanical system is

$$W_\Omega = \frac{1}{2} J_s \Omega^2 \tag{21}$$

The mechanical input power and work to the electric machine are respectively as

$$P_{\text{mech,in}} = -T_L \Omega \tag{22}$$

$$W_{\text{mech,in}} = \int_0^t P_{\text{mech,in}} \mathrm{d}t \tag{23}$$

where the negative sign indicates that the mechanical sources are in fact taking energy away from our system when $T_L > 0$.

1.4. Review on Circuit Fundamentals

Considering a circuit shown in Fig. 2, we have the following equation as per Kirchhoff's voltage law:

$$u_1 = R_1 i_1 + e_1 \tag{24}$$

where the voltage across the inductance L_1 is denoted as e_1. The direction of the voltage e_1 is defined such that it counters the terminal voltage u_1, hence also known as *counter electromagnetic force*.

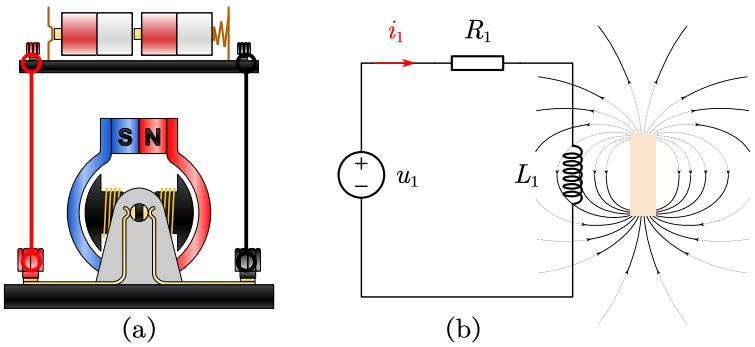

Figure 2. One phase of a generic inductive electric circuit linking to external magnetic field. (a) realistic drawing; (b) symbolic drawing.

1.5. The Energy Method

Recall that voltage times current is electric power, and integrating power over time gives electric work:

$$W_{\text{elec,in}} = \int_0^t u_1(t) i_1(t) \mathrm{d}t = \underbrace{\int_0^t i_1^2(t) R \mathrm{d}t}_{\text{Heat}} + \underbrace{\int_0^t i_1(t) e_1(t)\, \mathrm{d}t}_{\text{Magnetic energy}} \triangleq W_{\text{Cu}} + W_{\Phi} \tag{25}$$

where there are two kinds of work generated in the circuit: the copper loss W_{Cu} and the magnetic energy W_{Φ}. Note (25) is valid only if there exists no mechanical motion, i.e., $\Omega = 0$.

In case of a circuit involving mechanical part in motion, we must revise (25) to include the stored mechanical energy. Recall that the first law of thermodynamics states that "energy cannot be created or destroyed; it can only be converted from one form to another". Therefore, the stored mechanical energy must be further added to the right hand side of (25) to give

$$W_{\text{elec,in}} + W_{\text{mech,in}} = W_{\text{Cu}} + W_{\Phi} + W_{\Omega} \tag{26}$$

which reads [4]

$$\left(\begin{array}{c}\text{Energy input}\\ \text{from electric}\\ \text{sources}\end{array}\right) + \left(\begin{array}{c}\text{Energy input}\\ \text{from mechanical}\\ \text{sources}\end{array}\right) = \left(\begin{array}{c}\text{Energy}\\ \text{dissipated}\\ \text{as heat}\end{array}\right) + \left(\begin{array}{c}\text{Stored}\\ \text{magnetic field}\\ \text{energy}\end{array}\right) + \left(\begin{array}{c}\text{Stored}\\ \text{mechanical}\\ \text{energy}\end{array}\right) \tag{27}$$

where we have assumed only copper loss is contributing to heat.

Taking time derivative on both sides of (26) yields

$$\begin{aligned} & P_{\text{elec,in}} + P_{\text{mech,in}} = P_{\text{Cu}} + \frac{\mathrm{d}}{\mathrm{d}t} W_{\Phi} + \frac{\mathrm{d}}{\mathrm{d}t}\left(\frac{1}{2} J_s \Omega^2\right) \\ \Rightarrow\ & e_1 i_1 - T_L \Omega = \frac{\mathrm{d}}{\mathrm{d}t} W_{\Phi} + J_s \Omega \frac{\mathrm{d}}{\mathrm{d}t} \Omega \\ \Rightarrow\ & e_1 i_1 - T_L \Omega = \frac{\mathrm{d}}{\mathrm{d}t} W_{\Phi} + \Omega \left(T_{\text{em}} - T_L\right) \\ \Rightarrow\ & e_1 i_1 = \frac{\mathrm{d}}{\mathrm{d}t} W_{\Phi} + T_{\text{em}} \frac{\mathrm{d}}{\mathrm{d}t} \Theta \end{aligned} \tag{28}$$

where, apparently, T_{em} and W_Φ are unknown, and so is e_1.

We need to first derive an expression for W_Φ before we can get an expression for torque. As a side note, however, in the special case where the ac excitation has no reactive power component, such that the magnetic field energy W_Φ is time-invariant, then the torque can be derived for a three phase motor as simply as follows (see [5, (15)]) :

$$(28) \Rightarrow T_{\text{em}} = \frac{e_1 i_1 + e_2 i_2 + e_3 i_3 - \frac{\mathrm{d}}{\mathrm{d}t} W_\Phi}{\Omega} \tag{29}$$

Note (28) holds for any initial conditions. Let $\Theta = \text{Const.}$, and from (28), we can certainly derive an expression for magnetic field energy as a function of time t:

$$W_\Phi(t) = \int_0^t e_1 i_1 \mathrm{d}t + \text{Const.} \tag{30}$$

Here, the constant term Const. corresponds to the magnetic field energy due to the permanent magnet (PM), which exists before $t = 0$. But, what is the voltage across the inductance, that is, what is e_1?

1.6. Review on Faraday's Law of Induction

Faraday's law of induction states that *"The electromotive force around a closed path is equal to the* ***negative*** *of the time rate of change of the magnetic flux enclosed by the path."*[9]

$$e = -\frac{\mathrm{d}}{\mathrm{d}t}\Phi_1 \tag{31}$$

where Φ_1 denotes the magnetic flux enclosed by one turn of the coil. This is a macroscopic result of the fact that the curl of electric field equals to the time derivative of a magnetic field:

$$\nabla \times \vec{E} = -\frac{\partial \vec{B}}{\partial t} \tag{32}$$

The negative sign is explained by the Lenz's law, and one way to interpret it is that if a current is induced by the electromotive force e, the induced current's resulting magnetic field is in a direction that is against the original magnetic field.

1.6.1. Flux Linkage in an Electric Circuit

Flux linkage ψ_1 is a useful alternative to magnetic flux Φ_1 in an electric circuit, and it is defined as the integration of counter electromotive force e_1 over time:

$$\psi_1 = \pm \int e_1 \mathrm{d}t \tag{33}$$

[9] https : //en.wikipedia.org/wiki/Faraday%27s_law_of_induction

The main difference from the original law of induction (31) is that ψ_1 corresponds to the total linkage of an arbitrary coil #1 that has N_1 turns.

The question left is what sign should it take in (33)?

1.6.2. Motoring Convention

For this course, we are mainly studying the motoring operation of an electric machine, such that the electrical power is converted into mechanical power.[10]

The motoring convention states that by looking at the terminals of the circuit: (1) positive voltage generates positive current, giving positive power; (2) positive current generates positive flux linkage; (3) positive torque results in positive rotation:

$$\begin{aligned} &1.\ u_1 > 0 \Rightarrow i_1 > 0 \Rightarrow P_1 = u_1 i_1 > 0 \\ &2.\ i_1 > 0 \Rightarrow \psi_1 > 0 \Rightarrow e_1 > 0 \\ &3.\ T_{\text{em}} > 0 \Rightarrow \Omega > 0 \end{aligned} \tag{34}$$

Consider $R_1 = 0$, we have $u_1 = 0 \times i_1 + e_1 > 0$ and $i_1 > 0, \psi_1 > 0$. As a result, (33) takes the plus sign. Taking time derivative at both sides of (33) yields:

$$e_1 = \frac{\mathrm{d}}{\mathrm{d}t}\psi_1 = N_1 \frac{\mathrm{d}}{\mathrm{d}t}\Phi_1 \tag{35}$$

The last equal sign is only valid for a coil #1 that has N_1 turns and each turn links the same magnetic flux Φ_1. By (35), we view the electromotive force as a help such that positive electromotive force leads to the build-up of the flux linkage of a coil.

1.6.3. Flux Linkage as Integral over Current

In (33), the flux linkage is defined as an integral of voltage over time. In Newton's law, the momentum of a particle can be calculated by integrating force over time as well: $\vec{p} = \int \vec{F}\mathrm{d}t$. In this analogy, **voltage** becomes force and **flux linkage** becomes momentum.

Furthermore, by this voltage-force analogy, **current** becomes velocity, because for electrical charge Q_1 (that passes through a cross section), its "velocity" is simply by definition, the current $\frac{\mathrm{d}Q_1}{\mathrm{d}t} = i_1$.

We are now ready to derive the equivalent inertia quantity in a circuit. To see this, let's recall that momentum is defined as $\vec{p} = m\frac{\mathrm{d}\vec{r}}{\mathrm{d}t} = m\vec{v}$, that is, an inertia quantity m times the velocity $\vec{v}$. Similarly, for a circuit, the relation between flux linkage and current is defined as the self-inductance:[11]

$$\begin{aligned} e_1 &= \frac{\mathrm{d}}{\mathrm{d}t}\psi_1 = \frac{\mathrm{d}\psi_1}{\mathrm{d}i_1}\frac{\mathrm{d}}{\mathrm{d}t}i_1 = L_1\frac{\mathrm{d}}{\mathrm{d}t}i_1 \\ \Rightarrow L_1 &\triangleq \frac{\mathrm{d}\psi_1}{\mathrm{d}i_1} \\ \Rightarrow \mathrm{d}\psi_1 &= L_1 \mathrm{d}i_1 \end{aligned} \tag{36}$$

This is known as the small signal definition of self-inductance—which literally means

[10] In regenerating operation, the mechanical power is converted into electrical power using the electric machine–known as the generator.

[11] This equation assumes the only source to the electromotive force is i_1.

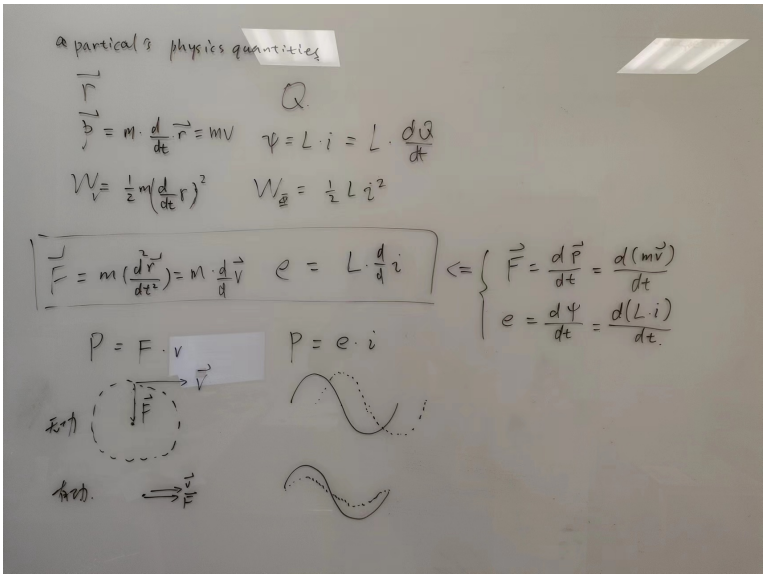

Figure 3. A duality of the physics between a particle and an electric charge.

flux linkage change per current change. Based on the definition for inductance, the flux linkage can as well be obtained as an integral of inductance over current:

$$\psi_1 = \int_0^{i_1} L_1(i_1)\,\mathrm{d}i_1 + C \tag{37}$$

where the inductance can be a modeled as a function of current to take into consideration of the saturation of iron core. Note the constant C is zero because we have assumed i_1 is the only source in this world. If self-inductance L_1 is not a function of current, we have $\psi_1 = L_1 i_1 = L_1 \frac{\mathrm{d}Q_1}{\mathrm{d}t}$, implying that the self-inductance L_1 is the inertia of electrical charge Q_1.

However, unlike a point particle, the "momentum" of an electrical charge can have multiple sources. Without loss of generality, when there are two magnetic sources, the differential of the flux linkage becomes:

$$\mathrm{d}\psi_1 = \frac{\partial \psi_1}{\partial i_1}\mathrm{d}i_1 + \frac{\partial \psi_1}{\partial i_2}\mathrm{d}i_2 \tag{38}$$

which can be used to calculate flux linkage in terms of states i_1 and i_2 as follows

$$\Rightarrow \psi_1(i_1, i_2) = \int_{(0,0)}^{(i_1,i_2)} \mathrm{d}\psi_1 = \int_{(0,0)}^{(i_1,0)} \frac{\partial \psi_1}{\partial i_1}\mathrm{d}i_1 + \int_{(i_1,0)}^{(i_1,i_2)} \frac{\partial \psi_1}{\partial i_2}\mathrm{d}i_2 = L_1 i_1 + L_{12} i_2 \tag{39}$$

where the integral path independency is valid only if the magnetic circuit is linear and time-invariant, such that inductance is not a function of currents or rotor angle Θ. We will soon have a refresh on the math involved above. The mutual inductance L_{12} is defined as the partial derivative of ψ_1 with respect to excitation i_2.

1.6.4. Electric Charge and Point Particle: A Duality

Let's stop for a moment dwelling on the name "electromotive force". By following the motoring convention, we have defined the equivalent "law of motion" to an electrical charge Q_1: "the time rate of an electric charge's "momentum" $\psi_1 = L_1 \frac{\mathrm{d}Q}{\mathrm{d}t}$ equals to the external (electromotive) force e_1."

See Fig. 3 for a better understanding of what flux linkage really is or mean in an electric circuit by comparing the physics about a point particle with that of an electric charge. The physics about a particle include: position, velocity, momentum, energy, law of motion, and power (including active power and reactive power).

1.7. Review on Multi-variable Calculus

Plug Faraday's law of induction (35) into the equation of energy conservation (28), and multiply both sides with $\mathrm{d}t$ to remove dependency on time t:

$$\mathrm{d}W_\Phi = i_1 \mathrm{d}\psi_1 - T_{\mathrm{em}} \mathrm{d}\Theta \tag{40}$$

What is this?

1.7.1. Exact Differential

The exact differential of a scalar function $Q(x, y, z)$ that depends on three states is defined as

$$\begin{aligned} \mathrm{d}Q &= \frac{\partial Q}{\partial x}\mathrm{d}x + \frac{\partial Q}{\partial y}\mathrm{d}y + \frac{\partial Q}{\partial z}\mathrm{d}z \\ \mathrm{d}Q &= \vec{\nabla} Q\left(x, y, z\right) \cdot \left(\mathrm{d}x, \mathrm{d}y, \mathrm{d}z\right) \end{aligned} \tag{41}$$

where the gradient is defined as

$$\vec{\nabla} Q = \frac{\partial Q}{\partial x}\hat{x} + \frac{\partial Q}{\partial y}\hat{y} + \frac{\partial Q}{\partial z}\hat{z} = \left(\frac{\partial Q}{\partial x}, \frac{\partial Q}{\partial y}, \frac{\partial Q}{\partial z}\right)$$

where $\vec{\nabla}$ is the nabla operator $\vec{\nabla} = \left(\frac{\partial}{\partial x}, \frac{\partial}{\partial y}, \frac{\partial}{\partial z}\right)$.

1.7.2. Gradient Theorem

The gradient theorem states that the integral of an exact differential is independent of the choice of an integral path between the two endpoints, i.e., line integral of exact differential has path independency:

$$\int_{(x_0,y_0,z_0)}^{(x,y,z)} \mathrm{d}Q = \int_{(x_0,y_0,z_0)}^{(x,y,z)} \nabla Q\left(x, y, z\right) \cdot \left(\mathrm{d}x, \mathrm{d}y, \mathrm{d}z\right) = Q\left(x, y, z\right) - Q\left(x_0, y_0, z_0\right) \tag{42}$$

This line integral can be performed along any path the connects the two endpoints (x_0, y_0, z_0) and (x, y, z).

1.8. The Conservative Nature of Magnetic Field Energy

Equation (40) reveals the exact differential of the magnetic field energy:

$$\mathrm{d}W_\Phi\left(\psi_1,\Theta\right)=\left.\frac{\partial W_\Phi}{\partial\psi_1}\right|_\Theta\mathrm{d}\psi_1+\left.\frac{\partial W_\Phi}{\partial\Theta}\right|_{\psi_1}\mathrm{d}\Theta \tag{43}$$

which means that the variation in magnetic energy is solely determined by the state variables of flux linkage ψ_1 and cylinder's angular position Θ. Recall that we have eliminated heat and mechanical load input during the derivation of (28), so one can state that the system that stores magnetic field energy is lossless.

Comparing between the math in (43) and the physics in (40), we know the electromagnetic torque T_{em} is the negative partial derivative of magnetic energy W_Φ with respect to cylinder angle Θ:

$$\left.\frac{\partial W_\Phi}{\partial\Theta}\right|_{\psi_1}=-T_{\mathrm{em}} \tag{44}$$

Our objective shall now be changed to derive an expression of W_Φ at an arbitrary state of (ψ_1,Θ) (rather than at time t) without needing to know the electromagnetic torque T_{em}, and this is possible because the line integral of $\mathrm{d}W_\Phi$ has *path independency*. To this end, we need to choose an initial state (ψ_1,Θ) such that $T_{\mathrm{em}}\equiv 0$. We know when $W_\Phi=0$, the electromagnetic torque T_{em} is always zero. However, as indicated in (30), at $t=0$, there is already constant magnetic energy due to the permanent magnet (PM).

In order to create a null state of W_Φ, there are two ways to deal with the PM, the fictitious winding method [4, Sec 3.7] and the equivalent field winding method [6, Ch. 3]. The former puts a fictitious winding around the PM to exactly cancel the magnetic field of the PM, hence allowing the integration starts at a zero magnetic energy state; while the latter simply models the PM as a field winding, i.e., the PM or the field winding must also be excited by external electric sources in order to become magnetic in the first place.

We are going to use the second approach. Let's denote the additional circuit that models the PM as the $(m+1)$-th circuit, and till now, phase number m is 1, meaning that we have only 1 armature circuit. This additional electric circuit is a new electric source to the system, so we need to rewrite (28), (40) accordingly

$$(28)\Rightarrow e_1i_1+e_{m+1}i_{m+1}=\frac{\mathrm{d}}{\mathrm{d}t}W_\Phi+T_{\mathrm{em}}\frac{\mathrm{d}}{\mathrm{d}t}\Theta \tag{45}$$

$$(40)\Rightarrow \mathrm{d}W_\Phi=i_1\mathrm{d}\psi_1+i_{m+1}\mathrm{d}\psi_{m+1}-T_{\mathrm{em}}\mathrm{d}\Theta \tag{46}$$

Now, we are able to make $W_\Phi=0$ by letting $\psi_1=\psi_{m+1}=0$. Since there is no magnetic energy, the electromagnetic torque must be zero:

$$W_\Phi\left(\psi_1=0,\psi_{m+1}=0,\Theta\right)\Rightarrow T_{\mathrm{em}}=0 \tag{47}$$

otherwise if $T_{\mathrm{em}}\neq 0$ when $W_\Phi=0$, one can build a perpetual motion machine based on this phenomenon, e.g., integrating over rotor angle Θ before T_{em} changes its sign to give: $W_\Phi=\int -T_{\mathrm{em}}\mathrm{d}\Theta\neq 0$.

Since $\mathrm{d}W_\Phi$ in (46) is an exact differential, we can integrate over one state variable at a time and during the integration, other two independent state variables are fixed. Therefore, in order to reach arbitrary state of $(\psi_1, \psi_{m+1}, \Theta)$ from $(0,0,0)$, it is of high priority to integrate over Θ, which allows Θ to pick any value. Next, without lost of generality, we integrate over state ψ_1 by keeping $\psi_{m+1} = 0$ and $\Theta = \text{Const.}$, and finally, we integrate over state ψ_{m+1} by keeping the other two states constant. In math language, this becomes:

$$\begin{aligned} W_\Phi(\psi_1, \psi_{m+1}, \Theta) &= \int_0^{\Theta} T_{\text{em}}(\psi_1 = 0, \psi_{m+1} = 0, \Theta)\,\mathrm{d}\Theta \\ &+ \int_0^{\psi_1} i_1(\psi_1, \psi_{m+1} = 0, \Theta)\,\mathrm{d}\psi_1 + \int_0^{\psi_{m+1}} i_{m+1}(\psi_1, \psi_{m+1}, \Theta)\,\mathrm{d}\psi_{m+1} \end{aligned} \tag{48}$$

The above integration is valid because we are dealing with a conservative system to which the work done by force or current is independent of path.

1.9. Mutual Flux Linkage and Mutual Inductance

According to the exact differential of the flux linkage (38), we have a formula to calculate flux linkage of circuit #1 as follows[12]

$$\psi_1 = \int_0^{i_1} L_1 \mathrm{d}i_1 + \int_0^{i_{m+1}} L_{1(m+1)} \mathrm{d}i_{m+1} \tag{49}$$

where L_1 denotes the self-inductance and $L_{1(m+1)}$ is the mutual inductance. In (49), the magnetic flux lines passing through the coil of circuit #1 have two sources, the first term is self linkage and the second one is mutual linkage.

1.10. Assumption of Non-saturated Magnetic Circuit

In order to get an analytical result, *the magnetic circuit is assumed to be non-saturated* and this assumption leads to the following large signal definition of (self and mutual) inductance:

$$\begin{aligned} \psi_1 &= L_1 i_1 + L_{1(m+1)} i_{m+1} \\ \psi_{m+1} &= L_{1(m+1)} i_1 + L_{m+1} i_{m+1} \end{aligned} \Leftrightarrow \begin{bmatrix} \psi_1 \\ \psi_{m+1} \end{bmatrix} = \begin{bmatrix} L_1 & L_{1(m+1)} \\ L_{(m+1)1} & L_{m+1} \end{bmatrix} \begin{bmatrix} i_1 \\ i_{m+1} \end{bmatrix} \tag{50}$$

Note we can rewrite (50) in terms of matrix and vector and note

$$\begin{bmatrix} a & b \\ c & d \end{bmatrix}^{-1} = \frac{1}{ad - bc} \begin{bmatrix} d & -b \\ -c & a \end{bmatrix}$$

[12] To be specific, (49) is valid only if a phenomenon called cross saturation does not occur, i.e., L_1 is not dependent on i_{m+1}, and L_{m+1} is not dependent on i_1. In case of cross saturation, the flux linkage and the associated magnetic flux can only be determined with the help of finite element analysis softwares (for solving the magnetic potential in a saturated iron core).

As a result, the currents can be explicitly expressed in terms of inductances and flux linkages as follows:

$$i_1\left(\psi_1, \psi_{m+1}=0, \Theta\right)=\frac{L_{m+1}\psi_1 - L_{1(m+1)}\psi_{m+1}}{D}=\frac{L_{m+1}\psi_1 - 0}{D} \tag{51}$$

$$i_{m+1}\left(\psi_1, \psi_{m+1}, \Theta\right)=\frac{-L_{1(m+1)}\psi_1 + L_1\psi_{m+1}}{D} \tag{52}$$

with the determinant of the inductance matrix: $D = L_1 L_{m+1} - L_{1(m+1)}^2$, and we are now able proceed the integration in (48) to reach:

$$W_\Phi\left(\psi_1, \psi_{m+1}, \Theta\right)=0+\frac{L_{m+1}}{2D}\psi_1^2+\left(\frac{L_1}{2D}\psi_{m+1}^2-\frac{L_{1(m+1)}}{D}\psi_1\psi_{m+1}\right) \tag{53}$$

where though not indicated, note the inductance is allowed to be dependent on Θ.

1.11. Torque Expression (Single Phase $m = 1$)

The following equation holds between exact differential and partial differentials:

$$\mathrm{d}W_\Phi\left(\psi_1, \psi_{m+1}, \Theta\right)=\left.\frac{\partial W_\Phi}{\partial \psi_1}\right|_{\substack{\psi_{m+1}\\ \Theta}}\mathrm{d}\psi_1+\left.\frac{\partial W_\Phi}{\partial \psi_{m+1}}\right|_{\substack{\psi_1\\ \Theta}}\mathrm{d}\psi_{m+1}+\left.\frac{\partial W_\Phi}{\partial \Theta}\right|_{\substack{\psi_1\\ \psi_{m+1}}}\mathrm{d}\Theta \tag{54}$$

where each partial derivative must be evaluated with all other states being constants.

Compare the math in (54) to physics in (46), we have again obtained the equation for calculating the electromagnetic torque T_{em} as follows

$$\left.\frac{\partial W_\Phi}{\partial \Theta}\right|_{\substack{\psi_1\\ \psi_{m+1}}}=-T_{\mathrm{em}} \tag{55}$$

However, looking at (53), one realizes that W_Φ's partial derivative with respect to Θ is not easy to calculate because of the presence of the determinant $D(\Theta)$ in the denominator. Moreover, it is preferred to express the torque in terms of currents instead of the flux linkages, for currents are easy to measure.

1.12. The Co-Energy Trick

As a math trick, let's define co-energy as:

$$W'_\Phi = i_1\psi_1 + i_{m+1}\psi_{m+1} - W_\Phi \tag{56}$$

Note that the exact differential of current times flux (which has a dimension of [Nm]) satisfies: $\mathrm{d}(i\psi) = i\mathrm{d}\psi + \psi\mathrm{d}i$, and from (46), we have

$$\mathrm{d}W'_\Phi\left(i_1, i_{m+1}, \Theta\right)=\psi_1\mathrm{d}i_1+\psi_{m+1}\mathrm{d}i_{m+1}+T_{\mathrm{em}}\mathrm{d}\Theta \tag{57}$$

The co-energy can as well be integrated from a null state of $(0,0,0)$, via $(0,0,\Theta)$ and then $(i_1,0,\Theta)$, and finally to an arbitrary state (i_1,i_{m+1},Θ) as

$$\begin{aligned} W'_\Phi &= 0 + \int_0^{i_1} \psi_1\left(i_1, i_{m+1}=0, \Theta\right) \mathrm{d}i_1 + \int_0^{i_{m+1}} \psi_{m+1}\left(i_1, i_{m+1}, \Theta\right) \mathrm{d}i_{m+1} \\ &\overset{(50)}{=} \int_0^{i_1} \left(L_1 i_1 + L_{1(m+1)} \times 0\right) \mathrm{d}i_1 + \int_0^{i_{m+1}} \left(L_{1(m+1)} i_1 + L_{m+1} i_{m+1}\right) \mathrm{d}i_{m+1} \\ &= \frac{1}{2} L_1 i_1^2 + L_{1(m+1)} i_1 i_{m+1} + \frac{1}{2} L_{m+1} i_{m+1}^2 \\ &= \frac{1}{2} \begin{bmatrix} i_1 & i_{m+1} \end{bmatrix} \begin{bmatrix} L_1 & L_{1(m+1)} \\ L_{1(m+1)} & L_{m+1} \end{bmatrix} \begin{bmatrix} i_1 \\ i_{m+1} \end{bmatrix} \triangleq \frac{1}{2} \boldsymbol{i}^{\mathrm{T}} \boldsymbol{L} \boldsymbol{i} \end{aligned} \tag{58}$$

Note this derivation depends on the non-saturation assumption.

The exact differential from (57) also satisfies

$$\mathrm{d}W'_\Phi\left(i_1, i_{m+1}, \Theta\right) = \left.\frac{\partial W'_\Phi}{\partial i_1}\right|_{\substack{i_{m+1} \\ \Theta}} \mathrm{d}i_1 + \left.\frac{\partial W'_\Phi}{\partial i_{m+1}}\right|_{\substack{i_1 \\ \Theta}} \mathrm{d}i_{m+1} + \left.\frac{\partial W'_\Phi}{\partial \Theta}\right|_{\substack{i_1 \\ i_{m+1}}} \mathrm{d}\Theta \tag{59}$$

Comparing between (59) and (57), the torque is then derived as

$$T_{\mathrm{em}} = \left.\frac{\partial W'_\Phi}{\partial \Theta}\right|_{\substack{i_1 \\ i_{m+1}}} \mathrm{d}\Theta = \frac{1}{2} \boldsymbol{i}^{\mathrm{T}} \frac{\partial \boldsymbol{L}}{\partial \Theta} \boldsymbol{i} \tag{60}$$

1.13. Example: Single Phase Motor

Consider a single phase motor, i.e., $m=1$, and its torque expression is:

$$T_{\mathrm{em}} = \frac{1}{2} \frac{\partial L_1}{\partial \Theta} i_1^2 + \frac{\partial L_{1(m+1)}}{\partial \Theta} i_1 i_{m+1} + \frac{1}{2} \frac{\partial L_{m+1}}{\partial \Theta} i_{m+1}^2 \tag{61}$$

Now let's further generalize our discussion by allowing i_{m+1} to be time-varying, which means that the PM is replaced with a actual field winding having time-varying current:

$$\begin{aligned} i_1 &= I_1 \cos\left(\phi_1\right) \\ i_2 &= I_2 \cos\left(\phi_2\right) \end{aligned} \tag{62}$$

where note ϕ_1 and ϕ_2 are your free design variables. Let's assume for now the mutual inductance between two coils is a cosine of electrical rotor angle

$$L_{1(m+1)} = M \cos\left(n_{\mathrm{pp}} \Theta\right) \tag{63}$$

and $\frac{\partial L_1}{\partial \Theta} = \frac{\partial L_{m+1}}{\partial \Theta} = 0$. We will show why this is a valid assumption later.

The torque of this single phase motor is:

$$\begin{aligned} T_{\text{em}} &= 0 + \frac{\partial L_{1(m+1)}}{\partial \Theta} i_1 i_{m+1} + 0 \\ &= \frac{\partial M \cos\left(n_{\text{pp}}\Theta\right)}{\partial \Theta} I_1 \cos\left(\phi_1\right) I_2 \cos\left(\phi_2\right) \\ &= -n_{\text{pp}} I_1 I_2 M \sin\left(n_{\text{pp}}\Theta\right) \cos\left(\phi_1\right) \cos\left(\phi_2\right) \\ &= -n_{\text{pp}} I_1 I_2 M \sin\left(n_{\text{pp}}\Theta\right) \frac{\cos\left(\phi_1+\phi_2\right)+\cos\left(\phi_1-\phi_2\right)}{2} \\ &= -n_{\text{pp}} I_1 I_2 M \frac{1}{4} \left[\begin{array}{c} \sin\left(n_{\text{pp}}\Theta+\left(\phi_1+\phi_2\right)\right)+\sin\left(n_{\text{pp}}\Theta-\left(\phi_1+\phi_2\right)\right) \\ +\sin\left(n_{\text{pp}}\Theta+\left(\phi_1-\phi_2\right)\right)+\sin\left(n_{\text{pp}}\Theta-\left(\phi_1-\phi_2\right)\right) \end{array} \right] \end{aligned} \tag{64}$$

which is dependent on rotor angle Θ.

1.13.1. AC PM Motor Example

Let $\phi_2 = 0$, we have constant field current $i_2 = I_2$ and the torque becomes:

$$T_{\text{em}} = \frac{-n_{\text{pp}} I_1 I_2 M}{2} \left[\sin\left(n_{\text{pp}}\Theta+\phi_1\right)+\sin\left(n_{\text{pp}}\Theta-\phi_1\right)\right] \tag{65}$$

In order to have a non-zero average value over one revolution, we need to eliminate Θ in sine function. For example, further letting $\phi_1 = n_{\text{pp}}\Theta + \phi_0$, which would require we measure the rotor angle Θ using a physical sensor, (65) becomes:

$$T_{\text{em}} = \frac{-n_{\text{pp}} I_1 I_2 M}{2} \left[\sin\left(2n_{\text{pp}}\Theta+\phi_0\right)+\sin\phi_0\right] \tag{66}$$

The torque is not steady but does have a non-zero average value over one revolution.

1.13.2. DC Motor Example

Figure 4. Commutated parallel-excited dc motor of which the rotor coil terminals are conductive for 180 degrees of the rotation (i.e., half of its insulation on rotor coil terminals has been stripped off). Photo credit: Douyin user @Dover.

Let $\phi_1 = \phi_2 = 0$, we have the torque of a dc motor from (65):

$$T_{\text{em}} = -n_{\text{pp}} I_1 I_2 M \sin\left(n_{\text{pp}}\Theta\right) \tag{67}$$

where we shall now emphasize that I_1 and I_2 are also at our disposal. Keep I_2 as a constant. If we can excite negative current I_1 only when the sine function $\sin(n_{\text{pp}}\Theta)$ is positive, the torque will always be positive even though it is not steady. An example working motor is shown in (4).

1.13.3. Flux Switched Alternator Example

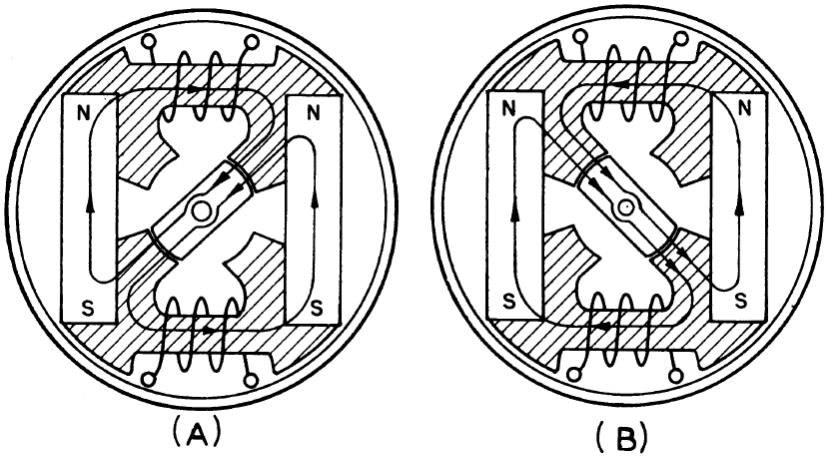

Figure 5. Flux switched alternator with four stator (salient) poles and two rotor (salient) poles. Figure credit: Rauch and Johnson (1955).

The flux switched alternator has been used as a generator and power supply for missile guiding system [7], and its working principle is illustrated in Fig. 5. Let the coils form circuit #1 and PMs form circuit #(m+1). Since the magnetic flux that links the coils in situation (A) has an opposite sign to that in situation (B), it is equivalent to say that the mutual inductance $L_{1(m+1)}$ takes values that have opposite signs between situation (A) and situation (B). Therefore, if we excite proper current, a torque with non-zero average value can be produced.

1.14. Torque Expression (Multi-Phases)

Now let's generalize the above results to a system with m phase armature circuits and an $(m+1)$-th additional equivalent field circuit that models the PM (such that i_{m+1} is a parameter rather than a control input):

$$\begin{aligned} T_{\text{em}} = \frac{1}{2}\boldsymbol{i}^{\mathrm{T}}\frac{\partial \boldsymbol{L}}{\partial \Theta}\boldsymbol{i} = &\left\{\frac{1}{2}\sum_{j=1}^{m} i_j^2\frac{\partial L_j}{\partial \Theta} + \sum_{j=1}^{m}\sum_{k=1}^{j-1}\frac{\partial L_{jk}}{\partial \Theta} i_j i_k\right\} \\ &+ \sum_{j=1}^{m}\frac{\partial L_{j(m+1)}}{\partial \Theta} i_j i_{m+1} + \frac{1}{2} i_{m+1}^2\frac{\partial L_{m+1}}{\partial \Theta} \end{aligned} \tag{68}$$

where the three terms on the right hand side are respectively the reluctance torque, reaction torque, and the cogging torque. The definition of the current vector and inductance matrix is accordingly extended as $\boldsymbol{i} \in \mathbb{R}^{m+1}$ and $\boldsymbol{L} \in \mathbb{R}^{m+1} \times \mathbb{R}^{m+1}$. Note the mutual inductance is allowed to have a negative value.

1.14.1. Reluctance Torque

Reluctance torque is the professional term to describe the force exserted to a piece of iron by an electro-magnet.[13] If i_j is direct current (DC), the integral of the reluctance torque over Θ from 0 rad to 2π rad is zero, because of the periodicity of the inductance functions. Therefore, in order to generate a non-zero reluctance torque, i_j must be turned off at proper moments dependent on the value of Θ. The sign of i_j does not affect the self linking i_j^2 term in reluctance torque, but affects the other mutual linking $i_j i_k$ term. For motors with zero mutual inductances $L_{jk} = 0$, unipolar semiconductor power amplifier is sufficient to control the reluctance torque.

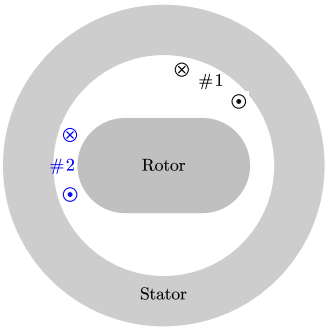

Figure 6. Illustration of a machine equipped with a two phase winding that works on reluctance torque.

An example reluctance toque with two phase stator winding is shown in Fig. 6. The rotor iron will be aligned to the center axis of a coil when the current is excited into the coil, and a reluctance torque is produced by the current.

1.14.2. Reaction Torque

Reaction torque[14] specifically refers to the torque due to the interaction between the armature field and the permanent magnetic field (which is not under our control, i.e., i_{m+1} is modelled as a constant). Recall that the $(m+1)$-th circuit is virtual, and therefore the mutual inductance between circuit j and circuit $m+1$, i.e., $L_{j(m+1)}$, is not ever measured in practice. However, the term $L_{j(m+1)}i_{m+1}$ does mean the circuit j has a mutual flux linking due to magnetic field generated by the virtual current i_{m+1}, which is known as the *permanent magnet flux linkage* of phase j, which can be measured by measuring the back electromotive force at the terminals of a winding.

1.14.3. Cogging Torque

The average contribution of cogging torque to mechanical work is zero, because of the fact that i_{m+1} is a constant and the partial derivative of L_{m+1} with respective to Θ is periodic. The existence of cogging torque is due to the fact the stator iron is slotted for manufacture purposes (i.e., for putting in stator winding). The amplitude of the cogging torque can be reduced by choosing a slot-pole combination (stator slot number Q_s and rotor pole pair number n_{pp}) such that $\text{LCM}(Q_s, 2n_{\text{pp}})$ is as large as possible.

[13] The magnetic flux lines act like a string that pulls the iron piece towards a new location such that the reluctance in the magnetic circuit is at a minimum.

[14] Jiahao: I did not find an official source why this torque is called reaction torque, but I do notice "action" and "reaction" appear in Newton's third law of motion. Therefore, the reaction torque is the equal and opposite reaction exserted back to the rotor.

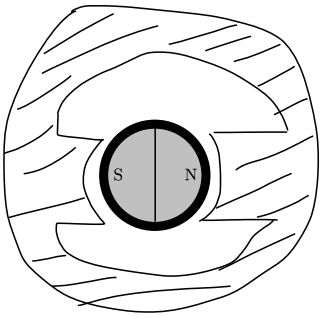

Figure 7. Illustration of a two-stator-slot machine that suffers from cogging torque.

The most significant cogging torque for a perfectly manufactured machine has a frequency of $\mathrm{LCM}(Q_s, 2n_{\mathrm{pp}})$ Hz per rotor revolution. For the machine in (7), it is calculated as $\mathrm{LCM}(Q_s, 2n_{\mathrm{pp}}) = \mathrm{LCM}(2, 2\times 1) = 2$ Hz, meaning the cogging torque profile (or the self inductance L_{m+1}) repeats twice as the PM rotor rotates 2π mechanical radians.

In a regular servo motor that has 18 stator slots and 4 pole pair PM rotor, this LCM is calculated as high as 72 Hz and the amplitude of the cogging torque is reduced as its frequency increases, so the cogging torque in a perfectly manufactured is negligible in practice.

The manufacturing of the machine in practice has tolerances on both stator iron and rotor iron.

- When only stator tolerance exists, the cogging torque has a component that has frequency of $2n_{\mathrm{pp}}, 4n_{\mathrm{pp}}, 6n_{\mathrm{pp}}, \dots$ per rotor revolution [8].
- When only rotor tolerance exists, the cogging torque has a component that has a frequency of $Q_s/n_{\mathrm{pp}}, 2Q_s/n_{\mathrm{pp}}, \dots$ per rotor revolution [8].
- When both stator and rotor tolerance exists, the cogging torque has a component that has a frequency of $0.5Q_s/n_{\mathrm{pp}}$ per rotor revolution [9].

Another possible cause of cogging torque is the radially or axially misplaced permanent magnets, and it will cause a cogging torque at a frequency of exactly stator slot number Q_s per rotor revolution.

1.15. Electrical Dynamics in Phase Quantities

The flux linkage expressions (50) can be extended using vector and matrix notations as simple as

$$\boldsymbol{\psi} = \boldsymbol{L}\boldsymbol{i}, \quad \text{with } \boldsymbol{L} = \begin{bmatrix} L_1 & L_{12} & \cdots & L_{1(m+1)} \\ L_{21} & L_2 & \cdots & L_{2(m+1)} \\ \vdots & \vdots & \ddots & \vdots \\ L_{(m+1)1} & L_{(m+1)2} & \cdots & L_{m+1} \end{bmatrix} \text{ and } \boldsymbol{i} = \begin{bmatrix} i_1 \\ i_2 \\ \vdots \\ i_{m+1} \end{bmatrix} \tag{69}$$

Substituting (69) into the following generalized version of (35), the dynamics of currents can be derived as:

$$\begin{aligned}\boldsymbol{u}-\boldsymbol{R}\boldsymbol{i}=\boldsymbol{e}=\frac{\mathrm{d}}{\mathrm{d}t}\boldsymbol{\psi}=\frac{\mathrm{d}}{\mathrm{d}t}\left(\boldsymbol{L}\boldsymbol{i}\right)=\left(\frac{\mathrm{d}}{\mathrm{d}t}\boldsymbol{L}\right)\boldsymbol{i}+\boldsymbol{L}\frac{\mathrm{d}}{\mathrm{d}t}\boldsymbol{i}\\ \Rightarrow \boldsymbol{L}\frac{\mathrm{d}}{\mathrm{d}t}\boldsymbol{i}=\boldsymbol{u}-\boldsymbol{R}\boldsymbol{i}-\frac{\mathrm{d}\boldsymbol{L}}{\mathrm{d}\left(n_{\mathrm{pp}}\Theta\right)}\frac{\mathrm{d}\left(n_{\mathrm{pp}}\Theta\right)}{\mathrm{d}t}\boldsymbol{i}\end{aligned} \tag{70}$$

where n_{pp} is short for "pole pair number" and it is a positive constant that generally counts how many times the motor back emf repeats during one full mechanical revolution. For a PM rotor machine, n_{pp} is the number of repeat of north-south pole pairs.

1.16. Brief Summary on Modeling in Phase Quantities

So far, we have derived the full model for electric machines, including the $(m+1)$-th order electrical dynamics (70), the 2nd order mechanical dynamics (19) and (20), and the electromechanical energy conversion principle (68) that bridges the gap between the electrical sub-system and the mechanical sub-system. The (2+m+1)-th order dynamics are summarized as follows

$$\begin{aligned}\frac{\mathrm{d}}{\mathrm{d}t}\Theta&=\Omega\\ J_s\frac{\mathrm{d}}{\mathrm{d}t}\Omega=T_{\mathrm{em}}-T_L&=\frac{1}{2}\boldsymbol{i}^{\mathrm{T}}\frac{\partial\boldsymbol{L}}{\partial\Theta}\boldsymbol{i}-T_L\\ \boldsymbol{L}\frac{\mathrm{d}}{\mathrm{d}t}\boldsymbol{i}&=\boldsymbol{u}-\boldsymbol{R}\boldsymbol{i}-\frac{\mathrm{d}\boldsymbol{L}}{\mathrm{d}\left(n_{\mathrm{pp}}\Theta\right)}\frac{\mathrm{d}\left(n_{\mathrm{pp}}\Theta\right)}{\mathrm{d}t}\boldsymbol{i}\end{aligned} \tag{71}$$

However, the modeling is not complete as the inductance function $\boldsymbol{L}(\Theta)$ has not been defined. In other words, the machine geometry and winding distribution are not defined. Great simplification can be made to the inductance matrix $\boldsymbol{L}$, if we put the armature circuits in a symmetric configuration, and use a uniform air gap, such that, for a three phase stator armature, $L_1, L_2, L_3, L_{12}, L_{23}, L_{31}, L_{m+1}$ are not dependent on rotor angle Θ:

$$\frac{\mathrm{d}\boldsymbol{L}}{\mathrm{d}\left(n_{\mathrm{pp}}\Theta\right)}=\frac{\mathrm{d}}{\mathrm{d}\left(n_{\mathrm{pp}}\Theta\right)}\begin{bmatrix}0&0&0&L_{1(m+1)}\\0&0&0&L_{2(m+1)}\\0&0&0&L_{3(m+1)}\\L_{1(m+1)}&L_{2(m+1)}&L_{3(m+1)}&0\end{bmatrix} \tag{72}$$

1.17. Review on Magnetic Flux Density and Magnetic Potential

The inductance reveals the circuit's ability to link magnetic flux. The magnetic flux is not an electric circuit variable, but a field variable, which is calculated as an surface integral over magnetic flux density $\vec{B}$ over the area that the coil encloses.

In most cases, we are interested in the magnetic field $\vec{B}(x,y,z)$ in a cross-section of a machine. Let z-axis be orthogonal to the cross-section. The distribution of the 2D vector field $\vec{B}(x,y,z)$ can be obtained as $\nabla\times A_z$ by solving a partial differential

equation (PDE) for z-axis magnetic potential A_z.[15] A numerical solution of such a PDE is often resorted to a finite element analysis software.

Note: to be consistent with the frames discussed in later chapters, the z-axis should be renamed to γ-axis.

1.18. Review on Lumped Parameter Model

As per Wikipedia, "the lumped-parameter model simplifies the description of the behaviour of spatially distributed physical systems, such as electrical circuits, into a topology consisting of discrete entities that approximate the behaviour of the distributed system under certain assumptions."

From a perspective of math, the lumped parameter model simplifies the partial differential equation (PDE) problem as an ordinary differential equation (ODE) problem for electric circuits. In other words, we do not solve for a vector field $\vec{E}(x, y, z)$ but use the Ohm's law to get current $I = U/R$.

The distribution of the magnetic field potential in the machine can be obtained by solving a PDE with certain boundary conditions, whereas for ideal machine, a lumped parameter model can be used to describe the magnetic field distribution, and based on this model, a magnetic circuit similar to electrical circuit can be drawn.

1.19. Review on Magnetic Circuit

In Section 1.5, we have naturally introduce the concept of magnetic energy by integrating electrical power $e_1 i_1$ over time, which implies that the energy consumed by inductance is converted into the magnetic field energy. Apparently, the magnetic field is distributed in the space. The *lumped parameter modeling* of the magnetic field leads to magnetic circuit.[16] In magnetic circuit, the current flows through inductance provides the source of voltage potential difference, known as magnetomotive force $\mathcal{F}$, the magnetic flux Φ serves as the role of current, and the magnetic induction B is analogue to current density. Iron core is often treated as the copper wire, and air gap is analogue to the resistance having a limited magnetic conductance Λ. The Ohm's law for magnetic circuit therefore follows as $\Phi = \mathcal{F}\Lambda$. It is worth mentioning that there are no dynamics for magnetic circuit. Refer to [10] for more information about magnetic circuit.

1.20. Review on Inductance Modeling in Magnetic Circuit

Recall the flux linkage expression for an electrical circuit [(38) and (39)], where we have derived that inductance as the partial derivative of flux linkage with respect to current.

---

[15] The PDE for scalar magnetic potential $A_z(x, y, z)$ is derived using its definition $\vec{B} = \vec{\nabla} \times A_z$:

$$\vec{\nabla} \times \vec{H} = \vec{\nabla} \times \left(\mu^{-1}\vec{B}\right) = \vec{\nabla} \times \left(\mu^{-1}\vec{\nabla} \times A_z\right) = \vec{J}$$

which, if we adopt the Coulomb gauge $\nabla \cdot A_z = 0$ and assume linear isotropic material, reduces to:

$$-\mu^{-1}\nabla^2 A_z = \vec{J}$$

where $\vec{\nabla} = \left(\frac{\partial}{\partial x}, \frac{\partial}{\partial y}, \frac{\partial}{\partial z}\right)$ is the nabla operator, and $\nabla^2 = \vec{\nabla} \cdot \vec{\nabla} = \Delta = \left(\frac{\partial^2}{\partial x^2} + \frac{\partial^2}{\partial y^2} + \frac{\partial^2}{\partial y^2}\right)$ is the Laplace operator. See also FEMM4.2 manual, available at: https://femm.info

[16] On the other hand, the lumped parameter modeling of the electrical field leads to electrical circuit.

In a magnetic circuit, we know the flux linkage is due to the magnetic flux (possibly produced by multiple sources) passing through the coils and current is the source of magnetomotive force $\mathcal{F}_1 = N_1 i_1,\ \mathcal{F}_2 = N_2 i_2$, so the flux linkage can be calculated as

$$\psi_1\left(i_1, i_2\right) = N_1(\Phi_{11} + \Phi_{12}) = N_1\left(\mathcal{F}_1\Lambda_{11} + \mathcal{F}_2\Lambda_{12}\right) = N_1\left(N_1 i_1\Lambda_{11} + N_2 i_2\Lambda_{12}\right) \quad (73)$$

where the Ohm's law for magnetic circuit has been applied. Since the inductance is the partial derivative with respect to source current, we have

$$\begin{aligned} L_1 = L_{11} &= \frac{\partial\psi_1}{\partial i_1} = N_1^2\Lambda_{11} \\ L_{12} &= \frac{\partial\psi_1}{\partial i_2} = N_1 N_2\Lambda_{12} \end{aligned} \quad (74)$$

Finally, the magnetic conductance Λ_g of an air gap is

$$\Lambda_g = \mu_0 S/g_e \quad (75)$$

with μ_0 the magnetic permeability, g_e the air gap length, and S the area that flux lines pass through. It is at our disposal whether to design $\Lambda_{11} = \Lambda_{12} = \Lambda_g$ or not.

The above result forms a simple and generic magnetic circuit consisting of source, conductance and flux. In this case, the magnetomotive force is modeled as a time variable: $\mathcal{F}(t)$ as current $i(t)$ depends on t.

1.21. Inductance Modeling in Electric Machine

However, when comes to modeling of the mutual inductance in a machine, the equation (74) cannot be directly used[17], because the coil (on the rotor) is potentially moving along the air gap. We are lacking a general analytic tool for describing the geometry of arbitrarily placed coils and their relative positions. We are going to introduce the concept of turn function and winding function before we can model inductance in electric machine [1] (see also the Appendix of my thesis [11]). In an actual machine, it turns out that the magnetomotive force $\mathcal{F}(t, \Theta) = N(\Theta)i(t)$ is a space variable along the air gap, as the "number of turns" $N(\Theta)$ is modeled as a Θ-dependent variable, known as winding function. On the other hand, the magnetic conductance Λ can be either dependent on rotor angle Θ or not, depending on the machine types. In this course, we are interested in machine types that prefer Λ being a constant[18].

Fig. 8 shows an ideal rotary machine, for which we are going to calculate the inductances among the coils. Stator inner radius is r_{si} and rotor outer radius is r_{or}.

---

[17] One example for calculating the mutual inductance when coil #1 and coil #$(m+1)$ are aligned is:

$$\begin{aligned} \Phi_{1(m+1)} &= F_{m+1}\Lambda = N_{m+1} i_{m+1}\Lambda \\ \Rightarrow L_{1(m+1)} &= N_1\frac{N_{m+1} i_{m+1}\Lambda}{i_{m+1}} = N_1 N_{m+1}\Lambda \end{aligned} \quad (76)$$

[18] TODO: add a section of essentials of flux modulation theory to show that one principle for designing motor is to see if the back emf exists.

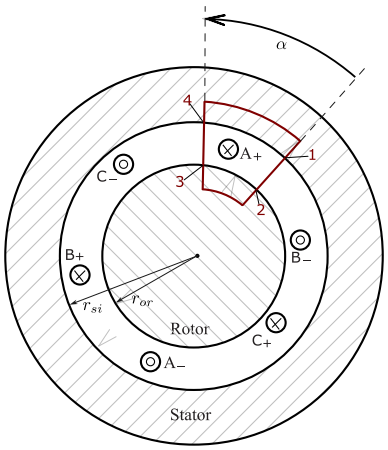

Figure 8. Cross section view of an ideal rotary machine with three place winding placed in the air gap. An enclosed path in passing through the air gap back and forth, on which the Ampère's circuital law will be applied. The angular location of path 3–4 with respect to the fixed path 1–2 is denoted by α.

1.21.1. Local Calculation of Flux

Our objective is to calculate the inductance using the large signal definition $L = \psi/i$ so we need to first calculate the flux linkage ψ and flux Φ. The Ohm's law for magnetic circuit is valid for an infinitesimal angular span $\mathrm{d}\alpha$ in the air gap, and for example, the winding A is producing a magnetic flux in the air gap passing through an area with a height of l_e and arc length of $r\mathrm{d}\phi$ that is located at α:

$$\mathrm{d}\Phi = \mathcal{F}_{\mathrm{A}}\mathrm{d}\Lambda = \mathcal{F}_{\mathrm{A}}(\alpha)\,\mu_0\frac{l_e r\mathrm{d}\alpha}{g_e} \tag{77}$$

where g_e is the air gap length, radius $r \in [r_{or}, r_{si}]$, and $\mathrm{d}\Lambda$ is the magnetic conductance of the infinitesimal area. From (77), to calculate flux, we need to model the magnetomotive force as a function of space variable α.

1.21.2. Turn Function

Consider a path passing through the air gap and back, denoted as 1–2–3–4–1 in Fig. 8. The side 1–2 is fixed and serves as a reference for the angular span between side 3–4 with respect to side 1–2, which is denoted as α. **It must be emphasized that α is in electrical radians throughout this course and it takes values from 0 degrees to $n_{\mathrm{pp}}360$ degrees per rotor revolution.**

An expression of magnetomotive force $\mathcal{F}(\alpha)$ at angular location α (i.e., at side 3–4) can be derived using the Ampère's circuital law:

$$\oint_{\partial S} H(\alpha)\,\mathrm{d}l = \iint_S J\mathrm{d}S \tag{78}$$

where the boundary ∂S of the surface is 1–2–3–4–1 and $H = B/\mu_0$ is the magnetic field intensity. Assuming the conductors are carrying the same current of i, we define

the turn function $n(\alpha)$ as follows:

$$\iint_S J\mathrm{d}S \triangleq n(\alpha)i = \mathcal{F}_{12} + \mathcal{F}_{23} + \mathcal{F}_{34} + \mathcal{F}_{41} = H(0)g_e + 0 - H(\alpha)g_e + 0 \tag{79}$$

Note path 2–3 and path 4–1 are in the iron, and we assume the magnetic potential drop in iron is zero, so $\mathcal{F}_{23} = \mathcal{F}_{41} = 0$. The turn function counts every time when side 3–4 moves across a conductor carrying positive current and is, according to the Ampère's circuital law, the net current enclosed by path 1–2–3–4–1.

We have assumed the magnetic field intensity H is only a variable of α so we have $\mathcal{F}_{12} = H(0)g_e$ that is unknown and $\mathcal{F}_{34} = -H(\alpha)g_e$ that is what we want for flux calculation as $\mathcal{F}_{\mathrm{A}}(\alpha)$ in (77).

According to the Gauss's law for magnetism, we can derive a constraint for $H(\alpha)$ as

$$\oiint_{\mathcal{S}'} B\mathrm{d}\mathcal{S}' = \mu_0 \int_0^{l_e}\int_0^{2\pi} rH(\alpha)\,\mathrm{d}\alpha\mathrm{d}z = 0 \tag{80}$$

$$\Rightarrow \int_0^{2\pi} H(\alpha)\,\mathrm{d}\alpha = 0 \tag{81}$$

$$\Rightarrow \int_0^{2\pi} F_{34}(\alpha)\,\mathrm{d}\alpha = 0 \tag{82}$$

where $\mathcal{S}'$ is a cylinder wall in the air gap covering the rotor with height of l_e. This result can be utilized for calculation of the constant $H(0)$. To see this, integrating both sides of (79) gives

$$\int_0^{2\pi} \mathcal{F}_{12}\mathrm{d}\alpha + \int_0^{2\pi} \mathcal{F}_{34}\mathrm{d}\alpha = \int_0^{2\pi} n(\alpha)\,i\mathrm{d}\alpha \tag{83}$$

$$\Rightarrow \mathcal{F}_{12} = H(0)g_e = i\left[\frac{1}{2\pi}\int_0^{2\pi} n(\alpha)\,\mathrm{d}\alpha\right] \tag{84}$$

which shows that $\mathcal{F}_{12}$ is the average value of the turn function $n(\alpha)$.

1.21.3. Winding Function

Substituting (84) into (79), it arrives at a definition for winding function:

$$-H(\alpha)g_e = \mathcal{F}_{34} = n(\alpha)i - \left[\frac{1}{2\pi}\int_0^{2\pi} n(\alpha)\,\mathrm{d}\alpha\right] i \triangleq N(\alpha)\,i \tag{85}$$

Winding function $N(\alpha) \triangleq n(\alpha) - \left[\frac{1}{2\pi}\int_0^{2\pi} n(\alpha)\,\mathrm{d}\alpha\right]$ is calculated as the difference between the turn function and its average, and its physical meaning is the magnetomotive force in the air gap generated by unit current.

Using winding function in replace of number of turns, we have a consistent expression for the magnetomotive force as $\mathcal{F}(t,\alpha) = N(\alpha)\,i(t)$, but keep in mind that the concept of winding function is based on the derivation of the magnetomotive force at location α.

In case of moving coils, we need to keep side 1–2 to be relatively stationary to the coils. The winding function is a property of the coils, and if the coils are moving along

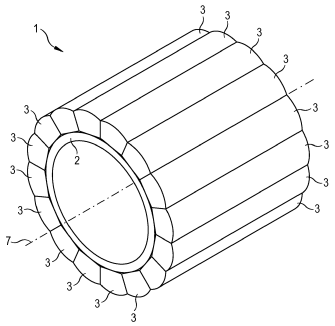

Figure 9. Bread loaf shaped magnets mounted on the surface of a piece of back iron ring.

the air gap, the reference for the winding function, i.e., side 1–2 (at which $\alpha = 0$), should also move, leading to a rotor angle dependent winding function:

$$\mathcal{F}\left(t, \alpha - n_{\mathrm{pp}}\Theta\right) = N\left(\alpha - n_{\mathrm{pp}}\Theta\right) i\left(t\right) \tag{86}$$

TODO: Examples of winding function.

TODO: Harmonic leakage inductance. Each electromotive force corresponds to some inductance. The fundamental flux is inducing a counter electromotive force. How about the harmonic flux? It turns out the harmonic flux caused by the fundamental current is inducing counter electromotive force of the same frequency as the fundamental current. In fact, the harmonic magnetomotive force must induce fundamental back electromotive force in an inductor, because the inductor is assumed as a linear system component. Harmonic leakage inductance can use the main magnetic circuit [1, Sec. 1.12].

1.22. Rotating Magnetic Field of Magnets

Consider a rotating iron core cylinder rotor with n_{pp} pole pairs of permanent magnets mounted on its cylinder surface, and the magnets have the shape of a bread loaf, as shown in Fig. 9.[19] As a result, the magnetomotive force of the magnets can be assumed to be sinusoidally distributed along a uniform air gap as:

$$\mathcal{F}_{m+1}\left(\alpha, \Theta\right) = N_{m+1}\left(\alpha, \Theta\right) i_{m+1} = N_{\mathrm{PM}} i_{m+1} \cos\left(\alpha - n_{\mathrm{pp}}\Theta\right) \tag{87}$$

Note the air gap location α is referred to rotor's electrical angle. For example, only when α is in advance to $n_{\mathrm{pp}}\Theta$ by 90 elec.deg, the magnetomotive force $\mathcal{F}_{m+1} \propto \cos(\frac{\pi}{2})$ becomes zero.

1.23. Mutual Inductance Calculation

The second use case of the concept of winding function is to calculate the mutual inductance in a machine. Recall the local calculation of flux (77), and the flux linkage

[19] Figure is adapted from an European patent entitled "Multipolar rotor with loaf-shaped permanent magnets" by Jens Schulze, which has been withdrawn.

of winding B due to excitation of winding A is

$$\psi_{BA} = \int_0^{2\pi} n_B(\alpha)\,\mathrm{d}\Phi = \frac{\mu_0 l_e r}{g_e}\int_0^{2\pi} \mathcal{F}_A(\alpha)\, n_B(\alpha)\,\mathrm{d}\alpha = \frac{\mu_0 l_e r}{g_e}\int_0^{2\pi} \mathcal{F}_A(\alpha)\, N_B(\alpha)\,\mathrm{d}\alpha \tag{88}$$

where note the relation $n_B(\alpha) = N_B(\alpha) + \left[\frac{1}{2\pi}\int_0^{2\pi} n_B(\alpha)\,\mathrm{d}\alpha\right]$ has been substituted. Note $\mathcal{F}_A = N_A i_A$ and the mutual inductance follows as

$$L_{BA} = \frac{\psi_{BA}}{i_A} = \frac{\mu_0 l_e r}{g_e}\int_0^{2\pi} N_A(\alpha)\, N_B(\alpha)\,\mathrm{d}\alpha \tag{89}$$

which implies that the mutual inductance of a linear magnetic system is not dependent on the excitation.

Let winding A be coil #(m+1), i.e., the magnet, let winding B be coil #1, #2, #3, and we have

$$\begin{cases} L_{1(m+1)}\Lambda^{-1} = N_{(1)}N_{\mathrm{PM}}\int_0^{2\pi}\cos(\alpha)\cos(\alpha - n_{\mathrm{pp}}\Theta)\,\mathrm{d}\alpha \\ L_{2(m+1)}\Lambda^{-1} = N_{(1)}N_{\mathrm{PM}}\int_0^{2\pi}\cos\left(\alpha-\frac{2}{3}\pi\right)\cos(\alpha - n_{\mathrm{pp}}\Theta)\,\mathrm{d}\alpha \\ L_{3(m+1)}\Lambda^{-1} = N_{(1)}N_{\mathrm{PM}}\int_0^{2\pi}\cos\left(\alpha-\frac{4}{3}\pi\right)\cos(\alpha - n_{\mathrm{pp}}\Theta)\,\mathrm{d}\alpha \end{cases}$$

$$\Rightarrow \begin{cases} L_{1(m+1)}\Lambda^{-1} = N_{(1)}N_{\mathrm{PM}}\int_0^{2\pi}\frac{\cos(n_{\mathrm{pp}}\Theta)+\cos(2\alpha-n_{\mathrm{pp}}\Theta)}{2}\mathrm{d}\alpha = N_{(1)}N_{\mathrm{PM}}\frac{2\pi\cos(n_{\mathrm{pp}}\Theta)}{2} \\ L_{2(m+1)}\Lambda^{-1} = N_{(1)}N_{\mathrm{PM}}\int_0^{2\pi}\frac{\cos\left(n_{\mathrm{pp}}\Theta-\frac{2}{3}\pi\right)+\cos\left(2\alpha-\frac{2}{3}\pi-n_{\mathrm{pp}}\Theta\right)}{2}\mathrm{d}\alpha = N_{(1)}N_{\mathrm{PM}}\frac{2\pi\cos\left(n_{\mathrm{pp}}\Theta-\frac{2}{3}\pi\right)}{2} \\ L_{3(m+1)}\Lambda^{-1} = N_{(1)}N_{\mathrm{PM}}\int_0^{2\pi}\frac{\cos\left(n_{\mathrm{pp}}\Theta-\frac{4}{3}\pi\right)+\cos\left(2\alpha-\frac{4}{3}\pi-n_{\mathrm{pp}}\Theta\right)}{2}\mathrm{d}\alpha = N_{(1)}N_{\mathrm{PM}}\frac{2\pi\cos\left(n_{\mathrm{pp}}\Theta-\frac{4}{3}\pi\right)}{2} \end{cases}$$

$$\Rightarrow \begin{cases} \psi_{1(m+1)} = L_{1(m+1)}i_{m+1} = \psi_{\mathrm{PM}}\cos(n_{\mathrm{pp}}\Theta) \\ \psi_{2(m+1)} = L_{2(m+1)}i_{m+1} = \psi_{\mathrm{PM}}\cos\left(n_{\mathrm{pp}}\Theta-\frac{2}{3}\pi\right) \\ \psi_{3(m+1)} = L_{3(m+1)}i_{m+1} = \psi_{\mathrm{PM}}\cos\left(n_{\mathrm{pp}}\Theta-\frac{4}{3}\pi\right) \end{cases} \tag{90}$$

where note $\psi_{\mathrm{PM}} = \Lambda N_{(1)}N_{\mathrm{PM}}\pi i_{m+1}$ has been substituted, but this expression is not very useful, as N_{PM} stays unknown. Alternatively, we should deem the amplitude of the permanent magnet flux linkage $\psi_{\mathrm{PM}} \triangleq i_{m+1}\times\max_{\Theta} L_{j(m+1)}$ as the peak of the mutual inductance times the field winding current.

In terms of calculation of reaction torque, the mutual flux linkage $\psi_{j(m+1)},\ j=1,2,3$ is useful, and we can already calculate the torque for a three phase PM motor.

1.24. Machines that Utilize Only Reaction Torque (Part 1)

We shall now look at two important examples of electric machines. In a rotary machine, we call the spinning cylinder the rotor, and the stationary part the stator. We may classify the machines based on their utilization of the torque: reaction torque, reluctance torque, or both.

1.24.1. Surface Mounted Permanent Magnet Synchronous Machine

The physical coils of circuit #1, circuit #2 and circuit #3 are equally spaced around the circumference of the cylinder rotor. In such machine configuration, the magnetic conductance Λ_g is invariant with respect to rotor angle Θ, and therefore self inductance

L_j and mutual inductance L_{jk} are independent on rotor angle Θ (i.e., their partial derivatives are zero).

From (90), the PM flux linking the coils of circuit #1, circuit #2 and circuit #3 are $\psi_{\mathrm{PM}}\cos(n_{\mathrm{pp}}\Theta)$, $\psi_{\mathrm{PM}}\cos\left[n_{\mathrm{pp}}\left(\Theta-\frac{2\pi}{3}\right)\right]$ and $\psi_{\mathrm{PM}}\cos\left[n_{\mathrm{pp}}\left(\Theta-\frac{4\pi}{3}\right)\right]$, respectively, where we have assumed that when $\Theta=0$, the magnet is aligned with the center of the coil of circuit #1.

The torque expression of this symmetrical $m=3$ phase machine can be derived as follows:

$$\begin{aligned}
T_{\mathrm{em}} &= 0+\sum_{j=1}^{m=3}\frac{\partial L_{j(m+1)}}{\partial\Theta}i_j i_{m+1}+0\\
&=\psi_{\mathrm{PM}}\left(\frac{\partial\cos\left(n_{\mathrm{pp}}\Theta\right)}{\partial\Theta}i_1+\frac{\partial\cos\left[n_{\mathrm{pp}}\left(\Theta-\frac{2\pi}{3}\right)\right]}{\partial\Theta}i_2+\frac{\partial\cos\left[n_{\mathrm{pp}}\left(\Theta-\frac{4\pi}{3}\right)\right]}{\partial\Theta}i_3\right)\\
&=n_{\mathrm{pp}}\psi_{\mathrm{PM}}\left(-\sin\left(n_{\mathrm{pp}}\Theta\right)i_1-\sin\left(n_{\mathrm{pp}}\Theta-n_{\mathrm{pp}}\frac{2\pi}{3}\right)i_2-\sin\left(n_{\mathrm{pp}}\Theta-n_{\mathrm{pp}}\frac{4\pi}{3}\right)i_3\right)\\
&\overset{\text{(A17)}}{=}-n_{\mathrm{pp}}\psi_{\mathrm{PM}}I_q\frac{3}{2}\sin\left(-\phi_0\right)=\frac{3}{2}n_{\mathrm{pp}}\psi_{\mathrm{PM}}I_q\sin\phi_0
\end{aligned}\tag{91}$$

in which the following symmetrical alternating current excitations with a synchronous angular speed of ω_{syn} have been imposed for obtaining a steady torque:

$$\omega_{\mathrm{syn}}=n_{\mathrm{pp}}\frac{\mathrm{d}\Theta}{\mathrm{d}t}=n_{\mathrm{pp}}\Omega\ [\text{elec.rad/s}]\tag{92}$$

$$\begin{aligned}
i_1&=I_q\cos\left(\omega_{\mathrm{syn}}t+\phi_0\right)=I_q\cos\left(n_{\mathrm{pp}}\Theta+\phi_0\right)\\
i_2&=I_q\cos\left(\omega_{\mathrm{syn}}t-\frac{2\pi}{3}+\phi_0\right)=I_q\cos\left(n_{\mathrm{pp}}\Theta-n_{\mathrm{pp}}\frac{2\pi}{3}+\phi_0\right)\\
i_3&=I_q\cos\left(\omega_{\mathrm{syn}}t-\frac{4\pi}{3}+\phi_0\right)=I_q\cos\left(n_{\mathrm{pp}}\Theta-n_{\mathrm{pp}}\frac{4\pi}{3}+\phi_0\right)
\end{aligned}\tag{93}$$

with I_q denoting the amplitude of the armature current, and ϕ_0 the initial phase angle of the alternating current. When $\phi_0=0.5\pi$, the torque is maximized.

Equation (92) states that the electrical angular speed of current equals the electrical rotor angular speed, which is called as the synchronization condition. A *synchronous machine* needs to excite proper currents to meet this condition to produce a steady torque, hence the name. According to (91), a simple linear control system can be implemented using I_q as the input to the mechanical system.

Remark: There is a unwanted magnetic field in the air gap generated by the three phase current excitation (93), known as *armature reaction* magnetic field. When there is a magnetic field, there is magnetic field energy W_Φ. This implies the fact that *reactive power* is drawn by a synchronous motor under load, thus its power factor is less than 1. We will come back to this topic later.

1.24.2. Permanent Magnet Induction Gear: A Concept

If we allow the coils on the stator to be freely movable along the air gap and short the coils such that $u_1=u_2=u_3=0$, then the rotating PM rotor will induce currents in the stator coils with proper phase angle to generate maximal torque that tries to stop the PM rotor from spinning. The reaction torque from PM to the stator coils will

"drag" them until the coils keep up with the rotating PM rotor.

One can show that the induced current in the stator coils has an angular frequency of $\omega_{\text{sl}} = n_{\text{pp}}(\Omega - \Omega_{\text{stator}})$. A machine with two rotors is mostly used for a bearing or gearbox. In our case, this machine is a PM gearbox based on the phenomenon of induction.

1.25. Rotating Magnetic Field of a Polyphase Winding

We have learned that current is the source of magnetic field, and now we are going to derive a pattern of current that can be useful to generate a steady torque in induction machine.

Based on the development in (B9), we know that a (stationary) polyphase winding is able to produce a rotating magnetomotive force as follows:

$$\mathcal{F}_{(k,v)}(\alpha, t) = \frac{m}{2} N_{(v)} I_{(k)} \sin\left(k\omega_{\text{syn}} t + \phi_{(k)} - v\alpha\right) \tag{94}$$

This is the first use case of the concept of winding function.

For a typical three phase winding, sinusoidal current is injected ($k = 1$) and therefore only the fundamental component of winding function ($v = 1$) serves as a "working" magnetomotive force in induction machine. It is worth additional explanation here about the word "working". In a synchronous machine, it is desired that a winding does not generate any magnetomotive force in the air gap, and in this case, the magnetomotive force is unwanted and therefore it is not considered a working magnetomotive force. However, in an induction machine, the main air gap field is produced by a three phase winding, and this field is interacting with the rotor currents to produce steady torque, and therefore, it is considered as a working magnetomotive force.

1.26. Machines that Utilize Only Reaction Torque (Part 2)

The induction machine is also known as asynchronous machine. For a synchronous machine, if we replace the PM field winding with a three-phase field winding, we are able to apply current at an asynchronous frequency (denoted as ω_{sl}) to that of the armature winding (denoted as ω_{syn}), hence the name.

1.26.1. Asynchronous Machine: a Concept

Let's now recap two important facts that we have developed so far.

(1) Recall the idea of using virtual field winding that carries a constant field current i_{m+1}, it implies that in terms of magnetic interaction with stator, permanent magnets can be replaced with other circuit(s) on the rotor. The magnetic field of the bread-loaf shaped magnets is sinusoidally distributed in electrical rotor angular angle θ.

(2) From the i–N–$\mathcal{F}$ (i.e., current–winding function–magnetomotive force) development, we know that stationary coils with alternating current can generate a rotating magnetic field that rotates at an electrical angular speed of $\frac{\mathrm{d}}{\mathrm{d}t}\theta = \mp\frac{k}{v}\omega_{\text{syn}}$ with current harmonic index k and winding function harmonic index v.

We therefore can infer that, in terms of magnetic interaction with stator winding, a poly-phase winding with symmetrical alternating current is equivalent to a rotating

field winding that carries constant current and we can use a poly-phase winding in replace of the rotor magnets. This seemingly obvious fact is indeed closely related to an important development for ac motor control, widely known as Park transformation. To see this, let's write down the magnetomotive force of a rotating poly-phase winding as follows

$$\mathcal{F}_{(1,1)}(\alpha, t) = \frac{m}{2} N_{(1)} I_{(1)} \sin\left(\phi_{(1)} - [\alpha - n_{\text{pp}}\Theta(t)] + \omega_{\text{sl}} t\right) \tag{95}$$

where the angular frequency of the alternating current is ω_{sl}, note $\Omega = \frac{\mathrm{d}}{\mathrm{d}t}\Theta$, and note that the angular location along the air gap is referred to the rotor angle of the cylinder, denoted as $\alpha - n_{\text{pp}}\Theta$. In order for (95) to replace of (87), we need to impose a constraint on the rotor current frequency ω_{sl}. When the current frequency is 0 Hz, i.e., $\omega_{\text{sl}} = 0$ rad/s, the rotor should spin at a synchronous speed of $\Omega = \frac{\omega_{\text{syn}}}{n_{\text{pp}}}$, which is the case of the virtual field winding replacing the magnets; when the current frequency is 1 Hz, the rotor should spin at an asynchronous speed of $\Omega = \frac{\omega_{\text{syn}} - 2\pi \times 1 \text{ Hz}}{n_{\text{pp}}}$; and we call this 1 Hz the slip frequency, and the corresponding slip angular speed is denoted by $\omega_{\text{sl}} = 2\pi \times 1$ rad/s. In other words, if we use multiple electric circuits on the rotor in replace of the magnets, we can relax the synchronization condition (92) by a slip angular speed of ω_{sl}. Here "slip" means the rotor is not synchronized with the frequency of the alternating current, hence such a machine is called as *asynchronous machine*.

The torque expression for an asynchronous machine is similar to that of a synchronous machine (91), since they both utilize the reaction torque. To avoid unnecessary derivation of the torque expression, let's rewrite the magnetomotive force in (95) following the form in (87) which is rewritten here for comparison:

$$\begin{aligned} &\mathcal{F}_{m+1}(\alpha, \Theta) = N_{m+1}(\alpha, \Theta)\, i_{m+1} = N_{\text{PM}} i_{m+1} \cos(\alpha - n_{\text{pp}}\Theta) \\ &\text{s.t. } \frac{\mathrm{d}}{\mathrm{d}t} n_{\text{pp}}\Theta = \omega_{\text{syn}} \end{aligned}$$

To replicate a field like this using a three-phase winding, let $\phi_{(1)} = 0.5\pi$, we have

$$\mathcal{F}_{(1,1)}(\alpha - n_{\text{pp}}\Theta, t) = \frac{m}{2} N_{(1)} I_{(1)} \cos(\alpha - n_{\text{pp}}\Theta(t) - \omega_{\text{sl}} t) \tag{96}$$

which states that the $m = 3$ phase current of amplitude $I_{(1)}$ is equivalent to a constant current of $\frac{m}{2} I_{(1)}$ that is rotating at a speed of $\frac{\mathrm{d}}{\mathrm{d}t}[n_{\text{pp}}\Theta(t) + \omega_{\text{sl}} t] = n_{\text{pp}}\Omega + \omega_{\text{sl}}$.

In order to satisfy the synchronization condition, we need to impose:

$$n_{\text{pp}}\Omega + \omega_{\text{sl}} = \omega_{\text{syn}} \tag{97}$$

which implies that the rotor speed of an asynchronous machine can be different from the synchronous angular speed $\omega_{\text{syn}}/n_{\text{pp}}$, hence it is called asynchronous machine.

Replace the three-phase field winding circuit with a $(m+1)$-th circuit, and let $i_{m+1} = \frac{m}{2} I_{(1)}$, and the torque of an asynchronous machine can be derived as [see (91)

for detailed derivation]

$$\begin{aligned} T_{\text{em}} &= 0 + \sum_{j=1}^{m} \frac{\partial L_{j(m+1)}}{\partial \Theta} i_j i_{m+1} + 0 \\ &= \frac{m}{2} I_q n_{\text{pp}} \psi_{\text{A}} \sin \phi_0 \end{aligned} \tag{98}$$

where ψ_{A} is amplitude of the active flux. We will introduce the concept of active flux later, and for now, it is safe to think it as the rotor flux linkage, i.e., the equivalent permanent magnetic flux linkage in an asynchronous machine.

1.26.2. Induction Machine

The conceptual asynchronous machine uses a rotating three-phase field winding on the rotor, and the armature winding is fixed to stator. Unlike synchronous machine or the conceptual asynchronous machine, the induction machine uses stationary three-phase field winding, and a rotating armature winding. Since only the relative movement between the stator and rotor matters, if we swap the stator and rotor for a conceptual asynchronous machine, we have an induction machine.

However, it is still difficult to excite alternating current into the rotating circuits, so it is preferred to utilize magnetic induction to excite the rotor circuits. This means we need to use the stator winding, for the first time so far in this course, to generate the main magnetic field in the air gap as follows

$$\mathcal{F}_{(1,1)}(\alpha, t) = \frac{m}{2} N_{(1)} I_{(1)} \cos(\alpha - \omega_{\text{syn}} t) \tag{99}$$

which means the stator three-phase field winding can be replaced with an $(m+1)$-th circuit.

Assume there is a polyphase winding on the rotor, and its Q_r-phase winding function is

$$\begin{cases} N_{r1}(\alpha - n_{\text{pp}}\Theta) = N_{r(1)} \cos(\alpha - n_{\text{pp}}\Theta) \\ N_{r2}(\alpha - n_{\text{pp}}\Theta) = N_{r(1)} \cos\left(\alpha - n_{\text{pp}}\Theta - \frac{2\pi}{Q_r}\right) \\ N_{r3}(\alpha - n_{\text{pp}}\Theta) = N_{r(1)} \cos\left(\alpha - n_{\text{pp}}\Theta - \frac{4\pi}{Q_r}\right) \\ \dots \\ N_{rQ_r}(\alpha - n_{\text{pp}}\Theta) = N_{r(1)} \cos\left(\alpha - n_{\text{pp}}\Theta - \frac{(Q_r-1)2\pi}{Q_r}\right) \end{cases} \tag{100}$$

Then, mutual flux linkage for the rotor circuits due to stator magnetic field can be derived as follows [cf. (90)]

$$\begin{cases} \psi_{1(m+1)} = \psi_{\text{A}} \cos(\omega_{\text{syn}} t - n_{\text{pp}}\Theta) \\ \psi_{2(m+1)} = \psi_{\text{A}} \cos\left(\omega_{\text{syn}} t - n_{\text{pp}}\Theta - \frac{2\pi}{Q_r}\right) \\ \psi_{3(m+1)} = \psi_{\text{A}} \cos\left(\omega_{\text{syn}} t - n_{\text{pp}}\Theta - \frac{4\pi}{Q_r}\right) \\ \dots \\ \psi_{Q_r(m+1)} = \psi_{\text{A}} \cos\left(\omega_{\text{syn}} t - n_{\text{pp}}\Theta - \frac{(Q_r-1)2\pi}{Q_r}\right) \end{cases} \tag{101}$$

According to Faraday's law of induction, the induced back electromotive forces on the rotor circuits are

$$\begin{cases} e_{1(m+1)} = \omega_{\text{syn}}\psi_{\text{A}}\cos\left(\left(\omega_{\text{syn}} - n_{\text{pp}}\Omega\right)t + \frac{1}{2}\pi\right) \\ e_{2(m+1)} = \omega_{\text{syn}}\psi_{\text{A}}\cos\left(\left(\omega_{\text{syn}} - n_{\text{pp}}\Omega\right)t - \frac{2\pi}{Q_r} + \frac{1}{2}\pi\right) \\ e_{3(m+1)} = \omega_{\text{syn}}\psi_{\text{A}}\cos\left(\left(\omega_{\text{syn}} - n_{\text{pp}}\Omega\right)t - \frac{4\pi}{Q_r} + \frac{1}{2}\pi\right) \\ \dots \\ e_{Q_r(m+1)} = \omega_{\text{syn}}\psi_{\text{A}}\cos\left(\left(\omega_{\text{syn}} - n_{\text{pp}}\Omega\right)t - \frac{(Q_r-1)2\pi}{Q_r} + \frac{1}{2}\pi\right) \end{cases} \tag{102}$$

Comparing (102) with the current excitations in (93), we learn that if we short all the circuits on the rotor, the electromotive forces in (102) are going to generate rotor currents at slip angular speed ω_{sl} that has the proper phase for maximizing the torque.

Note we did not assume $Q_r = 3$, and therefore, the rotor winding can be made of a symmetric winding that has higher phase number than stator winding. Since the rotor circuits are shorted, it is also feasible that we short all circuits using two end rings, making the rotor winding a squirrel cage, in which case the phase number m equals to the number of conductors. *This conclusion implies that the maximum of the phase number of a group of circuits depends on the number of conductors that having different phases.*

A squirrel cage rotor is a special case of the above rotor with the Q_r-phase symmetric winding, in which each phase of the winding is reduced to only one solid conductor.

1.27. Electrical Dynamics in Phase Quantities

TODO: remove npp in integral limit:

To derive the electrical dynamics in phase quantities, we need to compute the rest of the inductances. The mutual inductance is

$$\begin{aligned} L_{12} = \frac{\psi_{12}}{i_2} &= \frac{\mu_0 l_e r}{g_e}\int_0^{2\pi} N_1(\alpha) N_2(\alpha)\,\mathrm{d}\alpha \\ &= \frac{\mu_0 l_e r}{g_e} N_{(1)}^2 \int_0^{2\pi} \cos(\alpha)\cos\left(\alpha - \tfrac{2}{3}\pi\right)\mathrm{d}\alpha \\ &= \frac{\mu_0 l_e r}{g_e} N_{(1)}^2 \int_0^{2\pi} \frac{\cos\left(\alpha - \alpha + \frac{2}{3}\pi\right) + \cos\left(\alpha + \alpha - \frac{2}{3}\pi\right)}{2}\mathrm{d}\alpha \\ &= \frac{\mu_0 l_e r}{g_e} N_{(1)}^2 \int_0^{2\pi} \frac{\cos\left(\frac{2}{3}\pi\right) + \cos\left(2\alpha - \frac{2}{3}\pi\right)}{2}\mathrm{d}\alpha \\ &= \frac{\mu_0 l_e r}{g_e} N_{(1)}^2 \frac{\cos\left(\frac{2}{3}\pi\right) 2\pi}{2} \\ &= \frac{\mu_0 l_e r}{g_e} N_{(1)}^2 \frac{-\pi}{2} \end{aligned} \tag{103}$$

It is easy to show that $L_{12} = L_{13}$ and $L_1 = L_{11} = \frac{\mu_0 l_e r}{g_e} N_{(1)}^2 \pi$.

The electrical dynamics in phase quantities are (note $\boldsymbol{i} \in \mathbb{R}^4$ and $\boldsymbol{L} \in \mathbb{R}^{4\times 4}$)

$$\begin{aligned} \boldsymbol{u} &= R\boldsymbol{i} + \boldsymbol{L}\frac{\mathrm{d}}{\mathrm{d}t}\boldsymbol{i} + \boldsymbol{e}_{\Omega} \\ \boldsymbol{e}_{\Omega} &= \frac{\mathrm{d}\boldsymbol{L}}{\mathrm{d}\left(n_{\mathrm{pp}}\Theta\right)}\frac{\mathrm{d}\left(n_{\mathrm{pp}}\Theta\right)}{\mathrm{d}t}\boldsymbol{i} \end{aligned} \tag{104}$$

Let's only consider the case of a 3 phase permanent magnet motor and neglect the dynamics of the $m+1$ circuit, so we have

$$\begin{bmatrix} u_1 \\ u_2 \\ u_3 \end{bmatrix} = R\begin{bmatrix} 1 & 0 & 0 \\ 0 & 1 & 0 \\ 0 & 0 & 1 \end{bmatrix}\begin{bmatrix} i_1 \\ i_2 \\ i_3 \end{bmatrix} + \begin{bmatrix} L_1 & -\frac{1}{2}L_1 & -\frac{1}{2}L_1 \\ -\frac{1}{2}L_1 & L_1 & -\frac{1}{2}L_1 \\ -\frac{1}{2}L_1 & -\frac{1}{2}L_1 & L_1 \end{bmatrix}\frac{\mathrm{d}}{\mathrm{d}t}\begin{bmatrix} i_1 \\ i_2 \\ i_3 \end{bmatrix} + \begin{bmatrix} e_{\Omega 1} \\ e_{\Omega 2} \\ e_{\Omega 3} \end{bmatrix} \tag{105}$$

One basic idea to generate reaction torque using (106) is to excite current $i_j(t)$ that is in-phase to the rotary electromotive force $e_{\Omega j}$. To see this, apply a dot product with current vector to (105), the left-hand-side is electrical power input, the right-hand-side reads heating power, time derivative of stored magnetic energy in inductance, and electromagnetic power.

Further assume the stator winding is wye-connected such that neutral current is null: $i_1 + i_2 + i_3 = 0$, and therefore the mutual inductances can be eliminated to arrive at:

$$\begin{bmatrix} u_1 \\ u_2 \\ u_3 \end{bmatrix} = R\begin{bmatrix} i_1 \\ i_2 \\ i_3 \end{bmatrix} + \tfrac{3}{2}L_1\frac{\mathrm{d}}{\mathrm{d}t}\begin{bmatrix} i_1 \\ i_2 \\ i_3 \end{bmatrix} + \frac{\mathrm{d}\left(n_{\mathrm{pp}}\Theta\right)}{\mathrm{d}t}\left(\frac{\mathrm{d}}{\mathrm{d}\left(n_{\mathrm{pp}}\Theta\right)}\begin{bmatrix} L_{1(m+1)} \\ L_{2(m+1)} \\ L_{3(m+1)} \end{bmatrix}\right) i_{m+1} \tag{106}$$

1.27.1. Brushless DC Machine

A brushless dc machine can be controlled using the phase quantity model (106). The brushless dc machine only needs to know the rotor angle when the rotary electromotive force $e_{\Omega j}$ is positive for phase j. For a three phase implementation, this means one only needs three Hall sensors to measuring when one of the north-poles of the PM rotor is aligned with each phase of coils. Therefore, brushless dc motor is widely used in electric bicycles for its low cost in rotor angle sensor.

1.28. Correction for Inductance Calculation of Multiple Pole Pairs

When we are integrating over α for calculating inductance, the full integral limit for α should really be $[0, n_{\mathrm{pp}}2\pi]$, because α is in electrical radians. However, we have always been doing the integral from 0 to 2π, see e.g., (103). This is because there are distinct choices about how we want to connect the coils belonging to the same phase but under different PM pole pairs. If we decide to (for the same phase) connect coils under different PM pole pairs in series, the final inductance should be n_{pp} as large,

such that (103) should become:

$$\begin{aligned} L_{12} &= \frac{\psi_{12}}{i_2} = \frac{\mu_0 l_e r}{g_e} \int_0^{2\pi n_{\text{pp}}} N_1(\alpha) N_2(\alpha) \,\mathrm{d}\alpha \\ &= \frac{\mu_0 l_e r}{g_e} N_{(1)}^2 \int_0^{2\pi n_{\text{pp}}} \cos(\alpha) \cos\left(\alpha - \tfrac{2}{3}\pi\right) \mathrm{d}\alpha \\ &= \frac{\mu_0 l_e r}{g_e} N_{(1)}^2 \frac{-\pi n_{\text{pp}}}{2} \end{aligned} \tag{107}$$

If we decide to connect coils under different PM pole pairs in parallel, the final inductance should become much smaller.

For this course, the theoretical value of inductance does not matter that much, and we can always correct the calculated result of inductance by updating the value of winding function amplitude $N_{(1)}$. Therefore, it is safe for us to take integral in $[0, 2\pi]$ instead of $[0, n_{\text{pp}} 2\pi]$.

1.29. A Hindsight for Fast Deriving Torque Expression

Take $m = 1$ for example, we can write the electrical dynamics as follows

$$\begin{aligned} u_1 - R_1 i_1 = e_1 = \frac{\mathrm{d}\psi_1}{\mathrm{d}t} &= \frac{\frac{\partial \psi_1}{\partial i_1}\mathrm{d}i_1 + \frac{\partial \psi_1}{\partial i_2}\mathrm{d}i_2 + \frac{\partial \psi_1}{\partial \Theta}\mathrm{d}\Theta}{\mathrm{d}t} = L_{11}\frac{\mathrm{d}i_1}{\mathrm{d}t} + L_{12}\frac{\mathrm{d}i_2}{\mathrm{d}t} + \frac{\partial\left(L_{11} i_1 + L_{12} i_2\right)}{\partial \Theta}\frac{\mathrm{d}\Theta}{\mathrm{d}t} \\ u_2 - R_2 i_2 = e_2 = \frac{\mathrm{d}\psi_2}{\mathrm{d}t} &= \frac{\frac{\partial \psi_2}{\partial i_1}\mathrm{d}i_1 + \frac{\partial \psi_2}{\partial i_2}\mathrm{d}i_2 + \frac{\partial \psi_2}{\partial \Theta}\mathrm{d}\Theta}{\mathrm{d}t} = L_{21}\frac{\mathrm{d}i_1}{\mathrm{d}t} + L_{22}\frac{\mathrm{d}i_2}{\mathrm{d}t} + \frac{\partial\left(L_{21} i_1 + L_{22} i_2\right)}{\partial \Theta}\frac{\mathrm{d}\Theta}{\mathrm{d}t} \end{aligned} \tag{108}$$

where note the total/exact differential of the magnetic flux linkage, $\mathrm{d}\psi_j,\ j = 1, 2$ is dependent on there independent states: i_1, i_2, Θ, the partial derivatives of the linkage with respect to the currents are defined as self-inductance and mutual inductance, and the expression for flux linkage as function of only currents and inductance has been substituted. Further left multiplying the voltage equation with $\begin{bmatrix} i_1 & i_2 \end{bmatrix}$ yields the power balance equation:

$$\begin{aligned} &\begin{bmatrix} i_1 & i_2 \end{bmatrix} \begin{bmatrix} u_1 \\ u_2 \end{bmatrix} - \begin{bmatrix} i_1 & i_2 \end{bmatrix} \boldsymbol{R} \begin{bmatrix} i_1 \\ i_2 \end{bmatrix} = \begin{bmatrix} i_1 & i_2 \end{bmatrix} \begin{bmatrix} e_1 \\ e_2 \end{bmatrix} \\ &= \begin{bmatrix} i_1 & i_2 \end{bmatrix} \begin{bmatrix} L_{11} & L_{12} \\ L_{21} & L_2 \end{bmatrix} \begin{bmatrix} \frac{\mathrm{d}}{\mathrm{d}t} i_1 \\ \frac{\mathrm{d}}{\mathrm{d}t} i_2 \end{bmatrix} + \begin{bmatrix} i_1 & i_2 \end{bmatrix} \begin{bmatrix} \frac{\partial}{\partial \Theta} L_{11} & \frac{\partial}{\partial \Theta} L_{12} \\ \frac{\partial}{\partial \Theta} L_{21} & \frac{\partial}{\partial \Theta} L_2 \end{bmatrix} \frac{\mathrm{d}\Theta}{\mathrm{d}t} \begin{bmatrix} i_1 \\ i_2 \end{bmatrix} \end{aligned} \tag{109}$$

Assume a linear magnetic circuit such that magnetic energy and co-energy are equal to each other, and therefore, the stored magnetic energy in inductance is

$$W_\Phi = W'_\Phi = \frac{1}{2} \boldsymbol{i}^T \boldsymbol{L} \boldsymbol{i}$$

we can easily derive the change rate of W_Φ as[20]

$$\frac{\mathrm{d}}{\mathrm{d}t} W_\Phi = P_\Phi = \boldsymbol{i}^T \boldsymbol{L} \frac{\mathrm{d}}{\mathrm{d}t} \boldsymbol{i} + \frac{1}{2} \boldsymbol{i}^T \frac{\partial \boldsymbol{L}}{\partial \Theta} \frac{\partial \Theta}{\partial t} \boldsymbol{i} \tag{110}$$

[20]Note by assuming the linear magnetic circuit, the partial derivative with respect to Θ should be replaced with total derivative.

On the other hand, using the energy method, we know the power balance equation that takes mechanical dynamics into consideration can be written as

$$\begin{aligned} & P_{\text{elec,in}} - P_{\text{Cu}} = P_{\Phi} + P_{\text{em}} \\ \Rightarrow\ & \boldsymbol{i}^T\boldsymbol{u} - \boldsymbol{i}^T\boldsymbol{R}\boldsymbol{i} = \boldsymbol{i}^T\boldsymbol{e} = \left(\boldsymbol{i}^T\boldsymbol{L}\frac{\mathrm{d}}{\mathrm{d}t}\boldsymbol{i} + \frac{1}{2}\boldsymbol{i}^T\frac{\partial \boldsymbol{L}}{\partial \Theta}\frac{\partial \Theta}{\partial t}\boldsymbol{i}\right) + \Omega T_{\text{em}} \end{aligned} \tag{111}$$

where the electromagnetic torque T_{em} exerted to the rotor cylinder is what we desire to know. Compare (109) and (111), we know the electromagnetic torque should be:

$$T_{\text{em}} = \frac{1}{2}\begin{bmatrix} i_1 & i_2 \end{bmatrix}\begin{bmatrix} \frac{\partial}{\partial \Theta}L_{11} & \frac{\partial}{\partial \Theta}L_{12} \\ \frac{\partial}{\partial \Theta}L_{21} & \frac{\partial}{\partial \Theta}L_2 \end{bmatrix}\begin{bmatrix} i_1 \\ i_2 \end{bmatrix} = \frac{1}{2}\boldsymbol{i}^T\frac{\partial \boldsymbol{L}}{\partial \Theta}\boldsymbol{i}$$

with $\boldsymbol{i} \in \mathbb{R}^{m+1}$ and $\boldsymbol{L} \in \mathbb{R}^{(m+1)\times(m+1)}$.

2. Chapter 2: AC Machine Theory

The mathematic model in phase quantities derived in last chapter are theoretically enough for describing the dynamics of electric machines, but are unnecessarily complicated for engineering. In this chapter, we are going to further model electric machines for engineering purposes.

2.1. Motivation

The rotating magnetomotive force in (99) created by a stationary polyphase winding:

$$\mathcal{F}_{(1,1)}(\alpha, t) = \frac{m}{2} N_{(1)} I_{(1)} \cos(\alpha - \omega_{\text{syn}} t)$$

can be viewed as a result of a virtual coil that has number of turns of $N_{(1)}$ and carries a dc current of $\frac{m}{2} I_{(1)}$, and the virtual coil is rotating along the air gap at an electrical angular speed of $\frac{\mathrm{d}\alpha}{\mathrm{d}t} = \omega_{\text{syn}}$. In other words, the mechanical speed of the equivalent virtual coil is $n_{\text{pp}}^{-1} \omega_{\text{syn}}$.

Note the same rotating magnetic field can be generated when m is taking different values, which implies that we are able to model the electric machine with less than m state variables, e.g., down to 1. However, on the other hand, a $m = 3$ phase winding can do more than just creating one rotating magnetic field for magnetizing the air gap, and in fact, in an induction machine, the stator three-phase field winding is also able to also generate a magnetic field to cancel out the armature reaction field created by the rotor circuits. To see this, recall the desired three phase current for steady torque from last chapter (93):

$$\begin{aligned}
i_1 &= I_{(1)} \cos(\omega_{\text{syn}} t + \phi_0) = I_{(1)} [\cos(\omega_{\text{syn}} t) \cos\phi_0 - \sin(\omega_{\text{syn}} t) \sin\phi_0] \\
i_2 &= I_{(1)} \cos\left(\omega_{\text{syn}} t - \tfrac{2\pi}{3} + \phi_0\right) = I_{(1)} \left[\cos\left(\omega_{\text{syn}} t - \tfrac{2\pi}{3}\right) \cos\phi_0 - \sin\left(\omega_{\text{syn}} t - \tfrac{2\pi}{3}\right) \sin\phi_0\right] \\
i_3 &= I_{(1)} \cos\left(\omega_{\text{syn}} t - \tfrac{4\pi}{3} + \phi_0\right) = I_{(1)} \left[\cos\left(\omega_{\text{syn}} t - \tfrac{4\pi}{3}\right) \cos\phi_0 - \sin\left(\omega_{\text{syn}} t - \tfrac{4\pi}{3}\right) \sin\phi_0\right]
\end{aligned} \tag{112}$$

in which we have decomposed the sinusoidal current into two synchronous parts with $\frac{1}{2}\pi$ phase difference, one is responsible for magnetizing the air gap and one is for canceling armature reaction field.

2.2. The DQ Plane

To reveal both the redundancy and capability of a polyphase winding, we need to learn about the degree of freedoms of a symmetric electric system first. Consider a three phase current with phase angle $\phi(t)$

$$\begin{aligned}
i_1 &= I_{(1)} \cos(\phi) \\
i_2 &= I_{(1)} \cos\left(\phi - \tfrac{2\pi}{3}\right) \\
i_3 &= I_{(1)} \cos\left(\phi - \tfrac{4\pi}{3}\right)
\end{aligned} \tag{113}$$

It is a well known trigonometry identity that $i_1 + i_2 + i_3 = 0$. This is also a constraint when the three phase winding uses Wye connection with a neutral point.

The vector $\boldsymbol{i}_{abc} = (i_1, i_2, i_3) = i_1\vec{a} + i_2\vec{b} + i_3\vec{c}$ describes a point moving in the Cartesian coordinate system with its standard basis denoted by $\{\vec{a}, \vec{b}, \vec{c}\}$, and a direct corollary is that the point stays within the plane defined by equation $i_1 + i_2 + i_3 = 0$. We shall now look for an alternative basis related to this plane, i.e., three unit vectors that are perpendicular to each other, and two of the three are within the plane. We can call it the DQ plane.

2.3. Park Transformation

First, let's find a normal vector to the plane. Apparently, $(1,1,1) = \vec{a} + \vec{b} + \vec{c}$ is a normal vector of the plane because it is orthogonal to every vector in the plane (i.e., the dot product is null):

$$\left(\vec{a} + \vec{b} + \vec{c}\right) \cdot \left(i_1\vec{a} + i_2\vec{b} + i_3\vec{c}\right) = (1,1,1) \cdot (i_1, i_2, i_3) = 0$$

and the resulting unit normal vector is

$$\vec{n} = \frac{\vec{a} + \vec{b} + \vec{c}}{\sqrt{1^2 + 1^2 + 1^2}} = \frac{\vec{a} + \vec{b} + \vec{c}}{\sqrt{3}} = \left(\frac{1}{\sqrt{3}}, \frac{1}{\sqrt{3}}, \frac{1}{\sqrt{3}}\right) \tag{114}$$

The analytic geometry meaning of this coefficient $\sqrt{3}^{-1}$ is known as direction cosine. That is, the direction cosine of the vector $\vec{a}$ to the normal vector is

$$\frac{(1,0,0) \cdot (1,1,1)}{|(1,0,0)| \cdot |(1,1,1)|} = \frac{1}{\sqrt{3}} = \cos\left\langle \vec{a}, \vec{a} + \vec{b} + \vec{c} \right\rangle \approx \cos\left(54.7^\circ\right) \approx 0.577 \tag{115}$$

In addition, it can be shown that the plane $i_1 + i_2 + i_3 = 0$ passes through the origin, because the projection of the vector $(0,0,0)$ to the normal vector of the plane has a length of zero.

Second, it can be shown that the distance from the point to the origin is a constant

$$|\boldsymbol{i}_{abc}| = \sqrt{i_1^2 + i_2^2 + i_3^2} = I_{(1)}\sqrt{\cos^2(\phi) + \cos^2\left(\phi - \tfrac{2}{3}\pi\right) + \cos^2\left(\phi - \tfrac{4}{3}\pi\right)} = I_{(1)}\sqrt{\tfrac{3}{2}} \tag{116}$$

meaning the point $\boldsymbol{i}_{abc}$ is in a circular trajectory about the origin, and therefore, we can define a unit radial vector as

$$\vec{r} = \frac{\boldsymbol{i}_{abc}}{|\boldsymbol{i}_{abc}|} = \frac{i_1\vec{a} + i_2\vec{b} + i_3\vec{c}}{\sqrt{i_1^2 + i_2^2 + i_3^2}} \triangleq \vec{d} = \left(\frac{I_{(1)}\cos(\phi)}{I_{(1)}\sqrt{\frac{3}{2}}}, \frac{I_{(1)}\cos\left(\phi - \frac{2}{3}\pi\right)}{I_{(1)}\sqrt{\frac{3}{2}}}, \frac{I_{(1)}\cos\left(\phi - \frac{4}{3}\pi\right)}{I_{(1)}\sqrt{\frac{3}{2}}}\right) \tag{117}$$

note in this course we define the axis that is through origin and is parallel to the radial vector as the direct-axis or d-axis.

The third vector, the quadrature vector $\vec{q}$, that forms a new basis must satisfy the following cross product:

$$\vec{q} = \vec{n} \times \vec{d} \tag{118}$$

It turns out that the speed of the point $\frac{\mathrm{d}}{\mathrm{d}t}\boldsymbol{i}_{abc}$ is a proper candidate:

$$\vec{q} = \frac{\frac{\mathrm{d}}{\mathrm{d}t}\boldsymbol{i}_{abc}}{\left|\frac{\mathrm{d}}{\mathrm{d}t}\boldsymbol{i}_{abc}\right|} = \frac{\frac{\mathrm{d}}{\mathrm{d}t}i_1\vec{a} + \frac{\mathrm{d}}{\mathrm{d}t}i_2\vec{b} + \frac{\mathrm{d}}{\mathrm{d}t}i_3\vec{c}}{\omega_{\mathrm{syn}}I_q\sqrt{\frac{3}{2}}} = \frac{\omega_{\mathrm{syn}}I_q}{\omega_{\mathrm{syn}}I_q\sqrt{\frac{3}{2}}}\left(-\sin\left(\phi\right), -\sin\left(\phi - \tfrac{2}{3}\pi\right), -\sin\left(\phi - \tfrac{4}{3}\pi\right)\right) \tag{119}$$

A transformation matrix thus results (note a coordinate is a column vector)

$$\begin{bmatrix} \vec{d}^{\,T} \\ \vec{q}^{\,T} \\ \vec{n}^{\,T} \end{bmatrix} = \sqrt{\frac{2}{3}}\begin{bmatrix} \cos\left(\omega_{\mathrm{syn}}t\right) & \cos\left(\omega_{\mathrm{syn}}t - \frac{2}{3}\pi\right) & \cos\left(\omega_{\mathrm{syn}}t - \frac{4}{3}\pi\right) \\ -\sin\left(\omega_{\mathrm{syn}}t\right) & -\sin\left(\omega_{\mathrm{syn}}t - \frac{2}{3}\pi\right) & -\sin\left(\omega_{\mathrm{syn}}t - \frac{4}{3}\pi\right) \\ \sqrt{\frac{1}{3}}/\sqrt{\frac{2}{3}} & \sqrt{\frac{1}{2}} & \sqrt{\frac{1}{2}} \end{bmatrix} \triangleq \boldsymbol{T}\left(\omega_{\mathrm{syn}}t\right) \tag{120}$$

which is known as power invariant Park transformation matrix.[21] Left multiplying a vector by the matrix means to project the vector to each of the basis vectors.

Substituting $\phi = \omega_{\mathrm{syn}}t + \phi_0$, the current in phase quantities $\boldsymbol{i}_{abc}$ can now be represented as a constant vector in the new coordinates $\boldsymbol{i}_{dqn}$ as

$$\boldsymbol{i}_{dqn} = \begin{bmatrix} i_d \\ i_q \\ i_n \end{bmatrix} = \boldsymbol{T}\left(\omega_{\mathrm{syn}}t\right)\boldsymbol{i}_{abc} = \sqrt{\frac{2}{3}}\begin{bmatrix} \frac{3}{2}I_{(1)}\cos\phi_0 \\ \frac{3}{2}I_{(1)}\sin\phi_0 \\ 0 \end{bmatrix} \tag{121}$$

The Park transformation has the following properties:

$$\begin{cases} \boldsymbol{T}\left(\theta_d\right)^{-1} = \boldsymbol{T}(\theta_d)^T \\ \boldsymbol{T}\left(\theta_d\right)\frac{\mathrm{d}\boldsymbol{T}(\theta_d)^{-1}}{\mathrm{d}t} = \begin{bmatrix} 0 & -\frac{\mathrm{d}}{\mathrm{d}t}\theta_d & 0 \\ \frac{\mathrm{d}}{\mathrm{d}t}\theta_d & 0 & 0 \\ 0 & 0 & 0 \end{bmatrix} \\ \frac{\mathrm{d}\boldsymbol{T}(\theta_d)}{\mathrm{d}t}\boldsymbol{T}\left(\theta_d\right)^{-1} = \begin{bmatrix} 0 & \frac{\mathrm{d}}{\mathrm{d}t}\theta_d & 0 \\ -\frac{\mathrm{d}}{\mathrm{d}t}\theta_d & 0 & 0 \\ 0 & 0 & 0 \end{bmatrix} \end{cases} \tag{122}$$

where note the angle used in Park transformation (denoted as θ_d) does not need to equal to the phase angle of the currents, and $\boldsymbol{T}(0)$ is known as the Clarke transformation[22] and the resulting dqn-frame is also called as the $\alpha\beta\gamma$-frame:

$$\boldsymbol{T}\left(0\right) = \sqrt{\frac{2}{3}}\begin{bmatrix} 1 & -\frac{1}{2} & -\frac{1}{2} \\ 0 & \frac{\sqrt{3}}{2} & -\frac{\sqrt{3}}{2} \\ \frac{1}{\sqrt{2}} & \frac{1}{\sqrt{2}} & \frac{1}{\sqrt{2}} \end{bmatrix} \tag{123}$$

Applying Clarke transformation to each of the original basis vectors $\vec{a}, \vec{b}, \vec{c}$ results in

[21] R.H. Park, "Two-Reaction Theory of Synchronous Machines, Generalized Method of Analysis - Part I," Trans. of the AIEE, 1929, pp. 716–730.

[22] W. C. Duesterhoeft, Max W. Schulz, Edith Clarke. "Determination of Instantaneous Currents and Voltages by Means of Alpha, Beta, and Zero Components". July 1951. Transactions of the American Institute of Electrical Engineers. 70 (2): 1248–1255. doi:10.1109/T-AIEE.1951.5060554.

three new points

$$\boldsymbol{T}(0)\,\vec{a}=\boldsymbol{T}(0)\begin{bmatrix}1\\0\\0\end{bmatrix}=\begin{bmatrix}\sqrt{\frac{2}{3}}\\0\\\frac{1}{\sqrt{3}}\end{bmatrix},\boldsymbol{T}(0)\,\vec{b}=\begin{bmatrix}-\sqrt{\frac{1}{6}}\\\frac{1}{\sqrt{2}}\\\frac{1}{\sqrt{3}}\end{bmatrix},\boldsymbol{T}(0)\,\vec{c}=\begin{bmatrix}-\sqrt{\frac{1}{6}}\\-\frac{1}{\sqrt{2}}\\\frac{1}{\sqrt{3}}\end{bmatrix} \tag{124}$$

If we project the three points onto the dq-plane, it can be shown that the angles among the three projected phase-axes are 120 degrees. If you draw the three axes on the DQ plane, you will learn that the projected phase axes can be exactly aligned with the actual coils placed along the air gap. If we draw DQ plane on top of the motor geometry (i.e., the coils and the magnets), we are able to visualize space variable like magnetomotive force $\mathcal{F}_{(1,1)}(\alpha,t)$ and time variable $\boldsymbol{i}_{dqn}$ in the same plot.

2.4. Application of Park Transformation in Inductance Calculation

The Park transformation can be applied to other electric circuit quantities, including flux linkage and voltage. Recall the flux linkage is calculated as $\boldsymbol{\psi}_{abc}=\boldsymbol{L}_{abc}\boldsymbol{i}_{abc}$, and we have

$$\begin{aligned}\boldsymbol{T}\boldsymbol{\psi}_{abc}&=\boldsymbol{T}\boldsymbol{L}_{abc}\left[\boldsymbol{T}^{-1}\boldsymbol{T}\right]\boldsymbol{i}_{abc}\\\Rightarrow\boldsymbol{T}\boldsymbol{\psi}_{dqn}&=\boldsymbol{T}\boldsymbol{L}_{abc}\boldsymbol{T}^{-1}\boldsymbol{i}_{dqn}\end{aligned} \tag{125}$$

Recall the mutual inductance calculation in (89), we have

$$\begin{aligned}\boldsymbol{L}_{abc}&=\frac{\mu_0 l_e r}{g_e}\int_0^{2\pi}\begin{bmatrix}N_1N_1&N_1N_2&N_1N_3\\N_1N_2&N_2N_2&N_2N_3\\N_1N_3&N_2N_3&N_3N_3\end{bmatrix}\mathrm{d}\alpha\\&=\frac{\mu_0 l_e r}{g_e}\int_0^{2\pi}\begin{bmatrix}N_1&N_1&N_1\\N_2&N_2&N_2\\N_3&N_3&N_3\end{bmatrix}\begin{bmatrix}N_1&0&0\\0&N_2&0\\0&0&N_3\end{bmatrix}\mathrm{d}\alpha\\&=\frac{\mu_0 l_e r}{g_e}\int_0^{2\pi}\begin{bmatrix}N_1\\N_2\\N_3\end{bmatrix}\begin{bmatrix}1&1&1\end{bmatrix}\begin{bmatrix}N_1&0&0\\0&N_2&0\\0&0&N_3\end{bmatrix}\mathrm{d}\alpha\\&=\frac{\mu_0 l_e r}{g_e}\int_0^{2\pi}\begin{bmatrix}N_1\\N_2\\N_3\end{bmatrix}\begin{bmatrix}N_1&N_2&N_3\end{bmatrix}\mathrm{d}\alpha\end{aligned} \tag{126}$$

which leads to the following derivation

$$\begin{aligned}\Rightarrow\boldsymbol{T}\boldsymbol{L}_{abc}\boldsymbol{T}^{-1}&=\frac{\mu_0 l_e r}{g_e}\int_0^{2\pi}\boldsymbol{T}\begin{bmatrix}N_1\\N_2\\N_3\end{bmatrix}\begin{bmatrix}N_1&N_2&N_3\end{bmatrix}\boldsymbol{T}^T\mathrm{d}\alpha\\\Rightarrow\boldsymbol{L}_{dqn}\triangleq\boldsymbol{T}\boldsymbol{L}_{abc}\boldsymbol{T}^{-1}&=\frac{\mu_0 l_e r}{g_e}\int_0^{2\pi}\begin{bmatrix}N_d\\N_q\\N_n\end{bmatrix}\begin{bmatrix}N_d&N_q&N_n\end{bmatrix}\mathrm{d}\alpha\end{aligned} \tag{127}$$

where we have derived the *dqn*-frame winding function as follows

$$\begin{aligned}\begin{bmatrix} N_d \\ N_q \\ N_n \end{bmatrix} &\triangleq \boldsymbol{T}(\theta_d) \begin{bmatrix} N_1(\alpha) \\ N_2(\alpha) \\ N_3(\alpha) \end{bmatrix} \\ &= \sqrt{\frac{2}{3}} \begin{bmatrix} \cos\theta_d & \cos\left(\theta_d - \frac{2}{3}\pi\right) & \cos\left(\theta_d - \frac{4}{3}\pi\right) \\ -\sin\theta_d & -\sin\left(\theta_d - \frac{2}{3}\pi\right) & -\sin\left(\theta_d - \frac{4}{3}\pi\right) \\ \sqrt{\frac{1}{2}} & \sqrt{\frac{1}{2}} & \sqrt{\frac{1}{2}} \end{bmatrix} \begin{bmatrix} N_{(1)}\cos(\alpha) \\ N_{(1)}\cos\left(\alpha - \frac{2}{3}\pi\right) \\ N_{(1)}\cos\left(\alpha - \frac{4}{3}\pi\right) \end{bmatrix} \\ &= \sqrt{\frac{3}{2}} N_{(1)} \begin{bmatrix} \cos(\theta_d - \alpha) \\ -\sin(\theta_d - \alpha) \\ 0 \end{bmatrix}\end{aligned} \tag{128}$$

Note the winding function $N_j(\alpha)$ is a function of angular location α, while the *dqn*-frame version is further dependent on *d*-axis angle θ_d.

In conclusion, in terms of magnetic behavior, a symmetrical three phase winding with currents i_1, i_2, i_3 and winding function N_1, N_2, N_3 can be replaced with currents i_d, i_q, i_n with winding function N_d, N_q, N_n. The distribution of winding function N_d and N_q over angular location α is referred to *d*-axis angle θ_d. in other words, there are two virtual coils corresponding to N_d and N_q being fixed to the *d*-axis and *q*-axis, respectively.

It can be shown that the mutual inductance between the *d*-axis coil and *q*-axis coil is zero:

$$L_{dq} = \frac{\mu_0 l_e r}{g_e} \int_0^{2\pi} N_d N_q \mathrm{d}\alpha = 0 \tag{129}$$

The *d*-axis self-inductance and *q*-axis self-inductance are now in order:

$$\begin{aligned}\begin{bmatrix} L_{dd} \\ L_{qq} \end{bmatrix} &= \frac{\mu_0 l_e r}{g_e} \int_0^{2\pi} \frac{3}{2} N_{(1)}^2 \begin{bmatrix} \cos^2(\theta_d - \alpha) \\ \sin^2(\theta_d - \alpha) \end{bmatrix} \mathrm{d}\alpha \\ &= \frac{\mu_0 l_e r}{g_e} \int_0^{2\pi} \frac{3}{2} N_{(1)}^2 \frac{1}{2} \begin{bmatrix} 1 + \cos(2\theta_d - 2\alpha) \\ 1 - \cos(2\theta_d - 2\alpha) \end{bmatrix} \mathrm{d}\alpha = \frac{\mu_0 l_e r}{g_e} \frac{3}{2} N_{(1)}^2 \frac{1}{2} 2\pi \begin{bmatrix} 1 \\ 1 \end{bmatrix}\end{aligned} \tag{130}$$

2.5. Generalization to Multi-phase Winding

If the *abc*-axes are projected to the *dq*-plane, the angle among the three axes are $2\pi/3$.

For a symmetrical electrical system with more than $m = 3$ phases, e.g., the rotor circuits of an induction machine at standstill, the Park transformation can be extended.[23]

The motivation stays the same, and the derivation of the steady torque in (91) can be extended to require a multi-phase currents of $i_j = I_q \cos\left(\omega_{\text{syn}} t - (j-1)\frac{2\pi}{m}\right), j =$

[23] Jin Huang, "Transformation theory for p-pair pole n phase symmetric system", Transactions of China Electrotechnical Society, 1995(1), pp.53-57.

$1, 2, \ldots, m$, and the corresponding Park transformation to the dq-plane is

$$\boldsymbol{T}_m = \sqrt{\frac{2}{m}} \begin{bmatrix} \cos(\theta_d) & \cos\left(\theta_d - \frac{2\pi}{m}\right) & \cos\left(\theta_d - \frac{4\pi}{m}\right) & \ldots & \cos\left(\theta_d - \frac{(m-1)2\pi}{m}\right) \\ -\sin(\theta_d) & -\sin\left(\theta_d - \frac{2\pi}{m}\right) & -\sin\left(\theta_d - \frac{4\pi}{m}\right) & \ldots & -\sin\left(\theta_d - \frac{(m-1)2\pi}{m}\right) \end{bmatrix} \tag{131}$$

If we do a similar calculation as in (124) for the m-phase system, we will learn that the adjacent phase axes in the dq-plane has a angle of $360^\circ/m$. Recalling the conclusion from last sub-section, the extended Park transformation in (131) implies that a multi-phase winding can be replaced with a pair of coils in d-axis and q-axis, respectively. A corollary is that the squirrel cage of an induction motor at standstill can be modeled as a d-axis coil and q-axis coil.

When the rotor winding is rotating, it can be modeled through a change of reference for its winding functions as follows:

$$\begin{bmatrix} N_{r(1)} \cos(\alpha - n_{\text{pp}}\Theta) \\ N_{r(1)} \cos\left(\alpha - n_{\text{pp}}\Theta - \frac{1}{m}2\pi\right) \\ N_{r(1)} \cos\left(\alpha - n_{\text{pp}}\Theta - \frac{2}{m}2\pi\right) \\ \ldots \\ N_{r(1)} \cos\left(\alpha - n_{\text{pp}}\Theta - \frac{m-1}{m}2\pi\right) \end{bmatrix} \tag{132}$$

This means the winding functions are already rotating forward in the air gap at a speed of $\frac{\mathrm{d}}{\mathrm{d}t} n_{\text{pp}}\Theta$. Only fundamental component is considered here because we are only interested in the magnetomotive force that contributes to attain a steady reaction torque.

Our objective is to transform all circuits into dq-plane as virtual coils. Therefore, applying $\boldsymbol{T}_m(\theta_d - n_{\text{pp}}\Theta)$ from (131) to the winding function vector in (132) gives the winding function of the rotor dq virtual circuits:

$$\begin{bmatrix} N_{dr} \\ N_{qr} \end{bmatrix} = \sqrt{\frac{m}{2}} N_{r(1)} \begin{bmatrix} \cos(\theta_d - n_{\text{pp}}\Theta - \alpha + n_{\text{pp}}\Theta) \\ -\sin(\theta_d - n_{\text{pp}}\Theta - \alpha + n_{\text{pp}}\Theta) \end{bmatrix} \tag{133}$$

which is basically the multi-phase version of the stator dq-frame winding functions in (128).

As an interpretation, (133) shows that there is a virtual coil placed at d-axis such that its per ampere magnetomotive force waveform is referred to d-axis angle θ_d, i.e.,

$$N_{dr} = \sqrt{\frac{m}{2}} N_{r(1)} \cos(\alpha - \theta_d)$$

2.6. Modeling of Rotor Saliency

So far, we have assumed Λ is a constant and air gap length g_e is invariant with respect to angular location α. This can be true for a surface mounted permanent magnet synchronous machine, but is off for a wound-rotor synchronous machine with actual field winding or an interior/inset permanent magnet synchronous machine. A slip ring is needed to supply currents to the rotor.

For an interior/inset permanent magnet synchronous machine, the magnetic circuit passes through the magnets has low magnetic conductance. For an wound-rotor synchronous machine, the field winding needs to be placed in a slot where the magnetic

conductance is lower than the salient pole. We will now focus on the modeling of salient pole.

There are two approaches to model a salient pole rotor: Fourier expansion and infinitely deep slot. Either approach ends up with the modeling of the inverse air gap length function $g_e^{-1}(\alpha)$, which matters to the integral of the winding functions over α when calculating inductance.

2.6.1. Infinitely Deep Slot Approach [1]

For small synchronous machine, the air gap length function is a simple function, and we can model it as if the slot is infinitely deep such that the inverse of the air gap length is 0. Let's assume the salient pole of the rotor spans a pole arc of $\beta\pi$ over a pole pitch π, where $\beta \in (0, 1]$ denotes the per unit pole arc, and an attemptive design of the inverse air gap length function is

$$g_e^{-1}\left(\alpha - n_{\text{pp}}\Theta\right) = \begin{cases} g_{\min}^{-1}, (\alpha - n_{\text{pp}}\Theta) \in [0, \beta\pi] \cup [\pi, (1+\beta)\,\pi] \\ 0, \text{others} \end{cases} \tag{134}$$

The inductance calculation in (130) can be updated with the inver air gap length function in (134), but the expression is unnecessarily complicated as shown in the footnote here[24]. One can show that not only (134) leads to complicated inductance expressions, but also that it is a counter-intuitive design. The hint is that the function $g_e^{-1}\left(\alpha - n_{\text{pp}}\Theta\right)$ defines where the rotor iron core locates along the axis of the angular location α, while the winding function $N_d(\theta_d - \alpha)$ defines the virtual coil's location along the axis of the angular location α—they should be perfectly aligned for later decoupling between the stator d-(q-)axis coil and rotor q-(d-)axis coil.

A better option is to align the center of the salient pole to the zero rotor position $\Theta = 0$, giving a slightly different inverse gap function:

$$g_e^{-1}\left(\alpha - n_{\text{pp}}\Theta\right) = \begin{cases} g_{\min}^{-1}, (\alpha - n_{\text{pp}}\Theta) \in \left[-\frac{\beta\pi}{2}, \frac{\beta\pi}{2}\right] \cup \left[\pi - \frac{\beta\pi}{2}, \pi + \frac{\beta\pi}{2}\right] \\ 0, \text{others} \end{cases} \tag{135}$$

---

[24] The dq inductance calculation using the inverse air gap length function (134) goes:

$$\begin{aligned}
\begin{bmatrix} L_{dd} \\ L_{qq} \end{bmatrix} &= \mu_0 l_e r \int_0^{2\pi} \frac{3}{2} N_{(1)}^2 \begin{bmatrix} \cos^2(\theta_d - \alpha) \\ \sin^2(\theta_d - \alpha) \end{bmatrix} g_e^{-1} \mathrm{d}\alpha \\
&= \mu_0 l_e r \int_0^{2\pi} \frac{3}{2} N_{(1)}^2 \frac{1}{2} \begin{bmatrix} 1 + \cos(2\theta_d - 2\alpha) \\ 1 - \cos(2\theta_d - 2\alpha) \end{bmatrix} g_e^{-1} \mathrm{d}\alpha \\
&= \frac{\mu_0 l_e r}{g_{\min}} \frac{3}{2} N_{(1)}^2 \frac{1}{2} \cdot \left(\int_{n_{\text{pp}}\Theta}^{n_{\text{pp}}\Theta + \beta\pi} \begin{bmatrix} 1 + \cos(2\theta_d - 2\alpha) \\ 1 - \cos(2\theta_d - 2\alpha) \end{bmatrix} \mathrm{d}\alpha + \int_{n_{\text{pp}}\Theta + \pi}^{n_{\text{pp}}\Theta + (1+\beta)\pi} \begin{bmatrix} 1 + \cos(2\theta_d - 2\alpha) \\ 1 - \cos(2\theta_d - 2\alpha) \end{bmatrix} \mathrm{d}\alpha \right) \\
\Rightarrow L_{dd} &= \frac{\mu_0 l_e r}{g_{\min}} \frac{3}{2} N_{(1)}^2 \frac{1}{2} \cdot 2 \left(\beta\pi - \frac{1}{2} \sin(2\theta_d - 2n_{\text{pp}}\Theta - 2\beta\pi) + \frac{1}{2} \sin(2\theta_d - 2n_{\text{pp}}\Theta) \right) \\
&= \frac{\mu_0 l_e r}{g_{\min}} \frac{3}{2} N_{(1)}^2 \left(\beta\pi - \frac{1}{2} \left(\sin 2(\theta_d - n_{\text{pp}}\Theta)(\cos 2\beta\pi - 1) + \cos 2(\theta_d - n_{\text{pp}}\Theta) \sin 2\beta\pi \right) \right)
\end{aligned}$$

which leads to the following dq inductances results[25]

$$\begin{aligned} L_{dd} &= \frac{\mu_0 l_e r}{g_{\min}} \frac{3}{2} N_{(1)}^2 \left[\beta\pi + \cos 2\left(\theta_d - n_{\text{pp}}\Theta\right) \sin\left(\beta\pi\right)\right] \\ L_{qq} &= \frac{\mu_0 l_e r}{g_{\min}} \frac{3}{2} N_{(1)}^2 \left[\beta\pi - \cos 2\left(\theta_d - n_{\text{pp}}\Theta\right) \sin\left(\beta\pi\right)\right] \end{aligned} \tag{136}$$

from which we learn that if we use a reference frame whose d-axis angle is equal to the rotor's electrical angular position, we obtain dq inductances that are invariant with respect to rotor position, in which case, the assumed air gap shape $g_e^{-1}(\alpha)$ results in $L_{dd} > L_{qq}$ given that $\theta_d = n_{\text{pp}}\Theta$.

The rotor dq self-inductances can be as well calculated from (133)

$$\begin{aligned} L_{drdr} &= \frac{\mu_0 l_e r}{g_{\min}} \frac{m}{2} N_{r(1)}^2 \left[\beta\pi + \cos 2\left(\theta_d - n_{\text{pp}}\Theta\right) \sin\left(\beta\pi\right)\right] \\ L_{qrqr} &= \frac{\mu_0 l_e r}{g_{\min}} \frac{m}{2} N_{r(1)}^2 \left[\beta\pi - \cos 2\left(\theta_d - n_{\text{pp}}\Theta\right) \sin\left(\beta\pi\right)\right] \end{aligned} \tag{137}$$

From (136) and (137), one realizes that circuits with different phase numbers and even different motion states can all be transformed into dq-plane for potential simplification of the inductance calculation results, even when the rotor saliency is present. Therefore, it is desired to model AC machine in dq-plane.

2.6.2. Fourier Expansion Approach [2]

For larger synchronous machine, the salient pole is tapered to obtain a more better machine performance, and in this case, the inverse air gap length function is to be designed at will. A common practice is to design the air gap length as follows

$$g_e^{-1}\left(\alpha - n_{\text{pp}}\Theta\right) = \frac{g_{\min}^{-1} + g_{\max}^{-1}}{2} + \frac{g_{\min}^{-1} - g_{\max}^{-1}}{2} \cos 2\left(\alpha - n_{\text{pp}}\Theta\right) \triangleq g_0 + g_2 \cos 2\left(\alpha - n_{\text{pp}}\Theta\right) \tag{138}$$

where g_0 and g_2 are in dimension of m^{-1}. Like (135), we have intentionally design the phase angle to align the center of the salient pole to the zero rotor position. This design (138) can also be interpreted as a result of neglecting higher order terms in the Fourier expansion of some inverse air gap length function.

---

[25] The full derivation using (135) is listed here to save space:

$$\begin{aligned}
\begin{bmatrix} L_{dd} \\ L_{qq} \end{bmatrix} &= \mu_0 l_e r \int_0^{2\pi} \frac{3}{2} N_{(1)}^2 \begin{bmatrix} \cos^2\left(\theta_d - \alpha\right) \\ \sin^2\left(\theta_d - \alpha\right) \end{bmatrix} g_e^{-1} \mathrm{d}\alpha \\
&= \mu_0 l_e r \int_0^{2\pi} \frac{3}{2} N_{(1)}^2 \frac{1}{2} \begin{bmatrix} 1 + \cos\left(2\theta_d - 2\alpha\right) \\ 1 - \cos\left(2\theta_d - 2\alpha\right) \end{bmatrix} g_e^{-1} \mathrm{d}\alpha \\
&= \frac{\mu_0 l_e r}{g_{\min}} \frac{3}{2} N_{(1)}^2 \frac{1}{2} \cdot \left(\int_{n_{\text{pp}}\Theta - \frac{1}{2}\beta\pi}^{n_{\text{pp}}\Theta + \frac{1}{2}\beta\pi} \begin{bmatrix} 1 + \cos\left(2\theta_d - 2\alpha\right) \\ 1 - \cos\left(2\theta_d - 2\alpha\right) \end{bmatrix} \mathrm{d}\alpha + \int_{n_{\text{pp}}\Theta + \pi - \frac{1}{2}\beta\pi}^{n_{\text{pp}}\Theta + \pi + \frac{1}{2}\beta\pi} \begin{bmatrix} 1 + \cos\left(2\theta_d - 2\alpha\right) \\ 1 - \cos\left(2\theta_d - 2\alpha\right) \end{bmatrix} \mathrm{d}\alpha \right) \\
\Rightarrow L_{dd} &= \frac{\mu_0 l_e r}{g_{\min}} \frac{3}{2} N_{(1)}^2 \frac{1}{2} \cdot 2 \left(\beta\pi - \frac{1}{2} \sin\left(2\theta_d - 2n_{\text{pp}}\Theta - \beta\pi\right) + \frac{1}{2} \sin\left(2\theta_d - 2n_{\text{pp}}\Theta + \beta\pi\right) \right) \\
&= \frac{\mu_0 l_e r}{g_{\min}} \frac{3}{2} N_{(1)}^2 \begin{pmatrix} \beta\pi - \frac{1}{2} \sin\left(2\theta_d - 2n_{\text{pp}}\Theta\right) \cos\left(-\beta\pi\right) + \frac{1}{2} \sin\left(2\theta_d - 2n_{\text{pp}}\Theta\right) \cos\left(\beta\pi\right) \\ -\frac{1}{2} \cos\left(2\theta_d - 2n_{\text{pp}}\Theta\right) \sin\left(-\beta\pi\right) + \frac{1}{2} \cos\left(2\theta_d - 2n_{\text{pp}}\Theta\right) \sin\left(\beta\pi\right) \end{pmatrix} \\
&= \frac{\mu_0 l_e r}{g_{\min}} \frac{3}{2} N_{(1)}^2 \left[\beta\pi + \cos 2\left(\theta_d - n_{\text{pp}}\Theta\right) \sin\left(\beta\pi\right)\right]
\end{aligned}$$

Then, the dq self-inductances become[26]

$$\begin{aligned} L_{dd} &= \mu_0 l_e r \frac{3}{2} N_{(1)}^2 \pi \left(g_0 + g_2 \frac{\cos 2\left(\theta_d - n_{\text{pp}}\Theta\right)}{2} \right) \\ L_{qq} &= \mu_0 l_e r \frac{3}{2} N_{(1)}^2 \pi \left(g_0 - g_2 \frac{\cos 2\left(\theta_d - n_{\text{pp}}\Theta\right)}{2} \right) \end{aligned} \tag{139}$$

Similar results to the infinitely deep slot approach have been obtained. In addition, for a permanent magnet machine, since the magnets have almost the same magnetic conductivity as air, the coefficient g_2 should be modelled as a negative value, resulting in $L_{dd} < L_{qq}$.

In addition, the mutual inductance between d-axis coil and q-axis coil can as well be calculated using winding functions as

$$L_{dq} = \mu_0 l_e r \frac{3}{2} N_{(1)}^2 \frac{\pi}{2} g_2 \sin 2\left(\theta_d - n_{\text{pp}}\Theta\right) \tag{140}$$

2.7. Leakage Inductance Modeling

In practice, the phase inductance matrix should further incorporate leakage inductance terms. As a notation convention for this course, the matrix $\boldsymbol{L}_{abc}$ is defined solely using winding functions in (126) for an ideal machine; whereas, for an actual machine, the three phase **stator** phase inductance matrix is denoted by $\boldsymbol{L}_{abcs}$, which further accounts for self-leakage inductance L_σ and mutual leakage inductance M_σ:

$$\boldsymbol{L}_{abcs} = \boldsymbol{L}_{abc} + \boldsymbol{L}_{abc\sigma} \tag{141}$$

with the leakage inductance matrix and its dq-frame version as follows

$$\boldsymbol{L}_{abc\sigma} = \begin{bmatrix} L_\sigma & M_\sigma & M_\sigma \\ M_\sigma & L_\sigma & M_\sigma \\ M_\sigma & M_\sigma & L_\sigma \end{bmatrix} \text{ and } \boldsymbol{T}\boldsymbol{L}_{abc\sigma}\boldsymbol{T}^{-1} = \begin{bmatrix} L_\sigma - M_\sigma & 0 & 0 \\ 0 & L_\sigma - M_\sigma & 0 \\ 0 & 0 & L_\sigma + 2M_\sigma \end{bmatrix} \tag{142}$$

---

[26] The full derivation using (138) is

$$\begin{aligned}
\begin{bmatrix} L_{dd} \\ L_{qq} \end{bmatrix} &= \mu_0 l_e r \int_0^{2\pi} \frac{3}{2} N_{(1)}^2 \begin{bmatrix} \cos^2\left(\theta_d - \alpha\right) \\ \sin^2\left(\theta_d - \alpha\right) \end{bmatrix} g_e^{-1} \mathrm{d}\alpha \\
&= \mu_0 l_e r \int_0^{2\pi} \frac{3}{2} N_{(1)}^2 \frac{1}{2} \begin{bmatrix} 1 + \cos\left(2\theta_d - 2\alpha\right) \\ 1 - \cos\left(2\theta_d - 2\alpha\right) \end{bmatrix} \left(g_0 + g_2 \cos 2\left(\alpha - n_{\text{pp}}\Theta\right)\right) \mathrm{d}\alpha \\
\Rightarrow L_{dd} &= \mu_0 l_e r \frac{3}{2} N_{(1)}^2 \frac{1}{2} \cdot \int_0^{2\pi} \left(1 + \cos\left(2\theta_d - 2\alpha\right)\right) \left(g_0 + g_2 \cos 2\left(\alpha - n_{\text{pp}}\Theta\right)\right) \mathrm{d}\alpha \\
&= \mu_0 l_e r \frac{3}{2} N_{(1)}^2 \frac{1}{2} \cdot \int_0^{2\pi} \left(g_0 + g_2 \cos 2\left(\alpha - n_{\text{pp}}\Theta\right) + g_0 \cos\left(2\theta_d - 2\alpha\right) + g_2 \cos 2\left(\alpha - n_{\text{pp}}\Theta\right) \cos\left(2\theta_d - 2\alpha\right)\right) \mathrm{d}\alpha \\
&= \mu_0 l_e r \frac{3}{2} N_{(1)}^2 \frac{1}{2} \cdot \int_0^{2\pi} \left(g_0 + g_2 \cos 2\left(\alpha - n_{\text{pp}}\Theta\right) \cos\left(2\theta_d - 2\alpha\right)\right) \mathrm{d}\alpha \\
&= \mu_0 l_e r \frac{3}{2} N_{(1)}^2 \frac{1}{2} \cdot \int_0^{2\pi} \left(g_0 + g_2 \left(\frac{\cos\left(2\alpha - 2n_{\text{pp}}\Theta - 2\theta_d + 2\alpha\right)}{2} + \frac{\cos\left(2\alpha - 2n_{\text{pp}}\Theta + 2\theta_d - 2\alpha\right)}{2}\right)\right) \mathrm{d}\alpha \\
&= \mu_0 l_e r \frac{3}{2} N_{(1)}^2 \frac{1}{2} \cdot \int_0^{2\pi} \left(g_0 + g_2 \left(\frac{\cos\left(4\alpha - 2n_{\text{pp}}\Theta - 2\theta_d\right)}{2} + \frac{\cos\left(2\theta_d - 2n_{\text{pp}}\Theta\right)}{2}\right)\right) \mathrm{d}\alpha \\
\Rightarrow L_{dd} &= \mu_0 l_e r \frac{3}{2} N_{(1)}^2 \pi \left(g_0 + g_2 \frac{\cos 2\left(\theta_d - n_{\text{pp}}\Theta\right)}{2} \right)
\end{aligned}$$

As a result, the corresponding stator dq inductance matrix becomes

$$\begin{aligned}\boldsymbol{L}_{dqns} &= \begin{bmatrix} L_{dd} & L_{dq} & 0 \\ L_{qd} & L_{qq} & 0 \\ 0 & 0 & 0 \end{bmatrix} + \begin{bmatrix} L_\sigma - M_\sigma & 0 & 0 \\ 0 & L_\sigma - M_\sigma & 0 \\ 0 & 0 & L_\sigma + 2M_\sigma \end{bmatrix} \\ &= \begin{bmatrix} L_{\text{ave}} + L_{\text{diff}} \cos 2\left(\theta_d - n_{\text{pp}}\Theta\right) & -L_{\text{diff}} \sin 2\left(\theta_d - n_{\text{pp}}\Theta\right) & 0 \\ -L_{\text{diff}} \sin 2\left(\theta_d - n_{\text{pp}}\Theta\right) & L_{\text{ave}} - L_{\text{diff}} \cos 2\left(\theta_d - n_{\text{pp}}\Theta\right) & 0 \\ 0 & 0 & L_n \end{bmatrix}\end{aligned} \tag{143}$$

where, out of convenience, we have introduced three constant inductance parameters that take leakage inductance into account:

$$\begin{cases} L_d \triangleq L_\sigma - M_\sigma + \mu_0 l_e r \frac{3}{2} N_{(1)}^2 \pi \left(g_0 + \frac{1}{2} g_2\right) \\ L_q \triangleq L_\sigma - M_\sigma + \mu_0 l_e r \frac{3}{2} N_{(1)}^2 \pi \left(g_0 - \frac{1}{2} g_2\right) \\ L_n \triangleq L_\sigma + 2M_\sigma \end{cases} \tag{144}$$

that further derive the average and difference of the dq-frame inductances:

$$L_{\text{ave}} \triangleq \frac{L_d + L_q}{2} = \mu_0 l_e r \frac{3}{2} N_{(1)}^2 \pi g_0 + L_\sigma - M_\sigma \tag{145}$$

$$L_{\text{diff}} \triangleq \frac{L_d - L_q}{2} = \mu_0 l_e r \frac{3}{2} N_{(1)}^2 \pi \frac{1}{2} g_2 \tag{146}$$

*2.8. *Inductances in Stationary $\alpha\beta$ Frame*

Let $\theta_d = 0$, and the following results are useful for modeling of salient pole permanent magnet synchronous machines in stationary $\alpha\beta$-frame:

$$\boldsymbol{L}_{\alpha\beta\gamma s} = \boldsymbol{L}_{dqns}\big|_{\theta_d = 0} = \begin{bmatrix} L_\alpha & L_{\alpha\beta} & 0 \\ L_{\alpha\beta} & L_\beta & 0 \\ 0 & 0 & L_\gamma \end{bmatrix} \tag{147}$$

with

$$\begin{cases} L_\alpha = L_{\text{ave}} + L_{\text{diff}} \cos\left(2n_{\text{pp}}\Theta\right) \\ L_\beta = L_{\text{ave}} - L_{\text{diff}} \cos\left(2n_{\text{pp}}\Theta\right) \\ L_{\alpha\beta} = L_{\text{diff}} \sin\left(2n_{\text{pp}}\Theta\right) \\ L_\gamma = L_n \end{cases} \tag{148}$$

where unlike inductance parameters L_d and L_q, note $\alpha\beta$ inductances are function of rotor angle Θ, meaning this winding is capable of producing reluctance torque. A well acknowledged paper using those nonlinear inductances is [12].

2.9. Notations for Coils and Leakage Inductance

In sub-section 2.5, we have been adding subscript $_r$ to indicate **rotor**. From now on, since both stator and rotor circuits are modeled, we should stick with using full subscripts in the inductance symbols. In fact, the parameter symbols L_d and L_q are

only used when there is no rotor circuit, i.e., in a permanent magnet synchronous machine. Therefore, to be crystal clear, let's further add subscript $_s$ to indicate the inductance of **stator** coils such that

$$\begin{aligned} L_{dsds} &\triangleq L_{dd} \\ L_{dsqs} &\triangleq L_{dq} \\ L_{qsqs} &\triangleq L_{qq} \\ L_{ls} &\triangleq L_\sigma - M_\sigma \end{aligned} \tag{149}$$

where, for example, subscript $_{ds}$ indicate the virtual d-axis coil on stator, and $_{ls}$ means "stator leakage".

Finally, similar to the case of stator, in an actual machine. the magnetic circuit of the rotor coils also has leakage path, and generally speaking, the rotor leakage inductance is not equal to the stator leakage inductance. For this course, the rotor d-axis leakage inductance is denoted as L_{lr}.

2.10. DQ Modeling of AC Machine

Since this sub-section, we are considering actual machines that has leakage in magnetic circuit, so pay attention to the subscripts $_s$ and $_r$.

Consider a generic electrical machine. A three phase winding is placed within the stator, and the rotor is equipped with a multi-phase rotor winding (usually more than 3 phases) and a n_{pp}-pole-pair field winding.

2.10.1. Voltage Equations

The dynamics of stator circuits are according to Faraday's law of induction as follows

$$\boldsymbol{u}_{abcs} - \boldsymbol{R}_{abcs}\boldsymbol{i}_{abcs} = \frac{\mathrm{d}}{\mathrm{d}t}\boldsymbol{\psi}_{abcs} \tag{150}$$

where the symmetry assumption leads to $\boldsymbol{R}_{abcs} = R\boldsymbol{I}_3$. Applying Park transformation to each side of (150) yields

$$\begin{aligned} (150) &\Rightarrow \boldsymbol{T}\left(\boldsymbol{u}_{abcs} - \boldsymbol{R}_{abcs}\boldsymbol{i}_{abcs}\right) = \boldsymbol{T}\frac{\mathrm{d}}{\mathrm{d}t}\left(\left[\boldsymbol{T}^{-1}\boldsymbol{T}\right]\boldsymbol{\psi}_{abcs}\right) \\ &\Rightarrow \boldsymbol{u}_{dqns} - R\boldsymbol{i}_{dqns} = \boldsymbol{T}\frac{\mathrm{d}}{\mathrm{d}t}\left(\left[\boldsymbol{T}^{-1}\right]\boldsymbol{\psi}_{dqns}\right) = \boldsymbol{T}\left(\frac{\mathrm{d}}{\mathrm{d}t}\boldsymbol{T}^T\right)\boldsymbol{\psi}_{dqns} + \boldsymbol{T}\boldsymbol{T}^{-1}\frac{\mathrm{d}}{\mathrm{d}t}\boldsymbol{\psi}_{dqns} \\ &\Rightarrow \boldsymbol{u}_{dqns} - R\boldsymbol{i}_{dqns} = \boldsymbol{T}\left(\frac{\mathrm{d}}{\mathrm{d}t}\boldsymbol{T}^T\right)\boldsymbol{\psi}_{dqns} + \frac{\mathrm{d}}{\mathrm{d}t}\boldsymbol{\psi}_{dqns} \end{aligned} \tag{151}$$

Similarly, we can use a multi-phase transformation (131) to convert the rotor circuits into dq circuits. Even though we do not need to know the phase number of the rotor circuits, let's consider, without loss of generality, the symmetric $m = 5$ phase rotor

circuits:

$$\begin{bmatrix} u_1 \\ u_2 \\ u_3 \\ u_4 \\ u_5 \end{bmatrix} - R_r \begin{bmatrix} i_1 \\ i_2 \\ i_3 \\ i_4 \\ i_5 \end{bmatrix} = \frac{\mathrm{d}}{\mathrm{d}t} \begin{bmatrix} \psi_1 \\ \psi_2 \\ \psi_3 \\ \psi_4 \\ \psi_5 \end{bmatrix} \tag{152}$$

$$\Rightarrow \boldsymbol{T}_m \begin{bmatrix} u_1 \\ u_2 \\ u_3 \\ u_4 \\ u_5 \end{bmatrix} - R_r \boldsymbol{T}_m \begin{bmatrix} i_1 \\ i_2 \\ i_3 \\ i_4 \\ i_5 \end{bmatrix} = \boldsymbol{T}_m \frac{\mathrm{d}}{\mathrm{d}t} \left(\boldsymbol{T}_m^T \boldsymbol{T}_m \begin{bmatrix} \psi_1 \\ \psi_2 \\ \psi_3 \\ \psi_4 \\ \psi_5 \end{bmatrix} \right) \tag{153}$$

$$\Rightarrow \begin{bmatrix} u_{dr} \\ u_{qr} \end{bmatrix} - R_r \begin{bmatrix} i_{dr} \\ i_{qr} \end{bmatrix} = \boldsymbol{T}_m \left(\frac{\mathrm{d}}{\mathrm{d}t} \boldsymbol{T}_m^T \right) \begin{bmatrix} \psi_{dr} \\ \psi_{qr} \end{bmatrix} + \boldsymbol{T}_m \boldsymbol{T}_m^T \frac{\mathrm{d}}{\mathrm{d}t} \begin{bmatrix} \psi_{dr} \\ \psi_{qr} \end{bmatrix} \tag{154}$$

$$\Leftrightarrow \boldsymbol{u}_{dqr} - R_r \boldsymbol{i}_{dqr} = \boldsymbol{T}_m \left(\frac{\mathrm{d}}{\mathrm{d}t} {\boldsymbol{T}_m}^T \right) \boldsymbol{\psi}_{dqr} + \frac{\mathrm{d}}{\mathrm{d}t} \boldsymbol{\psi}_{dqr} \tag{155}$$

where $\boldsymbol{T}_m(\theta_d - n_{\mathrm{pp}}\Theta)$ is the extended version of the Park transformation for converting rotor m-phase coils (that are already rotating along the air gap) to dq-plane.[27]

Finally, the voltage equation for the circuit of the field winding is

$$u_{fr} - R_{fr} i_{fr} = \frac{\mathrm{d}}{\mathrm{d}t} \psi_{fr} \tag{156}$$

2.10.2. Flux Equations

We have transformed all winding into dq-plane (which is done by converting all electrical circuit variables and winding functions into dq-plane). Each symmetric polyphase winding corresponds to a pair of d-axis coil and q-axis coil, thus in total there are 5 coils denoted by a unique subscript among $_{ds}$, $_{qs}$, $_{dr}$, $_{qr}$, $_{fr}$. Note the neutral coil with subscript $_{ns}$ is not useful for this course and can be simply discarded. The flux

---

[27] One can verify that $\boldsymbol{T}_m^T \boldsymbol{T}_m \neq \boldsymbol{I}_{m\times m}$ and in fact, it is a constant matrix:

$$\boldsymbol{T}_m^T \boldsymbol{T}_m = \begin{bmatrix} 0.4 & -0.1+0.1\sqrt{5} & -0.1\sqrt{5}-0.1 & -0.1\sqrt{5}-0.1 & -0.1+0.1\sqrt{5} \\ -0.1+0.1\sqrt{5} & 0.4 & -0.1+0.1\sqrt{5} & -0.1\sqrt{5}-0.1 & -0.1\sqrt{5}-0.1 \\ -0.1\sqrt{5}-0.1 & -0.1+0.1\sqrt{5} & 0.4 & -0.1+0.1\sqrt{5} & -0.1\sqrt{5}-0.1 \\ -0.1\sqrt{5}-0.1 & -0.1\sqrt{5}-0.1 & -0.1+0.1\sqrt{5} & 0.4 & -0.1+0.1\sqrt{5} \\ -0.1+0.1\sqrt{5} & -0.1\sqrt{5}-0.1 & -0.1\sqrt{5}-0.1 & -0.1+0.1\sqrt{5} & 0.4 \end{bmatrix}$$

In order to derive an identity matrix to be used in (153), we actually must introduce the full square multiphase Park transformation matrix:

$$\boldsymbol{T}_{m\times m} = \sqrt{\frac{2}{5}} \begin{bmatrix} \cos(\theta_1(t)) & \sin\left(\theta_1(t)+\frac{\pi}{10}\right) & -\cos\left(\theta_1(t)+\frac{\pi}{5}\right) & -\sin\left(\theta_1(t)+\frac{3\pi}{10}\right) & \cos\left(\theta_1(t)+\frac{2\pi}{5}\right) \\ -\sin(\theta_1(t)) & \cos\left(\theta_1(t)+\frac{\pi}{10}\right) & \sin\left(\theta_1(t)+\frac{\pi}{5}\right) & -\cos\left(\theta_1(t)+\frac{3\pi}{10}\right) & -\sin\left(\theta_1(t)+\frac{2\pi}{5}\right) \\ \cos(\theta_3(t)) & -\sin\left(\theta_3(t)+\frac{3\pi}{10}\right) & \sin\left(\theta_3(t)+\frac{\pi}{10}\right) & \cos\left(\theta_3(t)+\frac{2\pi}{5}\right) & -\cos\left(\theta_3(t)+\frac{\pi}{5}\right) \\ -\sin(\theta_3(t)) & -\cos\left(\theta_3(t)+\frac{3\pi}{10}\right) & \cos\left(\theta_3(t)+\frac{\pi}{10}\right) & -\sin\left(\theta_3(t)+\frac{2\pi}{5}\right) & \sin\left(\theta_3(t)+\frac{\pi}{5}\right) \\ \frac{\sqrt{2}}{2} & \frac{\sqrt{2}}{2} & \frac{\sqrt{2}}{2} & \frac{\sqrt{2}}{2} & \frac{\sqrt{2}}{2} \end{bmatrix}$$

which satisfies $\boldsymbol{T}_{m\times m}^T \boldsymbol{T}_{m\times m} = \boldsymbol{I}_{m\times m}$. Note the full transformation will have two independent d-axis angles, denoted as $\theta_1 = \theta_d$ and θ_2, respectively. We will only concern the two equations involved with θ_1. It is interesting to mention that this is not the only form that a multiphase Park transformation matrix $\boldsymbol{T}_{m\times m}$ can take.

equation of stator coils and rotor coils are respectively:

$$\boldsymbol{\psi}_{dqns} = \boldsymbol{L}_{dqns}\boldsymbol{i}_{dqns} + \boldsymbol{L}_{dqnsr}\boldsymbol{i}_{dqfr} \tag{157}$$

$$\boldsymbol{\psi}_{dqfr} = \left(\boldsymbol{L}_{dqnsr}\right)^T \boldsymbol{i}_{dqns} + \boldsymbol{L}_{dqfr}\boldsymbol{i}_{dqfr} \tag{158}$$

where it is worth noting that the mutual linkage from stator to rotor is the same as the mutual linkage from rotor to stator, hence the presence of the transposed mutual inductance matrix term $\left(\boldsymbol{L}_{dqnsr}\right)^T$.

The inductance matrices are defined as

$$\boldsymbol{L}_{dqns} = \begin{bmatrix} L_{ls}+L_{dsds} & L_{dsqs} & L_{dsns} \\ L_{qsds} & L_{ls}+L_{qsqs} & L_{qsns} \\ L_{nsds} & L_{nsqs} & L_n+L_{nsns} \end{bmatrix} = \begin{bmatrix} L_{ls}+L_{dsds} & L_{dsqs} & 0 \\ L_{qsds} & L_{ls}+L_{qsqs} & 0 \\ 0 & 0 & L_n \end{bmatrix} \tag{159}$$

$$\boldsymbol{L}_{dqnsr} = \begin{bmatrix} L_{dsdr} & L_{dsqr} & L_{dsfr} \\ L_{qsdr} & L_{qsqr} & L_{qsfr} \\ L_{nsdr} & L_{nsqr} & L_{nsfr} \end{bmatrix} = \begin{bmatrix} L_{dsdr} & L_{dsqr} & L_{dsfr} \\ L_{qsdr} & L_{qsqr} & L_{qsfr} \\ 0 & 0 & 0 \end{bmatrix} \tag{160}$$

$$\boldsymbol{L}_{dqfr} = \begin{bmatrix} L_{lr}+L_{drdr} & L_{dsqr} & L_{drfr} \\ L_{qsdr} & L_{lr}+L_{qsqr} & L_{qsfr} \\ L_{fsdr} & L_{fsqr} & L_{fsfr} \end{bmatrix} \tag{161}$$

The mutual inductance between stator and rotor coils can be derived (cf. (139)) as

$$L_{dsdr} = \mu_0 l_e r \sqrt{\frac{3}{2}}\sqrt{\frac{m}{2}} N_{(1)} N_{r(1)} \pi \left(g_0 + g_2 \frac{\cos 2\left(\theta_d - n_{\text{pp}}\Theta\right)}{2} \right) \tag{162}$$

$$L_{qsqr} = \mu_0 l_e r \sqrt{\frac{3}{2}}\sqrt{\frac{m}{2}} N_{(1)} N_{r(1)} \pi \left(g_0 - g_2 \frac{\cos 2\left(\theta_d - n_{\text{pp}}\Theta\right)}{2} \right) \tag{163}$$

with no leakage inductance. The cross-axes-coupling inductance is

$$\begin{aligned} L_{dsqr} &= -\mu_0 l_e r \int_0^{2\pi} \sqrt{\frac{3}{2}} N_{(1)} \sqrt{\frac{m}{2}} N_{r(1)} \cos\left(\theta_d - \alpha\right) \sin\left(\theta_d - \alpha\right) g_e^{-1} \mathrm{d}\alpha \\ &= -\mu_0 l_e r \sqrt{\frac{3}{2}}\sqrt{\frac{m}{2}} N_{(1)} N_{r(1)} \int_0^{2\pi} \frac{1}{2} \sin 2\left(\theta_d - \alpha\right) \left(g_0 + g_2 \cos 2\left(\alpha - n_{\text{pp}}\Theta\right)\right) \mathrm{d}\alpha \\ &= -\mu_0 l_e r \sqrt{\frac{3}{2}}\sqrt{\frac{m}{2}} N_{(1)} N_{r(1)} \frac{\pi}{2} g_2 \sin 2\left(\theta_d - n_{\text{pp}}\Theta\right) \end{aligned} \tag{164}$$

which is apparently equal to zero when there is no rotor saliency, i.e., $g_2 = 0$.

2.10.3. Rotor Oriented Frame

Again, we find that the inductance matrices can be greatly simplified if we use a reference frame whose d-axis angle equals to rotor's electrical angular position $n_{\text{pp}}\Theta$. To reduce the number of inductance parameters, let the dq-frame be fixed to the rotor:

$$\theta_d = n_{\text{pp}}\Theta \tag{165}$$

and as a result, e.g., the stator inductance variables become constant:

$$L_{dsds} + L_{ls} = L_{dd} + L_{ls} = L_d \tag{166}$$
$$L_{qsqs} + L_{ls} = L_{qq} + L_{ls} = L_q \tag{167}$$

and the dq-axes are decoupled such that for example: $L_{dsqs} = L_{dsqr} = 0$ even when saliency is present, i.e., when $g_2 \neq 0$.

2.10.4. Over-parametrization Problem

The inductance parameters L_{dsds}, L_{dsdr} and L_{drdr} only differ by a factor, yet they are treated as three unknown circuit parameters. This inevitably leads to over-parametrization of our model, see also the previously derived model (71) from last chapter.

In order to reduce the number of parameters, the flux equations are rewritten componentwise in terms of the stator constant magnetizing inductances L_{dd} and L_{qq}:

$$\begin{aligned}
\psi_{ds} &= (L_{dsds} i_{ds} + 0 + 0) + \left(L_{dd} \frac{\sqrt{\frac{m}{2}} N_{r(1)}}{\sqrt{\frac{3}{2}} N_{(1)}} i_{dr} + 0 + L_{dsfr} i_{fr} \right) \\
\psi_{qs} &= (0 + L_{qsqs} i_{qs} + 0) + \left(0 + L_{qq} \frac{\sqrt{\frac{m}{2}} N_{r(1)}}{\sqrt{\frac{3}{2}} N_{(1)}} i_{qr} + 0 \right) \\
\psi_{dr} &= \left(L_{dd} \frac{\sqrt{\frac{m}{2}} N_{r(1)}}{\sqrt{\frac{3}{2}} N_{(1)}} i_{ds} + 0 + 0 \right) + \left(\left[L_{lr} + L_{dd} \left(\frac{\sqrt{\frac{m}{2}} N_{r(1)}}{\sqrt{\frac{3}{2}} N_{(1)}} \right)^2 \right] i_{dr} + 0 + L_{drfr} i_{fr} \right) \\
\psi_{qr} &= \left(0 + L_{qq} \frac{\sqrt{\frac{m}{2}} N_{r(1)}}{\sqrt{\frac{3}{2}} N_{(1)}} i_{qs} + 0 \right) + \left(0 + \left[L_{lr} + L_{qq} \left(\frac{\sqrt{\frac{m}{2}} N_{r(1)}}{\sqrt{\frac{3}{2}} N_{(1)}} \right)^2 \right] i_{qr} + 0 \right) \\
\psi_{fr} &= (L_{frds} i_{ds} + 0 + 0) + (L_{frdr} i_{dr} + 0 + L_{frfr} i_{fr})
\end{aligned} \tag{168}$$

Since the rotor flux linkage and rotor currents are not measured in practice, we are less concerned with their actual values. Let's define a change of variables using the turn ratio transformation $k_{sr} = \sqrt{\frac{m}{2}} N_{r(1)} / \left(\sqrt{\frac{3}{2}} N_{(1)} \right)$:

$$\boldsymbol{i}'_{dqr} = k_{sr} \boldsymbol{i}_{dqr} \tag{169}$$
$$\boldsymbol{\psi}'_{dqr} = (k_{sr})^{-1} \boldsymbol{\psi}_{dqr} \tag{170}$$
$$L'_{lr} = k_{sr}^{-2} L_{lr} \tag{171}$$

This practice is known as referring the rotor circuits to the stator, and the resulting

flux equations have even less inductance parameters:

$$
\begin{aligned}
\psi_{ds} &= (L_{dsds} i_{ds} + 0 + 0) + \left(L_{dd} i'_{dr} + 0 + L_{dsfr} i_{fr}\right) \\
\psi_{qs} &= (0 + L_{qsqs} i_{qs} + 0) + \left(0 + L_{qq} i'_{qr} + 0\right) \\
\psi'_{dr} &= (L_{dd} i_{ds} + 0 + 0) + \left(\left(L'_{lr} + L_{dd}\right) i'_{dr} + 0 + k_{sr}^{-1} L_{drfr} i_{fr}\right) \\
\psi'_{qr} &= (0 + L_{qq} i_{qs} + 0) + \left(0 + \left(L'_{lr} + L_{qq}\right) i'_{qr} + 0\right) \\
\psi_{fr} &= (L_{frds} i_{ds} + 0 + 0) + \left(L_{frdr} k_{sr}^{-1} i'_{dr} + 0 + L_{frfr} i_{fr}\right) \\
\Leftrightarrow &\begin{cases}
\boldsymbol{\psi}_{dqs} = \begin{bmatrix} L_{ls} + L_{dd} & 0 \\ 0 & L_{ls} + L_{qq} \end{bmatrix} \boldsymbol{i}_{dqs} + \begin{bmatrix} L_{dd} & 0 \\ 0 & L_{qq} \end{bmatrix} \boldsymbol{i}'_{dqr} + \begin{bmatrix} L_{dsfr} i_{fr} \\ 0 \end{bmatrix} \\
\boldsymbol{\psi}'_{dqr} = \begin{bmatrix} L_{dd} & 0 \\ 0 & L_{qq} \end{bmatrix} \boldsymbol{i}_{dqs} + \begin{bmatrix} L'_{lr} + L_{dd} & 0 \\ 0 & L'_{lr} + L_{qq} \end{bmatrix} \boldsymbol{i}'_{dqr} + \begin{bmatrix} k_{sr}^{-1} L_{drfr} i_{fr} \\ 0 \end{bmatrix} \\
\psi_{fr} = L_{frds} i_{ds} + L_{frdr} k_{sr}^{-1} i'_{dr} + L_{frfr} i_{fr}
\end{cases}
\end{aligned}
\tag{172}
$$

As a result of referring the rotor circuits to the stator, we find out that the stator flux $\boldsymbol{\psi}_{dqs}$ and the rotor flux $\boldsymbol{\psi}'_{dqr}$ are both related to an intermediate flux linkage, known as the air gap flux linkage (denoted as $\boldsymbol{\psi}_{dqg}$), which is a concept used in motor control, and it equals to stator flux minus stator leakage flux, or rotor flux minus rotor leakage flux:

$$
\begin{aligned}
\boldsymbol{\psi}_{dqg} &= \boldsymbol{\psi}_{dqs} - L_{ls} \boldsymbol{i}_{dqs} \\
\boldsymbol{\psi}_{dqg} &= \boldsymbol{\psi}'_{dqr} - L'_{lr} \boldsymbol{i}_{dqr}
\end{aligned}
\tag{173}
$$

which implies that $L_{dsfr} = k_{sr}^{-1} L_{drfr}$, and in other words, the mutual inductance L_{drfr} can be referred to stator and there is no need to use L_{drfr} anymore.

2.10.5. Results in Rotor Reference Frame $\theta_d = n_{\text{pp}}\Theta$

The dq-frame voltage equations are rewritten as

$$
\begin{cases}
\boldsymbol{u}_{dqns} - R\boldsymbol{i}_{dqns} = \boldsymbol{T}\left(\frac{\mathrm{d}}{\mathrm{d}t}\boldsymbol{T}^T\right)\boldsymbol{\psi}_{dqns} + \frac{\mathrm{d}}{\mathrm{d}t}\boldsymbol{\psi}_{dqns} \\
\boldsymbol{u}_{dqr} - R_r\boldsymbol{i}_{dqr} = \boldsymbol{T}_m\left(\frac{\mathrm{d}}{\mathrm{d}t}\boldsymbol{T}_m{}^T\right)\boldsymbol{\psi}_{dqr} + \frac{\mathrm{d}}{\mathrm{d}t}\boldsymbol{\psi}_{dqr} \\
u_{fr} - R_{fr} i_{fr} = \frac{\mathrm{d}}{\mathrm{d}t}\psi_{fr}
\end{cases}
\tag{174}
$$

which can be further simplified using the properties in (122) and a skew-symmetric matrix $\boldsymbol{J} = \left[\begin{smallmatrix} 0 & -1 \\ 1 & 0 \end{smallmatrix}\right]$ as follows

$$
(174) \Rightarrow \begin{cases}
\boldsymbol{u}_{dqs} - R\boldsymbol{i}_{dqs} = \boldsymbol{J}\frac{\mathrm{d}\theta_d}{\mathrm{d}t}\boldsymbol{\psi}_{dqs} + \frac{\mathrm{d}}{\mathrm{d}t}\boldsymbol{\psi}_{dqs} \\
\boldsymbol{u}_{dqr} - R_r\boldsymbol{i}_{dqr} = \boldsymbol{J}\frac{\mathrm{d}(\theta_d - n_{\text{pp}}\Theta)}{\mathrm{d}t}\boldsymbol{\psi}_{dqr} + \frac{\mathrm{d}}{\mathrm{d}t}\boldsymbol{\psi}_{dqr} \\
u_{fr} - R_{fr} i_{fr} = \frac{\mathrm{d}}{\mathrm{d}t}\psi_{fr}
\end{cases}
\tag{175}
$$

in which the rotor voltage equation needs to be referred to stator. To this end, multiplying k_{sr}^{-1} to both sides yields

$$
\frac{\boldsymbol{u}_{dqr}}{k_{sr}} - \frac{R_r}{k_{sr}}\frac{1}{k_{sr}}\boldsymbol{i}'_{dqr} = \boldsymbol{J}\frac{\mathrm{d}\left(\theta_d - n_{\text{pp}}\Theta\right)}{\mathrm{d}t}\boldsymbol{\psi}'_{dqr} + \frac{\mathrm{d}}{\mathrm{d}t}\boldsymbol{\psi}'_{dqr}
\tag{176}
$$

with the following definitions for rotor voltage and rotor resistance:

$$\begin{aligned} \boldsymbol{u}'_{dqr} &= \boldsymbol{u}_{dqr} k_{sr}^{-1} \\ R'_r &= R_r k_{sr}^{-2} \end{aligned} \tag{177}$$

To solve the ordinary differential equations (ODEs) (175), one needs to express currents in terms of flux linkages. You can choose to take inverse of the $\mathbb{R}^{5\times5}$ inductance matrix with the aid of SymPy package, but of course I have a better way to summarize the results. First, we need to re-order the vector and matrix:

$$\begin{bmatrix} \psi_{ds} \\ \psi'_{dr} \\ \psi_{fr} \\ \psi_{qs} \\ \psi'_{qr} \end{bmatrix} = \begin{bmatrix} L_{ls}+L_{dd} & L_{dd} & L_{df} & 0 & 0 \\ L_{dd} & L'_{lr}+L_{dd} & L_{df} & 0 & 0 \\ L_{df} & L_{df} & L_{fr} & 0 & 0 \\ 0 & 0 & 0 & L_{ls}+L_{qq} & L_{qq} \\ 0 & 0 & 0 & L_{qq} & L'_{lr}+L_{qq} \end{bmatrix} \begin{bmatrix} i_{ds} \\ i'_{dr} \\ i_{fr} \\ i_{qs} \\ i'_{qr} \end{bmatrix} \tag{178}$$

which apparently consists of two block matrices. Therefore, we have the following solutions for currents:

$$\begin{aligned} \begin{bmatrix} i_{ds} \\ i'_{dr} \\ i_{fr} \end{bmatrix} &= \frac{\begin{bmatrix} L_{fr}\left(L'_{lr}+L_{dd}\right)-L_{df}^2 & -L_{dd}L_{fr}+L_{df}^2 & -L_{df}L'_{lr} \\ -L_{dd}L_{fr}+L_{df}^2 & \left(L_{ls}+L_{dd}\right)L_{fr}-L_{df}^2 & -L_{df}L_{ls} \\ -L_{df}L'_{lr} & -L_{df}L_{ls} & L_{ls}L'_{lr}+L_{dd}\left(L'_{lr}+L_{ls}\right) \end{bmatrix} \begin{bmatrix} \psi_{ds} \\ \psi'_{dr} \\ \psi_{fr} \end{bmatrix}}{\left(L_{ls}+L_{dd}\right)L_{fr}L'_{lr}+L_{dd}L_{fr}L_{ls}-L_{df}^2\left(L'_{lr}+L_{ls}\right)} \\ \begin{bmatrix} i_{qs} \\ i'_{qr} \end{bmatrix} &= \frac{1}{L'_{lr}L_{ls}+L'_{lr}L_{qq}+L_{ls}L_{qq}} \begin{bmatrix} L'_{lr}+L_{qq} & -L_{qq} \\ -L_{qq} & L_{ls}+L_{qq} \end{bmatrix} \begin{bmatrix} \psi_{qs} \\ \psi'_{qr} \end{bmatrix} \end{aligned} \tag{179}$$

This simplified results are due to the fact that the rotor oriented frame decouples the magnetic linkage between the d-axis coils (ds, dr, fr) and the q-axis coils (qs, qr), i.e., $L_{dq}=0$.

In this DQ model, there are two kinds of electromotive forces, i.e., transformer electromotive force and rotary electromotive force. The latter exists only when the circuits are transformed into a dq-frame that is not stationary with respect to the original circuits.

The electrical power input is:

$$\begin{aligned} P_{\text{elec,in}} &= \boldsymbol{u}_{dqs}\cdot\boldsymbol{i}_{dqs} + \boldsymbol{u}'_{dqr}\cdot\boldsymbol{i}'_{dqr} + u_{fr}i_{fr} \\ &= \left(R\boldsymbol{i}_{dqs}\cdot\boldsymbol{i}_{dqs} + \boldsymbol{J}\frac{\mathrm{d}\theta_d}{\mathrm{d}t}\boldsymbol{\psi}_{dqs}\cdot\boldsymbol{i}_{dqs} + \frac{\mathrm{d}}{\mathrm{d}t}\boldsymbol{\psi}_{dqs}\cdot\boldsymbol{i}_{dqs}\right) + \left(R'_r\boldsymbol{i}'_{dqr}\cdot\boldsymbol{i}'_{dqr} + \frac{\mathrm{d}}{\mathrm{d}t}\boldsymbol{\psi}'_{dqr}\cdot\boldsymbol{i}'_{dqr}\right) + \left(R_{fr}i_{fr}^2 + i_{fr}\frac{\mathrm{d}}{\mathrm{d}t}\psi_{fr}\right) \end{aligned} \tag{180}$$

where the term containing rotary electromotive force is responsible for electromechanical power conversion or in other words, passing electrical power from stator to rotor shaft.

Based on (180), the electromagnetic torque can be obtained by the energy method as follows

$$\begin{aligned} \Omega T_{\text{em}} &= \boldsymbol{J}\frac{\mathrm{d}\theta_d}{\mathrm{d}t}\boldsymbol{\psi}_{dqs}\cdot\boldsymbol{i}_{dqs} = \boldsymbol{J}\frac{\mathrm{d}n_{\text{pp}}\Theta}{\mathrm{d}t}\boldsymbol{\psi}_{dqs}\cdot\boldsymbol{i}_{dqs} \\ \Rightarrow T_{\text{em}} &= \frac{\frac{\mathrm{d}n_{\text{pp}}\Theta}{\mathrm{d}t}}{\Omega}\boldsymbol{J}\boldsymbol{\psi}_{dqs}\cdot\boldsymbol{i}_{dqs} = n_{\text{pp}}\left(\boldsymbol{J}\boldsymbol{\psi}_{dqs}\right)^T\boldsymbol{i}_{dqs} = n_{\text{pp}}\boldsymbol{\psi}_{dqs}\times\boldsymbol{i}_{dqs} \end{aligned} \tag{181}$$

2.10.6. Brief Summary

Based on preceding development, a clean model taking all turn ratio conversions into account is finally derived as follows:

$$\begin{aligned}
&\frac{\mathrm{d}}{\mathrm{d}t}\boldsymbol{\psi}_{dqs} = \boldsymbol{u}_{dqs} - R\boldsymbol{i}_{dqs} - \boldsymbol{J}\frac{\mathrm{d}\theta_d}{\mathrm{d}t}\boldsymbol{\psi}_{dqs} \\
&\frac{\mathrm{d}}{\mathrm{d}t}\boldsymbol{\psi}'_{dqr} = \boldsymbol{u}'_{dqr} - R'_r\boldsymbol{i}'_{dqr} - \boldsymbol{J}\frac{\mathrm{d}(\theta_d - n_{\mathrm{pp}}\Theta)}{\mathrm{d}t}\boldsymbol{\psi}'_{dqr} \\
&\frac{\mathrm{d}}{\mathrm{d}t}\psi_{fr} = u_{fr} - R_{fr}i_{fr}
\end{aligned} \tag{182}$$

where the d-axis angle θ_d can still be arbitrarily set.

In order to solve this model numerically, we need to set a rotor oriented reference frame with $\theta_d = n_{\mathrm{pp}}\Theta$, and then represent currents in terms of flux linkages

$$\begin{aligned}
D_d i_{ds} &= \left[L_{fr}\left(L'_{lr} + L_{dd}\right) - L_{df}^2\right]\psi_{ds} + \left(-L_{dd}L_{fr} + L_{df}^2\right)\psi'_{dr} + \left(-L_{df}L'_{lr}\right)\psi_{fr} \\
D_d i'_{dr} &= \left[L_{fr}\left(L_{ls} + L_{dd}\right) - L_{df}^2\right]\psi'_{dr} + \left(-L_{dd}L_{fr} + L_{df}^2\right)\psi_{ds} + \left(-L_{df}L_{ls}\right)\psi_{fr} \\
D_d i_{fr} &= \left[L_{dd}\left(L'_{lr} + L_{ls}\right) + L_{ls}L'_{lr}\right]\psi_{fr} + \left(-L_{df}L'_{lr}\right)\psi_{ds} + \left(-L_{df}L_{ls}\right)\psi'_{dr} \\
D_q i_{qs} &= \left(L'_{lr} + L_{qq}\right)\psi_{qs} - L_{qq}\psi'_{qr} \\
D_q i'_{qr} &= \left(L_{ls} + L_{qq}\right)\psi'_{qr} - L_{qq}\psi_{qs}
\end{aligned} \tag{183}$$

where the determinants of the d-axis and q-axis inductance matrices are respectively:

$$\begin{aligned}
D_d &= \left(L_{ls} + L_{dd}\right)L_{fr}L'_{lr} + L_{dd}L_{fr}L_{ls} - L_{df}^2\left(L'_{lr} + L_{ls}\right) \\
D_q &= L'_{lr}L_{ls} + L'_{lr}L_{qq} + L_{ls}L_{qq}
\end{aligned} \tag{184}$$

The mechanical subsystem is:

$$\begin{aligned}
&\frac{\mathrm{d}}{\mathrm{d}t}\theta_d = n_{\mathrm{pp}}\frac{\mathrm{d}}{\mathrm{d}t}\Theta = n_{\mathrm{pp}}\Omega \\
&\frac{\mathrm{d}}{\mathrm{d}t}\Omega = \frac{1}{J_s}\left(T_{\mathrm{em}} - T_L\right) \\
&T_{\mathrm{em}} = n_{\mathrm{pp}}\left(\boldsymbol{J}\boldsymbol{\psi}_{dqs}\right)^T\boldsymbol{i}_{dqs} = n_{\mathrm{pp}}\left(-\psi_{qs}i_{ds} + \psi_{ds}i_{qs}\right)
\end{aligned} \tag{185}$$

We can do transient simulation of an electrically-excited wound-rotor synchronous machine using models of the electrical and mechanical sub-systems.

2.11. DQ Modeling of Induction Machine

Removing field winding $i_{fr} = 0$ and assuming there is no saliency $g_2 = 0$ and no rotor voltage $\boldsymbol{u}'_{dqr} = \boldsymbol{0}$, we have the dq model for induction machine as

$$\begin{aligned}
&\boldsymbol{\psi}_{dqs} = L_s\boldsymbol{i}_{dqs} + L_m\boldsymbol{i}'_{dqr} \\
&\boldsymbol{\psi}'_{dqr} = L_m\boldsymbol{i}_{dqs} + L_r\boldsymbol{i}'_{dqr} \\
&\boldsymbol{u}_{dqs} - R\boldsymbol{i}_{dqs} = \boldsymbol{J}\frac{\mathrm{d}\theta_d}{\mathrm{d}t}\boldsymbol{\psi}_{dqs} + \frac{\mathrm{d}}{\mathrm{d}t}\boldsymbol{\psi}_{dqs} \\
&\boldsymbol{u}'_{dqr} - R'_r\boldsymbol{i}'_{dqr} = \boldsymbol{J}\frac{\mathrm{d}\left(\theta_d - n_{\mathrm{pp}}\Theta\right)}{\mathrm{d}t}\boldsymbol{\psi}'_{dqr} + \frac{\mathrm{d}}{\mathrm{d}t}\boldsymbol{\psi}'_{dqr}
\end{aligned} \tag{186}$$

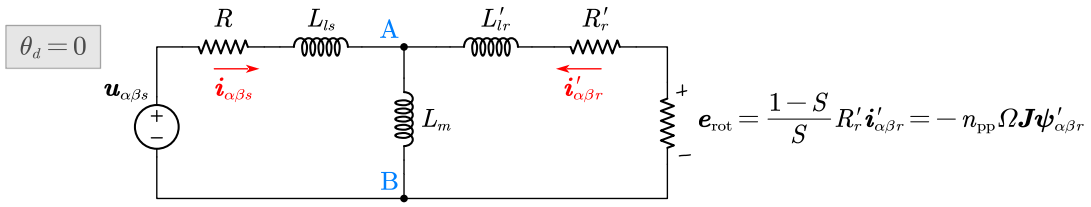

Figure 10. The T-equivalent-circuit of induction machine at steady state, derived using (190),(191), and (193).

where $L_s = L_m + L_{ls}$, $L_r = L_m + L'_{lr}$ and $L_m = L_{dd} = L_{qq}$.

Without the presence of saliency, there is no need to fix the dq-frame to the rotor anymore. Let $\theta_d = 0$, we have the $\alpha\beta$-frame model of induction machine as

$$\theta_d = 0 \Rightarrow \begin{cases} \boldsymbol{\psi}_{\alpha\beta s} = L_s \boldsymbol{i}_{\alpha\beta s} + L_m \boldsymbol{i}'_{\alpha\beta r} \\ \boldsymbol{\psi}'_{\alpha\beta r} = L_m \boldsymbol{i}_{\alpha\beta s} + L_r \boldsymbol{i}'_{\alpha\beta r} \\ \boldsymbol{u}_{\alpha\beta s} - R \boldsymbol{i}_{\alpha\beta s} = \frac{\mathrm{d}}{\mathrm{d}t} \boldsymbol{\psi}_{\alpha\beta s} \\ \boldsymbol{u}'_{\alpha\beta r} - R'_r \boldsymbol{i}'_{\alpha\beta r} = -n_{\text{pp}} \Omega \boldsymbol{J} \boldsymbol{\psi}'_{\alpha\beta r} + \frac{\mathrm{d}}{\mathrm{d}t} \boldsymbol{\psi}'_{\alpha\beta r} \end{cases} \tag{187}$$

where note the subscripts d and q are replaced with new subscripts α and β to emphasize the fact $\theta_d = 0$. Note from now on, symbol α no longer denotes the angular location in air gap, symbol β no longer stands for the per unit pole arc, whereas they are the axes of the $\alpha\beta$-frame.

2.12. Steady State Behavior of Induction Machine

It can be shown that at steady state, when all variables in $\alpha\beta$-frame are sinusoidal with angular speed of ω_{syn}, it is valid to simply do the following substitution:

$$\frac{\mathrm{d}}{\mathrm{d}t} = \boldsymbol{J} \omega_{\text{syn}} \tag{188}$$

The steady state voltage equation becomes:

$$(188) \Rightarrow \begin{cases} \boldsymbol{u}_{\alpha\beta s} - R \boldsymbol{i}_{\alpha\beta s} = \boldsymbol{J} \omega_{\text{syn}} \boldsymbol{\psi}_{\alpha\beta s} \\ \boldsymbol{u}'_{\alpha\beta r} - R'_r \boldsymbol{i}'_{\alpha\beta r} = (\omega_{\text{syn}} - n_{\text{pp}} \Omega) \boldsymbol{J} \boldsymbol{\psi}'_{\alpha\beta r} \end{cases} \tag{189}$$

2.12.1. The T Equivalent Circuit of Induction Machine

When drawing the equivalent circuit of the voltage equations (see Fig. 10), the following derivation is useful:

$$\begin{aligned} \boldsymbol{u}_{\alpha\beta s} - R \boldsymbol{i}_{\alpha\beta s} &= \boldsymbol{J} \omega_{\text{syn}} \boldsymbol{\psi}_{\alpha\beta s} \\ &= \boldsymbol{J} \omega_{\text{syn}} L_{ls} \boldsymbol{i}_{\alpha\beta s} + \boldsymbol{J} \omega_{\text{syn}} L_m \left(\boldsymbol{i}_{\alpha\beta s} + \boldsymbol{i}'_{\alpha\beta r} \right) \qquad (190) \\ \boldsymbol{u}'_{\alpha\beta r} - R'_r \boldsymbol{i}'_{\alpha\beta r} &= (\omega_{\text{syn}} - n_{\text{pp}} \Omega) \boldsymbol{J} \boldsymbol{\psi}'_{\alpha\beta r} \\ &= \boldsymbol{J} \omega_{\text{syn}} L'_{lr} \boldsymbol{i}'_{\alpha\beta r} + \boldsymbol{J} \omega_{\text{syn}} L_m \left(\boldsymbol{i}_{\alpha\beta s} + \boldsymbol{i}'_{\alpha\beta r} \right) - n_{\text{pp}} \Omega \boldsymbol{J} \boldsymbol{\psi}'_{\alpha\beta r} \qquad (191) \end{aligned}$$

The last voltage term in (191) is not in synchronous speed and therefore it seems it cannot be represented as electrical component in the equivalent circuit. In fact, it is closely related to the electromagnetic torque. To see this, let's derive the torque expression in terms of rotor side variables [recall the results in (181)]:

$$\begin{aligned}
T_{\text{em}} &= n_{\text{pp}}\left(L_s\boldsymbol{i}_{dqs} + L_m\boldsymbol{i}'_{dqr}\right)\times\boldsymbol{i}_{dqs} = n_{\text{pp}}L_m\boldsymbol{i}'_{dqr}\times\boldsymbol{i}_{dqs}\\
&= n_{\text{pp}}\frac{L_m}{L_r}L_r\boldsymbol{i}'_{dqr}\times\boldsymbol{i}_{dqs} = n_{\text{pp}}\frac{L_m}{L_r}\left(L_m\boldsymbol{i}_{dqs} + L_r\boldsymbol{i}'_{dqr}\right)\times\boldsymbol{i}_{dqs}\\
&= n_{\text{pp}}\frac{L_m}{L_r}\boldsymbol{\psi}'_{dqr}\times\boldsymbol{i}_{dqs} \equiv n_{\text{pp}}\frac{L_m}{L_r}\boldsymbol{\psi}'_{\alpha\beta r}\times\boldsymbol{i}_{\alpha\beta s}\\
&= n_{\text{pp}}\frac{L_m}{L_r}\boldsymbol{\psi}'_{\alpha\beta r}\times\frac{\boldsymbol{\psi}'_{\alpha\beta r} - L_r\boldsymbol{i}'_{\alpha\beta r}}{L_m}\\
&= n_{\text{pp}}\boldsymbol{\psi}'_{\alpha\beta r}\times\left(-\boldsymbol{i}'_{\alpha\beta r}\right) = n_{\text{pp}}\left(\boldsymbol{J}\boldsymbol{\psi}'_{\alpha\beta r}\right)^T\left(-\boldsymbol{i}'_{\alpha\beta r}\right)\\
&= n_{\text{pp}}\left(\frac{\boldsymbol{u}'_{\alpha\beta r} - R'_r\boldsymbol{i}'_{\alpha\beta r}}{\omega_{\text{sl}}}\right)^T\left(-\boldsymbol{i}'_{\alpha\beta r}\right)\\
&= n_{\text{pp}}\frac{R'_r}{\omega_{\text{sl}}}\boldsymbol{i}'^T_{\alpha\beta r}\boldsymbol{i}'_{\alpha\beta r} = n_{\text{pp}}\frac{\omega_{\text{syn}}}{\omega_{\text{sl}}}\frac{R'_r}{\omega_{\text{syn}}}\boldsymbol{i}'^T_{\alpha\beta r}\boldsymbol{i}'_{\alpha\beta r} = n_{\text{pp}}\frac{1}{\omega_{\text{syn}}}\frac{R'_r}{S}\boldsymbol{i}'^T_{\alpha\beta r}\boldsymbol{i}'_{\alpha\beta r}
\end{aligned} \tag{192}$$

where the slip ratio is defined as $S = \omega_{\text{sl}}/\omega_{\text{syn}}$ and the electrical slip angular speed defined as $\omega_{\text{sl}} = \omega_{\text{syn}} - n_{\text{pp}}\Omega$. Note it is possible to introduce the rotational back emf of the rotor circuit: $\boldsymbol{e}^T_{\text{rot}} \triangleq \Omega n_{\text{pp}}\left(\boldsymbol{J}\boldsymbol{\psi}'_{\alpha\beta r}\right)^T$ into (192), which leads to the following results by further evaluating electromagnetic power P_{em}:

$$\begin{aligned}
(192)\Rightarrow P_{\text{em}} = \Omega T_{\text{em}} &= \boldsymbol{e}^T_{\text{rot}}\left(-\boldsymbol{i}'_{\alpha\beta r}\right) = \Omega n_{\text{pp}}\left(\boldsymbol{J}\boldsymbol{\psi}'_{\alpha\beta r}\right)^T\left(-\boldsymbol{i}'_{\alpha\beta r}\right)\\
&= n_{\text{pp}}\frac{\Omega}{\omega_{\text{syn}}}\frac{R'_r}{S}\boldsymbol{i}'^T_{\alpha\beta r}\boldsymbol{i}'_{\alpha\beta r} = \frac{1-S}{S}R'_r\boldsymbol{i}'^T_{\alpha\beta r}\boldsymbol{i}'_{\alpha\beta r}\Rightarrow \text{Fig. 10}
\end{aligned} \tag{193}$$

It turns out the rotational back emf in rotor circuit $\boldsymbol{e}_{\text{rot}}$ can be modelled as the voltage drop across a "mechanical resistance" calculated as $\frac{1-S}{S}R'_r$. The power consumed by the "mechanical resistance" $\frac{1-S}{S}R'_r$ is equal to machine's mechanical power ΩT_{em}, i.e.,

$$\frac{1-S}{S}R'_r\left(\boldsymbol{i}'_{\alpha\beta r}\cdot\boldsymbol{i}'_{\alpha\beta r}\right) = \Omega T_{\text{em}}$$

2.12.2. Complex Number Analysis

In order to do circuit analysis, we are going to map any steady state $\mathbb{R}^2$ circuit variable into a complex number, e.g., the $\alpha\beta$-frame voltage becomes

$$\begin{aligned}
\boldsymbol{u}_{\alpha\beta s} &= \begin{bmatrix} u_{\alpha s}\\ u_{\beta s}\end{bmatrix} = \begin{bmatrix} U\cos\left(\omega_{\text{syn}}t+\phi\right)\\ U\sin\left(\omega_{\text{syn}}t+\phi\right)\end{bmatrix}\\
&\equiv U\cos\left(\omega_{\text{syn}}t+\phi\right) + jU\sin\left(\omega_{\text{syn}}t+\phi\right) = u_{\alpha s} + ju_{\beta s} = U\text{e}^{j(\omega_{\text{syn}}t+\phi)}
\end{aligned} \tag{194}$$

2.12.3. Torque Slip Curve (Mechanical Characteristics of Grid Fed Induction Motor)

It is of interest to derive the torque expression when an induction machine (that is already rotating at a speed Ω) is directly connected to the three phase grid (which is a

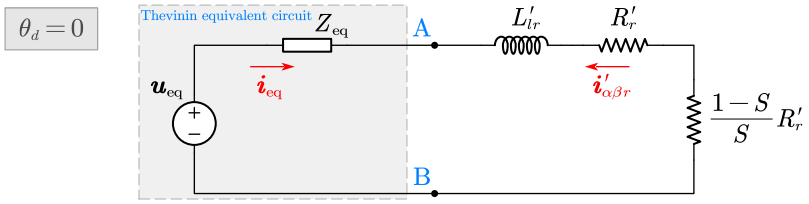

Figure 11. The T-equivalent-circuit of the induction machine at steady state with the network to the left of point A and B has been transformed using an equivalent voltage source $\boldsymbol{u}_{\text{eq}}$ and equivalent impedance Z_{eq}.

constant-voltage, constant-frequency voltage source). In fact, most of the three phase induction machines at service are excited in this way.

To derive a torque expression in terms of its input (which is voltage) instead of inductance state (which is current), we need to use the Ohm's law to eliminate rotor currents in torque (192). The rotor currents can be calculated with the aid of the Thevenin's theorem (see Fig. 11) as

$$\boldsymbol{i}'_{\alpha\beta r} = -\frac{\boldsymbol{u}_{\text{eq}}}{Z_{\text{eq}} + j\omega_{\text{syn}} L'_{lr} + R'_r S^{-1}} \tag{195}$$

where the equivalent voltage and equivalent impedance are:

$$\begin{aligned}
\boldsymbol{u}_{\text{eq}} &= \boldsymbol{u}_{\alpha\beta s} \frac{j\omega_{\text{syn}} L_m}{R + j\omega_{\text{syn}} (L_{ls} + L_m)} \approx \boldsymbol{u}_{\alpha\beta s} \\
Z_{\text{eq}} &= R_{\text{eq}} + jX_{\text{eq}} = \left(\frac{1}{R + j\omega_{\text{syn}} L_{ls}} + \frac{1}{j\omega_{\text{syn}} L_m} \right)^{-1} = \left(\frac{j\omega_{\text{syn}} L_m + R + j\omega_{\text{syn}} L_{ls}}{(R + j\omega_{\text{syn}} L_{ls})\, j\omega_{\text{syn}} L_m} \right)^{-1}
\end{aligned} \tag{196}$$

With the expression for rotor currents available, now the torque as a function of slip S can be derived as:

$$T_{\text{em}}(S) = \frac{n_{\text{pp}}}{\omega_{\text{syn}}} \frac{R'_r}{S} \left| \boldsymbol{i}'_{\alpha\beta r} \right|^2 = \frac{n_{\text{pp}}}{\omega_{\text{syn}}} \frac{R'_r}{S} \frac{\left| \boldsymbol{u}_{\text{eq}} \right|^2}{\left(R_{\text{eq}} + R'_r S^{-1} \right)^2 + \left(X_{\text{eq}} + j\omega_{\text{syn}} L'_{lr} \right)^2} \tag{197}$$

which described the torque-slip curve of an induction machine. An example of the function $T_{\text{em}}(S)$ is plotted in Fig. 12.

The maximum torque is also known as breakdown torque—if the load torque is higher than the maximum torque, the motor operation is going to break down. The

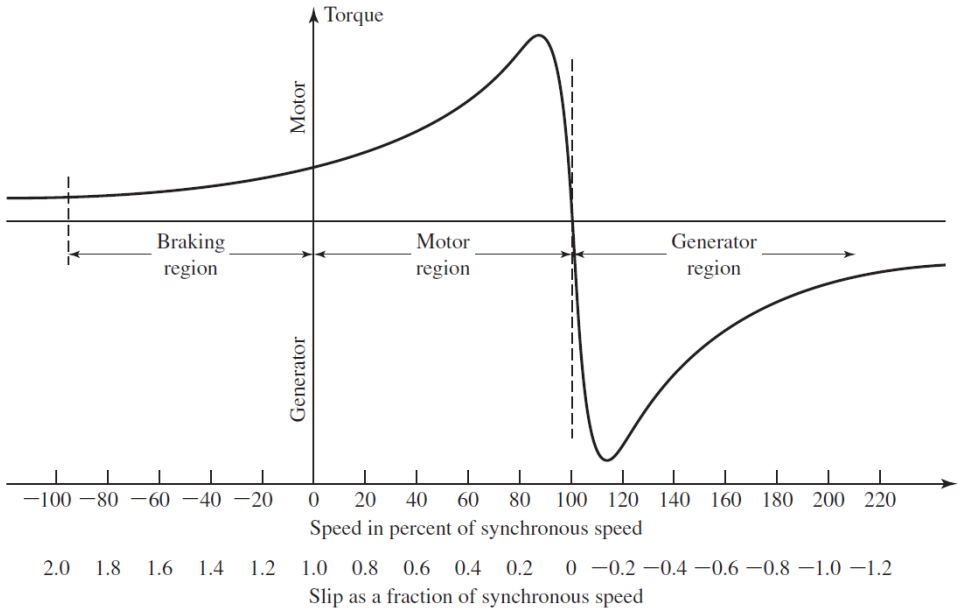

Figure 12. The torque-slip curve for constant-voltage, constant-frequency operation. Figure credit: [4].

breakdown slip corresponding to the breakdown torque is[28]

$$S_{\max T_{\text{em}}} = \frac{R'_r}{\sqrt{R_{\text{eq}}^2 + \left(X_{\text{eq}} + j\omega_{\text{syn}} L'_{lr}\right)^2}} \tag{198}$$

and the breakdown torque is

$$T_{\text{em}}(S_{\max T_{\text{em}}}) = \frac{n_{\text{pp}} \left|\boldsymbol{u}_{\text{eq}}\right|^2}{\omega_{\text{syn}} 2} \frac{1}{\sqrt{R_{\text{eq}}^2 + \left(X_{\text{eq}} + j\omega_{\text{syn}} L'_{lr}\right)^2} + R_{\text{eq}}} \tag{199}$$

[28]The full derivation is

$$\begin{aligned}
T_{\text{em}} &= \frac{n_{\text{pp}}}{\omega_{\text{syn}}} \frac{R'_r}{S} \frac{\left|\boldsymbol{u}_{\text{eq}}\right|^2}{\left(R_{\text{eq}} + \frac{R'_r}{S}\right)^2 + \left(X_{\text{eq}} + j\omega_{\text{syn}} L'_{lr}\right)^2} \\
&= \frac{n_{\text{pp}}}{\omega_{\text{syn}}} \frac{R'_r}{S} \frac{\left|\boldsymbol{u}_{\text{eq}}\right|^2}{R_{\text{eq}}^2 + 2\frac{R'_r}{S} R_{\text{eq}} + \frac{R'^2_r}{S^2} + \left(X_{\text{eq}} + j\omega_{\text{syn}} L'_{lr}\right)^2} \\
&= \frac{n_{\text{pp}} R'_r \left|\boldsymbol{u}_{\text{eq}}\right|^2}{\omega_{\text{syn}}} \frac{1}{S\left[R_{\text{eq}}^2 + \left(X_{\text{eq}} + j\omega_{\text{syn}} L'_{lr}\right)^2\right] + \frac{R'^2_r}{S} + 2R'_r R_{\text{eq}}} \\
&= \frac{n_{\text{pp}} R'_r \left|\boldsymbol{u}_{\text{eq}}\right|^2}{\omega_{\text{syn}}} \frac{1}{SZ^2 + \frac{R'^2_r}{S} + 2R'_r R_{\text{eq}}} \quad \text{with } Z^2 = R_{\text{eq}}^2 + \left(X_{\text{eq}} + j\omega_{\text{syn}} L'_{lr}\right)^2 \\
\frac{\mathrm{d}T_{\text{em}}}{\mathrm{d}S} &= \frac{n_{\text{pp}} R'_r \left|\boldsymbol{u}_{\text{eq}}\right|^2}{\omega_{\text{syn}}} \frac{-1}{\left(SZ^2 + \frac{R'^2_r}{S} + 2R'_r R_{\text{eq}}\right)^2} \left(Z^2 + \frac{-R'^2_r}{S^2}\right) = 0 \Rightarrow \left(Z^2 + \frac{-R'^2_r}{S^2}\right) = 0 \\
\Rightarrow S &= \pm\frac{R'_r}{Z} = \pm\frac{R'_r}{\sqrt{R_{\text{eq}}^2 + \left(X_{\text{eq}} + j\omega_{\text{syn}} L'_{lr}\right)^2}}
\end{aligned}$$

2.12.4. No Load Test

Let $S = 0$, which can be achieved by connecting the induction motor's shaft to a prime mover that spins at the synchronous speed of the induction motor, and we have

$$\begin{aligned} S = 0 \Rightarrow & \begin{cases} \boldsymbol{u}_{\alpha\beta s} - R\boldsymbol{i}_{\alpha\beta s} = \boldsymbol{J}\omega_{\text{syn}}\boldsymbol{\psi}_{\alpha\beta s} = \boldsymbol{J}\omega_{\text{syn}}\left(L_{ls}\boldsymbol{i}_{\alpha\beta s} + L_m\boldsymbol{i}_{\alpha\beta s}\right) = \boldsymbol{J}\omega_{\text{syn}}L_s\boldsymbol{i}_{\alpha\beta s} \\ \boldsymbol{u}'_{\alpha\beta r} - R'_r\boldsymbol{i}'_{\alpha\beta r} = \boldsymbol{0} \Rightarrow \boldsymbol{i}'_{\alpha\beta r} = \boldsymbol{0} \end{cases} \\ \Rightarrow Z_0 = \frac{\boldsymbol{u}_{\alpha\beta s}}{\boldsymbol{i}_{\alpha\beta s}} &= \frac{R\boldsymbol{i}_{\alpha\beta s} + \boldsymbol{J}\omega_{\text{syn}}L_s\boldsymbol{i}_{\alpha\beta s}}{\boldsymbol{i}_{\alpha\beta s}} = R + \boldsymbol{J}\omega_{\text{syn}}L_s \end{aligned} \tag{200}$$

where we have abused the $\mathbb{R}^2$ vector notation to mean complex number accordingly. As a result, R and L_s can be solved by measuring the no load impedance Z_0.

2.12.5. Blocked Rotor Test

Let $S = 1$, which is done by mechanically blocking the rotor from rotation, and we have [29]

$$Z_L = R_L + \boldsymbol{J}X_L = \frac{\boldsymbol{u}_{\alpha\beta s}}{\boldsymbol{i}_{\alpha\beta s}} = \left(R + \frac{R'_r \left(\omega_{\text{syn}} L_m\right)^2}{{R'_r}^2 + \left(\omega_{\text{syn}} L_r\right)^2} \right) + \boldsymbol{J} \left(\omega_{\text{syn}} L_{ls} + \omega_{\text{syn}} L_m \frac{{R'_r}^2 + \left(\omega_{\text{syn}} L_r\right)\left(\omega_{\text{syn}} L'_{lr}\right)}{{R'_r}^2 + \left(\omega_{\text{syn}} L_r\right)^2} \right) \tag{201}$$

which is not enough for solving the circuit parameters, because there are three unknown parameters L'_{lr}, L_{ls}, R'_r given the two equations.

There is an iteration based solution provided in IEEE Std 112-2004 [13, Sec. 5.9], where an assumption of the form $L_{ls} = kL'_{lr}$ is a must. I have no idea how this iteration trick is derived, but note the iteration itself is no magic while the assumption $L_{ls} = kL'_{lr}$ is the key (which reduces the unknown parameter by one) to our dilemma.

---

[29] The full derivation is here:

$$S = 1$$

$$\Rightarrow \boldsymbol{u}'_{\alpha\beta r} - R'_r \boldsymbol{i}'_{\alpha\beta r} = \omega_{\text{syn}} \boldsymbol{J} \boldsymbol{\psi}'_{\alpha\beta r}$$

$$\Rightarrow \boldsymbol{i}'_{\alpha\beta r} = -\frac{\omega_{\text{syn}}}{R'_r} \boldsymbol{J} \boldsymbol{\psi}'_{\alpha\beta r} = -\frac{\omega_{\text{syn}}}{R'_r} \boldsymbol{J} \left(L_m \boldsymbol{i}_{\alpha\beta s} + L_r \boldsymbol{i}'_{\alpha\beta r} \right)$$

$$\Rightarrow \boldsymbol{i}'_{\alpha\beta r} = -\frac{\omega_{\text{syn}}}{R'_r} \boldsymbol{J} L_m \boldsymbol{i}_{\alpha\beta s} - \frac{\omega_{\text{syn}}}{R'_r} \boldsymbol{J} L_r \boldsymbol{i}'_{\alpha\beta r}$$

$$\Rightarrow \boldsymbol{i}'_{\alpha\beta r} = -\frac{\omega_{\text{syn}}}{R'_r} \boldsymbol{J} L_m \boldsymbol{i}_{\alpha\beta s} \left(1 + \frac{\omega_{\text{syn}}}{R'_r} \boldsymbol{J} L_r \right)^{-1}$$

$$\boldsymbol{u}_{\alpha\beta s} - R \boldsymbol{i}_{\alpha\beta s} = \boldsymbol{J} \omega_{\text{syn}} \boldsymbol{\psi}_{\alpha\beta s} = \boldsymbol{J} \omega_{\text{syn}} L_{ls} \boldsymbol{i}_{\alpha\beta s} + \boldsymbol{J} \omega_{\text{syn}} L_m \left[\boldsymbol{i}_{\alpha\beta s} - \frac{\omega_{\text{syn}}}{R'_r} \boldsymbol{J} L_m \boldsymbol{i}_{\alpha\beta s} \left(1 + \frac{\omega_{\text{syn}}}{R'_r} \boldsymbol{J} L_r \right)^{-1} \right]$$

$$\Rightarrow Z_L = \frac{\boldsymbol{u}_{\alpha\beta s}}{\boldsymbol{i}_{\alpha\beta s}} = R + \boldsymbol{J} \omega_{\text{syn}} L_{ls} + \boldsymbol{J} \omega_{\text{syn}} L_m \left[1 - \frac{\frac{\omega_{\text{syn}}}{R'_r} \boldsymbol{J} L_m}{1 + \frac{\omega_{\text{syn}}}{R'_r} \boldsymbol{J} L_r} \right]$$

$$\Rightarrow Z_L = \frac{\boldsymbol{u}_{\alpha\beta s}}{\boldsymbol{i}_{\alpha\beta s}} = R + \boldsymbol{J} \omega_{\text{syn}} L_{ls} + \boldsymbol{J} \omega_{\text{syn}} L_m \left[\frac{1 + \frac{\omega_{\text{syn}}}{R'_r} \boldsymbol{J} L'_{lr}}{1 + \frac{\omega_{\text{syn}}}{R'_r} \boldsymbol{J} L_r} \right]$$

$$\Rightarrow Z_L = \frac{\boldsymbol{u}_{\alpha\beta s}}{\boldsymbol{i}_{\alpha\beta s}} = R + \boldsymbol{J} \omega_{\text{syn}} L_{ls} + \boldsymbol{J} \omega_{\text{syn}} L_m \frac{\left(1 + \frac{\omega_{\text{syn}}}{R'_r} \boldsymbol{J} L'_{lr} \right) \left(1 - \frac{\omega_{\text{syn}}}{R'_r} \boldsymbol{J} L_r \right)}{1 + \left(\frac{\omega_{\text{syn}}}{R'_r} L_r \right)^2}$$

$$\Rightarrow Z_L = \frac{\boldsymbol{u}_{\alpha\beta s}}{\boldsymbol{i}_{\alpha\beta s}} = R + \boldsymbol{J} \omega_{\text{syn}} L_{ls} + \boldsymbol{J} \omega_{\text{syn}} L_m \frac{\left(1 - \frac{\omega_{\text{syn}}}{R'_r} \boldsymbol{J} L_r \right) + \left(\frac{\omega_{\text{syn}}}{R'_r} \boldsymbol{J} L'_{lr} - \frac{\omega_{\text{syn}}}{R'_r} \boldsymbol{J} L_r \frac{\omega_{\text{syn}}}{R'_r} \boldsymbol{J} L'_{lr} \right)}{1 + \left(\frac{\omega_{\text{syn}}}{R'_r} L_r \right)^2}$$

$$\Rightarrow Z_L = \frac{\boldsymbol{u}_{\alpha\beta s}}{\boldsymbol{i}_{\alpha\beta s}} = R + \boldsymbol{J} \omega_{\text{syn}} L_{ls} + \boldsymbol{J} \omega_{\text{syn}} L_m \frac{1 - \frac{\omega_{\text{syn}}}{R'_r} \boldsymbol{J} L_m + \frac{\omega_{\text{syn}} L_r}{R'_r} \frac{\omega_{\text{syn}} L'_{lr}}{R'_r}}{1 + \left(\frac{\omega_{\text{syn}}}{R'_r} L_r \right)^2}$$

$$\Rightarrow Z_L = \frac{\boldsymbol{u}_{\alpha\beta s}}{\boldsymbol{i}_{\alpha\beta s}} = R + \boldsymbol{J} \omega_{\text{syn}} L_{ls} + \frac{\boldsymbol{J} \omega_{\text{syn}} L_m + \frac{\left(\omega_{\text{syn}} L_m\right)^2}{R'_r} + \frac{\omega_{\text{syn}} L_r}{R'_r} \frac{\omega_{\text{syn}} L'_{lr}}{R'_r} \boldsymbol{J} \omega_{\text{syn}} L_m}{1 + \left(\frac{\omega_{\text{syn}}}{R'_r} L_r \right)^2}$$

$$\Rightarrow Z_L = \frac{\boldsymbol{u}_{\alpha\beta s}}{\boldsymbol{i}_{\alpha\beta s}} = R + \boldsymbol{J} \omega_{\text{syn}} L_{ls} + \frac{\boldsymbol{J} \omega_{\text{syn}} L_m {R'_r}^2 + R'_r \left(\omega_{\text{syn}} L_m\right)^2 + \left(\omega_{\text{syn}} L_r\right)\left(\omega_{\text{syn}} L'_{lr}\right) \boldsymbol{J} \omega_{\text{syn}} L_m}{{R'_r}^2 + \left(\omega_{\text{syn}} L_r\right)^2}$$

$$\Rightarrow Z_L = R_L + \boldsymbol{J} X_L = \left(R + \frac{R'_r \left(\omega_{\text{syn}} L_m\right)^2}{{R'_r}^2 + \left(\omega_{\text{syn}} L_r\right)^2} \right) + \boldsymbol{J} \left(\omega_{\text{syn}} L_{ls} + \frac{\omega_{\text{syn}} L_m {R'_r}^2 + \left(\omega_{\text{syn}} L_r\right)\left(\omega_{\text{syn}} L'_{lr}\right) \omega_{\text{syn}} L_m}{{R'_r}^2 + \left(\omega_{\text{syn}} L_r\right)^2} \right)$$

$$\Rightarrow Z_L = R_L + \boldsymbol{J} X_L = \left(R + \frac{R'_r \left(\omega_{\text{syn}} L_m\right)^2}{{R'_r}^2 + \left(\omega_{\text{syn}} L_r\right)^2} \right) + \boldsymbol{J} \left(\omega_{\text{syn}} L_{ls} + \omega_{\text{syn}} L_m \frac{{R'_r}^2 + \left(\omega_{\text{syn}} L_r\right)\left(\omega_{\text{syn}} L'_{lr}\right)}{{R'_r}^2 + \left(\omega_{\text{syn}} L_r\right)^2} \right)$$

2.12.6. Inverse-Γ Equivalent Circuit of Induction Machine

Let's look at the rotor flux linkage definition and play with the two variables that have been referred to stator, i.e., the two primed symbols—$\boldsymbol{\psi}'_{dqr}$ and $\boldsymbol{i}'_{dqr}$

$$\begin{aligned} \boldsymbol{\psi}'_{dqr} &= L_m \boldsymbol{i}_{dqs} + L_r \boldsymbol{i}'_{dqr} \\ \Rightarrow \frac{L_m}{L_r}\boldsymbol{\psi}'_{dqr} &= \frac{L_m}{L_r} L_m \boldsymbol{i}_{dqs} + \frac{L_m}{L_r} L_m \frac{L_r}{L_m} \boldsymbol{i}'_{dqr} \\ \Rightarrow \boldsymbol{\psi}_{dq\mu} &= L_\mu \boldsymbol{i}_{dqs} + L_\mu \boldsymbol{i}_{dq,\text{req}} \end{aligned} \tag{202}$$

from which, we have reduced the number of unknown circuit parameter by one and L_μ is our new magnetizing inductance. In other words, with a simple change of variables for rotor current and rotor flux linkage:

$$\boldsymbol{i}_{dq,\text{req}} = \left(\frac{L_m}{L_r}\right)^{-1} \boldsymbol{i}'_{dqr} \tag{203}$$

$$\boldsymbol{\psi}_{dq\mu} = \frac{L_m}{L_r}\boldsymbol{\psi}'_{dqr} \tag{204}$$

the electrical circuit of induction machine can be parameterized using only four parameters: $R, L_s, L_\mu, R_\text{req}$ [14], as shown in Fig. 13, where note $L_s - L_\mu$ corresponds to the total leakage inductance, and the definition of equivalent rotor resistance $R_\text{req} \triangleq \frac{L_m^2}{L_r^2} R'_r$ is a natural result by using new variables in rotor voltage equation.

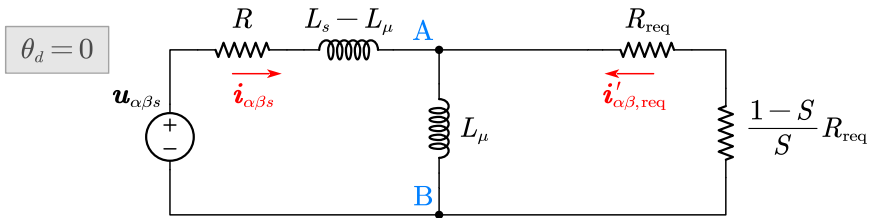

Figure 13. The inverse Γ equivalent circuit of induction machine.

As a result, the blocked rotor test gives an impedance measurement as follows:

$$Z_L = R_L + jX_L = \frac{\boldsymbol{u}_{\alpha\beta s}}{\boldsymbol{i}_{\alpha\beta s}} = \left(R + \frac{R_\text{req}\left(\omega_\text{syn} L_\mu\right)^2}{R_\text{req}^2 + \left(\omega_\text{syn} L_\mu\right)^2}\right) + \boldsymbol{J}\left(\omega_\text{syn}\left(L_s - L_\mu\right) + \omega_\text{syn} L_\mu \frac{R_\text{req}^2}{R_\text{req}^2 + \left(\omega_\text{syn} L_\mu\right)^2}\right) \tag{205}$$

which gives two equations for solving two unknowns of R_req and L_μ (note R and L_s are already known):

$$R_\text{req} = \left[\left(\frac{R_L - R}{X_L - \omega_\text{syn} L_s}\right)^2 + 1\right]\left(R_L - R\right) \tag{206}$$

$$\omega_\text{syn} L_\mu = \sqrt{\frac{\left(R_L - R\right) R_\text{req}^2}{R_\text{req} - \left(R_L - R\right)}} \tag{207}$$

and finally if we assume that the stator leakage inductance is equal to rotor leakage

inductance: $L_{ls} = L'_{lr}$, we can convert the inverse-Γ circuit into T-equivalent circuit:

$$\begin{cases} L_r = L_s \\ L_m = \sqrt{L_\mu L_r} \\ L_{ls} = L_s - L_m \\ L'_{lr} = L_r - L_m \\ R'_r = \left(\frac{L_m}{L_r}\right)^{-2} R_{\text{req}} \end{cases} \tag{208}$$

2.12.7. Improvement with Multiple Measurement of No-Load Data

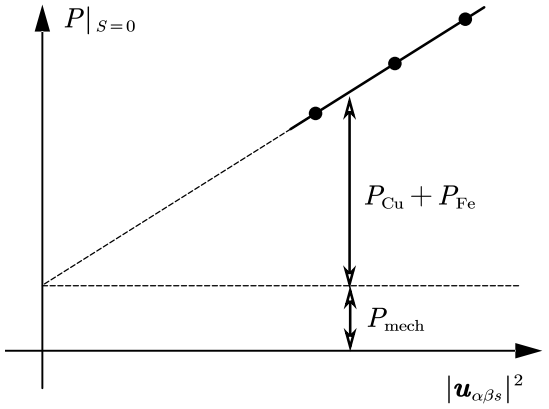

Figure 14. The no-load measurement results of an induction motor at $S \approx 0$. If $S = 0$, then the mechanical power should be $P_{\text{mech}} = 0$, and in this case the friction and windage loss are compensated by another motor coupled to the shaft.

If we have multiple Z_0 measurement at different voltages, draw the no-load power $P|_{S=0}$ versus voltage squared $\boldsymbol{u}_{\alpha\beta s}$ curve, and fit the data points to a straight line, as shown in Fig. 14. It is shown that the no load power consists of three parts:

$$P|_{S=0} = P_{\text{Fe}} + P_{\text{Cu}} + P_{\text{mech}} \tag{209}$$

Since the copper loss power can be easily calculated as $R|\boldsymbol{i}_{\alpha\beta s}|^2$, the iron loss power can be measured approximately as a function of voltage squared. In finite element analysis software (e.g., JMAG Designer), the iron loss power can be calculated as a volume integral using the following loss equation:

$$P_{\text{Fe}} = \int_V \left(K_{\text{hyst}} B^2 f + K_{\text{eddy}} B^2 f^2\right) \mathrm{d}V \tag{210}$$

Since the frequency is fixed to the synchronous value, P_{Fe}'s voltage squared dependency stems from the coefficient of magnetic flux density squared B^2. Example values for the hysteresis loss coefficient and eddy-current loss coefficient are provided for M-19 Gauge 29 steel as follows:

$$\begin{aligned} K_{\text{hyst}} &= 143 \text{ W}/\left(\text{m}^3\text{T}^2\text{Hz}\right) \\ K_{\text{eddy}} &= 0.53 \text{ W}/\left(\text{m}^3\text{T}^2\text{Hz}^2\right) \end{aligned} \tag{211}$$

The iron loss is zero if an ideal magnetic circuit is assumed, so it is not predicted in our derived "linear magnetic circuit" model.

If your experimental data show that the fitted curve has a nonzero intercept with y-axis as is in Fig. 14, this indicates that the condition $S = 0$ is likely violated. In this situation, the no-load test data can still be used by subtracting P_{mech} from $P|_{s=0}$ at all data points.

2.13. DQ Modeling of Permanent Magnet Synchronous Machine

Removing rotor winding from the DQ model (175), i.e., letting $\boldsymbol{i}'_{dqr} = \mathbf{0}$, we have the 2nd-order dq model for permanent magnet synchronous machine:

$$\begin{aligned}
&\theta_d = n_{\text{pp}}\Theta \\
&\boldsymbol{\psi}_{dqs} = \begin{bmatrix} L_d & 0 \\ 0 & L_q \end{bmatrix} \boldsymbol{i}_{dqs} + \begin{bmatrix} \psi_{\text{PM}} \\ 0 \end{bmatrix} \\
&\boldsymbol{u}_{dqs} - R\boldsymbol{i}_{dqs} = \boldsymbol{J}\frac{\mathrm{d}\theta_d}{\mathrm{d}t}\boldsymbol{\psi}_{dqs} + \frac{\mathrm{d}}{\mathrm{d}t}\boldsymbol{\psi}_{dqs} = \boldsymbol{J}\frac{\mathrm{d}\theta_d}{\mathrm{d}t}\left(\begin{bmatrix} L_d i_{ds} + \psi_{\text{PM}} \\ L_q i_{qs} \end{bmatrix}\right) + \frac{\mathrm{d}}{\mathrm{d}t}\left(\begin{bmatrix} L_d & 0 \\ 0 & L_q \end{bmatrix} \boldsymbol{i}_{dqs}\right)
\end{aligned} \tag{212}$$

where recall the parameters L_d and L_q from (144) that include leakage inductance, and the mutual flux linkage due to the PM is defined as $\psi_{\text{PM}} \triangleq L_{dsfr} i_{fr}$.

Unlike induction machine, since L_{dq} is not zero when $\theta_d = 0$, the stationary $\alpha\beta$ model for a PM motor uses inductances defined in (148) (in which the inductance's dependency on rotor angle Θ leads to nonlinear electrical dynamics that are difficult to be analyzed), and is not discussed in this course.

The electrical power flowing into the rotary electromotive force

$$\boldsymbol{J}\frac{\mathrm{d}\theta_d}{\mathrm{d}t}\left(\begin{bmatrix} L_d i_{ds} + \psi_{\text{PM}} \\ L_q i_{qs} \end{bmatrix}\right)$$

is converted into mechanical power via the electromagnetic torque:

$$\begin{aligned}
&T_{\text{em}}\Omega = (\boldsymbol{i}_{dqs})^T \boldsymbol{J}\frac{\mathrm{d}\theta_d}{\mathrm{d}t}\left(\begin{bmatrix} L_d i_{ds} + \psi_{\text{PM}} \\ L_q i_{qs} \end{bmatrix}\right) \\
&\Rightarrow T_{\text{em}} = n_{\text{pp}}\left[\left(L_d i_{ds} + \psi_{\text{PM}}\right) i_{qs} - L_q i_{qs} i_{ds}\right] = n_{\text{pp}}\psi_{\text{PM}} i_{qs} + n_{\text{pp}}\left(L_d - L_q\right) i_{ds} i_{qs}
\end{aligned}$$

in which $n_{\text{pp}}\psi_{\text{PM}} i_{qs}$ is the reaction torque between the PM and the armature, and $n_{\text{pp}}\left(L_d - L_q\right) i_{ds} i_{qs}$ is the reluctance torque due to the saliency: $L_d \neq L_q$.

2.14. Steady State Behavior of Permanent Magnet Synchronous Machine

2.14.1. The Equivalent Circuit and Two Reaction Theory

An attentive equivalent circuit based on the dq model (212) is shown in Fig. 15. Apparently, since the two axes are not symmetric in the presence of rotor saliency, it is better to separate the "vector equivalent circuit" into two component circuit at

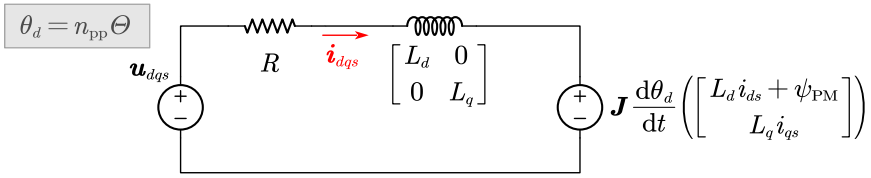

Figure 15. The equivalent circuit of a permanent magnet synchronous machine using (212).

d-axis and q-axis as:

$$\begin{aligned} u_{ds} - Ri_{ds} &= -L_q i_{qs}\frac{\mathrm{d}\theta_d}{\mathrm{d}t} + L_d\frac{\mathrm{d}}{\mathrm{d}t}i_{ds} \\ u_{qs} - Ri_{qs} &= \left(L_d i_{ds} + \psi_{\text{PM}}\right)\frac{\mathrm{d}\theta_d}{\mathrm{d}t} + L_q\frac{\mathrm{d}}{\mathrm{d}t}i_{qs} \end{aligned} \tag{213}$$

The analysis based on the steady-state behaviors using the d-axis equation and q-axis equation, is known as two reaction analysis. At steady state, since phase currents are balanced and sinusoidal, the dq-frame currents are constant, thus (213) becomes

$$\begin{aligned} u_{ds} - Ri_{ds} &= -L_q i_{qs}\omega_{\text{syn}} \\ u_{qs} - Ri_{qs} &= \left(L_d i_{ds} + \psi_{\text{PM}}\right)\omega_{\text{syn}} \end{aligned} \overset{R=0}{\Rightarrow} \begin{cases} i_{qs} = -u_{ds}/\left(\omega_{\text{syn}} L_q\right) \\ i_{ds} = \left(u_{qs} - \omega_{\text{syn}}\psi_{\text{PM}}\right)/\left(\omega_{\text{syn}} L_d\right) \end{cases} \tag{214}$$

where it is often to assume R can be neglected as it is small enough as compared with the reactance, such that a cleaner expression can be derived for dq-currents. Finally, the apparent power S, active power P and reactive power Q can be calculated as voltage times the conjugate of current:

$$S = P + jQ = \left(u_{ds} + ju_{qs}\right)\left(i_{ds} - ji_{qs}\right) = \left(u_{ds}i_{ds} + u_{qs}i_{qs}\right) + j\left(u_{qs}i_{ds} - u_{ds}i_{qs}\right)$$

2.14.2. Power Angle

When the synchronous machine is connected to the grid, it is desired to reveal the relation between the active power (or torque) and the voltage excitation from the grid. To this end, define the power angle δ_P as the angle between the q-axis and the terminal voltage vector $\boldsymbol{u}_{dqs}$[30]

$$\delta_P = \frac{\pi}{2} - \angle\boldsymbol{u}_{dqs} = \frac{\pi}{2} - \arctan\frac{u_{qs}}{u_{ds}} \tag{215}$$

We can rewrite the d-axis and q-axis voltages in terms of power angle as follows:

$$\begin{aligned} u_{qs} &= \left|\boldsymbol{u}_{dqs}\right|\cos\delta_P \\ u_{ds} &= \left|\boldsymbol{u}_{dqs}\right|\sin\delta_P \end{aligned} \tag{216}$$

[30]In the conventional two reaction theory, with the help of steady state phasor diagram, the power angle is derived by subtracting the displacement power factor angle from the internal power factor angle.

Note our derivation is always based on motoring convention, and the active power can be calculated in terms of power angle δ_P as

$$\begin{aligned}
P &= u_{ds}i_{ds} + u_{qs}i_{qs} \\
&= u_{ds}\left(u_{qs} - \omega_{\text{syn}}\psi_{\text{PM}}\right)/\left(\omega_{\text{syn}}L_d\right) - u_{qs}u_{ds}/\left(\omega_{\text{syn}}L_q\right) \\
&= \left(\frac{u_{ds}u_{qs}}{\omega_{\text{syn}}L_d} - \frac{u_{ds}\omega_{\text{syn}}\psi_{\text{PM}}}{\omega_{\text{syn}}L_d}\right) - \frac{u_{qs}u_{ds}}{\omega_{\text{syn}}L_q} \\
&= \left(\frac{|\boldsymbol{u}_{dqs}|\sin\delta_P\,|\boldsymbol{u}_{dqs}|\cos\delta_P}{\omega_{\text{syn}}L_d} - \frac{|\boldsymbol{u}_{dqs}|\sin\delta_P\omega_{\text{syn}}\psi_{\text{PM}}}{\omega_{\text{syn}}L_d}\right) - \frac{|\boldsymbol{u}_{dqs}|\cos\delta_P\,|\boldsymbol{u}_{dqs}|\sin\delta_P}{\omega_{\text{syn}}L_q} \\
&= -|\boldsymbol{u}_{dqs}|\sin\delta_P\frac{\omega_{\text{syn}}\psi_{\text{PM}}}{\omega_{\text{syn}}L_d} + \frac{|\boldsymbol{u}_{dqs}|^2\sin 2\delta_P}{2}\left(\frac{1}{\omega_{\text{syn}}L_d} - \frac{1}{\omega_{\text{syn}}L_q}\right) = \Omega T_{\text{em}}
\end{aligned} \tag{217}$$

where power angle δ_P has to be negative to keep a positive active power P, and in other words, $\boldsymbol{u}_{dqs}$ should be leading to the back electromotive force $\omega_{\text{syn}}j\boldsymbol{\psi}_{dqs}$ to make $P > 0$.

This analysis in terms of power angle is only valid when we assume the excitation is constant voltage and constant frequency, e.g., the grid, and note we have neglected resistance such that $R = 0$.

2.14.3. Power Factor

In theoretical analysis, when we use the term of "power factor", in most cases we mean the displacement power factor, which is defined as the cosine of the angle between the fundamental voltage and current, which is a straightforward idea because we assume electrical variables are sinusoidal:

$$\cos\varphi = \cos\left\langle\boldsymbol{u}_{dqs}, \boldsymbol{i}_{dqs}\right\rangle = \frac{P}{|S|} = \frac{\Omega T_{\text{em}} + |\boldsymbol{i}_{dqs}|^2 R}{|\boldsymbol{u}_{dqs}|\,|\boldsymbol{i}_{dqs}|} \tag{218}$$

where the last equal sign is only valid when there is no rotor resistance and the magnetic circuit is linear.

When the synchronous machine is loaded $i_q \neq 0$, the power factor is not zero even when $i_d = 0$, because some reactive power is inevitably consumed on the q-axis reactance $\omega_{\text{syn}}L_q$ to maintain a nonzero i_q. This can be shown in math language as follows (note $R = 0$ has been assumed):

$$\begin{aligned}
Q &= u_{qs}i_{ds} - u_{ds}i_{qs} = \omega_{\text{syn}}\psi_{\text{PM}}i_{ds} + \omega_{\text{syn}}L_d i_{ds}^2 + \omega_{\text{syn}}L_q i_{qs}^2 \\
Q|_{i_{ds}=0} &= \omega_{\text{syn}}L_q i_{qs}^2
\end{aligned} \tag{219}$$

This q-axis magnetic field is known as the q-axis armature reaction field. We can excite a negative d-axis current to make power factor to be unity:

$$\begin{aligned}
&Q = 0 \Rightarrow L_d i_{ds}^2 + \psi_{\text{PM}}i_{ds} + L_q i_{qs}^2 = 0 \\
&i_{ds} = \frac{-b \pm \sqrt{b^2 - 4ac}}{2a} = \frac{-\psi_{\text{PM}} \pm \sqrt{\psi_{\text{PM}}^2 - 4L_d L_q i_{qs}^2}}{2L_d}
\end{aligned} \tag{220}$$

which will have a real solution for i_{ds} if ψ_{PM} is large enough and i_{qs} is small enough.

The true/distortion power factor that assumes a stiff voltage source, needs to further take the total harmonic distortion of the current THD_i into account to give:

$$\begin{aligned} \text{PF} &= \frac{\cos\varphi}{\sqrt{1+\text{THD}_i^2}} \\ \text{THD}_i &= \frac{\sqrt{\sum_{h=2}^{\infty} I_h^2}}{I_1} \end{aligned} \tag{221}$$

where note I_h is the amplitude of the h-th order harmonic current.

2.14.4. Static Stability of the Synchronous Generator

In most analysis, the grid is assumed to be infinitely large such that the grid voltage applied at the terminal of the synchronous generator is assumed to be invariant and unchanged (i.e., stiff), which makes a perfect reference for phasor analysis. If we take the stator voltage as the reference of the phasor diagram, the angle (with respect to the reference phasor) of the armature current (the q-axis current) phasor is known as the power angle δ_P:

$$\delta_P = \theta_q - \theta_{\boldsymbol{u}\alpha\beta s} = \theta_d + \frac{\pi}{2} - \theta_{\boldsymbol{u}\alpha\beta s} = n_{\text{pp}}\Theta + \frac{\pi}{2} - \theta_{\boldsymbol{u}\alpha\beta s} = \frac{\pi}{2} - \theta_{\boldsymbol{u}dqs} \tag{222}$$

which has redefined the power angle in the stationary $\alpha\beta$ frame. The q-axis is aligned with the rotor field induced emf because emf is 90° leading to the rotor magnetic flux that is chosen as the d-axis.

When the synchronous motor is connected to the grid, it is most likely being used as a generator, and its active power P versus power angle δ_P curve indicates its maximal power before it losses its synchronism, assuming the prime mover is able to provide arbitrary large power P_L. This is equivalently to assume the prime mover's power is a horizontal line in the power versus power angle plot that is based on (217).

If the generator's load power $P_L(\delta_P, \Omega)$ is also a function of the power angle and rotor speed, the stability can ba assessed through linearization[31] of the state space

[31] The linearization of a state space model is based on the Taylor's expansion of a vector field:

$$\begin{aligned} & sx = f(x) \\ \Rightarrow\ & s(x+\Delta x) = f(x+\Delta x) \\ \Rightarrow\ & s(x+\Delta x) = f(x) + \frac{\partial f}{\partial x}(x+\Delta x - x) + \text{H.O.T.} \\ \Rightarrow\ & s\Delta x \approx \frac{\partial f}{\partial x}(\Delta x) \end{aligned}$$

where $\frac{\partial f}{\partial x}$ is the Jacobian matrix.

model of the mechanical system as follows:[32]

$$
\begin{aligned}
&\begin{cases} n_{\mathrm{pp}}\Theta = \delta_P + \theta_{\boldsymbol{u}\alpha\beta s} - \frac{\pi}{2} \\ J_s \frac{\mathrm{d}}{\mathrm{d}t}\Omega = T_{\mathrm{em}}\left(\delta_P\right) - T_L\left(\delta_P, \Omega\right) \end{cases} \\
&\begin{cases} s\delta_P = n_{\mathrm{pp}}\Omega - \omega_{\boldsymbol{u}\alpha\beta s} \\ J_s s\Omega = T_{\mathrm{em}}\left(\delta_P\right) - T_L\left(\delta_P, \Omega\right) \end{cases} \\
&\Rightarrow \begin{cases} s\delta_P = n_{\mathrm{pp}}\Omega - \omega_{\boldsymbol{u}\alpha\beta s} \\ s\Omega = \frac{P_{\mathrm{em}}(\delta_P) - P_L(\delta_P, \Omega)}{J_s \Omega} \end{cases} \\
&\Rightarrow s \begin{bmatrix} \Delta\delta_P \\ \Delta\Omega \end{bmatrix} = \begin{bmatrix} -\frac{\partial \omega_{\boldsymbol{u}\alpha\beta s}}{\partial \delta_P} & n_{\mathrm{pp}} \\ \frac{1}{J_s\Omega}\left(\frac{\partial P_{\mathrm{em}}}{\partial \delta_P} - \frac{\partial P_L}{\partial \delta_P}\right) & \frac{-1}{J_s\Omega}\frac{\partial P_L}{\partial \Omega} \end{bmatrix} \begin{bmatrix} \Delta\delta_P \\ \Delta\Omega \end{bmatrix}
\end{aligned}
\tag{223}
$$

If there exists viscous load torque, then we have $\frac{\partial P_L}{\partial \Omega} = B$, where B is the viscous coefficient. If the grid is assumed to be infinitely large, then we have $\frac{\partial \omega_{\boldsymbol{u}\alpha\beta s}}{\partial \delta_P} = 0$, i.e., the angular speed of the grid voltage is not a function of the power angle of this synchronous machine. Evaluating the eigenvalues, a necessary condition for the system to be stable is to have

$$
\left(\frac{\partial P_{\mathrm{em}}}{\partial \delta_P} - \frac{\partial P_L}{\partial \delta_P}\right) < 0 \tag{224}
$$

based on which, further consider the case $B = 0$, and then the eigenvalues reside in the imaginary axis, in this case we cannot state the stability of the nonlinear state space model through linearization (i.e., small signal analysis), but (224) is still a necessary condition for stability.

2.14.5. Direct Starting of Synchronous Machine

The permanent magnet synchronous machine cannot be directly started from standstill (i.e., $\Omega = 0$) by connecting three phase winding to the grid that is at a fixed electrical frequency of $\omega_{\mathrm{syn}}/(2\pi) = 50$ Hz.

2.15. Parameter Identification Through Impedance Measurement

There are various ways to measure the inductance of a permanent magnet motor, depending on which equipment is used: the LCR meter or the inverter.

---

[32] Click the link and see the phase portrait of the power angle vs. dot power angle:
https://anvaka.github.io/fieldplay/?cx=0.0005999999999999339&cy=-0.
0005999999999999339&w=8.542000000000002&h=8.542000000000002&dt=0.01&fo=0.998&dp=0.
009&cm=3&vf=%2F%2F%20p.x%20and%20p.y%20are%20current%20coordinates%0A%2F%2F%20v.
x%20and%20v.y%20is%20a%20velocity%20at%20point%20p%0Avec2%20get_velocity%28vec2%
20p%29%20%7B%0A%20%20vec2%20v%20%3D%20vec2%280.%2C%200.%29%3B%0A%0A%20%20%2F%2F%
20change%20this%20to%20get%20a%20new%20vector%20field%0A%20%20v.x%20%3D%20p.y%3B%0A%
20%20v.y%20%3D%20%28-10.0*sin%28p.x%29%20-%205.0%29%20%2F%20%28p.y%20%2B%2050.0%29%
3B%0A%0A%20%20return%20v%3B%0A%7D&code=%2F%2F%20p.x%20and%20p.y%20are%20current%
20coordinates%0A%2F%2F%20v.x%20and%20v.y%20is%20a%20velocity%20at%20point%20p%
0Avec2%20get_velocity%28vec2%20p%29%20%7B%0A%20%20vec2%20v%20%3D%20vec2%280.%2C%
200.%29%3B%0A%0A%20%20%2F%2F%20change%20this%20to%20get%20a%20new%20vector%20field%
0A%20%20v.x%20%3D%20p.y%3B%0A%20%20v.y%20%3D%20%2810.0*sin%28p.x%29%20-%205.0%29%20%
2F%20%28p.y%20%2B%2050.0%29%3B%0A%0A%20%20return%20v%3B%0A%7D&pc=50000

2.15.1. Impedance Measurement for Identification of DQ Inductances

Unfortunately, we do not know L_d and L_q and there is no way for a direct measurement. In practice, impedance measurement at the terminals of a Wye-connected three phase machine is feasible.

Let phase 1 to be open and apply the impedance probes to phase 2 and phase 3. This is rewritten in math languages as follows

$$i_1 = 0 \Rightarrow \begin{cases} i_2 = i_Z \\ i_3 = -i_Z \end{cases} \tag{225}$$

In this case, the three phase flux linkages are

$$\begin{bmatrix} \psi_1 \\ \psi_2 \\ \psi_3 \end{bmatrix} = \boldsymbol{L}_{abcs}\boldsymbol{i}_{abcs} = \begin{bmatrix} 0 \\ (L_2 - L_{23})\, i_Z \\ (L_{32} - L_3)\, i_Z \end{bmatrix} \tag{226}$$

Pick a reasonable excitation frequency, e.g., $f_Z = 100$ Hz such that $i_Z = I_Z \sin(2\pi f_Z t)$ is an alternating sinusoidal current. Note I_Z is so small, the motor will be at standstill even without a blocked rotor. The impedance meter will give you a read on the inductance between terminal #2 and #3, which will equal to a linear combination of the phase self- and mutual-inductances:

$$L_{Z1} = \frac{\psi_2 - \psi_3}{i_Z} = (L_2 - L_{23}) - (L_{32} - L_3) = L_2 + L_3 - 2L_{23} \tag{227}$$

Here, we realize that we have never derived an expression for our phase self- and mutual-inductances. It can be calculated using the original definition in terms of winding functions N_1, N_2, N_3 (see (126) and (141)); or, we can apply Park transformation to

$\boldsymbol{L}_{dqns}$. The detailed derivation is shown in the footnote.[33] The phase self-inductances are

$$\begin{aligned} L_1 &= \tfrac{2}{3}\left[L_{\text{ave}} + L_{\text{diff}}\cos\left(2n_{\text{pp}}\Theta\right)\right] + \tfrac{1}{3}L_n \\ L_2 &= \tfrac{2}{3}\left[L_{\text{ave}} + L_{\text{diff}}\cos\left(2n_{\text{pp}}\Theta + \tfrac{2}{3}\pi\right)\right] + \tfrac{1}{3}L_n \\ L_3 &= \tfrac{2}{3}\left[L_{\text{ave}} + L_{\text{diff}}\cos\left(2n_{\text{pp}}\Theta + \tfrac{4}{3}\pi\right)\right] + \tfrac{1}{3}L_n \end{aligned} \tag{228}$$

and the phase mutual-inductances are

$$\begin{aligned} L_{12} &= -\tfrac{1}{2}\tfrac{2}{3}L_{\text{ave}} + \tfrac{2}{3}L_{\text{diff}}\cos\left(2n_{\text{pp}}\Theta - \tfrac{2}{3}\pi\right) + \tfrac{1}{3}L_n \\ L_{13} &= -\tfrac{1}{2}\tfrac{2}{3}L_{\text{ave}} + \tfrac{2}{3}L_{\text{diff}}\cos\left(2n_{\text{pp}}\Theta + \tfrac{2}{3}\pi\right) + \tfrac{1}{3}L_n \\ L_{23} &= -\tfrac{1}{2}\tfrac{2}{3}L_{\text{ave}} + \tfrac{2}{3}L_{\text{diff}}\cos\left(2n_{\text{pp}}\Theta\right) + \tfrac{1}{3}L_n \end{aligned} \tag{229}$$

Now the measurement in (227) can be expressed in terms of L_{ave} and L_{diff}.

---

[33] The phase inductance matrix can be deduced using Park transformation as

$$\boldsymbol{L}_{abcs} = \boldsymbol{T}^{-1}\boldsymbol{L}_{dqns}\boldsymbol{T} = \boldsymbol{T}\left(0\right)^{-1}\boldsymbol{L}_{\alpha\beta\gamma s}\boldsymbol{T}\left(0\right) = \sqrt{\frac{2}{3}}\begin{bmatrix} 1 & 0 & \frac{1}{\sqrt{2}} \\ -\frac{1}{2} & \frac{\sqrt{3}}{2} & \frac{1}{\sqrt{2}} \\ -\frac{1}{2} & -\frac{\sqrt{3}}{2} & \frac{1}{\sqrt{2}} \end{bmatrix}\begin{bmatrix} L_\alpha & L_{\alpha\beta} & 0 \\ L_{\alpha\beta} & L_\beta & 0 \\ 0 & 0 & L_n \end{bmatrix}\sqrt{\frac{2}{3}}\begin{bmatrix} 1 & -\frac{1}{2} & -\frac{1}{2} \\ 0 & \frac{\sqrt{3}}{2} & -\frac{\sqrt{3}}{2} \\ \frac{1}{\sqrt{2}} & \frac{1}{\sqrt{2}} & \frac{1}{\sqrt{2}} \end{bmatrix}$$

$$= \frac{2}{3}\begin{bmatrix} L_\alpha & L_{\alpha\beta} & \frac{1}{\sqrt{2}}L_n \\ -\frac{1}{2}L_\alpha + \frac{\sqrt{3}}{2}L_{\alpha\beta} & -\frac{1}{2}L_{\alpha\beta} + \frac{\sqrt{3}}{2}L_\beta & \frac{1}{\sqrt{2}}L_n \\ -\frac{1}{2}L_\alpha - \frac{\sqrt{3}}{2}L_{\alpha\beta} & -\frac{1}{2}L_{\alpha\beta} - \frac{\sqrt{3}}{2}L_\beta & \frac{1}{\sqrt{2}}L_n \end{bmatrix}\begin{bmatrix} 1 & -\frac{1}{2} & -\frac{1}{2} \\ 0 & \frac{\sqrt{3}}{2} & -\frac{\sqrt{3}}{2} \\ \frac{1}{\sqrt{2}} & \frac{1}{\sqrt{2}} & \frac{1}{\sqrt{2}} \end{bmatrix}$$

$$= \frac{2}{3}\begin{bmatrix} L_\alpha + \frac{1}{2}L_n & -\frac{1}{2}L_\alpha + \frac{\sqrt{3}}{2}L_{\alpha\beta} + \frac{1}{2}L_n & -\frac{1}{2}L_\alpha - \frac{\sqrt{3}}{2}L_{\alpha\beta} + \frac{1}{2}L_n \\ -\frac{1}{2}L_\alpha + \frac{\sqrt{3}}{2}L_{\alpha\beta} + \frac{1}{2}L_n & -\frac{1}{2}\left(-\frac{1}{2}L_\alpha + \frac{\sqrt{3}}{2}L_{\alpha\beta}\right) + \frac{\sqrt{3}}{2}\left(-\frac{1}{2}L_{\alpha\beta} + \frac{\sqrt{3}}{2}L_\beta\right) + \frac{1}{2}L_n & -\frac{1}{2}\left(-\frac{1}{2}L_\alpha + \frac{\sqrt{3}}{2}L_{\alpha\beta}\right) - \frac{\sqrt{3}}{2}\left(-\frac{1}{2}L_{\alpha\beta} + \frac{\sqrt{3}}{2}L_\beta\right) + \frac{1}{2}L_n \\ -\frac{1}{2}L_\alpha - \frac{\sqrt{3}}{2}L_{\alpha\beta} + \frac{1}{2}L_n & -\frac{1}{2}\left(-\frac{1}{2}L_\alpha - \frac{\sqrt{3}}{2}L_{\alpha\beta}\right) + \frac{\sqrt{3}}{2}\left(-\frac{1}{2}L_{\alpha\beta} - \frac{\sqrt{3}}{2}L_\beta\right) + \frac{1}{2}L_n & -\frac{1}{2}\left(-\frac{1}{2}L_\alpha - \frac{\sqrt{3}}{2}L_{\alpha\beta}\right) - \frac{\sqrt{3}}{2}\left(-\frac{1}{2}L_{\alpha\beta} - \frac{\sqrt{3}}{2}L_\beta\right) + \frac{1}{2}L_n \end{bmatrix}$$

$$L_1 = \frac{2}{3}L_\alpha = \frac{L_d + L_q}{3} + \frac{L_d - L_q}{3}\cos\left(2n_{\text{pp}}\Theta\right) + \frac{1}{3}L_n$$

$$L_2 = \frac{2}{3}\left[-\frac{1}{2}\left(-\frac{1}{2}L_\alpha + \frac{\sqrt{3}}{2}L_{\alpha\beta}\right) + \frac{\sqrt{3}}{2}\left(-\frac{1}{2}L_{\alpha\beta} + \frac{\sqrt{3}}{2}L_\beta\right)\right] + \frac{1}{3}L_n$$

$$L_3 = \frac{2}{3}\left[-\frac{1}{2}\left(-\frac{1}{2}L_\alpha - \frac{\sqrt{3}}{2}L_{\alpha\beta}\right) - \frac{\sqrt{3}}{2}\left(-\frac{1}{2}L_{\alpha\beta} - \frac{\sqrt{3}}{2}L_\beta\right)\right] + \frac{1}{3}L_n$$

$$L_3 - \frac{1}{3}L_n = \frac{1}{2}\left(\frac{1}{3}L_\alpha + L_\beta\right) + \frac{\sqrt{3}}{3}L_{\alpha\beta}$$

$$= \frac{1}{2}\left(\frac{1}{3}\frac{L_d + L_q}{2} + \frac{1}{3}\frac{L_d - L_q}{2}\cos\left(2n_{\text{pp}}\Theta\right) + \frac{L_d + L_q}{2} - \frac{L_d - L_q}{2}\cos\left(2n_{\text{pp}}\Theta\right)\right) + \frac{\sqrt{3}}{3}\frac{L_d - L_q}{2}\sin\left(2n_{\text{pp}}\Theta\right)$$

$$= \frac{1}{2}\left(\frac{4}{3}\frac{L_d + L_q}{2} - \frac{2}{3}\frac{L_d - L_q}{2}\cos\left(2n_{\text{pp}}\Theta\right)\right) + \frac{\sqrt{3}}{3}\frac{L_d - L_q}{2}\sin\left(2n_{\text{pp}}\Theta\right)$$

$$= \frac{2}{3}\frac{L_d + L_q}{2} + \frac{2}{3}\frac{L_d - L_q}{2}\left(-\frac{1}{2}\cos\left(2n_{\text{pp}}\Theta\right) + \frac{\sqrt{3}}{2}\sin\left(2n_{\text{pp}}\Theta\right)\right)$$

$$= \frac{2}{3}\frac{L_d + L_q}{2} + \frac{2}{3}\frac{L_d - L_q}{2}\left(\cos\left(-\frac{4}{3}\pi\right)\cos\left(2n_{\text{pp}}\Theta\right) + \sin\left(-\frac{4}{3}\pi\right)\sin\left(2n_{\text{pp}}\Theta\right)\right)$$

$$= \frac{2}{3}\frac{L_d + L_q}{2} + \frac{2}{3}\frac{L_d - L_q}{2}\cos\left(2n_{\text{pp}}\Theta + \frac{4}{3}\pi\right)$$

$$\left(\frac{2}{3}\right)^{-1}L_{12} = -\frac{1}{2}L_\alpha + \frac{\sqrt{3}}{2}L_{\alpha\beta} + \frac{1}{2}L_n = -\frac{1}{2}\frac{L_d + L_q}{2} - \frac{1}{2}\frac{L_d - L_q}{2}\cos\left(2n_{\text{pp}}\Theta\right) + \frac{\sqrt{3}}{2}\frac{L_d - L_q}{2}\sin\left(2n_{\text{pp}}\Theta\right) + \frac{1}{2}L_n$$

$$= -\frac{1}{2}\frac{L_d + L_q}{2} + \cos\left(\frac{2}{3}\pi\right)\frac{L_d - L_q}{2}\cos\left(2n_{\text{pp}}\Theta\right) + \sin\left(\frac{2}{3}\pi\right)\frac{L_d - L_q}{2}\sin\left(2n_{\text{pp}}\Theta\right) + \frac{1}{2}L_n$$

$$= -\frac{1}{2}\frac{L_d + L_q}{2} + \frac{L_d - L_q}{2}\cos\left(2n_{\text{pp}}\Theta - \frac{2}{3}\pi\right) + \frac{1}{2}L_n$$

Repeat the impedance measurement for other two phases, we have the following results:

$$\begin{aligned} L_{Z1} &= 2\left[L_{\text{ave}} - L_{\text{diff}}\cos 2\theta\right] \\ L_{Z2} &= 2\left[L_{\text{ave}} - L_{\text{diff}}\cos 2\left(\theta - \tfrac{2}{3}\pi\right)\right] \\ L_{Z3} &= 2\left[L_{\text{ave}} - L_{\text{diff}}\cos 2\left(\theta - \tfrac{4}{3}\pi\right)\right] \end{aligned} \tag{230}$$

where the electrical rotor angle has been used $\theta \triangleq n_{\text{pp}}\Theta$.

Now, if we slowly rotate the motor shaft such that $\cos 2\theta = 1$, we can have a measurement of L_q, which is the maximum read for a permanent magnet motor.

And if we slowly rotate the motor shaft such that $\cos 2\theta = -1$, we can have a measurement of L_d, which is the minimum read for a permanent magnet motor.

However, those measurement depending on manual rotation of the motor shaft is not always reliable in practice owing to the cogging torque or large shaft inertia. It is desired to have a measurement of L_d and L_q at standstill. To this end, we have the following three equalities using the measurement results L_{Z1}, L_{Z2}, L_{Z3}.

$$\text{Equality 1}: \; {L_{Z1}}^2 + {L_{Z2}}^2 + {L_{Z3}}^2 = 12{L_{\text{ave}}}^2 + 6{L_{\text{diff}}}^2 \tag{231}$$

$$\text{Equality 2}: \; L_{Z1}L_{Z2} + L_{Z2}L_{Z3} + L_{Z3}L_{Z1} = 12{L_{\text{ave}}}^2 - 3{L_{\text{diff}}}^2 \tag{232}$$

$$\text{Equality 3}: \; L_{Z1} + L_{Z2} + L_{Z3} = 6L_{\text{ave}} \tag{233}$$

As a result, we have the following formula for measurement of L_q:

$$\begin{aligned} 6L_q &= L_{Z1} + L_{Z2} + L_{Z3} + 2\sqrt{{L_{Z1}}^2 + {L_{Z2}}^2 + {L_{Z3}}^2 - L_{Z1}L_{Z2} - L_{Z2}L_{Z3} - L_{Z3}L_{Z1}} \\ &= 6L_{\text{ave}} + 2\sqrt{12{L_{\text{ave}}}^2 + 6{L_{\text{diff}}}^2 - \left[12{L_{\text{ave}}}^2 - 3{L_{\text{diff}}}^2\right]} = 6L_{\text{ave}} + 2\sqrt{9{L_{\text{diff}}}^2} \\ &= 6L_{\text{ave}} + 6\left(\pm L_{\text{diff}}\right) \end{aligned} \tag{234}$$

Since we know L_q is larger than L_d for a PM motor, the undetermined sign in last row can be easily determined.

Similarly, L_d can be measured as:

$$6L_d = L_{Z1} + L_{Z2} + L_{Z3} - 2\sqrt{{L_{Z1}}^2 + {L_{Z2}}^2 + {L_{Z3}}^2 - L_{Z1}L_{Z2} - L_{Z2}L_{Z3} - L_{Z3}L_{Z1}} \tag{235}$$

As a side note, the above phase inductance matrix results are expressed in terms of three parameters of $L_{\text{ave}}, L_{\text{diff}}, L_n$. If the phase inductance is derived directly using phase winding functions N_1, N_2, N_3, a different set of parameters denoted by L_{s0}, M_{s0}, L_{s2} can be adopted:

$$\begin{aligned} 1.5L_{s0} &= L_{\text{ave}} + 0.5L_n \\ 1.5L_{s2} &= L_{\text{diff}} \\ 3M_{s0} &= L_n - L_{\text{ave}} \end{aligned} \tag{236}$$

where it is clear that the *dq* inductances are 1.5 times as large as the phase inductance parameters. Those parameters are motivated to provide a clean definition of the phase inductances as follows:

$$\begin{cases} L_1 = L_{s0} + L_{s2}\cos\left(2n_{\text{pp}}\Theta\right) \\ L_2 = L_{s0} + L_{s2}\cos\left(2n_{\text{pp}}\Theta + \frac{2}{3}\pi\right) \\ L_3 = L_{s0} + L_{s2}\cos\left(2n_{\text{pp}}\Theta + \frac{4}{3}\pi\right) \end{cases}$$
$$\begin{cases} L_{12} = M_{s0} + L_{s2}\cos\left(2n_{\text{pp}}\Theta - \frac{2}{3}\pi\right) \\ L_{13} = M_{s0} + L_{s2}\cos\left(2n_{\text{pp}}\Theta + \frac{2}{3}\pi\right) \\ L_{23} = M_{s0} + L_{s2}\cos\left(2n_{\text{pp}}\Theta\right) \end{cases}$$

from which the third parameter (the dc component of the phase mutual inductance) can be derived as: $M_{s0} \triangleq M_\sigma - \frac{1}{2}\left(L_{s0} - L_\sigma\right)$. The impedance measurement becomes:

$$\begin{aligned} L_{Z1} &= 2\left[L_{s0} - M_{s0} - 1.5L_{s2}\cos 2\theta\right] \\ L_{Z2} &= 2\left[L_{s0} - M_{s0} - 1.5L_{s2}\cos 2\left(\theta - \tfrac{2}{3}\pi\right)\right] \\ L_{Z3} &= 2\left[L_{s0} - M_{s0} - 1.5L_{s2}\cos 2\left(\theta - \tfrac{4}{3}\pi\right)\right] \end{aligned} \tag{237}$$

and *dq* inductances become:

$$\begin{aligned} L_d &= L_{\text{ave}} + L_{\text{diff}} = \left(L_{s0} - M_{s0}\right) + 1.5L_{s2} \\ L_q &= L_{\text{ave}} - L_{\text{diff}} = \left(L_{s0} - M_{s0}\right) - 1.5L_{s2} \end{aligned} \tag{238}$$

where it is worth mentioning for PM motor we have $L_{s2} < 0$ (recall $g_2 < 0$).

2.16. Winding Theory for AC Machine

We have been using the coefficient of Fourier analysis, e.g., $N_{(1)}$ to denote the winding function's amplitude. Those coefficients can be calculated using star of slots.

2.16.1. Statement of the Objective

Consider an m-phase stator winding that is going to fit into a Q_s slot stator iron core, and we are expecting it to generate a n_{pp}-pole-pair magnetomotive force as follows:

$$\mathcal{F}_{(1,1)}\left(\alpha, t\right) = \frac{m}{2}N_{(1)}I_{(1)}\cos\left(\alpha - \omega_{\text{syn}}t\right)$$

where the electrical angular location in the air gap is $\alpha = n_{\text{pp}}\alpha_{\text{mech}}$ with α_{mech} the mechanical angular location in the air gap.

Now assume there are z_Q conductors in each stator slot, and the induced electromotive force shares the same amplitude but has different phase angle. The shift in phase angle with respect to a reference conductor (let's say, conductor i) depends on the conductor's angular location (let's say, $i + y$). In particular, the phase shift between two adjacent slots (i.e., the case of $y = 1$) is called as *slot angle* that is calculated as

follows[34]

$$\alpha_{\text{slot}} = h2\pi/Q_s \tag{239}$$

where h is an arbitrary harmonic order number, which could be equal to n_{pp} or not. In the following, we are going to iterate h from 1 to a large enough integer to validate the stator wining's capability to induce electromotive force (or equivalently, generate magnetomotive force) that is h pole pairs.

TODO: How do you prove (239)? The frequency of the electromotive force is much higher when it is induced by the harmonic field that has higher pole pair number than the fundamental. The fundamental field and harmonic field has the same mechanical speed.

2.16.2. Complex Number Pitch Factor

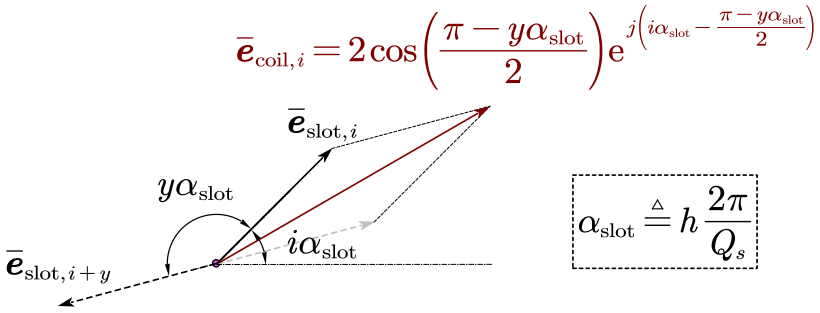

Figure 16. Deriving the complex number pitch factor for the coil whose two sides are respectively placed at slot i and slot $i+y$, i.e., it spans y slots. *This figure is a phasor plot because all the arrows are not rotating or you can say the time elapse is irrelevant in this plot, and only the relative location of the arrows matter.*

Each coil has two coil sides, and the two coil sides cannot be placed in the same slot, otherwise this coil is useless. Consider that one of the coil side is placed in slot i and the other slot $i+y$. We can draw the electromotive force induced in the conductors in these two slots in the DQ plane, but the time elapse does not really matter to us when we are analyzing the capability of a winding. Therefore, we can draw the arrow at any time we like, and we would like to let the arrow indicating the location of the conductor, as is done in Fig. 16, where the electromotive force phasor of conductor in slot i is located at $\alpha = i\alpha_{\text{slot}}$. In Fig. 16, the symbol $\bar{e}_{\text{slot},i}$ denotes a complex number electromotive force phasor of the conductors at slot i. For convenience, we are assuming $\bar{e}_{\text{slot},i}$ has a modulus of unity. Symbol $\bar{e}_{\text{coil},i}$ stands for the complex number electromotive force phasor sum of a coil whose coil sides locates in slot i and slot $i+y$. When doing the phasor sum, please note a simple fact that the two coil sides are connected in reverse series. As a result, the complex number pitch factor of a coil

[34]Imagine there is a harmonic rich field in the air gap moving and the electromotive force's phase difference between the two slots due to different harmonic that moves at the same mechanical speed is h times mechanical slot angle $2\pi/Q_s$.

that spans slot i and slot $i+y$ is:

$$\begin{aligned} \bar{\boldsymbol{k}}_{p,i}(h) &= \cos\left(\frac{\pi - y\alpha_{\text{slot}}}{2}\right) \mathrm{e}^{j\left(i\alpha_{\text{slot}} - \frac{\pi - y\alpha_{\text{slot}}}{2}\right)} \\ \Rightarrow \bar{\boldsymbol{k}}_{p,i}(h) &= \sin\left(\frac{yh\pi}{Q_s}\right) \exp\left\{j\left[\frac{h\pi}{Q_s}(2i+y) - \frac{\pi}{2}\right]\right\} \end{aligned} \tag{240}$$

which is a phasor and has a modulus that is less or equal than 1. The pitch factor shows that a short pitched ($y < \frac{Q_s}{2}$) or long pitched ($y > \frac{Q_s}{2}$) coil always induces less electromotive force (or generates magnetomotive force) than a full pitched coil with $y = \frac{Q_s}{2}$.

Note the pitch factor depends only on winding parameters: coil pitch in slot count y and stator slot number Q_s.

2.16.3. Complex Number Winding Factor

Each phase of winding consists of a group of coils that occupy $1/m$-th of the Q_s slots. In other words, one phase means one coil group. If we take the sum of complex number pitch factors of all coils in the same group, we get the complex number *winding factor* as follows:

$$\begin{aligned} \bar{\boldsymbol{k}}_{w,\mathcal{U}}(h) &= \frac{1}{N_{\mathcal{U}}} \sum_{i \in \mathcal{U}} \bar{\boldsymbol{k}}_{p,i}(h) \\ &\triangleq k_{w,\mathcal{U}}(h) \angle \alpha_{w,\mathcal{U}}(h) \end{aligned} \tag{241}$$

where $\mathcal{U}$ is the set of coil indices belonging to phase U, and $N_{\mathcal{U}}$ is the number of coils of phase U.

2.16.4. Star of Slots Plot

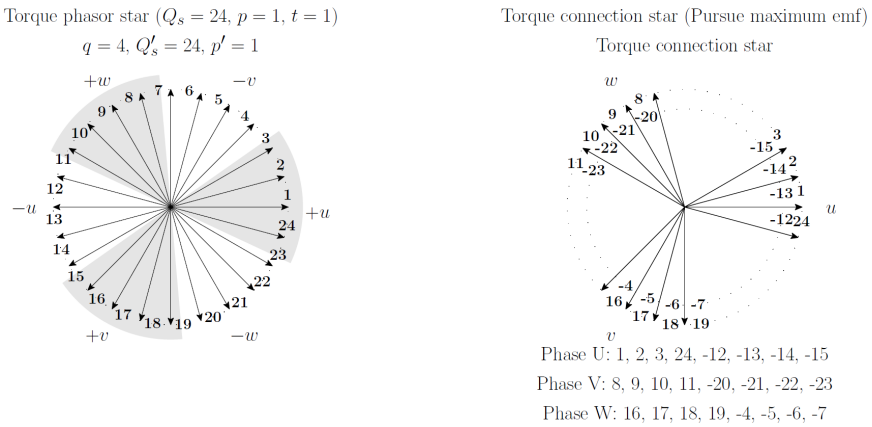

Figure 17. Example star of slots plot for $Q_s = 24$ and $n_{\text{pp}} = 1$. In literature, p is often used to denote n_{pp}. Phase U coil set is $\mathcal{U} = \{i \in \mathbb{N} | 1, 2, 3, 24, -12, 13, 14, 15\}$

We need to figure out a way to assign coils to phase. To this end, let's draw all upper coil side phasor of a coil in the same phasor plot, neglecting the lower coil side phasor (meaning that the pitch factor is not considered yet). Such a phasor plot is known as *star of slots plot*.

Using the open-sourced script[35], we can easily draw star of slots for any winding. For example, for a $Q_s = 24$, $n_{\text{pp}} = 1$ three phase winding, we have the results shown in Fig. 17.

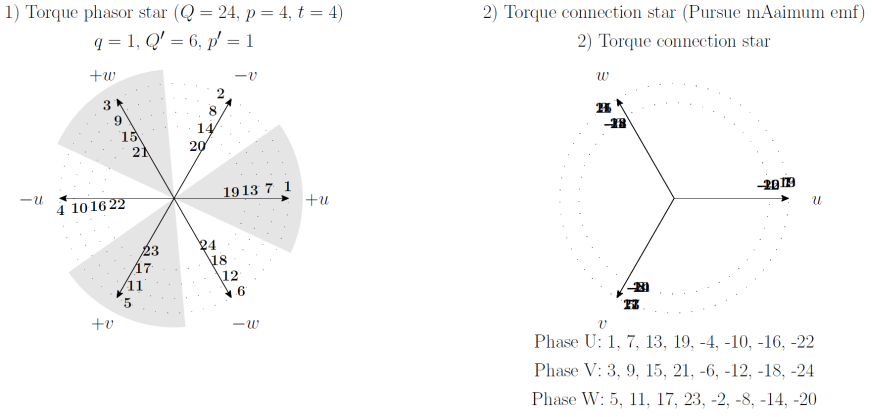

Figure 18. Star of slots plot for $Q_s = 24$ and $n_{\text{pp}} = 4$.

The same stator iron core with $Q_s = 24$ slots can be used to generate a $n_{\text{pp}} = 4$ pole-pair magnetic field, as shown in Fig. 18. Unlike the previous example, now the star phasors repeat $t = 4$ times with $t = \text{GCD}(Q_s, n_{\text{pp}})$.[36] This implies that the trick, for this particular winding, used to generate a four pole pair field is to repeat a one pole pair field four times per mechanical revolution. along the air gap.

[35] https://github.com/horychen/ACMOP/blob/better_framework/codes3/winding_layout_derivation_ismb2021_asymetry.py#L929

[36] GCD stands for greatest common divisor. By the way, the GCD of any two integers can be found by Euclid's algorithm as exemplified in the screenshot below in which Euclid algorithm is used to find the GCD(32769, 77). Credit: @Veritasium.

In the above two examples, the "$2\pi/m/2$ phase band" has been adopted to pursue a larger phasor sum per phase than the less used "$2\pi/m$ phase band". For a three phase winding, the grey area in Figs. 17 and 18 spans 60 degrees and we need to connect the coils in the white are in reverse to the coils in grey area. In order to indicate the connecting direction of the coils, we can draw a *connection star* based off the star of slots plot, as shown in Figs. 17 and 18. From the connection star, we can define the set $\mathcal{U}$ for coil group U, and calculate the winding factor using (241).

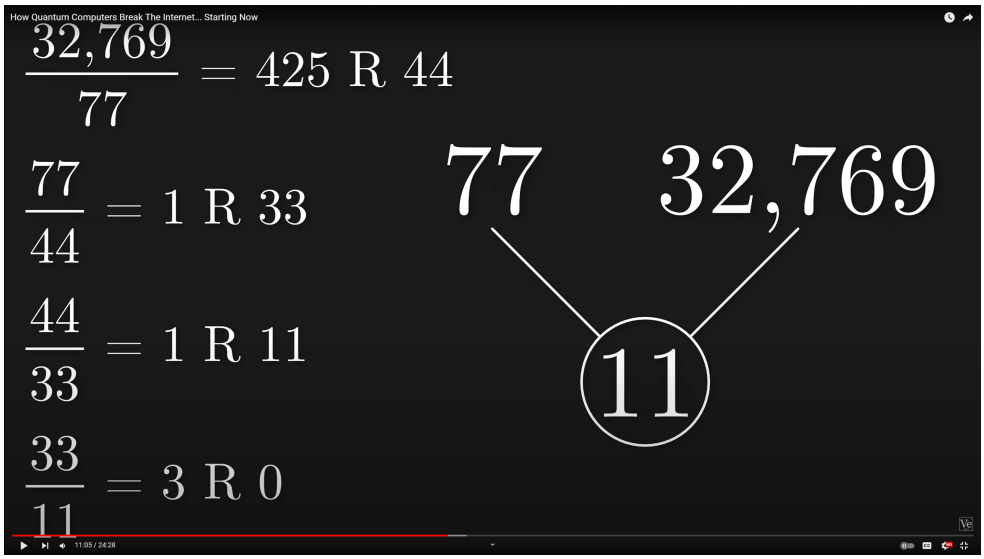

2.16.5. Phase Magnetomotive Force

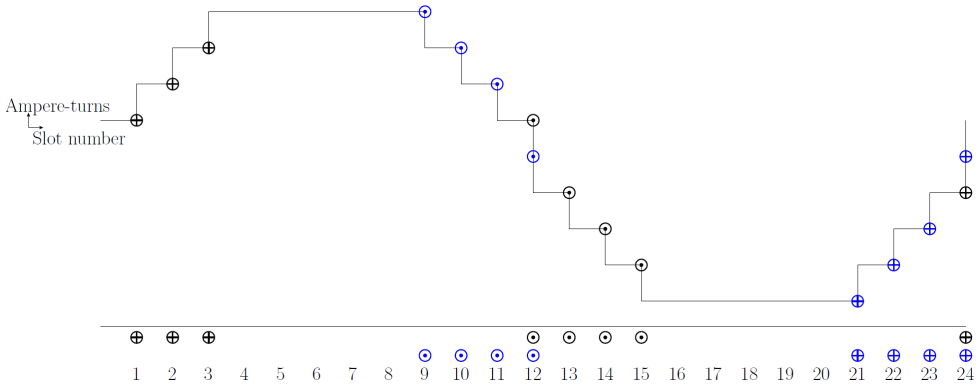

Figure 19. Phase turn function for $Q_s = 24$ and $n_{\text{pp}} = 1$ winding using a short coil pitch $y = 9$.

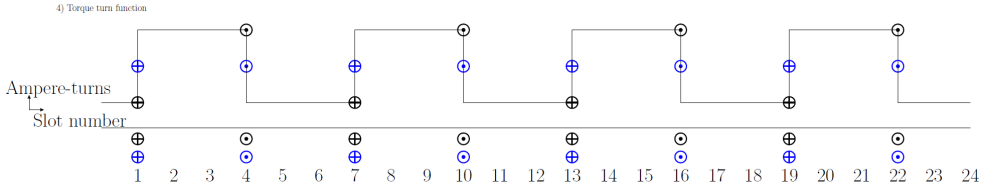

Figure 20. Phase turn function for $Q_s = 24$ and $n_{\text{pp}} = 4$ winding using a full coil pitch $y = 3$.

With the coil group $\mathcal{U}$ available, we need to further specify the coil pitch y to finish the winding design and we can draw turn function, as shown in Figs 19 and 20.

The coefficients of Fourier analysis of the corresponding winding functions can be calculated using the winding factors (241), see Figs 21a and 21b.

Torque winding factor at h freq.:

1: 0.885

3: -0.250

5: -0.079

7: 0.146

9: -0.250

11: 0.048

13: 0.048

15: -0.250

17: 0.146

19: -0.079

21: -0.250

23: 0.885

(a) $n_{\text{pp}} = 1$, and $y = 9$

Torque winding factor at h freq.:

4: 1.000

12: -1.000

20: 1.000

(b) $n_{\text{pp}} = 4$ and $y = 3$

Figure 21. Winding factor modulus $k_w(h)$ (of any phase, since the winding is symmetric). $Q_s = 24$. A consequence of using a $2\pi/m/2$ phase band (such that for any coil there is a same coil placed 180 electrical degrees) is that there is no $h = 2n_{\text{pp}}$ harmonic field.

2.16.6. Winding Layout

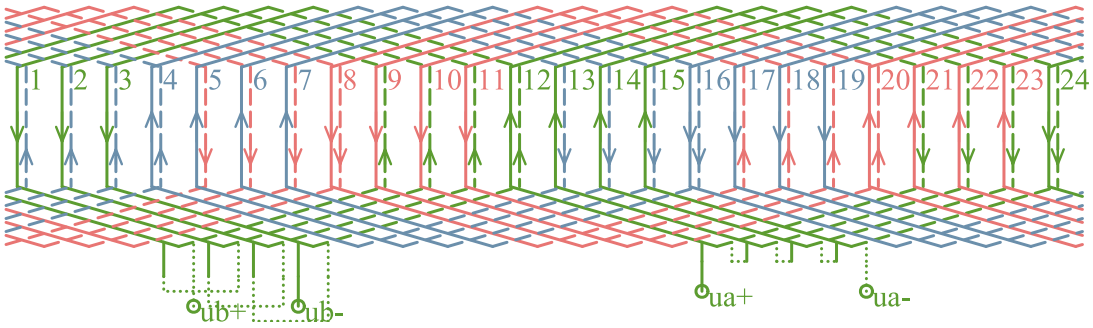

(a) $Q_s = 24$, $n_{\text{pp}} = 1$, and $y = 9$.

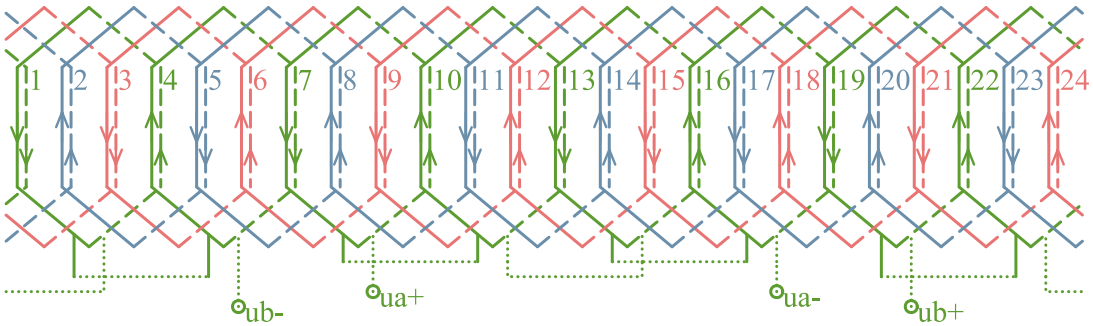

(b) $Q_s = 24$, $n_{\text{pp}} = 4$ and $y = 3$

Figure 22. Winding layout for phase U.

The winding layout or diagram is required by the electric machine manufacturer. In particular, machine designer needs to specify the terminals of the winding, see Figs 22a and 22b. For a coil group consists of a coils, we can choose to connect all a coils in parallel. For example, in Figs 22a and 22b, if we connect the ua coil group and ub coil group in parallel, the number of parallel branch is equal to $a = 2$.

As can be seen in the layout plot, a winding with large y value tends to have more "overlap" in the end winding region, such that the axial length of the winding is increased. One benefit to use $y = 1$ winding (a.k.a., coil wound winding) is to save axial length space in end winding region.

3. Chapter 3: Nonlinear Control for Electric Machine

We now have the model, winning us a ticket entering the world of model based control.

3.1. Motor Control: a Perspective (Part I)

There is a survey paper by Åström and Kumar (2014) published in Automatica [15], in which various control techniques developed for different models and environments are reviewed. I have heard multiple times complains about how the control theory has been developed disconnected from control target in real life. Fortunately, we have a real control target with its grey box model already available, and that's what makes engineer a satisfactory job.

Before we really work on motor control problem, it is high time to learn some professional keywords or ideas used in control theory. As a notation convention, we are going to use the time derivative operator $s = \frac{\mathrm{d}}{\mathrm{d}t}$.[37]

3.1.1. Regulator Problem

Design a control law for the control input T_{em} to regulate the state Ω, whose undisturbed dynamics are

$$s\Omega = \frac{1}{J_s}\left(T_{\mathrm{em}} - 0\right) \tag{242}$$

towards a constant command or reference signal $\Omega^* = \mathrm{Const}$.

If you have no clue what to do with a control problem, it is often a good idea to write down its control error dynamics:

$$se_\Omega = s\left(\Omega - \Omega^*\right) = \frac{1}{J_s}\left(T_{\mathrm{em}}\right) - s\Omega^* = \frac{1}{J_s}\left(T_{\mathrm{em}}\right) - 0 = -K_P e_\Omega \tag{243}$$

which motivates us to use a simple feedback control law

$$T_{\mathrm{em}} = -J_s K_P e_\Omega \tag{244}$$

with a proportional gain $K_P > 0$, such that the closed loop controlled system stays linear.

To predict how the error e_Ω evolves, recall basics in solving an ODE (that is, we need find an analytical function whose derivative is proportional to itself) and its analytical solution is:

$$e_\Omega(t) = e_\Omega(0)\exp(-K_P t) \tag{245}$$

which means the control error exponentially converges to null. The convergence rate of $e_\Omega(t)$ [see (245)] or the pole of the linear system (243) (which is $-K_P$) can be arbitrarily set if a continuous control system is implemented, provided J_s is perfectly known (otherwise the pole location has uncertainty due to the mismatched inertia parameter used).

[37] Note s is Laplace variable rather than Laplace operator. If you wonder what is a Laplace operator, search this PDF document to find out.

3.1.2. Lyapunov Stability and Lyapunov Function

Generally speaking, we should not expect an analytical solution can be derived and we do not really need it anyhow.

Our truly desired property is the closed loop system having property of "error modulus converging to zero", which is closely related to the core concept in control theory, the stability. For a linear system, its stability is evaluated by inspecting the negativity of the real parts of the poles. For nonlinear system, however, the negativity of the changing rate of an auxiliary energy function is evaluated to see if the system is stable in the sense of Lyapunov.

As an example, define an energy function $V = \frac{1}{2}e_\Omega^2$ for (243), and its time derivative along the error dynamics (243) is as follows

$$sV = e_\Omega s e_\Omega = -K_P e_\Omega^2 \tag{246}$$

which is negative everywhere except at $e_\Omega = 0$, meaning that $V \geq 0$ is always decreasing until $e_\Omega = 0$. Such a system is said to be asymptotically stable and its function V is called Lyapunov function.[38]

3.1.3. Constant Disturbance Problem and Input-to-State Stability

Further consider the disturbed dynamics

$$s\Omega = \frac{1}{J_s}\left(T_{\text{em}} - T_L\right) \tag{247}$$

and derive a new control law T_{em} to have asymptotically stable control error e_Ω regardless of the unknown disturbance $T_L = \text{Const}$.

The control error dynamics using the old control law (244) become

$$se_\Omega = -K_P e_\Omega - \frac{T_L}{J_s} \tag{248}$$

and we have

$$\begin{aligned} sV = e_\Omega s e_\Omega &= -K_P e_\Omega^2 - e_\Omega \frac{T_L}{J_s} \\ &\leq -K_P e_\Omega^2 + |e_\Omega| \left|\frac{T_L}{J_s}\right| \\ &\leq -K_P e_\Omega^2 + \frac{\varrho}{2}|e_\Omega|^2 + \frac{1}{2\varrho}\left|\frac{T_L}{J_s}\right|^2 \end{aligned} \tag{249}$$

[38] A formal proof of the asymptotical stability needs to refer to Barbalat's Lemma [16].

where the following basic inequality has been used[39]

$$\frac{\varrho}{2}\left|e_\Omega\right|^2+\frac{1}{2\varrho}\left|\frac{T_L}{J_s}\right|^2\geq 2\sqrt{\frac{\varrho}{2}\left|e_\Omega\right|^2}\sqrt{\frac{1}{2\varrho}\left|\frac{T_L}{J_s}\right|^2}=\left|e_\Omega\right|\left|\frac{T_L}{J_s}\right| \tag{250}$$

We choose a positive constant $\varrho<2K_P$ so the positive definiteness of $\frac{\varrho}{2}\left|e_\Omega\right|^2$ is "weak enough" to not cancel the negative definiteness of $-K_P e_\Omega^2$.

Owing to the existence of the unknown disturbance T_L, now sV is negative only when the "error energy" e_Ω^2 is large enough such that

$$e_\Omega^2>\frac{1}{\left(K_P-\frac{\varrho}{2}\right)}\frac{1}{2\varrho}\left|\frac{T_L}{J_s}\right|^2 \tag{251}$$

which leads to an estimate of the converging region for the control error e_Ω in the sense of Lyapunov. In other words, the error would still converge outside the "1D circle" that has a radius of

$$\left|\frac{T_L}{J_s}\right|/\sqrt{2\varrho\left(K_P-\frac{\varrho}{2}\right)} \tag{252}$$

which, however, is larger than the actual radius at which the control error stops to converge. To see this, one can show directly from (248) that the steady state error is

$$\left|e_\Omega(\infty)\right|=\left|\frac{T_L}{J_s}\right|/K_P \tag{253}$$

Both radii in (252) and (253) can be set arbitrarily small if we use arbitrarily large proportional gain K_P, provided a continuous control system is implemented. We call the region beyond the radii the converging region, and apparently, the converging region predicted by the Lyapunov stability is much smaller. This example shows the conservative nature of the Lyapunov stability based analysis.

This steady-state result shows that the disturbed control error state is still stable under unknown disturbance, we may say the dynamics have "disturbance-to-state stability". Note for this particular example, T_L and T_{em} have the same entry in the dynamics (247), that is, they both "accelerate" the rotor shaft, so one may argue it is unfair to call T_L a disturbance rather than an *unknown input*. If we view the disturbance T_L as an input, disturbance-to-state stability becomes *input-to-state stability* (ISS) [16].

3.1.4. Constant Disturbance Problem and Adaptive Control

Writing out the error dynamics (248) does not gives us useful information. However, according to (253), the existence of the disturbance T_L does causes steady state control

[39]There are plenty of proofs. A simple one is

$$\begin{aligned}&a=\frac{a+b}{2}+\frac{a-b}{2}>0;\ b=\frac{a+b}{2}-\frac{a-b}{2}>0\\ \Rightarrow\ &ab=\left(\frac{a+b}{2}+\frac{a-b}{2}\right)\left(\frac{a+b}{2}-\frac{a-b}{2}\right)=\left(\frac{a+b}{2}\right)^2-\left(\frac{a-b}{2}\right)^2\leq\left(\frac{a+b}{2}\right)^2\end{aligned}$$

error $e_\Omega(t)|_{t=\infty}$ that is nonzero as long as T_L is unknown. In turn, we can use this information to produce an estimate of the unknown load torque T_L by integrating the control error over time:

$$s\hat{T}_L = \frac{\gamma_{TL}}{J_s} e_\Omega \tag{254}$$

which is known as the *adaptation law* and is a quite straightforward idea that we update the load torque estimate as long as the speed control error exists.

Now that we got an estimate of the load torque, we shall update the old control law as follows:

$$T_{\text{em}} = -J_s K_P e_\Omega + \hat{T}_L \tag{255}$$

which gives new error dynamics as follows

$$se_\Omega = -K_P e_\Omega - \frac{\tilde{T}_L}{J_s}$$

where $\tilde{T}_L \triangleq T_L - \hat{T}_L$.

To prove the stability of the adaptive control system with the extended error state $\tilde{T}_L$, we shall choose a new quadratic energy function:

$$\begin{aligned}
V &= \frac{1}{2} e_\Omega^2 + \frac{1}{2\gamma_{TL}} \tilde{T}_L^2 \\
&\Rightarrow sV = -K_P e_\Omega^2 - e_\Omega \frac{\tilde{T}_L}{J_s} + \frac{1}{\gamma_{TL}} \tilde{T}_L s\tilde{T}_L \\
&\Rightarrow \begin{cases} sV = -K_P e_\Omega^2 \\ -e_\Omega \frac{\tilde{T}_L}{J_s} + \frac{1}{\gamma_{TL}} \tilde{T}_L s\tilde{T}_L = 0 \end{cases} \\
&\Rightarrow s\tilde{T}_L = sT_L - s\hat{T}_L = \frac{\gamma_{TL}}{J_s} e_\Omega
\end{aligned} \tag{256}$$

where note the adaptation law (254) has been derived; and $sV = -K_P e_\Omega^2$ states that the positive definite function V is going to decrease everywhere except e_Ω is zero. Using Barbalat's Lemma [16], we can shows that as $e_\Omega \to 0$ as $t \to \infty$.

An important fact is that there is no conclusion made for the convergence of $\tilde{T}_L$. In fact, the adaptation rule (254) is designed only to make e_Ω converge to zero. To show the convergence of the load torque estimated error $\tilde{T}_L$, consider an auxiliary function W that is proportional to the derivative of $\tilde{T}_L^2$:

$$\begin{aligned}
W &= \frac{1}{2} s\tilde{T}_L^2 = \tilde{T}_L \left(\frac{\gamma_{TL}}{J_s} e_\Omega \right) \\
\Rightarrow sW &= \left(s\tilde{T}_L \right) \left(\frac{\gamma_{TL}}{J_s} e_\Omega \right) + \tilde{T}_L \left(\frac{\gamma_{TL}}{J_s} se_\Omega \right) \\
&= \left(s\tilde{T}_L \right) \left(\frac{\gamma_{TL}}{J_s} e_\Omega \right) - \tilde{T}_L \frac{\gamma_{TL}}{J_s} \left(K_P e_\Omega + \frac{\tilde{T}_L}{J_s} \right) \\
&= \left(\frac{\gamma_{TL}}{J_s} e_\Omega \right)^2 - \left(\frac{\gamma_{TL}}{J_s} K_P e_\Omega \tilde{T}_L + \frac{\gamma_{TL}}{J_s^2} \tilde{T}_L^2 \right)
\end{aligned} \tag{257}$$

which shows that the error $\tilde{T}_L$ is asymptotically stable according to the Matrosov's theorem [16]. Roughly speaking, when e_Ω has converged to zero such that $W = 0$, meaning the energy of the estimated load torque error, $\frac{1}{2}\tilde{T}_L^2$, is not changing. **Let's assume** $\tilde{T}_L \neq 0$, so we have a *positive* time derivative $sW = \frac{\gamma_{TL}}{J_s^2}\tilde{T}_L^2$, which is the second derivative of $\frac{1}{2}\tilde{T}_L^2$ and means that the changing rate of the load torque error energy $\tilde{T}_L^2$ is increasing. This violates the fact that V is not changing (because $sV = -K_P e_\Omega^2 = 0$). Therefore, $\tilde{T}_L$ must be null and this proves the asymptotical stability of $\tilde{T}_L$.

The condition to keep $sW > 0$ when $\tilde{T}_L \neq 0$ is called *persistency of excitation (PE) condition*. In this simple example, sW is always positive when $\tilde{T}_L \neq 0$ so the PE condition always holds.

3.1.5. The Proportional Integral (PI) Regulator

The above adaptive control is also known as PI regulator. To see this, let's rewrite the adaptive control law:

$$\begin{aligned} T_{\text{em}} &= -J_s K_P e_\Omega - \left(-\hat{T}_L\right) \\ s\left(-\hat{T}_L\right) &= \frac{\gamma_{TL}}{J_s} e_\Omega \\ \Rightarrow T_{\text{em}} &= -\left(J_s K_P + \frac{1}{s}\frac{\gamma_{TL}}{J_s}\right) e_\Omega = \left(P_\Omega + \frac{I_\Omega}{s}\right)(\Omega^* - \Omega) \end{aligned} \tag{258}$$

where P_Ω and I_Ω are two trial-and-error-tuning buttons that are widely commended for not needing to know model parameters.

3.1.6. The Derivative Control

The PI regulator is effective for system with relative degree of 1 with a constant disturbance input. As a counter example, let's change our control objective to control the rotor angle Θ to follow a constant command $\Theta^* = \text{Const.}$:

$$\begin{aligned} s\Theta &= \Omega \\ \Rightarrow se_\Theta = s(\Theta - \Theta^*) &= \Omega - 0 = -K_P e_\Theta \end{aligned} \tag{259}$$

of which the last equation requires we can treat the angular speed Ω as if it is our control input. Due to the existence of inertia, there is no way we can directly set the value of Ω. Alternatively, we need to take a another differentiation to make our actual control input T_{em} appear in the dynamics:

$$(259) \Rightarrow s^2 e_\Theta = s\Omega = \frac{1}{J_s}(T_{\text{em}} - 0) = -K_D s e_\Theta$$

which requires implementing a derivative control: $T_{\text{em}} = -J_s K_D s e_\Theta$. Such a system needing to take twice differentiation until we can modify the dynamics is said to be of relative degree of 2. Apparently, we can show that error dynamics $s^2 e_\Theta = -K_D s e_\Theta$ is not stable.

3.1.7. The Proportional Integral Derivative (PID) Control:

Control Target having Relative Degree of 2

There are different situations in which a PID regulator is needed. We are only considering one relevant example of using PID regulator to control a target with relative degree of 2 here, but keep in mind this is not the only use case of PID regulator.

Let's change our control objective to control the rotor angle Θ to follow a smooth[40] command Θ^*:

$$\begin{aligned} s\Theta &= \Omega \\ s\Omega &= \frac{1}{J_s}\left(T_{\text{em}} - T_L\right) \end{aligned} \tag{260}$$

Now we need to be clear that rotor angle is the output of the system that can be measured and the system (260) has a relative degree of 2, as we need to differentiate the output twice to get input T_{em}.[41] Let

$$\frac{1}{J_s}T_{\text{em}} = -K_P\left(\Theta - \Theta^*\right) - K_D\left(s\Theta - s\Theta^*\right) + s^2\Theta^* + \frac{1}{J_s}\left(-\hat{T}_L\right)$$

and we have a second order rotor angle control error system as follows[42]

$$\begin{aligned} &s^2\Theta = s\Omega = -K_P\left(\Theta - \Theta^*\right) - K_D\left(s\Theta - s\Theta^*\right) + s^2\Theta^* + \left(-\hat{T}_L\right) + \left(-T_L\right) \\ &\Rightarrow s^2 e_\Theta + K_D s e_\Theta + K_P e_\Theta + K_I s^{-1} e_\Theta = 0 \end{aligned} \tag{261}$$

where $e_\Theta \triangleq \Theta - \Theta^*$ and the adaptive control law $-\hat{T}_L = -K_I\frac{1}{s}\left(\Theta - \Theta^*\right)$ is motivated by the previous adaptive control example. Apparently, the introduction of the integral control increases or extends the system order by one.

Now, you can try to find a Lyapunov function for the error dynamics in (261), and soon you will realize it is not trivial to find one candidate, but there is a theorem that assures you that you can find one for it since it is a linear system [17, Theorem A.6]. For linear system $\dot{x} = Ax$, the Lyapunov function is $V = x^T P x$ with $P = \int_0^\infty \mathrm{e}^{A^{\mathrm{T}}t} Q \mathrm{e}^{At}\,\mathrm{d}t$ and Q a proper positive definite matrix, and the time derivative of V along $\dot{x}$ is $\dot{V} = A^{\mathrm{T}}P + PA = -Q$.

3.1.8. Two Degrees-of-Freedom Control

There are two problems about the adaptation law for load torque (254). First, the drive force for adaptation is the control error and it is potentially confused with "initial" regulating error. Second, the load torque disturbance has to be a dc signal or a slow-varying signal.

When there exists a sudden nonzero control error, it could be due to either sudden command change or sudden disturbance. It is desired to separate the two control objectives of command tracking and disturbance rejection, and a control method that achieve two objectives at the same time is called *two degrees-of-freedom control*.

The principle is rather simple: "don't change the command suddenly". That's it. As a result, if there is a sudden control error change, it is due to disturbance.

---

[40] Smooth means the existence of time derivative.

[41] See Lecture 19, EE222 2016, UC Berkeley.

[42] For more information about characteristics of second order system, refer to classic control theory textbook, e.g., Modern Control Engineering (2010) by Katsuhiko Ogata.

3.1.9. Command Tracking

Tracking implies the command is time-varying. There are two basic ideas to have time-varying command that does not sudden change: make sure the command is smooth [e.g., $\Omega^*(t) \in \mathcal{C}^2$], or use a low pass filter to filter your step command. There are alternative topologies (playing with the control blocks) but the basic idea is nothing more than: "don't change the command suddenly".

3.1.10. Faster Disturbance Rejection

Let's now assume the load torque is changing really fast such that we need to literally solve for T_L instantaneously to estimate it:

$$\begin{aligned} &-T_L = J_s s\Omega - T_{\text{em}} \\ &\Rightarrow -\hat{T}_L = Q(s)\left(J_s s\Omega - T_{\text{em}}\right) \\ &\Rightarrow -\hat{T}_L = \frac{\omega_c}{s+\omega_c}\left(J_s s\Omega - T_{\text{em}}\right) \end{aligned} \tag{262}$$

where a low pass filter $Q(s)$ is added to avoid taking pure differentiation of rotor angular speed. This is knows as a *disturbance observer*. The cut-off angular speed ω_c is tuned to adjust the disturbance observer's bandwidth.

3.1.11. Multi-variable Control and Decoupling Control

When there are two states appearing in each other's dynamics...

3.1.12. Input Output Linearizing Problem

The objective of the control design is to track both the speed command and the flux amplitude command.

The main trick here is to use state as the control input. In fact, such a trick has been used when we are deriving the PID control law in (261), where the derivative control is meant to use the state Ω as the control input to rotor angle dynamics $s\Theta$.

3.1.13. Insight from this Course

By learning through this course, students are going to grasp an understanding to the following three statements:

- The integral control is a dynamic control. Dynamic means there is a state introduced in the input variable.
- The derivative control is trick to use state as control input.
- The proportional control is a straightforward idea to use control input to modify the control error's dynamics. It is basically a different name for negative feedback control.

3.2. Field Orientation for AC Motors

The motivation for field orientation is a rather simple idea. The electrical engineers want to have a torque expression for AC motors that is as simple as that of a brushed

DC motor[43]

$$T_{\text{em}} = n_{\text{pp}} \psi_{\text{A}} i_{Ts} \tag{263}$$

where ψ_{A} is the amplitude of the active flux (linkage) and i_{Ts} is the torque producing stator current.

3.2.1. Field Orientation as Aligning d-Axis to a Space Vector

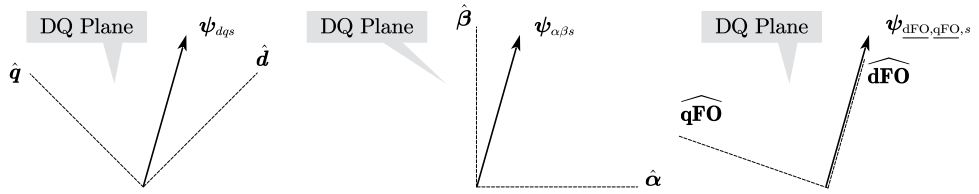

Figure 23. Choices for putting the dq-frame. From left to right: arbitrary θ_d, $\theta_d = 0$, $\theta_d = \theta_{\psi s}$.

As shown in Fig. 23, we have three different choices for putting the dq-frame. It should be emphasized that these three cases are describing exactly the same stator flux linkage space vector that exists in the DQ plane and the only difference is how we put the reference frame. Apparently, the $\widehat{\mathbf{qFO}}$-component of the stator flux linkage is exactly 0. Since the flux linkage space vector corresponds to the magnetic field that exists in the air gap, we call the alignment to a flux linkage space vector as the field orientation (FO). The field oriented frame subscript like $\underline{\text{dFO}}$ is lengthy, thus we shall take advantage of the arbitrariness of the dq-frame to use d instead of $\underline{\text{dFO}}$ in the sequel. Now, we are ready to see if our previously derived DQ models fit (263) or not.

3.2.2. PM Motor: Attempt 1—Stator FO

Let's rewrite the torque expression (185) for an AC machine in rotor oriented dq reference frame:

$$T_{\text{em}} = n_{\text{pp}} \left(\boldsymbol{J} \boldsymbol{\psi}_{dqs} \right)^T \boldsymbol{i}_{dqs} = n_{\text{pp}} \left(-\psi_{qs} i_{ds} + \psi_{ds} i_{qs} \right)$$

If we decide to use i_{qs} as the torque-producing current, we need to choose a field orientation such that the q-axis component of stator flux $\psi_{qs} \equiv 0$. The stator flux vector is not aligned with the rotor field winding (recall the angular position of the rotor field winding defines the rotor angle variable Θ). If we change the rotor orientation to field orientation, the mutual inductance between d-axis and q-axis would be non-zero, i.e., $L_{dq} \neq 0$, resulting in complicated DQ model. In conclusion, stator field orientation is no good for PM motor that has saliency, i.e., $g_2 \neq 0$.

3.2.3. PM Motor: Attempt 2—Rotor FO

For PM motor with saliency, the orientation of the d-axis is not at our disposal, and therefore, we cannot align the d-axis location to stator flux linkage space vector. Let's

[43]For DC motors, this expression is possible because of a physical component called carbon brush that supplies electricity to the rotor armature. The existence of carbon brush limits power rating. For AC motors, such a brush is not needed for armature so AC motors/generators can be made up to a higher power ratings.

get rid of stator flux linkage then.

Consider the PM motor model in rotor oriented dq reference frame:

$$\begin{aligned}
&\theta_d = n_{\text{pp}}\Theta \\
&\boldsymbol{\psi}_{dqs} = \begin{bmatrix} L_d & 0 \\ 0 & L_q \end{bmatrix} \boldsymbol{i}_{dqs} + \begin{bmatrix} \psi_{\text{PM}} \\ 0 \end{bmatrix} \\
&\boldsymbol{u}_{dqs} - R\boldsymbol{i}_{dqs} = \boldsymbol{J}\frac{\mathrm{d}\theta_d}{\mathrm{d}t}\boldsymbol{\psi}_{dqs} + \frac{\mathrm{d}}{\mathrm{d}t}\boldsymbol{\psi}_{dqs} \\
&T_{\text{em}} = n_{\text{pp}}\left[\left(L_d i_{ds} + \psi_{\text{PM}}\right) i_{qs} - L_q i_{qs} i_{ds}\right] = n_{\text{pp}}\psi_{\text{PM}} i_{qs} + n_{\text{pp}}\left(L_d - L_q\right) i_{ds} i_{qs}
\end{aligned}$$

where we have substituted the stator flux linkage expression in the torque expression. Apparently, if we define an active flux amplitude

$$\psi_{\text{A}} = \psi_{\text{PM}} + \left(L_d - L_q\right) i_{ds}$$

we then have

$$T_{\text{em}} = n_{\text{pp}}\psi_{\text{A}} i_{qs}$$

In this case, the q-axis stator current i_{qs} is the torque-producing current i_{Ts}. The unusual property about the new flux variable ψ_{A} is that it is a scalar rather than a $\mathbb{R}^2$ vector. The underlying relation between the new flux variable and the old stator flux variable is:

$$\boldsymbol{\psi}_{dqA} = \begin{bmatrix} \psi_{d\text{A}} \\ \psi_{q\text{A}} \end{bmatrix} = \begin{bmatrix} \psi_{\text{A}} \\ 0 \end{bmatrix} = \boldsymbol{\psi}_{dqs} - L_q \boldsymbol{i}_{dqs} \tag{264}$$

from which we realize that there is no necessity to introduce the $\mathbb{R}^2$ vector and its dq components, and we can eliminate stator flux linkage using ψ_{A} and currents, yielding the following new stator voltage equations

$$\begin{aligned}
s\psi_{\text{A}} + L_q s i_{ds} &= u_{ds} - R i_{ds} + \omega_d L_q i_{qs} \\
\omega_d \psi_{\text{A}} + L_q s i_{qs} &= u_{qs} - R i_{qs} - \omega_d L_q i_{ds}
\end{aligned} \tag{265}$$

with $\omega_d = s\theta_d = n_{\text{pp}} s\Theta$. Note how parameter L_d has disappeared from the model. This result implies that the two reaction theory from chapter 2 is not needed if we introduce a change state variable for flux linkage.

An hidden yet interesting fact is that the active flux vector $\boldsymbol{\psi}_{dqA}$ is aligned with the rotor PM magnetic field in the DQ plane, because their q-axis components in the field oriented frame are both zero, or in math terms they satisfy:

$$\boldsymbol{\psi}_{dqA} = \begin{bmatrix} \psi_{\text{A}} \\ 0 \end{bmatrix} \parallel \boldsymbol{\psi}_{dq\text{PM}} = \begin{bmatrix} \psi_{\text{PM}} \\ 0 \end{bmatrix}$$

Therefore, the original rotor oriented frame for PM motor is in fact a rotor field oriented frame.

3.2.4. Induction Motor: Attempt 1—Stator FO

Since there is no rotor saliency for induction motor, the freedom of definition of dq-frame is now ours. In other words, the d-axis can be arbitrarily placed anywhere in the air gap and therefore, the stator flux orientation seems feasible. That is, let $\psi_{qs} \equiv 0$, such that $T_{\text{em}} = n_{\text{pp}} (0 + \psi_{ds} i_{qs})$. Consequently, the stator voltage equation becomes

$$\begin{aligned} \boldsymbol{u}_{dqs} - R\boldsymbol{i}_{dqs} &= \boldsymbol{J}\frac{\mathrm{d}\theta_d}{\mathrm{d}t}\boldsymbol{\psi}_{dqs} + \frac{\mathrm{d}}{\mathrm{d}t}\boldsymbol{\psi}_{dqs} \\ \Rightarrow &\begin{cases} u_{ds} - Ri_{ds} = 0 + s\psi_{ds} \\ u_{qs} - Ri_{qs} = \omega_d \psi_{ds} + 0 \end{cases} \end{aligned}$$

from which we learn that u_{ds} can be used to control ψ_{ds}, but the control input for the torque producing current i_{qs} seems not clear. In fact, a dynamic control can be adopted to control the dynamics of i_{qs}, such that $u_{qs} = \omega_d \psi_{ds} + Rs^{-1} v_q$, with v_q as the new control input for the q-axis subsystem.

The stator field orientation defines a d-axis angle as follows

$$\begin{aligned} \cos\theta_d &= \frac{\psi_{\alpha s}}{\sqrt{\psi_{\alpha s}^2 + \psi_{\beta s}^2}} \\ \sin\theta_d &= \frac{\psi_{\beta s}}{\sqrt{\psi_{\alpha s}^2 + \psi_{\beta s}^2}} \end{aligned}$$

from which one can verify that we have

$$\boldsymbol{\psi}_{dqs} = \begin{bmatrix} \psi_{ds} \\ \psi_{qs} \end{bmatrix} = \begin{bmatrix} |\boldsymbol{\psi}_{\alpha\beta s}| \\ 0 \end{bmatrix} = \begin{bmatrix} \cos\theta_d & \sin\theta_d \\ -\sin\theta_d & \cos\theta_d \end{bmatrix} \begin{bmatrix} \psi_{\alpha s} \\ \psi_{\beta s} \end{bmatrix}$$

TODO: add figure of torque slip curve here.

3.2.5. Induction Motor: Attempt 2—Rotor FO

Motivated by success of not using stator flux linkage for PM motors, consider an induction motor using inverse Γ circuit parametrization represented in a dq reference frame that uses an orientation such that the q-axis component of the rotor flux linkage is null, i.e., $\psi_{q\mu} \equiv 0$:

$$\begin{aligned} &\boldsymbol{\psi}_{dqs} = (L_s - L_\mu)\, \boldsymbol{i}_{dqs} + \boldsymbol{\psi}_{dq\mu} \\ &\boldsymbol{\psi}_{dq\mu} = L_\mu (\boldsymbol{i}_{dqs} + \boldsymbol{i}_{dq\text{req}}) \Rightarrow \begin{cases} \psi_{d\mu} = L_\mu (i_{ds} + i_{d\text{req}}) \\ \psi_{q\mu} = L_\mu (i_{qs} + i_{q\text{req}}) = 0 \Rightarrow i_{qs} = -i_{q\text{req}} \end{cases} \\ &\boldsymbol{u}_{dqs} - R\boldsymbol{i}_{dqs} = \boldsymbol{J}\frac{\mathrm{d}\theta_d}{\mathrm{d}t}\boldsymbol{\psi}_{dqs} + \frac{\mathrm{d}}{\mathrm{d}t}\boldsymbol{\psi}_{dqs} \\ &0 - R_{\text{req}}\boldsymbol{i}_{dq\text{req}} = \boldsymbol{J}\frac{\mathrm{d}\,(\theta_d - n_{\text{pp}}\Theta)}{\mathrm{d}t}\boldsymbol{\psi}_{dq\mu} + \frac{\mathrm{d}}{\mathrm{d}t}\boldsymbol{\psi}_{dq\mu} \Rightarrow \begin{cases} -R_{\text{req}} i_{d\text{req}} = -(\omega_d - n_{\text{pp}}\Omega)\,\psi_{q\mu} + \frac{\mathrm{d}}{\mathrm{d}t}\psi_{d\mu} \\ -R_{\text{req}} i_{q\text{req}} = (\omega_d - n_{\text{pp}}\Omega)\,\psi_{d\mu} + \frac{\mathrm{d}}{\mathrm{d}t}\psi_{q\mu} \end{cases} \end{aligned}$$

From the q-axis rotor voltage equation, the choice of rotor field orientation leads to a constraint for slip angular speed ω_{sl}:

$$\begin{aligned}
&\psi_{q\mu} = 0 \\
&\Rightarrow -R_{\mathrm{req}} i_{q\mathrm{req}} = (\omega_d - n_{\mathrm{pp}}\Omega)\,\psi_{d\mu} + 0 \\
&\Rightarrow n_{\mathrm{pp}}\Omega - \frac{R_{\mathrm{req}} i_{q\mathrm{req}}}{\psi_{d\mu}} = \omega_d = \frac{\mathrm{d}}{\mathrm{d}t}\theta_d \\
&\Rightarrow n_{\mathrm{pp}}\Omega + \frac{R_{\mathrm{req}} i_{qs}}{\psi_{d\mu}} = \omega_d = \frac{\mathrm{d}}{\mathrm{d}t}\theta_d \\
&\Rightarrow \omega_{\mathrm{sl}} = \frac{R_{\mathrm{req}} i_{qs}}{\psi_{d\mu}} = \omega_d - n_{\mathrm{pp}}\Omega = \omega_{\mathrm{syn}} - n_{\mathrm{pp}}\Omega
\end{aligned} \tag{266}$$

where it has assumed that the angular speed of the rotor field orientated frame ω_d is equal to synchronous angular speed ω_{syn} of current excitation. If you feel uncomfortable about this assumption, keep it in mind, as we will come back to this assumption later.[44]

The torque expression becomes

$$\begin{aligned}
T_{\mathrm{em}} &= n_{\mathrm{pp}} \boldsymbol{J}\boldsymbol{\psi}_{dqs} \cdot \boldsymbol{i}_{dqs} = n_{\mathrm{pp}}\left(-\psi_{qs} i_{ds} + \psi_{ds} i_{qs}\right) \\
&= n_{\mathrm{pp}} \boldsymbol{J}\boldsymbol{\psi}_{dq\mu} \cdot \boldsymbol{i}_{dqs} = n_{\mathrm{pp}}\left(-\psi_{q\mu} i_{ds} + \psi_{d\mu} i_{qs}\right) \\
\Rightarrow T_{\mathrm{em}} &= n_{\mathrm{pp}}\left(-\psi_{q\mu} i_{ds} + \psi_{d\mu} i_{qs}\right) = n_{\mathrm{pp}} \psi_{d\mu} i_{qs} = n_{\mathrm{pp}} \psi_{d\mu} \frac{\psi_{d\mu}\omega_{\mathrm{sl}}}{R_{\mathrm{req}}} = n_{\mathrm{pp}} \psi_{d\mu}^2 \frac{\omega_{\mathrm{syn}}}{R_{\mathrm{req}}} S \\
\Rightarrow T_{\mathrm{em}} &= n_{\mathrm{pp}} \psi_{\mathrm{A}} i_{qs}
\end{aligned}$$

in which we have defined the active flux amplitude $\psi_{\mathrm{A}} = \psi_{d\mu}$ for induction motor. Note the rotor field orientation gives linear mechanical characteristics, a.k.a. torque-slip curve.

3.2.6. Brief Summary: The Rotor Field Oriented Modeling for AC Motors

In order to derive a unified model for two distinct types of AC machines, we need to choose to use the rotor field orientation, as the stator field orientation for PM motor leads to a model with $L_{dq} \neq 0$. Note the rotor oriented frame for PM synchronous motor is in fact also a rotor field oriented frame because the rotor field winding defines the rotor angle Θ.

---

[44] As a side note, the speed of the $\mathbb{R}^2$ vector $\boldsymbol{\psi}_{dq\mu}$ can be calculated by

$$\omega_d = s\theta_d = \mathrm{Im}\left[\frac{s\boldsymbol{\psi}_{dq\mu}}{\boldsymbol{\psi}_{dq\mu}}\right]$$

where note there is no such thing as vector division, so the $\mathbb{R}^2$ vector is interpreted as a complex number as is done chapter 2.

In summary, the induction motor has a fifth order model as follows:

$$\frac{\mathrm{d}}{\mathrm{d}t}\theta_d = \frac{\mathrm{d}}{\mathrm{d}t}\theta_{\boldsymbol{\psi}\mu} = n_{\mathrm{pp}}\Omega + \frac{R_{\mathrm{req}} i_{qs}}{\psi_{d\mu}} \tag{267a}$$

$$s\Omega = \frac{1}{J_s}\left(T_{\mathrm{em}} - T_L\right) = \frac{1}{J_s}\left(n_{\mathrm{pp}}\psi_{d\mu} i_{qs} - T_L\right) \tag{267b}$$

$$\frac{\mathrm{d}}{\mathrm{d}t}\psi_{d\mu} = -R_{\mathrm{req}} i_{d\mathrm{req}} = -R_{\mathrm{req}}\left(L_\mu^{-1}\psi_{d\mu} - i_{ds}\right) \tag{267c}$$

$$\boldsymbol{u}_{dqs} - R\boldsymbol{i}_{dqs} = \boldsymbol{J}\frac{\mathrm{d}\theta_d}{\mathrm{d}t}\left[\left(L_s - L_\mu\right)\boldsymbol{i}_{dqs} + \boldsymbol{\psi}_{dq\mu}\right] + \frac{\mathrm{d}}{\mathrm{d}t}\left[\left(L_s - L_\mu\right)\boldsymbol{i}_{dqs} + \boldsymbol{\psi}_{dq\mu}\right] \tag{267d}$$

where the field orientation is defined using the inverse Γ circuit rotor flux linkage vector such that

$$\cos\theta_d = \frac{\psi_{\alpha\mu}}{\sqrt{\psi_{\alpha\mu}^2 + \psi_{\beta\mu}^2}}$$
$$\sin\theta_d = \frac{\psi_{\beta\mu}}{\sqrt{\psi_{\alpha\mu}^2 + \psi_{\beta\mu}^2}}$$

The name "inverse Γ circuit rotor flux linkage vector" is too long, and we are going to call it "active flux vector" for short: $\psi_{\mathrm{A}} = \psi_{d\mu}$.

The PM synchronous motor has a fourth order model as follows:

$$\begin{aligned}
&\frac{\mathrm{d}}{\mathrm{d}t}\theta_d = n_{\mathrm{pp}}\frac{\mathrm{d}}{\mathrm{d}t}\Theta = n_{\mathrm{pp}}\Omega \\
&s\Omega = \frac{1}{J_s}\left(T_{\mathrm{em}} - T_L\right) = \frac{1}{J_s}\left[n_{\mathrm{pp}}\psi_{\mathrm{A}} i_{qs} - T_L\right] \\
&\psi_A = \psi_{\mathrm{PM}} + \left(L_d - L_q\right) i_{ds} \\
&\boldsymbol{u}_{dqs} - R\boldsymbol{i}_{dqs} = \boldsymbol{J}\frac{\mathrm{d}\theta_d}{\mathrm{d}t}\left(\begin{bmatrix} L_d i_{ds} + \psi_{\mathrm{PM}} \\ L_q i_{qs} \end{bmatrix}\right) + \frac{\mathrm{d}}{\mathrm{d}t}\left(\begin{bmatrix} L_d & 0 \\ 0 & L_q \end{bmatrix}\boldsymbol{i}_{dqs}\right)
\end{aligned} \tag{268}$$

It needs to be emphasized that the two types of machines, given their distinct natures (e.g., different armature excitations), end up with the same field orientation choice, the rotor field orientation, in order to reach a unified torque expression using active flux as follows:

$$T_{\mathrm{em}} = n_{\mathrm{pp}}\psi_{\mathrm{A}} i_{qs}$$

Apparently, the model for induction motor is "nastier" than that of PM motor because there are dynamics for the active flux, i.e., $s\psi_{\mathrm{A}}$. Therefore, we shall take induction motor model for controller design in the sequel, and of course the controller design also applies to the simpler PM motor.

3.3. Direct Rotor Field Oriented Control

Assume that the rotor flux $\boldsymbol{\psi}_{dq\mu}$ is known such that the following cosine and sine values become available

$$\cos\theta_d = \frac{\psi_{\alpha\mu}}{\sqrt{\psi_{\alpha\mu}^2 + \psi_{\beta\mu}^2}}$$
$$\sin\theta_d = \frac{\psi_{\beta\mu}}{\sqrt{\psi_{\alpha\mu}^2 + \psi_{\beta\mu}^2}}$$

The direct rotor field oriented control (DRFOC) is easily achieved by first converting the measured currents $\boldsymbol{i}_{\alpha\beta\gamma s} = \boldsymbol{T}(0)[i_1, i_2, i_3]^T$ into FO dq-frame:

$$\begin{bmatrix} i_{ds} \\ i_{qs} \end{bmatrix} = \begin{bmatrix} \cos\theta_d & \sin\theta_d \\ -\sin\theta_d & \cos\theta_d \end{bmatrix} \begin{bmatrix} i_{\alpha s} \\ i_{\beta s} \end{bmatrix} \tag{269}$$

and then design two independent controllers for the two linear systems that have relative degree of two:

$$\text{Active Flux Subsystem} \quad \begin{cases} s\psi_{d\mu} = -R_{\text{req}} i_{d\text{req}} = -R_{\text{req}} \left(L_\mu^{-1} \psi_{d\mu} - i_{ds} \right) \\ \left(L_s - L_\mu \right) s i_{ds} + s\psi_{d\mu} = u_{ds} - R i_{ds} + \omega_d \left[\left(L_s - L_\mu \right) i_{qs} + \psi_{q\mu} \right] \end{cases} \tag{270}$$

$$\text{Rotor Speed Subsystem} \quad \begin{cases} J_s s\Omega = n_{\text{pp}} \psi_{d\mu} i_{qs} - T_L \\ \left(L_s - L_\mu \right) s i_{qs} + 0 = u_{qs} - R i_{qs} - \omega_d \left[\left(L_s - L_\mu \right) i_{ds} + \psi_{d\mu} \right] \end{cases} \tag{271}$$

where the system input is voltages u_{ds}, u_{qs} and the system output is active flux amplitude $\psi_{d\mu}$ and rotor angular speed Ω.

We haven't derived any control law for the voltage input, but we have already covered the essentials of the field oriented control—the Park transformation to a field oriented reference frame and that's it. This field oriented frame has almost decouples the ac motors into two subsystems.

Note how the output of the active flux subsystem, which is $\psi_{d\mu}$, appears in the rotor angular speed subsystem. Therefore, if we really go with the topology of using two **independent** controllers, it is recommended that we need to first build up a magnetic field before we can control the rotor speed through the ideal linear mechanical characteristics. From the perspective of control, the flux control error $\psi_{d\mu} - \psi_{d\mu}^*$ is a disturbance to the rotor speed subsystem:

$$J_s s\Omega = n_{\text{pp}} \psi_{d\mu}^* i_{qs} - T_L + n_{\text{pp}} \left(\psi_{d\mu} - \psi_{d\mu}^* \right) i_{qs}$$

We will also use the symbol $\psi^* \in \mathbb{R}_+$ to designate the active flux amplitude command.

3.3.1. Active Flux Subsystem

The error dynamics for active flux subsystem to track command ψ^* are

$$s\left(\psi_{d\mu} - \psi^* \right) = R_{\text{req}} i_{ds} - R_{\text{req}} L_\mu^{-1} \psi_{d\mu} - s\psi^* \tag{272}$$

Since the voltage input u_{ds} is not seen yet, further differentiating the dynamics yields

$$s^2\left(\psi_{d\mu}-\psi^*\right)=R_{\text{req}}si_{ds}-R_{\text{req}}L_\mu^{-1}s\psi_{d\mu}-s^2\psi^*=\frac{R_{\text{req}}}{(L_s-L_\mu)}u_{ds}+\Gamma_\psi-s^2\psi^* \quad (273)$$

where the disturbance is

$$\Gamma_\psi=\frac{R_{\text{req}}}{(L_s-L_\mu)}\left(-Ri_{ds}+\omega_d\left[\left(L_s-L_\mu\right)i_{qs}+\psi_{q\mu}\right]+R_{\text{req}}\left(L_\mu^{-1}\psi_{d\mu}-i_{ds}\right)\right)-R_{\text{req}}L_\mu^{-1}s\psi_{d\mu} \quad (274)$$

which consists of known signals thus can be compensated using feedforward control:

$$\frac{R_{\text{req}}}{(L_s-L_\mu)}u_{ds}=-\Gamma_\psi+s^2\psi^*+v_d$$

with the design term v_d being used to modify the error dynamics into a standard second order system using PD control:

$$v_d=-K_P\left(\psi_{d\mu}-\psi^*\right)-K_Ds\left(\psi_{d\mu}-\psi^*\right)$$

3.3.2. Rotor Speed Subsystem

The error dynamics for rotor speed subsystem to track command Ω^* are

$$J_ss\left(\Omega-\Omega^*\right)=n_{\text{pp}}\psi_{d\mu}^*i_{qs}-T_L+n_{\text{pp}}\left(\psi_{d\mu}-\psi_{d\mu}^*\right)i_{qs}-J_s s\Omega^* \quad (275)$$

Since the voltage input u_{qs} is not yet seen, further differentiating the dynamics yields

$$\begin{aligned}J_ss^2\left(\Omega-\Omega^*\right)&=n_{\text{pp}}\psi_{d\mu}^*si_{qs}+n_{\text{pp}}\left(s\psi_{d\mu}^*\right)i_{qs}-sT_L+s\left[n_{\text{pp}}\left(\psi_{d\mu}-\psi_{d\mu}^*\right)i_{qs}\right]-J_ss^2\Omega^*\\&=\frac{n_{\text{pp}}\psi_{d\mu}^*}{(L_s-L_\mu)}u_{qs}+\Gamma_\Omega-J_ss^2\Omega^*+s\left[n_{\text{pp}}\left(\psi_{d\mu}-\psi_{d\mu}^*\right)i_{qs}\right]\end{aligned} \quad (276)$$

where the disturbance is

$$\Gamma_\Omega=\frac{n_{\text{pp}}\psi_{d\mu}^*}{(L_s-L_\mu)}\left\{-Ri_{qs}-\omega_d\left[\left(L_s-L_\mu\right)i_{ds}+\psi_{d\mu}\right]\right\}-sT_L+n_{\text{pp}}\left(s\psi_{d\mu}^*\right)i_{qs} \quad (277)$$

which consists of known signals (and we can make constant load torque assumption $sT_L=0$) thus can be compensated using feedforward control:

$$\frac{n_{\text{pp}}\psi_{d\mu}^*}{(L_s-L_\mu)}u_{qs}=-\Gamma_\Omega+J_ss^2\Omega^*+v_q$$

with the design term v_q being used to modify the error dynamics into a standard second order system using PD control:

$$v_q=-K_P\left(\Omega-\Omega^*\right)-K_Ds\left(\Omega-\Omega^*\right)$$

As a result, the controlled error dynamics become

$$J_ss^2\left(\Omega-\Omega^*\right)+K_Ds\left(\Omega-\Omega^*\right)+K_P\left(\Omega-\Omega^*\right)=s\left[n_{\text{pp}}\left(\psi_{d\mu}-\psi_{d\mu}^*\right)i_{qs}\right] \quad (278)$$

where an uncompensated disturbance appears on the right hand side. This disturbance is nonzero as long as the flux control error is nonzero. This disturbance reveals that the rotor speed subsystem is coupled to the active flux subsystem in a nonlinear fashion.

TODO: If the load torque is unknown, refer to Marino (2010) for load torque estimator design.

3.4. Input Output Feedback Linearizing Control (IOFLC)

From the perspective of speed controller design, the proposal of the idea of rotor field orientation is not natural, because the speed state never appears in the motivation. Let's apply the standard input-output linearizing to derive the controller law to the induction motor model in $\alpha\beta$-frame, pretending we do not know anything about field orientation and Park transformation.

It starts with a change of state variables to this 5th order nonlinear system

$$\begin{aligned}
z_1 &= \Omega \\
z_2 &= pz_1 = J_s^{-1}\left[n_{\text{pp}}\left(\psi_{\alpha\mu}i_{\beta s} - \psi_{\beta\mu}i_{\alpha s}\right) - T_L\right] \\
z_3 &= \psi_{\alpha\mu}^2 + \psi_{\beta\mu}^2 \\
z_4 &= pz_3 = -2\frac{R_{\text{req}}}{L_\mu}\left(\psi_{\alpha\mu}^2 + \psi_{\beta\mu}^2\right) + 2R_{\text{req}}\left(\psi_{\alpha\mu}i_{\alpha s} + \psi_{\beta\mu}i_{\beta s}\right) \\
z_5 &= \arctan\left(\psi_{\beta\mu}/\psi_{\alpha\mu}\right)
\end{aligned} \tag{279}$$

Assume $sT_L = 0$, and the motor dynamics in the new state variables are:

$$\begin{bmatrix} \dot{z}_1 \\ \dot{z}_2 \\ \dot{z}_3 \\ \dot{z}_4 \\ \dot{z}_5 \end{bmatrix} = \begin{bmatrix} z_2 \\ \Gamma_1 \\ z_4 \\ \Gamma_2 \\ \Omega + \frac{R_{\text{req}}(\psi_{\alpha\mu}i_{\beta s} - \psi_{\beta\mu}i_{\alpha s})}{\left(\psi_{\alpha\mu}^2 + \psi_{\beta\mu}^2\right)} \end{bmatrix} + \begin{bmatrix} 0 & 0 \\ \frac{1}{(L_s - L_\mu)J_s} & 0 \\ 0 & 0 \\ 0 & \frac{2R_{\text{req}}}{(L_s - L_\mu)} \\ 0 & 0 \end{bmatrix} \begin{bmatrix} -\psi_{\beta\mu} & \psi_{\alpha\mu} \\ \psi_{\alpha\mu} & \psi_{\beta\mu} \end{bmatrix} \begin{bmatrix} u_{\alpha s} \\ u_{\beta s} \end{bmatrix} \tag{280}$$

where terms like Γ_1 and Γ_2 are internal disturbances that are assumed known:

$$\begin{aligned}
J_s\Gamma_1 &= -\frac{1}{(L_s - L_\mu)}\Omega\left(\psi_{\alpha\mu}^2 + \psi_{\beta\mu}^2\right) - \left(\frac{R_{\text{req}}}{L_\mu} + \frac{R + R_{\text{req}}}{(L_s - L_\mu)}\right)\left(\psi_{\alpha\mu}i_{\beta s} - \psi_{\beta\mu}i_{\alpha s}\right) - \Omega\left(\psi_{\alpha\mu}i_{\alpha s} + \psi_{\beta\mu}i_{\beta s}\right) \\
\Gamma_2 &= \frac{R_{\text{req}}^2}{L_\mu^2}\left(4 + 2\frac{L_\mu}{(L_s - L_\mu)}\right)\left(\psi_{\alpha\mu}^2 + \psi_{\beta\mu}^2\right) + 2R_{\text{req}}\Omega\left(\psi_{\alpha\mu}i_{\beta s} - \psi_{\beta\mu}i_{\alpha s}\right) \\
&\quad - \left(6\frac{R_{\text{req}}^2}{L_\mu} + 2R_{\text{req}}\frac{R + R_{\text{req}}}{(L_s - L_\mu)}\right)\left(\psi_{\alpha\mu}i_{\alpha s} + \psi_{\beta\mu}i_{\beta s}\right) + 2R_{\text{req}}^2\left(i_{\alpha s}^2 + i_{\beta s}^2\right)
\end{aligned} \tag{281}$$

which can be compensated using feedforward control. Let's introduce a feedforward controller as follows

$$\begin{aligned}
\begin{bmatrix} u_{\alpha s} \\ u_{\beta s} \end{bmatrix} &= \frac{1}{\psi_{\alpha\mu}^2 + \psi_{\beta\mu}^2}\begin{bmatrix} -\psi_{\beta\mu} & \psi_{\alpha\mu} \\ \psi_{\alpha\mu} & \psi_{\beta\mu} \end{bmatrix}\begin{bmatrix} u_{qs}^* \\ u_{ds}^* \end{bmatrix} \\
&= \frac{1}{\psi_{\alpha\mu}^2 + \psi_{\beta\mu}^2}\begin{bmatrix} -\psi_{\beta\mu} & \psi_{\alpha\mu} \\ \psi_{\alpha\mu} & \psi_{\beta\mu} \end{bmatrix}\begin{bmatrix} J_s\left(L_s - L_\mu\right)\left(-\Gamma_1 + v_\alpha\right) \\ \frac{(L_s - L_\mu)}{2R_{\text{req}}}\left(-\Gamma_2 + v_\beta\right) \end{bmatrix}
\end{aligned} \tag{282}$$

where the intermediate controller commands u_{qs}^*, u_{ds}^* has been defined for ease of comparison to DRFOC, but note their dimensions are not V but VWb, and $v_\alpha,\ v_\beta$ are the outputs of a PD tracking controller. After the feedforward compensation, the feedforward compensated dynamics become

$$\begin{bmatrix} \dot{z}_1 \\ \dot{z}_2 \\ \dot{z}_3 \\ \dot{z}_4 \\ \dot{z}_5 \end{bmatrix} = \begin{bmatrix} z_2 \\ v_\alpha \\ z_4 \\ v_\beta \\ \Omega + R_{\text{req}} \left(J_s z_2 + T_L\right)/z_3 \end{bmatrix} \tag{283}$$

based on which, by using "deep" state as control input to a "shallow" state,[45] we have the following controller law design for v_α and v_β

$$\begin{aligned} v_\alpha &= -k_{\omega P}\left(\Omega - \Omega^*\right) - k_{\omega D} J_s^{-1}\left[\left(\psi_{\alpha\mu} i_{\beta s} - \psi_{\beta\mu} i_{\alpha s}\right) - T_L - J_s s\Omega^*\right] + s^2\Omega^* \\ v_\beta &= -k_{\psi P}\left[\left(\psi_{\alpha\mu}^2 + \psi_{\beta\mu}^2\right) - \psi^{*2}\right] - k_{\psi D}\left[-2\alpha\left(\psi_{\alpha\mu}^2 + \psi_{\beta\mu}^2\right) + 2\alpha M\left(\psi_{\alpha\mu} i_{\alpha s} + \psi_{\beta\mu} i_{\beta s}\right) - 2\psi^*\dot{\psi}^*\right] + 2\dot{\psi}^{*2} + 2\psi^*\ddot{\psi}^* \end{aligned} \tag{284}$$

where note expressions for $s\Omega$ and sz_3 have been substituted, and therefore the external disturbance T_L appears (and we have to assume T_L is known for this controller design). Finally, the controlled error dynamics are

$$\begin{aligned} &s^2\left(\Omega - \Omega^*\right) + k_{\omega D} s\left(\Omega - \Omega^*\right) + k_{\omega P}\left(\Omega - \Omega^*\right) = 0 \\ &s^2\left(\psi_{\alpha\mu}^2 + \psi_{\beta\mu}^2 - \psi^{*2}\right) + k_{\psi D} s\left(\psi_{\alpha\mu}^2 + \psi_{\beta\mu}^2 - \psi^{*2}\right) + k_{\psi P}\left(\psi_{\alpha\mu}^2 + \psi_{\beta\mu}^2 - \psi^{*2}\right) = 0 \end{aligned} \tag{285}$$

from which it shows that the derivative control is added to tune the damping of the second order systems.

As a conclusion, the Park transformation for field orientation (269) is in fact closely related to the decoupling matrix needed in IOFLC:

$$\boldsymbol{D}\left(\boldsymbol{\psi}_{\alpha\beta\mu}\right) = \begin{bmatrix} -\psi_{\beta\mu} & \psi_{\alpha\mu} \\ \psi_{\alpha\mu} & \psi_{\beta\mu} \end{bmatrix} \tag{286}$$

with its determinant $\det \boldsymbol{D} = \psi_{\alpha\mu}^2 + \psi_{\beta\mu}^2 \neq 0$ if the rotor flux amplitude is not null, and its inverse matrix as

$$\boldsymbol{D}^{-1}\left(\boldsymbol{\psi}_{\alpha\beta\mu}\right) = \frac{1}{\psi_{\alpha\mu}^2 + \psi_{\beta\mu}^2}\begin{bmatrix} -\psi_{\beta\mu} & \psi_{\alpha\mu} \\ \psi_{\alpha\mu} & \psi_{\beta\mu} \end{bmatrix} \tag{287}$$

From this perspective, the DRFOC is an asymptotic IOFLC for controlling the two tracking objectives of active flux amplitude and the rotor speed.

3.5. Indirect Rotor Field Oriented Control

Direct rotor field orientated control (DRFOC) assumes the rotor flux is available. In practice, the rotor flux is almost never measured[46], while the rotor angular position is

[45] "Deeper" means the state takes more time derivatives of the output to get.

[46] However, it is possible to measure the rotor flux angle by installing search coil to stator tooth, but one cannot exactly measure the rotor flux amplitude because it is a property associated with the linked winding, as we

relatively easy to be measured. For PM synchronous motor, knowing the rotor angular position Θ means the rotor field orientation is done. We need to find a way to utilize the information of measured rotor angular position to achieve rotor field orientation for induction motor.

Recall the angular speed assumption (266). Let's assume the rotor angular speed $\Omega = s\Theta$ is somehow available. From (267a), we know that the d-axis angle can be determined in a feedforward fashion as follows

$$\theta_M = \frac{1}{s}\omega_{\text{syn}}^* \tag{288}$$

which defines a new reference frame called MT-frame. Note this MT-frame does not necessarily be aligned with the rotor field, and the M-axis angle θ_M as an internal state implies we are designing a *dynamic control law*.

Transforming the rotor voltage equations into MT-frame yields

$$\begin{aligned} &i_{M\text{req}} = L_\mu^{-1}\psi_{M\mu} - i_{Ms} \\ &i_{T\text{req}} = L_\mu^{-1}\psi_{T\mu} - i_{Ts} \\ &0 - R_{\text{req}}\boldsymbol{i}_{MT\text{req}} = \boldsymbol{J}\frac{\mathrm{d}\left(\theta_M - n_{\text{pp}}\Theta\right)}{\mathrm{d}t}\boldsymbol{\psi}_{MT\mu} + \frac{\mathrm{d}}{\mathrm{d}t}\boldsymbol{\psi}_{MT\mu} \end{aligned} \tag{289}$$

which is decomposed into

$$\Rightarrow \begin{cases} -R_{\text{req}}i_{M\text{req}} = -\left(\frac{\mathrm{d}\theta_M}{\mathrm{d}t} - n_{\text{pp}}\Omega\right)\psi_{T\mu} + \frac{\mathrm{d}}{\mathrm{d}t}\psi_{M\mu} \\ -R_{\text{req}}i_{T\text{req}} = \left(\frac{\mathrm{d}\theta_M}{\mathrm{d}t} - n_{\text{pp}}\Omega\right)\psi_{M\mu} + \frac{\mathrm{d}}{\mathrm{d}t}\psi_{T\mu} \end{cases}$$

The current-source-inverter-fed induction motor is then represented by

$$\Rightarrow \begin{cases} J_s s\Omega = -\psi_{T\mu}i_{Ms} + \psi_{M\mu}i_{Ts} - T_L \\ s\psi_{M\mu} = -R_{\text{req}}L_\mu^{-1}\psi_{M\mu} + R_{\text{req}}i_{Ms} + \left(s\theta_M - n_{\text{pp}}\Omega\right)\psi_{T\mu} \\ s\psi_{T\mu} = -R_{\text{req}}L_\mu^{-1}\psi_{T\mu} + R_{\text{req}}i_{Ts} - \left(s\theta_M - n_{\text{pp}}\Omega\right)\psi_{M\mu} \end{cases}$$

The control error dynamics are:

$$\Rightarrow \begin{cases} J_s s e_\Omega = J_s s\left(\Omega - \Omega^*\right) = -\psi_{T\mu}i_{Ms} + \psi_{M\mu}i_{Ts} - T_L - s\Omega^* \\ s e_{\psi M\mu} = s\left(\psi_{M\mu} - \psi^*\right) = -R_{\text{req}}L_\mu^{-1}\psi_{M\mu} + R_{\text{req}}i_{Ms} + \left(s\theta_M - n_{\text{pp}}\Omega\right)\psi_{T\mu} - s\psi^* \\ s e_{\psi T\mu} = s\left(\psi_{T\mu} - 0\right) = -R_{\text{req}}L_\mu^{-1}\psi_{T\mu} + R_{\text{req}}i_{Ts} - \left(s\theta_M - n_{\text{pp}}\Omega\right)\psi_{M\mu} \end{cases}$$

which can be rewritten into

$$\Rightarrow \begin{cases} J_s s e_\Omega = -e_{\psi T\mu}i_{Ms} + e_{\psi M\mu}i_{Ts} + \psi^* i_{Ts} - T_L - s\Omega^* \\ s e_{\psi M\mu} = -R_{\text{req}}L_\mu^{-1}e_{\psi M\mu} + \left(s\theta_M - n_{\text{pp}}\Omega\right)e_{\psi T\mu} - s\psi^* - R_{\text{req}}L_\mu^{-1}\psi^* + R_{\text{req}}i_{Ms} \\ s e_{\psi T\mu} = -R_{\text{req}}L_\mu^{-1}e_{\psi T\mu} - \left(s\theta_M - n_{\text{pp}}\Omega\right)e_{\psi M\mu} - \left(s\theta_M - n_{\text{pp}}\Omega\right)\psi^* + R_{\text{req}}i_{Ts} \end{cases}$$

$$\Rightarrow \begin{cases} \psi^* i_{Ts} - T_L - s\Omega^* = -k_P e_\Omega \\ -s\psi^* - R_{\text{req}}L_\mu^{-1}\psi^* + R_{\text{req}}i_{Ms} = 0 \\ -\left(s\theta_M - n_{\text{pp}}\Omega\right)\psi^* + R_{\text{req}}i_{Ts} = 0 \end{cases}$$

have learned in Chapter 2.

where the control law design is possible because by introducing an internal state, we have obtained a third control DoF so we can impose three constraints. The design constraints imposed above give us a dynamic control law as follows:

$$\begin{aligned} i_{Ts} &= \frac{-k_P e_\Omega + T_L + s\Omega^*}{\psi^*} \\ i_{Ms} &= \frac{1}{R_{\text{req}}} s\psi^* + \frac{1}{L_\mu}\psi^* \\ s\theta_M &= n_{\text{pp}}\Omega + \frac{R_{\text{req}} i_{Ts}}{\psi^*} \end{aligned} \tag{290}$$

in which the last equation defines the synchronous speed and slip speed:

$$\omega^*_{\text{syn}} \triangleq n_{\text{pp}}\Omega + \omega^*_{\text{sl}} \tag{291}$$

$$\omega^*_{\text{sl}} \triangleq \frac{R_{\text{req}} i_{Ts}}{\psi^*} \tag{292}$$

This dynamic control law is known as the indirect rotor field oriented control (IRFOC).

Finally, let's prove the Lyapunov stability of the above dynamic control law. Consider the following Lyapunov function for the flux control subsystem:[47]

$$V = \frac{1}{2} e^2_{\psi M\mu} + \frac{1}{2} e^2_{\psi T\mu} \tag{293}$$

which can be used to show that the flux control error will converge to zero as time approaches infinity. We say the field orientation is asymptotically achieved. As a result, the speed control error can be shown to be bounded or stable in the sense of Lyapunov.

3.6. Nested Loops PI Control versus PID Control

There are two ways that motivate we use a nested loops PI control.

First, for the DRFOC, there is a problem about the PD controller, we need to take time derivative of the measured signals. The measurement noises will be amplified if we take pure differentiation.

Second, for the IRFOC, we only derive desired values for the M-axis current and T-axis current, but we do not know how to regulate currents towards theses goals yet.

We are going to introduce the nested loop PI control in the coding project.

TODO:

Consider a second order system:

$$G(s) = \frac{\Omega}{u_q} = \frac{n_{\text{pp}}\psi_{\text{A}}}{J_s s} \frac{1}{L_q s + R} \tag{294}$$

Let's define a intermediate state i_q as

$$i_q(s) = \frac{1}{L_q s + R} u_q \tag{295}$$

[47] One can show that the third order error dynamics further including speed error is a nonlinear system, which makes the stability proof much more involved.

and use this intermediate state as the input to the speed dynamics.

By doing this, we have separated the two system We

3.7. Tuning PI Coefficients for Nested Loops

See Chapter 11 of TI InstaSPIN user's guide. The conclusion made there about the choice of damping factor is actually not very useful because a output saturation or clamping is always used in practice, which makes the speed or current control a nonlinear control law, thus the conclusion made assuming the speed or current controller a linear system is not final.

4. Chapter 4: Observer

There are three main topics in the field of artificial intelligence, i.e., unsupervised learning, supervised learning, and reinforced learning.[48] Those three topics can actually be mapped to the three classic topics in the field of control engineering.

- Unsupervised learning deals with pattern recognition from data, which assembles diagnosis. **Diagnosis**, in its simplest form, is to detect specific frequency component in the spectrum of the measured signals, and it gets involved when the signal is non-stationary, thus further needing tools (e.g., wavelet analysis) that generates time-frequency map. The time-frequency map is essentially a 2D picture that can further be used as input to the convolution neural network (CNN) [18], and the learning transfer is able to facilitate the training of the neural network for a distinct application.
- Supervised learning needs to further put a label to each datum before the datum can be used for training, and a similar requirement is imposed on the data for constructing an observer, estimator, or identifier. **Observer, estimator or identifier** uses a pair of input and output signals for reconstructing state or estimating parameter of a system. In discrete time domain, the reconstruction of the state at the next step based on the history data in the past is also called as prediction. Generally speaking, a filter is different from an observer, because the filter does not need a feedback loop to direct output back to calculate the estimated error. However, at the times of R. E. Kalman, there was no concept of observer yet and he needed a term that would be easier to be accepted by the community so the linear quadratic estimator (LQE) he develops was named as Kalman filter.
- Reinforced learning introduces the concepts of agent and environment, and the agent is able to influence the environment. **Control**, unlike diagnosis and observer, interacts with the real world based on the measurement of signals.

This chapter focuses on the observer design for ac motor but the concept is generally applicable to other systems.

[48] See, e.g., the lecture notes of MIT 6.S191 at `http://introtodeeplearning.com/`.

4.1. Review on Modern Control System Theory

Consider a linear system:

$$\begin{aligned} s\boldsymbol{x} &= \boldsymbol{A}\boldsymbol{x} + \boldsymbol{B}\boldsymbol{u} \\ \boldsymbol{y} &= \boldsymbol{C}\boldsymbol{x} \end{aligned} \tag{296}$$

where $\boldsymbol{x} \in \mathbb{R}^{n_x}$, $\boldsymbol{y} \in \mathbb{R}^{n_y}$, $\boldsymbol{u} \in \mathbb{R}^{n_u}$.

Unfortunately, we will see soon that this kind of design cannot be used in control of ac machines.

4.2. Motivation

In last chapter, the controller design is dependent on feedback of states of the ac machines, including the $\alpha\beta$-frame current, the rotor (angular) speed, and the $\alpha\beta$-frame active flux. Note the $\alpha\beta$-frame active flux is not needed in IRFOC.

The states of an ac machine include circuit states and mechanical states. It is important to be able to map those states with the feedback signals.

- The $\alpha\beta$-frame current is math representation of the currents of the multi-phase stator circuits. The currents of the physical circuits can be measured using either Hall sensors or shunt resistors (with a typical resistance value of 5 mΩ, see e.g., the GaN evaluation board by Texas Instruments).
- The $\alpha\beta$-frame active flux is mutual flux linkage of the $\alpha\beta$ frame coils. The active flux is in most cases not measured.
- The rotor (angular) speed is in most cases not measured and instead the rotor angle is measured.

The problem is how we can get active flux or rotor speed. If the active flux is known, the DRFOC can be implemented; if the rotor speed is available, the IRFOC can be implemented. In order to implement the controller in practice, we need to learn about the status of a system via sensors.

There are three kinds of problems needed to be solved in this chapter.

(1) Do flux estimation and the DRFOC can be implemented using the cosine and sine of the active flux angle.
(2) Do speed estimation with a reference signal for active flux angle available, so speed control based on DRFOC can be implemented.
(3) Do speed estimation and implement IRFOC where the d-axis angle is simply the integral of estimated field speed.

4.3. Sensor Imperfection

There is no perfect measurement, and noises, temperature drift and quantization error are three main issues we encounter in practice.

4.3.1. Sensors for Inverse Pendulum

Taking the state measurement of an inverse pendulum for example, an accelerometer and a gyroscope are often used. The measured rotor angle Θ_m by an accelerometer is

noisy

$$\Theta_m = \Theta + n_\Theta$$

where n_Θ denotes measurement noise. A simple observer for rotor angle can be designed as

$$s\hat{\Theta} = 0 + k_0\left(\Theta_m - \hat{\Theta}\right)$$

which can be rewritten as a low pass filter:

$$\hat{\Theta} = \frac{1}{s + k_0}\left(\Theta + n_\Theta\right)$$

To reduce the influence of the noise, we need to adjust the pole $-k_0$ of the low pass filter, which often sacrifices the bandwidth of the estimation.

The measured angular speed Ω_m has temperature drift

$$\Omega_m = \Omega + C_\Omega$$

where C_Ω is an unknown constant disturbance that makes the following integration unbounded:

$$\hat{\Theta} = \frac{1}{s}\Omega_m$$

A simple sensor fusion algorithm becomes apparent

$$s\hat{\Theta} = \underbrace{\Omega_m}_{\text{Prediction}} + k_0\underbrace{\left(\Theta_m - \hat{\Theta}\right)}_{\text{Innovation}}$$

which forms a basic observer with prediction term and innovation term, provided by the gyroscope and accelerometer, respectively.

Another well known method to deal with the noise n_Θ is the Kalman filter, which is also a sensor fusion algorithm that takes useful information from both Θ_m and Ω_m, by introducing time-varying observer coefficients.

4.3.2. Sensors for AC Machine

For ac machines, the rotor angle Θ can be measured by, for example, an incremental encoder, as shown in Fig. 24. The encoder has two key parameters, i.e., the pulse per revolution (ppr) and the resolution. Higher ppr value does not always means higher resolution. A typical low-end incremental encoder has 1024 ppr or 2500 ppr, while a high-end encoder integrated into a servo motor, e.g., Sigma-7 series from Yaskawa, has a ppr value up to 2^{24}, which is 16,777,216 pulses per revolution. The measured of the rotor angle is a digital quantity and there is quantization error. In most cases, it is safe to neglect the quantization error and assume the measured signal by an encoder is the actual rotor angle Θ.

The current is sampled by ADC (analog-to-digital-converter). The resulting measured current quantity has both temperature drift and the quantization error. In most

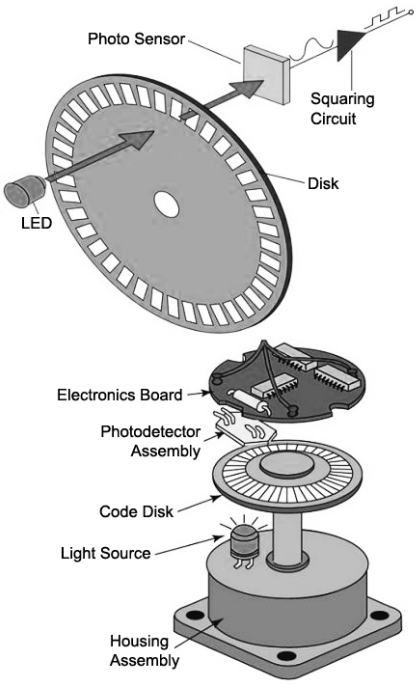

Figure 24. The working principle of an encoder. Figure credit: `https://www.anaheimautomation.com/manuals/forms/encoder-guide.php`

cases, it is safe to neglect the temperature drift and quantization error, expect the case when a pure integration is applied to the measured current signal.

4.3.3. Speed Signal Reconstruction based on Rotor Angle Measurement

The speed measurement using the encoder can be simply implemented as the number of pulse counts divided by a fixed time duration. The pulses will be decoded by a QEP module and several practical considerations are needed.

(1) Identify the angle between the index signal (Z signal) of the encoder and the d-axis of the rotor.
(2) Take care of the incremental in pulse counts when the QEP module's QPOSCNT gets reset.
(3) Decide the time duration (i.e., the width of the moving average window) of speed measurement considering the speed measurement resolution at steady state.

I believe for this engineering method, the talk is cheap, and I'd better show you the code.

TODO: Add code snippet.

4.4. Problem Formulation: A Unified Approach

We have derived the field oriented models for induction motor (267) and synchronous motor (268). It is desired that we only design observer for one model. To this end,

both ac machines can be described by the unified active field oriented model

$$s\theta_d = \omega_d = n_{\rm pp}\Omega + \omega_{\rm sl} \tag{297a}$$

$$s\Omega = \frac{1}{J_s}\left(T_{\rm em} - T_L\right) = \frac{1}{J_s}\left(n_{\rm pp}\psi_{\rm A} i_{qs} - T_L\right) \tag{297b}$$

$$\psi_{\rm A} = \frac{L_d - L_q}{\frac{L_d - L_q}{R_{\rm req}}s + 1} i_{ds} + \psi_{\rm PM} \tag{297c}$$

$$\begin{bmatrix} u_{ds} \\ u_{qs} \end{bmatrix} - R\begin{bmatrix} i_{ds} \\ i_{qs} \end{bmatrix} = \left(\boldsymbol{J}\omega_d + s\right)\boldsymbol{\psi}_{dqs} = \left(\boldsymbol{J}\omega_d + s\right)\left(\begin{bmatrix} \psi_{\rm A} \\ 0 \end{bmatrix} + L_q\begin{bmatrix} i_{ds} \\ i_{qs} \end{bmatrix}\right) \tag{297d}$$

When (297) describes the PM synchronous machine, we need to put $\omega_{\rm sl} = 0$ and $R_{\rm req} = \infty$. When (297) describes induction machine, we put $\psi_{\rm PM} = 0$, $\omega_{\rm sl} = R_{\rm req} i_{qs}/\psi_{\rm A}$, redefine L_d as the stator inductance L_s, and redefine L_q as the leakage inductance $L_s - L_\mu$.

Note that we have avoided using the rotor angle Θ as the state but choose to use the angle of the active flux, θ_d, as the state. As a result, this model shows that the ac machine can be described using a current vector $\boldsymbol{i}_{dqs}$, an active flux vector $\psi_{\rm A}\angle\theta_d$ and a rotor angular speed Ω.

4.5. Speed Estimation based on the Unified Active Field Oriented Model

Let's now design an encoderless observer using the unified model (297). Encoderless means the encoder is not used in the motor drive, which is a particularly interesting topic for induction motor, as the general purpose converter for induction motor often does no use any position feedback signal. This means we need to design the prediction part and the innovation part for the d-axis angle estimate.

The prediction part needs to be an estimate of the rotor angular speed Ω or angular speed of the active flux, i.e., ω_d. The motion dynamics (297b) are useless because there is an unknown disturbance T_L. The q-axis voltage equation, on the other hand, gives an estimate of d-axis angular speed as follows

$$\hat{\omega}_d = \frac{u_{qs} - Ri_{qs} - sL_q i_{qs}}{\psi_A + L_q i_{ds}} \tag{298}$$

where a hat has been added to ω_d because the dq frame quantities are obtained by an estimated angle $\hat{\theta}_d$ rather than the actual angle θ_d.

The innovation part can be anything that is exactly zero when the rotor angle estimate $\hat{\theta}_d$ is exactly equal to the real one θ_d. The d-axis equation comes handy for this purpose:

$$e_{d,\rm ss} \triangleq u_{ds} - Ri_{ds} - \hat{\omega}_d\left(L_q i_{qs}\right) \tag{299}$$

where the estimate $\hat{\omega}_d$ has been substituted and therefore, whenever ω_d or θ_d is erroneous, $e_{d,\rm ss}$ is nonzero. In ideal case, $e_{d,\rm ss}$ is equal to $s\left(\psi_{\rm A} + L_q i_{ds}\right)$, which is zero at steady state.

Therefore, an encoderless observer can be designed as

$$\begin{aligned} s\hat{\theta}_d &= \hat{\omega}_d + k_0 e_{d,\text{ss}} \\ &= \underbrace{\frac{u_{qs} - Ri_{qs} - sL_q i_{qs}}{\psi_A + L_q i_{ds}}}_{\text{Prediction}} + k_0 \underbrace{[u_{ds} - Ri_{ds} - \hat{\omega}_d (L_q i_{qs})]}_{\text{Innovation}} \end{aligned} \tag{300}$$

where all dq-frame quantities are obtained using $\hat{\theta}_d$ rather than θ_d. This is not the only way to construct prediction and innovation. For example, it is also possible to design observers for dq-frame currents and use the estimated d-axis current error as the innovation, and use the integral of q-axis current error as the prediction [19, Eq.(18)], from which it can be shown that the d-axis current prediction (i.e., the open loop estimate) error reveals angle error while the q-axis current prediction error indicates speed error.

4.6. The Arbitrary DQ Model

You might remind me that we have chosen to adopt the DQ model considering the saliency of the PM motor. However, another cool thing about the active flux concept based DQ model we use is that the saliency does not appear with arbitrary choice of DQ frame angular speed ω_d:

$$s\theta_d = \omega_d \tag{301a}$$

$$s\Omega = \frac{1}{J_s}(T_{\text{em}} - T_L) = \frac{1}{J_s}\left[n_{\text{pp}}\left(\psi_{d\text{A}} i_{qs} - \psi_{q\text{A}} i_{ds}\right) - T_L\right] \tag{301b}$$

$$\begin{bmatrix} u_{ds} \\ u_{qs} \end{bmatrix} - R \begin{bmatrix} i_{ds} \\ i_{qs} \end{bmatrix} = (\boldsymbol{J}\omega_d + s)\,\boldsymbol{\psi}_{dqs} \tag{301c}$$

$$\begin{bmatrix} u_{d\text{req}} \\ u_{q\text{req}} \end{bmatrix} - R_{\text{req}} \begin{bmatrix} i_{d\text{req}} \\ i_{q\text{req}} \end{bmatrix} = [\boldsymbol{J}(\omega_d - n_{\text{pp}}\Omega) + s]\,\boldsymbol{\psi}_{dq\text{A}} \tag{301d}$$

where $\omega_d = n_{\text{pp}}\Omega + \omega_{\text{sl}}$ must use a new expression for slip angular speed, i.e., $\omega_{\text{sl}} = R_{\text{req}} T_{\text{em}}/\|\boldsymbol{\psi}_{dq\text{A}}\|^2/n_{\text{pp}}$ rather than $\omega_{\text{sl}} = R_{\text{req}} i_q/\|\boldsymbol{\psi}_{dq\text{A}}\|$ because i_q directly relates torque only in rotor field oriented frame.

In order to get of the dependency on angular speed, a wise choice is to choose $\theta_d = 0$, and of course we can also design observers in this stationary reference frame.

4.7. Flux Estimator

In (297d), there is a simple relation between the stator flux and the active flux:

$$\begin{aligned} \boldsymbol{\psi}_{dqs} &= \boldsymbol{\psi}_{dq\text{A}} + L_q \boldsymbol{i}_{dqs} = \begin{bmatrix} \psi_{\text{A}} \\ 0 \end{bmatrix} + L_q \boldsymbol{i}_{dqs} \\ \Rightarrow \boldsymbol{\psi}_{\alpha\beta s} &= \boldsymbol{\psi}_{\alpha\beta\text{A}} + L_q \boldsymbol{i}_{\alpha\beta s} \end{aligned} \tag{302}$$

which turns the active flux estimation problem into a stator flux estimation problem.

Theoretically speaking, the stator flux can be directly obtained in $\alpha\beta$-frame by integrating the stator back electromotive force and the active field oriented d-axis angle can easily be calculated:

$$\begin{aligned} \boldsymbol{\psi}_{\alpha\beta s} &= \frac{1}{s}\left(\boldsymbol{u}_{\alpha\beta s} - R\boldsymbol{i}_{\alpha\beta s}\right) \\ \boldsymbol{\psi}_{\alpha\beta \mathrm{A}} &= \boldsymbol{\psi}_{\alpha\beta s} - L_q \boldsymbol{i}_{\alpha\beta s} \\ \theta_d &= \operatorname{arctan2}\left(\psi_{\beta \mathrm{A}}, \psi_{\alpha \mathrm{A}}\right) \end{aligned} \tag{303}$$

This is a typical open loop estimation that is vulnerable to disturbance. For instance, the temperature drift in the measured current $\boldsymbol{i}_{\alpha\beta s,m} = \boldsymbol{i}_{\alpha\beta s} + [C_\alpha, C_\beta]^T$ would result in unbounded integral. Therefore, we need to close the loop by feeding back some innovation term.

A typical flux estimator has a form as follows:

$$s\hat{\boldsymbol{\psi}}_{\alpha\beta s} = \underbrace{\boldsymbol{u}_{\alpha\beta s} - R\boldsymbol{i}_{\alpha\beta s,m}}_{\text{Prediction}} + \underbrace{\hat{\boldsymbol{D}}}_{\substack{\text{Innovation+} \\ \text{Compensation}}} \tag{304}$$

which also consists of a prediction term and an innovation term.

Before we move on to show how one can design $\hat{\boldsymbol{D}}$, I believe there is a more heuristic way to design an observer.

Step 1 implement the open loop predictor (i.e., without any innovation term);
Step 2 observe which quantity can be used for innovation;
Step 3 add innovation term and test the synthesized observer.

In our case, if you simulate the open loop flux estimator from various perspectives, you will possibly find different ideas for constructing an innovation term. The said perspectives include:

- The time domain waveform of the $\alpha\beta$ components of the estimated flux.
- The amplitude and angle of the estimated flux.
- The Lissajour figure of the estimated flux.

We are going to show some typical designs from literature.

4.7.1. Time Domain Approach: a Nonlinear System Perspective

According to literature, there are two effective innovation terms, which belong to the time domain approaches [19]. The first one is to compare the amplitude of the estimated active flux with that in (297c) and if they do not match, a correction to the integrand is needed. The second one is to record the peak value of the active flux estimate profile and if the maximum and minimum do not match, a correction can be made to the integrator's input or output.

From the perspective of nonlinear systems, we are particularly interested in the problem formulation detailed in [20], where the temperature drift is ignored such that $\boldsymbol{i}_{\alpha\beta s,m} = \boldsymbol{i}_{\alpha\beta s}$ and saliency must not exist, i.e., $L_d = L_q$. The flux estimation problem

can be regarded as a nonlinear system estimation problem as follows:

$$\begin{aligned} s\boldsymbol{x} = \boldsymbol{f}(\boldsymbol{x}) \;&\Leftrightarrow\; s\boldsymbol{\psi}_{\alpha\beta s} = \boldsymbol{u}_{\alpha\beta s} - R\boldsymbol{i}_{\alpha\beta s} \\ y = h(\boldsymbol{x}) = \|\boldsymbol{x} - L_q\boldsymbol{i}_{\alpha\beta s}\|^2 \;&\Leftrightarrow\; \psi_{\mathrm{A}} = \frac{L_d - L_q}{\frac{L_d - L_q}{R_{\mathrm{req}}}s + 1} i_{ds} + \psi_{\mathrm{PM}} = \boldsymbol{\psi}_{\alpha\beta s} - L_q\boldsymbol{i}_{\alpha\beta s} \end{aligned} \tag{305}$$

where the output function $h(\cdot)$ is a nonlinear function of the state $\boldsymbol{x}$, and in the case of non-saliency assumption $L_d = L_q$, we have the following algebraic constraint as our output function:

$$y = h(\boldsymbol{x}) \equiv 0 = \psi_{\mathrm{PM}}^2 - \left\|\boldsymbol{\psi}_{\alpha\beta s} - L_q\boldsymbol{i}_{\alpha\beta s}\right\|^2$$

from which a output function *gradient descent* observer results:

$$s\hat{\boldsymbol{\psi}}_{\alpha\beta s} = \boldsymbol{u}_{\alpha\beta s} - R\boldsymbol{i}_{\alpha\beta s} - \frac{K_P}{4}\underbrace{\nabla_{\hat{\boldsymbol{x}}} h(\hat{\boldsymbol{x}})}_{\text{gradient}}\underbrace{(0 - h(\hat{\boldsymbol{x}}))}_{\text{output error}} \tag{306}$$

where "descent" corresponds to the minus sign before the gradient term, and the negative gradient (or Jacobian) is computed as

$$-\nabla_{\hat{\boldsymbol{x}}} h(\hat{\boldsymbol{x}}) = \begin{bmatrix} \frac{\partial}{\partial\hat{\psi}_{\alpha s}}\left(\left(\hat{\psi}_{\alpha s} - L_q i_{\alpha s}\right)^2 + \left(\hat{\psi}_{\beta s} - L_q i_{\beta s}\right)^2\right) \\ \frac{\partial}{\partial\hat{\psi}_{\beta s}}\left(\left(\hat{\psi}_{\alpha s} - L_q i_{\alpha s}\right)^2 + \left(\hat{\psi}_{\beta s} - L_q i_{\beta s}\right)^2\right) \end{bmatrix} = 2\begin{bmatrix} \left(\hat{\psi}_{\alpha s} - L_q i_{\alpha s}\right) \\ \left(\hat{\psi}_{\beta s} - L_q i_{\beta s}\right) \end{bmatrix}$$

The observer can be written in its one-liner form as follows:

$$(306) \Leftrightarrow s\hat{\boldsymbol{\psi}}_{\alpha\beta s} = \boldsymbol{u}_{\alpha\beta s} - R\boldsymbol{i}_{\alpha\beta s} + \frac{K_P}{2}\begin{bmatrix} \left(\hat{\psi}_{\alpha s} - L_q i_{\alpha s}\right) \\ \left(\hat{\psi}_{\beta s} - L_q i_{\beta s}\right) \end{bmatrix}\left(\psi_{\mathrm{PM}}^2 - \left\|\hat{\boldsymbol{\psi}}_{\alpha\beta s} - L_q\boldsymbol{i}_{\alpha\beta s}\right\|^2\right)$$

which works as long as the motor parameter ψ_{PM} is known, and the detailed stability analysis involves a proper change of state for its error dynamics, where the number of equilibriums depends on the choice of both K_P value and motor operating speed [20].

4.7.2. Frequency Domain Approach

From a perspective of frequency domain performance, the open loop integral is critically stable as its dc gain is infinite. The integrator can be stabilized by moving the pole to the left of the complex number plane. However, the resulting flux estimate becomes lagging to the real flux.

There are suggestions of adding exact compensation at the current working frequency:

$$\hat{\boldsymbol{\psi}}_s = \frac{j\hat{\omega} + k|\hat{\omega}|}{j\hat{\omega}}\frac{1}{s + k|\hat{\omega}|}(e_{\alpha s} + je_{\beta s}) = \frac{[\boldsymbol{I} - k\boldsymbol{J}\mathrm{sign}(\hat{\omega})]\,\boldsymbol{e}_s}{s + k|\hat{\omega}|} \tag{307}$$

with k a scalar gain. The stator electromotive force is $\boldsymbol{e}_s = \boldsymbol{u}_s - R\boldsymbol{i}_s$ and this estimator must be implemented in $\alpha\beta$-frame, thus omitting indication of $\alpha\beta$ in the vector

subscript. However, the compensation is only exact at steady state.

In my opinion, trying to get a perfect flux estimation using frequency domain approach is ineffective. A better approach would be sticking with the IRFOC and use the lagged flux estimate to produce a fast speed estimate, as is done by Schauder (1992) [21].

4.8. Disturbance EMF Reconstruction using Sliding Mode Observer

We only show the most famous disturbance observer in literature [19], i.e., the super-twisting algorithm based second order sliding mode observer. The target dynamics are:

$$L_q s\boldsymbol{i}_{\alpha\beta s} = s\boldsymbol{\psi}_{\alpha\beta s} - s\boldsymbol{\psi}_{\alpha\beta \mathrm{A}} \tag{308}$$

and the corresponding generic sliding mode observer is:

$$L_q s\hat{\boldsymbol{i}}_{\alpha\beta s} = s\boldsymbol{\psi}_{\alpha\beta s} + \boldsymbol{f}\left(\boldsymbol{S}\right) \tag{309}$$

where the dynamic switching function $\boldsymbol{f}(\cdot)$ is

$$\boldsymbol{f}\left(\boldsymbol{S}\right) = \begin{bmatrix} k_1\sqrt{|S_\alpha|}\mathrm{sign}\left(S_\alpha\right) + k_2\frac{1}{s}\mathrm{sign}\left(S_\alpha\right) \\ k_1\sqrt{|S_\beta|}\mathrm{sign}\left(S_\beta\right) + k_2\frac{1}{s}\mathrm{sign}\left(S_\beta\right) \end{bmatrix}$$

and the sliding mode surface is simply the current error vector:

$$\boldsymbol{S} = \begin{bmatrix} S_\alpha \\ S_\beta \end{bmatrix} = \begin{bmatrix} i_{\alpha s} - \hat{i}_{\alpha s} \\ i_{\beta s} - \hat{i}_{\beta s} \end{bmatrix}$$

which is essentially the output error vector. Please note the two axes are completely decoupled.

The error dynamics can be derived by subtracting both sides of (308) from (309):

$$L_q s\boldsymbol{i}_{\alpha\beta s} - L_q s\hat{\boldsymbol{i}}_{\alpha\beta s} = \left(s\boldsymbol{\psi}_{\alpha\beta s} - s\boldsymbol{\psi}_{\alpha\beta \mathrm{A}}\right) - \left(s\boldsymbol{\psi}_{\alpha\beta s} + \boldsymbol{f}\left(\boldsymbol{S}\right)\right)$$

When the sliding mode surface is reached, i.e., $\boldsymbol{S} = 0$, the error dynamics are reduced to

$$\Rightarrow \boldsymbol{f}\left(\boldsymbol{S}\right) = -s\boldsymbol{\psi}_{\alpha\beta \mathrm{A}}$$

which suggests that the switching function is an estimate of the active emf.

4.9. Speed and Load Torque Reconstruction by Position Output Observer

The noise in the measured rotor angle is essentially a quantization error rather than white noise, thus speed observer is not a good application for Kalman filter. Instead, the speed signal can be reconstructed from the measured rotor angle Θ by designing

a Luenberger observer:

$$\begin{aligned} s\hat{\Theta} &= \hat{\Omega} + k_0\left(\Theta - \hat{\Theta}\right) \\ s\hat{\Omega} &= T_{\text{em}} + 0 + k_1\left(\Theta - \hat{\Theta}\right) \end{aligned} \tag{310}$$

where note the load torque is unknown and is substituted by a zero, and the error dynamics are

$$\begin{cases} s\tilde{\Theta} = \tilde{\Omega} - k_0\tilde{\Theta} \\ s\tilde{\Omega} = -T_L - k_1\tilde{\Theta} \end{cases} \tag{311}$$

which can be rewritten into a matrix form as follows:

$$s\begin{bmatrix} \tilde{\Theta} \\ \tilde{\Omega} \end{bmatrix} = \begin{bmatrix} -k_0 & 1 \\ -k_1 & 0 \end{bmatrix}\begin{bmatrix} \tilde{\Theta} \\ \tilde{\Omega} \end{bmatrix} + \begin{bmatrix} 0 \\ -T_L \end{bmatrix} \tag{312}$$

Neglecting the disturbance $-T_L$ in the error dynamics, the stability of the autonomous system is determined by the eigenvalues of the homogeneous matrix:

$$\det\left(\begin{bmatrix} s+k_0 & -1 \\ k_1 & s \end{bmatrix}\right) = s^2 + k_0 s + k_1 \tag{313}$$

$$\Rightarrow s = \frac{-k_0 \pm \sqrt{k_0^2 - 4k_1}}{2} \tag{314}$$

There are two issues about the above design, one obvious and one hidden. The hidden issue is the electromagnetic torque's dependency on the d-axis angle: $T_{\text{em}} = T_{\text{em}}(\theta_d)$, while the obvious one is the load torque disturbance.

- One way to deal with the T_{em}'s dependency to d-axis angle, is to use d-axis angle as the state instead of rotor angle Θ.
- The load torque disturbance can be estimated if we further increase the order of our observer; Or, implementing a dedicated load torque disturbance observer will do the job.

4.9.1. Load Torque Disturbance Observer

We have mentioned that we can do fast disturbance estimation by designing a disturbance observer (262), if the speed is measured. However, since the speed is not measured while the rotor angle is measured, we can do a second order disturbance estimation as follows

$$\begin{aligned} \hat{T}_L &= Q(s)\left(T_{\text{em}} - J_s s\Omega\right) \\ &= Q(s)\left(T_{\text{em}} - J_s s^2\Theta\right) \end{aligned} \tag{315}$$

where $Q(s)$ is a proper low pass filter that is of at least order 2.

4.9.2. Joint Speed and Load Torque Estimation

From a different perspective, the load torque is not necessarily a disturbance.

Since the load torque is unknown, it is inevitable to assume its dynamics before estimating it. The simplest model for load torque is to assume it is a constant, and in this case, we shall interpret it as a parameter of the system. Therefore, the load torque estimation is an adaptive observer design problem according to the classics [22]. However, it can be shown that the extended state observer (or to be specific, the extended Kalman filter in deterministic environment) is equivalent to the adaptive observer [23]. So it also fine to treat the load torque as an extended state.

In fact, treating the disturbance as an extended state is more general. For example, when we want to model a hand grip on the rotor shaft, the time domain profile of the load torque can be considered linear to time, i.e., $T_L = c_0 t$, and we can model it as a type-II linear system response: $T_L = \frac{c_0}{s^2}$. This leads to the following position output observer:

$$\begin{aligned} s\hat{\vartheta} &= \left(n_{\text{pp}}\hat{\Omega} + \omega_{\text{sl}}\right) + k_0\left(\vartheta - \hat{\vartheta}\right) \\ J_s s\hat{\Omega} &= T_{\text{em}}(\vartheta) + \hat{d} + k_1\left(\vartheta - \hat{\vartheta}\right) \\ s\hat{d} &= \left(k_2 + \frac{k_3}{s}\right)\left(\vartheta - \hat{\vartheta}\right) \end{aligned} \tag{316}$$

where note the dependency of T_{em} to the reference signal ϑ. It can be shown that the state space approach here limits the design choices of speed estimation, and a more general approach to define the speed estimation is pending.

4.9.3. The Generalized Speed Estimation

Taking the above discussion into account, we can further summarize the existing designs of speed observer into the following generalized form:

$$\begin{aligned} s\hat{\vartheta} &= f(\vartheta) + \sum_{j=0}^{n} k_j \frac{|\tilde{\vartheta}|^{\kappa_j}\text{sign}(\tilde{\vartheta})}{s^j}, \quad \text{with } k_j, \kappa_j \geq 0 \\ f(\vartheta) &= \omega_{\text{sl}} + \tfrac{n_{\text{pp}}}{sJ_s} T_{\text{em}} \end{aligned} \tag{317}$$

where to avoid confusion, we use a different symbol for the reference signal $\vartheta = \hat{\theta}_d$. Examples of the general position observer in literature are listed in (25). The resulting general speed estimate is

$$\hat{\omega}_{j_0} = f(\vartheta) + \sum_{j=j_0}^{n} k_j \frac{|\tilde{\vartheta}|^{\kappa_j}\text{sign}(\tilde{\vartheta})}{s^j} \text{ with } j_0 = 0, 1, 2, ..., n \tag{318}$$

Different choices of j_0 affect the tracking performance, disturbance rejection capability, and noise attenuation performance, which we will discuss in chapter 6.

The d-axis angle dynamics is not the only model that contains speed. In other words, any model that has speed in it can be used for extraction of the speed signal. See [24] for a q-axis current output observer used for speed estimation.

4.9.4. Trick for Calculation of the Angle Error

1. Calculate the sine of the angle error, assuming angle error is small enough.

Speed estimation	Order n	Gain design	Alternative names	Assumed motion dynamics
Linear correction	2	Const. ($k_2 = 0$)	PLL, Adaptive system	$\omega_r = \text{Const.}$, $f = \omega_{\text{sl}}$
$\kappa_0 = 1$	3	Const.	Generalized PLL	$\omega_r = kt$, $f = \omega_{\text{sl}}$
$\kappa_1 = 1$	3	Time-varying	EKF, ELO	$\omega_r = kt$, $f = \omega_{\text{sl}}$
$\kappa_2 = 1$	3	Const.	Speed observer, LESO, PI observer	$T_L = \text{Const.}$, $f = \omega_{\text{sl}} + \frac{n_{\text{pp}}}{sJ_s} T_{\text{em}}$
$\cdots$	4	Const.	Generalized LESO, Generalized PI observer	$T_L = kt$, $f = \omega_{\text{sl}} + \frac{n_{\text{pp}}}{sJ_s} T_{\text{em}}$
Nonlinear correction	1	Const. ($k_1 = k_2 = 0$)	1st-order SMDO ($\kappa_0 = 0$)	ω is bounded
$\exists j \in \{0, 1, 2\}$	2	Const. ($k_2 = 0$)	2nd-order SMDO ($\kappa_0 = \frac{1}{2}, \kappa_1 = 0$)	T_L is bounded
s.t. $\kappa_j \neq 1$	3	Const.	Nonlinear ESO ($\kappa_0 = 1, \kappa_1 = \frac{1}{2}, \kappa_2 = \frac{1}{4}$)	$T_L = \text{Const.}$, $f = \omega_{\text{sl}} + \frac{n_{\text{pp}}}{sJ_s} T_{\text{em}}$

PLL: phase locked loop. EKF: extended Kalman filter. LESO: linear extended state observer. ELO: extended Luenberger observer.

Figure 25. Examples for the general speed observers [19].

2. Use if-else-clauses.
3. Use q-axis flux linkage as the indicator.

4.10. Observability

In short, the speed cannot be observed when the excitation frequency to the ac machine is dc or 0 Hz. Note 0 Hz means zero speed for PM motor but a loaded induction motor shaft can still rotate because the slip frequency is nonzero such that slip speed and rotor speed add up to zero. However, it has been shown that the locally weak observability can be preserved at $\omega_{\text{syn}} = 0$, if an auxiliary observability vector in dq-frame

$$\boldsymbol{\psi}_{\mathcal{O}}^{dq} \triangleq \begin{bmatrix} \psi_{\text{A}} \\ -(L_d - L_q)\, i_q \end{bmatrix} \tag{319}$$

should rotate or change its direction with respect to the d-axis. See [19, Sec.VI] for details.

4.11. Joint Observer-Controller Stability

So far, we haven't really analyzed the stability of the observers we discussed. In fact, since the ac machine is a nonlinear system, the separation principle[49] does not work anymore. Therefore, there is a need to do the analyze observer-controller stability

We are now going to show one elegant nonlinear speed tracking control design that assumes flux feedback is available. In other words, it is a cascaded design with stage one being the flux estimator and stage two being the nonlinear control.

See [25] for the nonlinear controller design. It is interesting to note the procedure used in the stability proof is very alike to our adaptive controller design development in section 3.1.4.

If you want to move one step further such that there is no need of flux feedback assumption, see the work published with Automatica [26]. The stability proof of this system is beyond the scope of this course.

[49] See, e.g., equation (11.22) in the 14th edition book by Bishop.

5. Chapter 5: Inverter

The emergence of the power electronic devices and inverter gives us the capability to apply the voltage input to the ac machines. In this chapter, we are only interested with voltage stiff inverter (VSI). As a comparison, the current stiff inverter (CSI) that has a dc bus inductor needs to be implemented using a semiconductor power switch that features reverse blocking (i.e., no free-wheeling), see e.g., [27, 28].

5.1. Motor Control: a Perspective (Part II)

Let's revisit the topic of motor control with practical considerations. A physical system does not allow arbitrary large input. From the perspective of the current control, the input voltage is limited by the dc bus voltage of the inverter or the insulation of copper wires. From the perspective of the speed control, the armature current is limited by the thermal capability of the machine, which is often evaluated by the i^2t metric.

5.1.1. Limit to the Control Input for Linear System

Motivation for LQR. The objective and contradiction in optimal control.

5.1.2. Limit to the Control Input using a Nonlinear System

Paste Figure 11-14, 11-15 from InstaSPIN.

5.1.3. PID with Dynamic Anti-Windup

In Chapter 11 of TI InstaSPIN user's guide, there is one section about the dynamic anti-windup of the current controller. I do not recommend this implementation, but it is still useful to demonstrate the basic idea of anti-windup.

Here is a code snippet that implements the PID with anti-windup mechanism using Tustin's method (ode2).

```
1  @njit(nogil=True)
2  def tustin_pid(reg):
3
4      # Error signal
5      error = reg.setpoint - reg.measurement
6
7      # Proportional
8      proportional = reg.Kp * error
9
10     # Integral
11     reg.integrator = reg.integrator + 0.5 * reg.Ki * reg.T * (error
           + reg.prevError) # Tustin
12     # reg.integrator = reg.integrator + reg.Ki * reg.T * (error) #
          Euler
13
14     # Anti-wind-up via integrator clamping */
15     if reg.integrator  >  reg.IntLimit:
16         reg.integrator =  reg.IntLimit
17     elif reg.integrator< -reg.IntLimit:
18         reg.integrator = -reg.IntLimit
19
```

```
    # Derivative (band-limited differentiator) # Note: derivative
        on measurement, therefore minus sign in front of equation!
        */
    reg.differentiator = -(2.0 * reg.Kd * (reg.measurement - reg.
        prevMeasurement) \
                        + (2.0 * reg.tau - reg.T) * reg.
                            differentiator) \
                        / (2.0 * reg.tau + reg.T)

    # Compute output and apply limits
    reg.Out = proportional + reg.integrator + reg.differentiator

    if reg.Out  >  reg.OutLimit:
        reg.Out =  reg.OutLimit
    elif reg.Out< -reg.OutLimit:
        reg.Out = -reg.OutLimit

    # Store error and measurement for later use */
    reg.prevError       = error
    reg.prevMeasurement = reg.measurement

    # Return controller output */
    return reg.Out
```

Low pass filter for proper derivative control Derivative on measurement rather than the set-point. ODE2 for implementation of a differential operator.

$$s = \frac{2}{T_{\text{samp}}} \frac{z-1}{z+1}$$

Let IntLimit = OutLimit - proportional to implement dynamic clamping.

5.1.4. Incremental PI

Let's implement an ode1 version for incremental PI, in which the dynamic clamping is naturally implemented with only one block of output saturation.

```
@njit(nogil=True)
def incremental_pi(reg):
    reg.Err = reg.setpoint - reg.measurement
    reg.Out = reg.OutPrev + \
        reg.Kp * (reg.Err - reg.ErrPrev) + \
        reg.Ki * reg.Err
    if reg.Out >    reg.OutLimit:
        reg.Out =   reg.OutLimit
    elif reg.Out < -reg.OutLimit:
        reg.Out =  -reg.OutLimit
    reg.ErrPrev = reg.Err
    reg.OutPrev = reg.Out
```

5.1.5. When Speed Is Too High or Too Low

When the modulation-to-sampling rate is higher than 1.15 for SVPWM.

The regenerative braking mode at very low speeds, the inverter becomes a boost converter.

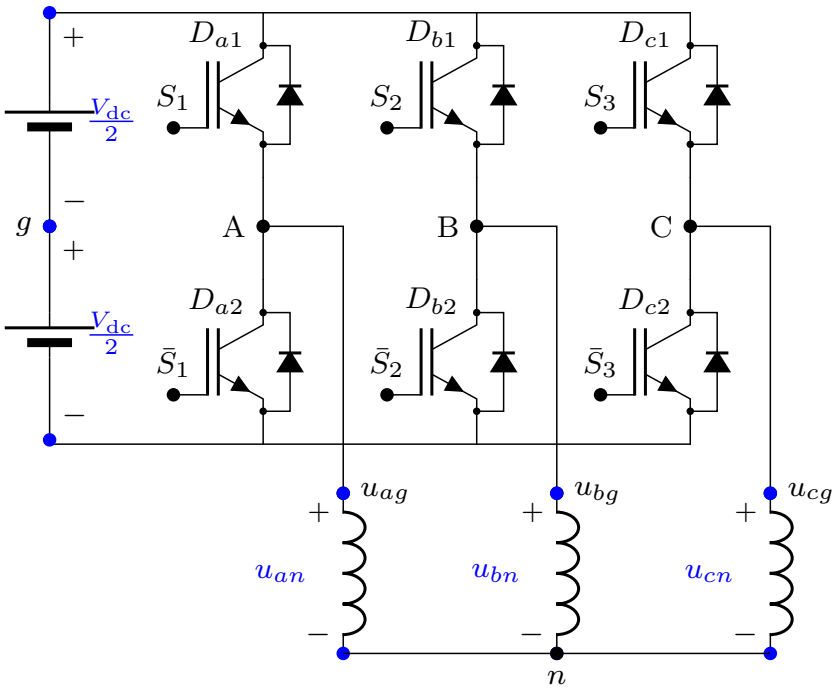

Figure 26. Three phase inverter and symbol definitions.

5.1.6. Bandwidth and Change Rate

The highest current bandwidth is determined by the dc bus voltage.

5.2. Three-Phase Three-Wire Inverter

Consider the electrical system of a 3 phase half bridge inverter and a wye-connected stator winding as in Fig. 26. This is a typical 3 phase 3 wire system with the neutral open.[50]

5.3. Control of Voltage Source Inverter

On the one hand, given a 3 phase 3 wire inverter (see e.g., 26), what is at our control is the duty ratio $S_x,\ x = a, b, c$ that ideally produces the following inverter terminal voltages:

$$\begin{aligned} u_{aG} &= S_a V_{\rm dc} > 0, S_a \in [0, 1] \\ u_{bG} &= S_b V_{\rm dc} > 0, S_b \in [0, 1] \\ u_{cG} &= S_c V_{\rm dc} > 0, S_c \in [0, 1] \end{aligned} \tag{320}$$

with subscript $_G$ denoting the negative of the dc bus, in which the concept of volt-second equivalence has been adopted.

On the other hand, the controller law we developed in previous chapters specifies the desired voltage commands in $\alpha\beta$-frame, i.e., $\boldsymbol{u}_{\alpha\beta s}$. The rest of this chapter aims

[50] If point n and point g are electrically connected, it becomes a 3 phase 4 wire system, in which phase voltage equals to terminal voltage, i.e., neutral to dc bus center voltage.

to develop the bridge between u_{xG} and $\boldsymbol{u}_{\alpha\beta s}$.

5.3.1. Sine-triangle PWM

A very natural idea is to simply use the inverse Clarke transformation that gives the phase voltages:

$$\begin{aligned}\begin{bmatrix} u_{\alpha s} \\ u_{\beta s} \\ u_{\gamma s} \end{bmatrix} &= \sqrt{\frac{2}{3}} \begin{bmatrix} 1 & \frac{-1}{2} & \frac{-1}{2} \\ 0 & \frac{\sqrt{3}}{2} & \frac{-\sqrt{3}}{2} \\ \frac{1}{\sqrt{2}} & \frac{1}{\sqrt{2}} & \frac{1}{\sqrt{2}} \end{bmatrix} \begin{bmatrix} u_{an} \\ u_{bn} \\ u_{cn} \end{bmatrix} = \sqrt{\frac{2}{3}} \begin{bmatrix} 1 & \frac{-1}{2} & \frac{-1}{2} \\ 0 & \frac{\sqrt{3}}{2} & \frac{-\sqrt{3}}{2} \\ \frac{1}{\sqrt{2}} & \frac{1}{\sqrt{2}} & \frac{1}{\sqrt{2}} \end{bmatrix} \begin{bmatrix} u_{aG} + u_{Gn} \\ u_{bG} + u_{Gn} \\ u_{cG} + u_{Gn} \end{bmatrix} \\ &= \sqrt{\frac{2}{3}} \begin{bmatrix} 1 & \frac{-1}{2} & \frac{-1}{2} \\ 0 & \frac{\sqrt{3}}{2} & \frac{-\sqrt{3}}{2} \\ \frac{1}{\sqrt{2}} & \frac{1}{\sqrt{2}} & \frac{1}{\sqrt{2}} \end{bmatrix} \begin{bmatrix} u_{aG} \\ u_{bG} \\ u_{cG} \end{bmatrix} + \begin{bmatrix} 0 \\ 0 \\ \sqrt{3} u_{Gn} \end{bmatrix}\end{aligned} \tag{321}$$

where our voltage control law specifies zero neutral-axis voltage: $u_{\gamma s} = 0$.

In order to impose the constraint $S_x \in [0, 1]$, let's assume the phase voltages are sinusoidal

$$\begin{aligned} u_{an} &= V_{\text{SPWM}} \sin\phi_a = \underbrace{(V_{\text{SPWM}} \sin\phi_a + V_{\text{SPWM}})}_{u_{aG}} \underbrace{- V_{\text{SPWM}}}_{u_{Gn}} = u_{aG} + u_{Gn} \\ u_{bn} &= V_{\text{SPWM}} \sin\phi_b \\ u_{cn} &= V_{\text{SPWM}} \sin\phi_c \end{aligned} \tag{322}$$

where V_{SPWM} is the phase voltage amplitude that needs to be bounded by our choice of inverter control law S_x.

Our objective is to derive inverter control law $S_x \in [0, 1]$. One straightforward idea is simply adding a dc bias to phase voltage:

$$u_{aG} = S_a V_{\text{dc}} = V_{\text{SPWM}} \sin\phi_a + V_{\text{SPWM}} \tag{323}$$

$$\Rightarrow S_a = S_a(\phi_a; V_{\text{SPWM}}) = \frac{V_{\text{SPWM}} \sin\phi_a + V_{\text{SPWM}}}{V_{\text{dc}}} \tag{324}$$

which ensures $S_a \in [0, 1]$. In literature, this idea is known as the sine-triangle PWM or SPWM. "Sine" is due to the assumption of the modulation waveform u_{aG} to be a biased sinusoidal, and "triangle" is related to the hardware implementation for calculating duty ratio S_x involves triangular carrier signal.

When over-modulation is not allowed, that is, when $S_x \leq 1$, we can derive the maximal allowed phase voltage amplitude is:[51]

$$\max_{V_{\text{SPWM}}} \left(\max_{\phi_a} (S_a) \right) \leq 1 \Rightarrow V_{\text{SPWM}} \leq \frac{1}{2} V_{\text{dc}} \tag{325}$$

The maximal phase voltage amplitude by SPWM is half the dc bus voltage.

[51] For more information about over-modulation, see this article of Microchip: `https://developerhelp.microchip.com/xwiki/bin/view/applications/motors/control-algorithms/3-phase-foc/`.

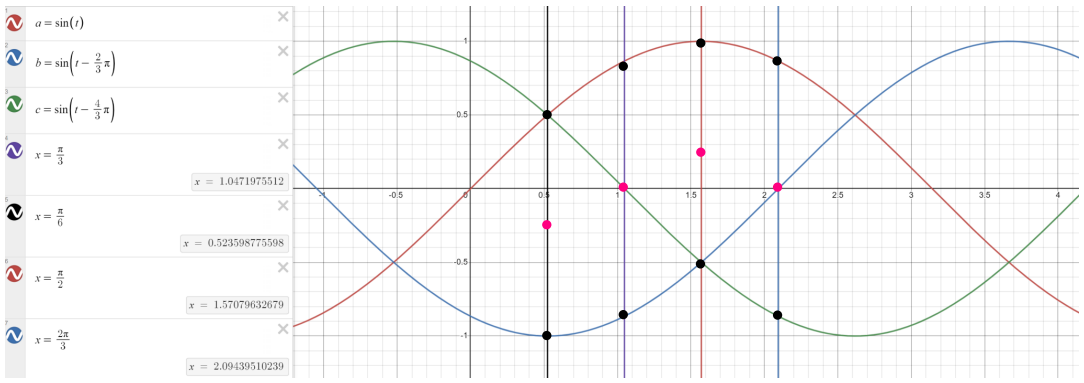

Figure 27. Differences in phase voltage u_{xn} are always less than the sinusoidal amplitude.

The maximal line-to-line voltage is

$$u_{ab} = V_{\text{SPWM}} \left(\sin \phi_a - \sin \left(\phi_a - \frac{2}{3}\pi \right) \right) = \sqrt{3} V_{\text{SPWM}} \sin \phi_{ab} \tag{326}$$

and the maximal line-to-line voltage amplitude by SPWM is

$$\max \left(u_{ab} \right) = \sqrt{3} \max \left(V_{\text{SPWM}} \right) = \frac{\sqrt{3}}{2} V_{\text{dc}} = 0.866 V_{\text{dc}} < V_{\text{dc}} \tag{327}$$

5.3.2. DC Bus Voltage Utilization

It is easy to validate that maximal instantaneous value for line-to-line voltage must be V_{dc}. For example, when terminal a is connected to dc bus positive, and terminal b is connected to dc bus negative. Therefore, we may conclude that the inverter control law, SPWM (324), does not take full capability of the inverter as is revealed in (327).

Let's draw all phase voltages in one plot in Fig. 27. Without loss of generality, let's assume $V_{\text{dc}} = 1$ V and apparently $\max(S_x) = 1$. From Fig. 27, it is seen that at any time instant, the maximal difference among the three phase voltages is less than the amplitude of the sinusoidal, 1 V.

This motivates us to visualize the dc bus voltage utilization by calculating "maximal difference among the three phase voltages", which can be rewritten in math language as

$$\eta_{\text{Vdc}} = \frac{\max \left(u_{an}, u_{bn}, u_{cn} \right) - \min \left(u_{an}, u_{bn}, u_{cn} \right)}{2} \tag{328}$$

where η_{Vdc} is known as the span of the three phase voltages. The time domain waveform of the SPWM span $\eta_{\text{Vdc}} < 1$ V is visualized in Fig. 28. Our objective is to increase the span η_{Vdc} to be equal to V_{dc}, but using SPWM, the black dots in Fig. 27 are already reaching the limits of -1 V and 1 V.

5.3.3. Space Vector PWM

In order to improve the dc bus voltage utilization ratio, the span η_{Vdc} needs to be maximized. The maximal allowed span η_{Vdc} occurs when the black dots in Fig. 27

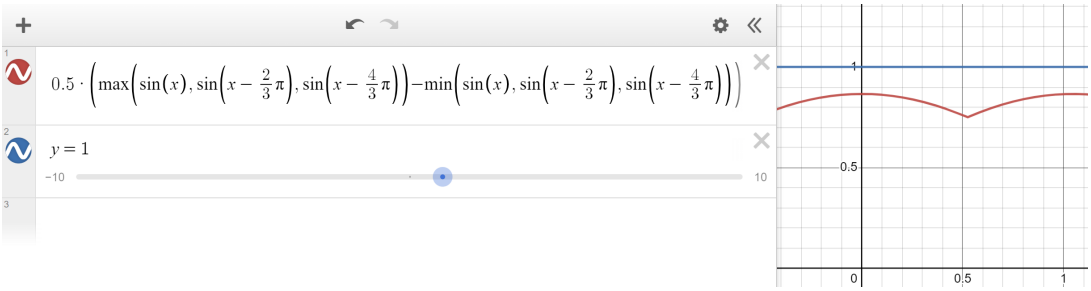

Figure 28. The utilization ratio of the SPWM corresponding to Fig. 27.

reaching $V_{\text{dc}} = \pm 1$ V, and the span is simply the distance between the two black dots at the same instant. Let's call the vertical line between the two black dots as the "span dimension line". The red dots in Fig. 27 are the middle points of the "span dimension line". The location of the red dots can be calculated as

$$\frac{\max\left(u_{an}, u_{bn}, u_{cn}\right) + \min\left(u_{an}, u_{bn}, u_{cn}\right)}{2} \tag{329}$$

In order to create more space for the black dots, one idea is to move the red dots to 0 V. This can be achieved by deliberately injecting some neutral-axis voltage as follows:

$$\frac{u_{\gamma s}}{\sqrt{3}} = -\frac{\max\left(u_{an}, u_{bn}, u_{cn}\right) + \min\left(u_{an}, u_{bn}, u_{cn}\right)}{2} \tag{330}$$

and the resulting phase voltage becomes:

$$(330) \Rightarrow u_{an} = \underbrace{V_{\text{SVPWM}} \sin\phi_a}_{\text{due to } u_{\alpha s} \text{ and } u_{\beta s}} \underbrace{- \frac{\max\left(u_{an}, u_{bn}, u_{cn}\right) + \min\left(u_{an}, u_{bn}, u_{cn}\right)}{2}}_{\text{due to zero seuqence voltage } u_{\gamma s}} \tag{331}$$

which effectively forces the red dots in Fig. 27 to stay at 0 V.

Finally, the terminal voltage and inverter control law can be accordingly determined as:

$$(331) \Rightarrow S_a V_{\text{dc}} = u_{aG} = V_{\text{SVPWM}} \sin\phi_a + V_{\text{SVPWM}} - \frac{\max\left(u_{an}, u_{bn}, u_{cn}\right) + \min\left(u_{an}, u_{bn}, u_{cn}\right)}{2} \tag{332}$$

and note this injects a zero sequence component in the three phase duty ratio control variables:

$$\sum_{x=a,b,c} S_x = S_a + S_b + S_c = \frac{3}{V_{\text{dc}}} \left(V_{\text{SVPWM}} - \frac{\max\left(u_{an}, u_{bn}, u_{cn}\right) + \min\left(u_{an}, u_{bn}, u_{cn}\right)}{2} \right) \tag{333}$$

This inverter control law is also known as the middle-point clamping of the zero sequence modulation (ZSM). In other words, its key idea is to move the three phase voltages up and down such that at any instant, the "span dimension line" of the three phase voltages are centered about the horizontal axis in Fig. 27, hence the name middle point clamping.

Middle-point clamped zero sequence modulation (ZSM)[52] is also known as space vector PWM (SVPWM). For a different derivation for the same inverter control law (331), see Appendix G.

Regarding the dc bus voltage utilization ratio, the constraint $S_a \leq 1$ leads to the maximal terminal voltage:

$$\begin{aligned}
&\max(u_{aG}) = \max\left[V_{\text{SVPWM}}\sin\phi_a + V_{\text{SVPWM}} - \frac{\max(u_{an},u_{bn},u_{cn}) + \min(u_{an},u_{bn},u_{cn})}{2}\right] \leq V_{\text{dc}} \\
&\Rightarrow V_{\text{SVPWM}} = \frac{1}{\sqrt{3}}V_{\text{dc}} > \frac{V_{\text{dc}}}{2}
\end{aligned} \tag{334}$$

in which the existence of the ZSM voltage helps amplitude V_{SVPWM} to achieve higher terminal voltage than SPWM ($\frac{V_{\text{dc}}}{2}$). The maximum of the line-to-line voltage is

$$(331) \Rightarrow \max(u_{ab}) = \max(u_{aG} - u_{bG}) = V_{\text{dc}}$$

We conclude that the SVPWM is able to achieve a unity dc bus voltage utilization ratio, as we have desired in section 5.3.2.

5.3.4. ZSM in SVPWM

The SVPWM inverter control law S_a^* can be summarized in the following process:

$$\begin{aligned}
&\sqrt{\frac{2}{3}}u_{\alpha s}^* + \frac{u_{\gamma s}^*}{\sqrt{3}} = u_{an}^* + u_{\text{ZSM}}^* = u_{aG}^* + u_{Gn} \\
&= S_a^* V_{\text{dc}} + u_{Gn} = \left(V_{\text{SVPWM}}\sin\phi_a + V_{\text{SVPWM}} - \frac{\max(u_{an},u_{bn},u_{cn}) + \min(u_{an},u_{bn},u_{cn})}{2}\right) - V_{\text{SVPWM}} \\
&\Rightarrow \text{Inverter Control Law}: S_a^* = \frac{V_{\text{SVPWM}}\sin\phi_a + V_{\text{SVPWM}} - \frac{\max(u_{an},u_{bn},u_{cn})+\min(u_{an},u_{bn},u_{cn})}{2}}{V_{\text{dc}}}
\end{aligned} \tag{335}$$

where we have injected the ZSM voltage as follows

$$u_{\text{ZSM}}^* = -\frac{\max(u_{an},u_{bn},u_{cn}) + \min(u_{an},u_{bn},u_{cn})}{2} \tag{336}$$

and $V_{\text{SVPWM}} = \left|\boldsymbol{u}_{\alpha\beta s}^*\right|$ and ϕ_a is the angle between the voltage vector $\boldsymbol{u}_{\alpha\beta s}^*$ and the phase-a axis.

[52] See the tutorial of the zero sequence modulation and space vector modulation by Microchip at https://developerhelp.microchip.com/xwiki/bin/view/applications/motors/control-algorithms/zsm/zsm/best-zsm/

5.4. Change of Voltage Reference

Previously, we have assumed that the terminal voltage is $u_{xG} = S_x V_{\rm dc}$ with S_x the duty ratio of the power switch. The duty ratio is equal to the conducting time divided by PWM period:

$$S_x = \frac{T_x}{T_{\rm PWM}} \tag{337}$$

where $T_{\rm PWM}$ designates the PWM period and $T_x \in [0, T_{\rm PWM}]$ denotes the actual conducting-time of phase x inverter leg. A typical value range of $T_{\rm PWM}$ silicon based power switch is $T_{\rm PWM} \in$ [0.5e-4, 2.5e-4] s. The resulting terminal voltage is

$$\begin{aligned} (337) \Rightarrow u_{xG} &= V_{\rm dc} S_x = V_{\rm dc} \frac{T_x}{T_{\rm PWM}} \\ \Rightarrow u_{xg} &= \frac{V_{\rm dc}}{2} (2S_x - 1) = \frac{V_{\rm dc}}{2} \left(\frac{2T_x}{T_{\rm PWM}} - 1 \right) \end{aligned} \tag{338}$$

where point G is the dc bus negative and point g denotes dc bus center. In the sequel, we will refer the voltage to g instead of G.

5.5. Time Average Inverter Model Considering Voltage Drops

In reality, the voltage source inverter is not a perfect power supply and its terminal voltage u_{xg} is dependent on its load current i_x. One well known $T_{\rm PWM}$-period average model for terminal voltage u_{xg} is [29]

$$u_{xg} = \frac{V_{\rm dc} - V_{ce} + V_d}{2} \left(\frac{2T_x}{T_{\rm PWM}} - 1 \right) - \frac{1}{2} \text{sign}(i_x) (V_{ce} + V_d) \tag{339}$$

where V_{ce} and V_d are the voltage drop of the switching device[53] and the freewheeling diode, respectively, and they can be further modelled as $V_{ce} = V_{ce0} + r_{ce}|i_x|$ and $V_d = V_{d0} + r_d|i_x|$ with V_{ce0} and V_{d0} positive constants; r_{ce} and r_d are the resistance of the switching device and the freewheeling diode, respectively. The expression for u_{xg} can be rewritten as

$$u_{xg} = \frac{V_{\rm dc} - V_{ce} + V_d}{2} \left(\frac{2T_x}{T_{\rm PWM}} - 1 \right) - \frac{1}{2} \text{sign}\,(i_x) (V_{ce0} + V_{d0}) - \frac{1}{2} (r_{ce} + r_d)\, i_x \tag{340}$$

which implies that the inverter has internal resistance of $r_{ce} + r_d$ that will be connected to the stator winding. It is desired that $R \gg r_{ce} + r_d$, which serves as one rule for pairing motor and inverter.

This model seems complicated but it is in fact rather intuitive if we consider two extreme cases when $T_x = 0$ or $T_x = T_{\rm PWM}$, leading to 4 scenarios further considering

[53] Subscript c and e stand for collector and emitter, respectively.

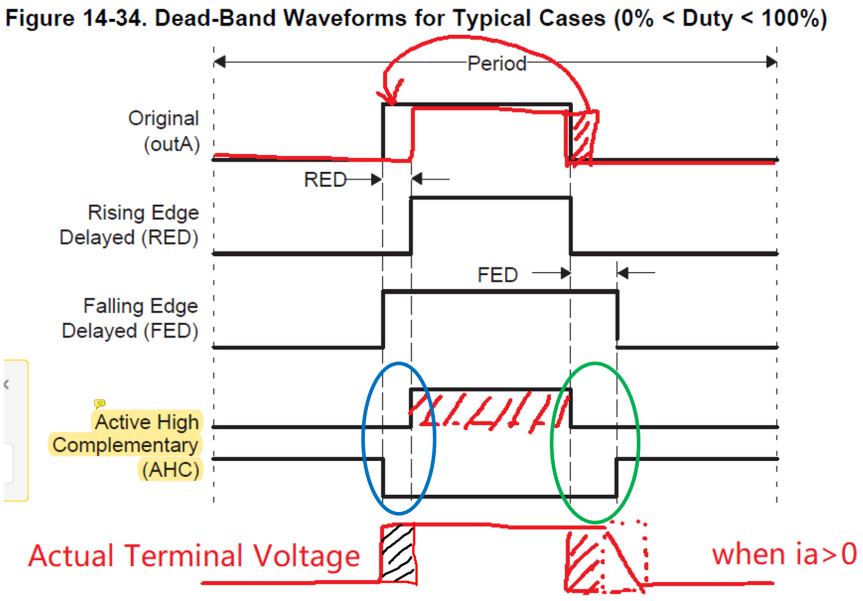

Figure 29. Three options for inserting dead time. The original figure is a screenshot from the technical reference for DSP 2837x ePWM module.

the load current direction:

$$\begin{aligned} u_{xg} &= -\frac{V_{\text{dc}}}{2} - V_d, \text{ if } T_x = 0 \text{ and } i_x > 0 \\ u_{xg} &= -\frac{V_{\text{dc}}}{2} + V_{ce}, \text{ if } T_x = 0 \text{ and } i_x < 0 \\ u_{xg} &= \frac{V_{\text{dc}}}{2} - V_{ce}, \text{ if } T_x = T_{\text{PWM}} \text{ and } i_x > 0 \\ u_{xg} &= \frac{V_{\text{dc}}}{2} + V_d, \text{ if } T_x = T_{\text{PWM}} \text{ and } i_x < 0 \end{aligned} \tag{341}$$

5.6. Dead Time

The semiconductor power switch has rise time and fall time such that there is a delay between the gate signal and the switch action and there is a risk both switches from the same half bridge leg are ON at the same time instant. Additional dead time (when both switches are OFF) is inserted into the gate signal. Three different delay implementations of dead time are shown in Fig. 29.

5.7. Time Average Inverter Model Further Considering Dead Time

In practice, the actual conducting time T_x is not at our control, and it is equal to:

$$T_x = T_x^* + \text{sign}(i_x)(-T_{\text{on}} + T_{\text{off}} - T_{\text{dead}}) \tag{342}$$

where $T_{\text{dead}}, T_{\text{on}}, T_{\text{off}}$ are dead time, rising time and falling time, respectively, The resulting terminal-to-center voltage becomes

$$\begin{aligned} u_{xg} &= \frac{V_{\text{dc}} - V_{ce} + V_d}{2} \left(2 \frac{T_x^* + \text{sign}(i_x) \left(-T_{\text{on}} + T_{\text{off}} - T_{\text{dead}} \right)}{T_{\text{PWM}}} - 1 \right) - \frac{1}{2} \text{sign}(i_x) \left(V_{ce} + V_d \right) \\ &= \frac{V_{\text{dc}} - V_{ce} + V_d}{2} \left(2 \frac{T_x^*}{T_{\text{PWM}}} - 1 \right) + V_{\text{dist}} \text{sign}(i_x) - \frac{1}{2} \left(r_{ce} + r_d \right) i_x \end{aligned} \tag{343}$$

with an inverter distortion voltage parameter defined as

$$V_{\text{dist}} \triangleq \left(V_{\text{dc}} - V_{ce} + V_d \right) \left(\frac{-T_{\text{on}} + T_{\text{off}} - T_{\text{dead}}}{T_{\text{PWM}}} \right) - \frac{1}{2} \left(V_{ce0} + V_{d0} \right)$$

which reveals that there are two kinds of distortion, one is due to the voltage drops of the power switches and the other is due to the conducting time error.

5.8. The Neutral to Center Voltage

From (321), recall

$$u_{xg} = u_{xn} + u_{ng}, \ x = a, b, c \tag{344}$$

$$u_{\gamma s} = \sqrt{\frac{2}{3}} \frac{1}{\sqrt{2}} \left(u_{an} + u_{bn} + u_{cn} \right) \tag{345}$$

and we can now derive the expression for neutral to center voltage u_{ng}:

$$u_{ng} = \frac{1}{3} \left(u_{ag} + u_{bg} + u_{cg} \right) - \frac{1}{3\sqrt{3}} u_{\gamma s} \tag{346}$$

which means the voltage difference u_{ng} is closely related to the zero sequence component of the inverter's terminal voltage and the zero sequence component of the winding phase voltage.

According to (346), u_{ng} can be derived as

$$\begin{aligned} u_{ng} &= \frac{1}{3} \left(u_{ag} + u_{bg} + u_{cg} \right) - \frac{1}{3\sqrt{3}} u_{\gamma s} \\ &= \frac{V_{\text{dc}} - V_{ce} + V_d}{3} \left(\frac{\sum_{x=a,b,c} T_x^*}{T_{\text{PWM}}} - \frac{3}{2} \right) + \frac{V_{\text{dist}}}{3} \sum_{x=a,b,c} \text{sign}(i_x) - \frac{r_{ce} + r_d}{6} \sum_{x=a,b,c} i_x - \frac{1}{3\sqrt{3}} u_{\gamma s} \end{aligned} \tag{347}$$

where note the term involving V_{dist} collects all distortion, and note for wye connected winding we have $\sum_{x=a,b,c} i_x = 0$.

What we are really interested in is the phase voltage u_{xn} and its expression is, however, a function of 3 phase conducting time T_a^*, T_b^*, T_c^*, because of the neutral-to-

center voltage $u_{ng}(T_a^*, T_b^*, T_c^*)$. The phase voltage is

$$\begin{aligned} u_{xn} &= u_{xg} - u_{ng} = \frac{V_{\mathrm{dc}} - V_{ce} + V_d}{2}\left(2\frac{T_x^*}{T_{\mathrm{PWM}}} - 1\right) + V_{\mathrm{dist}}\mathrm{sign}(i_x) - \frac{1}{2}\left(r_{ce} + r_d\right) i_x \\ &- \left[\frac{V_{\mathrm{dc}} - V_{ce} + V_d}{3}\left(\frac{\sum_{x=a,b,c} T_x^*}{T_{\mathrm{PWM}}} - \frac{3}{2}\right) + \frac{V_{\mathrm{dist}}}{3}\sum_{x=a,b,c}\mathrm{sign}(i_x) - 0 - \frac{1}{3\sqrt{3}}u_{\gamma s}\right] \\ &= \frac{V_{\mathrm{dc}} - V_{ce} + V_d}{3}\frac{3T_x^* - \sum_{x=a,b,c} T_x^*}{T_{\mathrm{PWM}}} + \frac{3V_{\mathrm{dist}}\mathrm{sign}(i_x) - \sum_{x=a,b,c}\mathrm{sign}(i_x)}{3} - \frac{1}{2}\left(r_{ce} + r_d\right) i_x + \frac{1}{3\sqrt{3}}u_{\gamma s} \end{aligned} \tag{348}$$

which shall be rearranged into a form of "command + distortion + ZSM term + resistor voltage drop" as follows

$$u_{xn} = u_{xn}^* - D_x + u_{\mathrm{ZSM}} - \frac{1}{2}\left(r_{ce} + r_d\right) i_x \tag{349}$$

For instance, when $x = a$, recall (333) and the phase a voltage is

$$\begin{aligned} u_{an} &= \frac{V_{\mathrm{dc}} - V_{ce} + V_d}{3}\left(3S_a^* - \sum_{x=a,b,c} S_x^*\right) + \frac{3V_{\mathrm{dist}}\mathrm{sign}(i_x) - \sum_{x=a,b,c}\mathrm{sign}(i_x)}{3} - \frac{1}{2}\left(r_{ce} + r_d\right) i_x + \frac{1}{3\sqrt{3}}u_{\gamma s} \\ &= \underbrace{V_{\mathrm{SVPWM}}\sin\phi_a}_{u_{an}^*} + \underbrace{\left(-V_{ce} + V_d\right) S_a^* - \left(V_{\mathrm{dist}}\left[2\mathrm{sign}(i_a) - \mathrm{sign}(i_b) - \mathrm{sign}(i_c)\right]\right)}_{-D_a} + \underbrace{\frac{1}{3\sqrt{3}}u_{\gamma s}}_{u_{\mathrm{ZSM}}} - \frac{1}{2}\left(r_{ce} + r_d\right) i_a \end{aligned} \tag{350}$$

in which it is of interest to note the following expression for phase voltage:

$$u_{an}^* = V_{\mathrm{dc}}\left(S_a^* - \frac{1}{3}\sum_{x=a,b,c} S_x^*\right) = V_{\mathrm{SVPWM}}\sin\phi_a \tag{351}$$

In practice, V_{dc} is often large enough to assume that

$$\left(V_{\mathrm{dc}} - V_{ce} + V_d\right) S_a^* \approx V_{\mathrm{dc}} S_a^* \tag{352}$$

or equivalently that

$$\left(-V_{ce} + V_d\right) S_a^* \approx 0 \tag{353}$$

so the distortion voltage can be simplified into

$$\begin{aligned} D_a &= V_{\mathrm{dist}}\left[2\mathrm{sign}(i_a) - \mathrm{sign}(i_b) - \mathrm{sign}(i_c)\right] + \left(V_{ce} + V_d\right) S_a^* && (354) \\ &\approx V_{\mathrm{dist}}\left[2\mathrm{sign}(i_a) - \mathrm{sign}(i_b) - \mathrm{sign}(i_c)\right] && (355) \\ &= 3V_{\mathrm{dist}}\mathrm{sign}(i_a) - V_{\mathrm{dist}}\sum_{x=a,b,c}\mathrm{sign}(i_x) && (356) \end{aligned}$$

in which the last equation allows us to write $D_a(i_a)$ as a function of phase current i_a, because the dependency on other phase currents is a zero sequence component. In

conclusion, the inverter distortion voltage has one phase voltage component that has a peak value of $3V_{\text{dist}}$ and one zero sequence component.

5.9. Converting Inverter Model to αβ Quantities

By applying the Clarke transformation, the phase voltage quantities are transformed into α-β quantities

$$\begin{aligned}\boldsymbol{u}^*_{\alpha\beta s} = \begin{bmatrix} u^*_{\alpha s} \\ u^*_{\beta s} \end{bmatrix} &= \frac{V_{\text{dc}} - V_{ce} + V_d}{3T_{\text{PWM}}}\sqrt{\frac{2}{3}}\begin{bmatrix} 3T^*_a - 1.5T^*_b - 1.5T^*_c \\ \frac{\sqrt{3}}{2}\left(3T^*_b - 3T^*_c\right) \end{bmatrix} = \boldsymbol{T}(0)\begin{bmatrix} u^*_{an} \\ u^*_{bn} \\ u^*_{cn} \end{bmatrix} \\ \boldsymbol{u}^*_{\alpha\beta s} = \begin{bmatrix} u^*_{\alpha s} \\ u^*_{\beta s} \end{bmatrix} &= \left(V_{\text{dc}} - V_{ce} + V_d\right)\sqrt{\frac{2}{3}}\begin{bmatrix} S^*_a - \frac{1}{2}S^*_b - \frac{1}{2}S^*_c \\ \frac{\sqrt{3}}{2}\left(S^*_b - S^*_c\right) \end{bmatrix} = \boldsymbol{T}(0)\begin{bmatrix} u^*_{an} \\ u^*_{bn} \\ u^*_{cn} \end{bmatrix}\end{aligned} \tag{357}$$

and the distorted voltages are derived as

$$\boldsymbol{D}_{\alpha\beta} = \begin{bmatrix} D_\alpha \\ D_\beta \end{bmatrix} = 3V_{\text{dist}}\sqrt{\frac{2}{3}}\begin{bmatrix} \text{sign}\left(i_a\right) - \frac{1}{2}\text{sign}\left(i_b\right) - \frac{1}{2}\text{sign}\left(i_c\right) \\ \frac{\sqrt{3}}{2}\left(\text{sign}\left(i_b\right) - \text{sign}\left(i_c\right)\right) \end{bmatrix} = \boldsymbol{T}(0)\begin{bmatrix} D_a \\ D_b \\ D_c \end{bmatrix} \tag{358}$$

5.10. Inverter Voltage Error Compensation in Phase Quantities

Recall the stator voltage equation in $\alpha\beta$ frame is

$$\boldsymbol{u}_{\alpha\beta s} = R\boldsymbol{i}_{\alpha\beta s} + s\boldsymbol{\psi}_{\alpha\beta s} \tag{359}$$

where the stator voltage $\boldsymbol{u}$ is generally defined as

$$\boldsymbol{u}_{\alpha\beta s} = \boldsymbol{u}^{**}_{\alpha\beta s} - \boldsymbol{D}_{\alpha\beta} = \boldsymbol{u}^*_{\alpha\beta s} + \hat{\boldsymbol{D}}_{\alpha\beta} - \boldsymbol{D}_{\alpha\beta} \tag{360}$$

Here we introduce a inverter error compensated voltage command $\boldsymbol{u}^{**}_{\alpha\beta s}$.

Alternatively, we can compensate the inverter in terms of phase quantities:

$$u_{ag} = u^{**}_{ag} - D_a\left(i_a\right) = u^*_{ag} + \hat{D}\left(i_a\right) - D\left(i_a\right) = u_{an} + u_{ng} \tag{361a}$$

$$u_{bg} = u^{**}_{bg} - D_b\left(i_b\right) = u^*_{bg} + \hat{D}\left(i_b\right) - D\left(i_b\right) = u_{bn} + u_{ng} \tag{361b}$$

$$u_{cg} = u^{**}_{cg} - D_c\left(i_c\right) = u^*_{cg} + \hat{D}\left(i_c\right) - D\left(i_c\right) = u_{cn} + u_{ng} \tag{361c}$$

where $u_{xn},\ x = a,b,c$, is the actual phase voltage applied to the stator winding; $D_x(\cdot),\ x = a,b,c$ is the *sampling-time-average* distorted voltage of one inverter leg, which is assumed to be a function of its phase current; $u_{xg},\ x = a,b,c$, is the actual motor terminal voltage; and $u^{**}_{xg},\ x = a,b,c$, is the commanded terminal voltage including compensation as follows

$$u^{**}_{xg} = u^*_{xg} + \hat{D}_x\left(i_x\right), \quad x = a,b,c \tag{362}$$

where $\hat{D}_x(\cdot)$ is the compensation voltage per phase, and u^*_{xg} is the motor controller output voltage.

In our simulation, when an ideal inverter is assumed, the "zero sequence voltage" u_{ng} is neglected and assume that the motor controller can control phase voltage directly, i.e., $u^*_{xg} = u_{xn}$. However, the same codes can be directly used in experiment where zero sequence voltage is indeed present. This is due to the following attribute of the Clarke transformation:

$$\begin{bmatrix} u_{\alpha s} \\ u_{\beta s} \\ u_{\gamma s} \end{bmatrix} = \sqrt{\frac{2}{3}} \begin{bmatrix} 1 & \frac{-1}{2} & \frac{-1}{2} \\ 0 & \frac{\sqrt{3}}{2} & \frac{-\sqrt{3}}{2} \\ \frac{1}{\sqrt{2}} & \frac{1}{\sqrt{2}} & \frac{1}{\sqrt{2}} \end{bmatrix} \begin{bmatrix} u_{ag} \\ u_{bg} \\ u_{cg} \end{bmatrix} = \sqrt{\frac{2}{3}} \begin{bmatrix} 1 & \frac{-1}{2} & \frac{-1}{2} \\ 0 & \frac{\sqrt{3}}{2} & \frac{-\sqrt{3}}{2} \\ \frac{1}{\sqrt{2}} & \frac{1}{\sqrt{2}} & \frac{1}{\sqrt{2}} \end{bmatrix} \begin{bmatrix} u_{an} \\ u_{bn} \\ u_{cn} \end{bmatrix} + \begin{bmatrix} 0 \\ 0 \\ u_{ng} \end{bmatrix} \tag{363}$$

Therefore, we can neglect the zero sequence component without introducing any simulation error in $\alpha\beta$-axes quantities. This is one of the many reasons why we have to solve the motor dynamics in a direct-quadrature reference frame. Do remember that the zero sequence voltage affects the dc bus voltage utilization ratio.

5.10.1. Brief Summary

To recap, in virtue of the Clarke transformation attribute (363), the commanded terminal voltage $u^{**}_{xg} = u^*_{xg} + \hat{D}_x$ of a 3 phase 3 wire system is converted into $\alpha\beta$-frame voltage $\boldsymbol{u}_{\alpha\beta s}$ and $\alpha\beta$-frame compensation $\hat{\boldsymbol{D}}_{\alpha\beta}$. The latter rejects the voltage disturbance $\boldsymbol{D}_{\alpha\beta}$, and the former regulates stator current or stator flux through the voltage equation (359).

In practice, the following procedure is implemented in C codes:

(1) The voltage commands $\boldsymbol{u}^*_{\alpha\beta s}$ are first given from motor controller, and the inverter control aims to produce an actual voltage $\boldsymbol{u}_{\alpha\beta s}$ that equals to the command; Inverse Clarke transformation $\boldsymbol{T}(0)^{-1}$ gives the voltage commands in phase quantities u^*_{xn}; For example, $u^*_{an} = V_{\text{SVPWM}} \sin\phi_a$;

(2) A voltage compensation $\hat{D}_a$ is added, resulting in $u^{**}_{an} = u^*_{an} + \hat{D}_a(i_a)$ and the compensation is dependent on one parameter V_{dist} only:

$$\hat{D}_a\left(i_a\right) = V_{\text{dist}} \left(3\text{sign}(i_a) - \sum_{x=a,b,c} \text{sign}(i_x) \right)$$

(3) From u^{**}_{an}, the commanded conducting time T^{**}_a is computed by SVPWM:

$$S^{**}_a = \frac{u^{**}_{an}}{V_{\text{dc}}} + \frac{V_{\text{SVPWM}}}{V_{\text{dc}}} - \frac{\max\left(u_{an}, u_{bn}, u_{cn}\right) + \min\left(u_{an}, u_{bn}, u_{cn}\right)}{2V_{\text{dc}}} = \frac{T^{**}_a}{T_{\text{PWM}}} = \frac{u^{**}_{aG}}{V_{\text{dc}}}$$

in which the command T^{**}_a contains the compensation time for rise time, falling time and dead time.

(4) Substitute T^{**}_a into (343) to calculate the actual terminal voltage; Note terminal voltage u_{xG} or u_{xg} is equivalent to u_{xn} in $\alpha\beta$ frame as per (363).

The above compensation scheme depends on one key parameter is V_{dist}, so we need to experimentally determine V_{dist} before we can execute dead-time compensation.

5.10.2. Square-wave Compensation

As a comparison, in Choi and Sul's paper [29], the compensation voltage is

$$\hat{D}_a = 3V_{\text{dist}}\text{sign}\left(i_a\right) \tag{364}$$

which is also known as the square-wave dead time compensation in literature. Note the zero sequence component is not compensated, and therefore the ZSM will be disturbed such that the voltage utilization ratio will be degraded.

In practice, the experimental measured distorted phase voltage $\hat{D}_a$ is really a function of i_a value, as is later discussed in Section 5.11.

5.11. Experimental Measurement of Inverter Nonlinearity

We can measure the inverter nonlinearity by exciting the motor with dc current. For example, we excite $i_{\alpha s} = \sqrt{\frac{3}{2}}$ A. The resulting phase a distortion voltage will be:

$$\begin{aligned} D_a &= V_{\text{dist}}\left[2\text{sign}\left(i_a\right) - \text{sign}\left(i_b\right) - \text{sign}\left(i_c\right)\right] \\ &= V_{\text{dist}}\left[2\text{sign}\left(1\text{A}\right) - \text{sign}\left(-0.5\text{A}\right) - \text{sign}\left(-0.5\text{A}\right)\right] \\ &= 4V_{\text{dist}} \end{aligned} \tag{365}$$

which is a function of the signs of phase currents. Thus, one might conclude that the distorted voltage can be identified by applying a constant α-axis current.

However, the measured voltage-current characteristics of an inverter indicates that D_a is a function of current value, as exemplified in Fig. 30, i.e., $D_a = f(i_a)$. As a result, if i_α is regulated to be constant, it means the three phase currents will have different amplitudes, such that the $0 \neq |D_a| \neq |D_b| \neq 0$, i.e., the inverter nonlinearity cannot be easily identified.

5.11.1. Standstill DC Test

As suggested in [29], to make sure phase distorted voltages are at the same current level, we can measure voltage-current characteristics at β-axis. By applying a dc current at β-axis such that the current vector angle is $\theta_i = 90°$, from Clarke transformation, we have $i_a = i_\alpha = 0$ and $i_b = -i_c = \sqrt{\frac{2}{3}}\frac{\sqrt{3}}{2}i_{\beta s}$. Since the current at phase b is of the same amplitude of phase c, it is valid to assume the distorted voltage D_b equals to D_c.

During a β-axis dc test, the maximum of measured dc phase voltage is $3V_{\text{dist}}$ and as a result, the D_b trace in Fig. 30 has a plateau voltage of $V_{\text{plateau}} = 3V_{\text{dist}}$,

5.11.2. Blocked Rotor Rotating Field Test

The disadvantage of a standstill dc test is that it involves only open-loop measurements. Owing to measurement errors, the 3 phase current after compensation does not necessarily look sinusoidal.

If we can block the motor rotor, by applying a dc q-axis current in a slow rotating dq frame, we can measure the inverter nonlinearity as the disturbance voltage that is rejected by the current loop PI regulator.

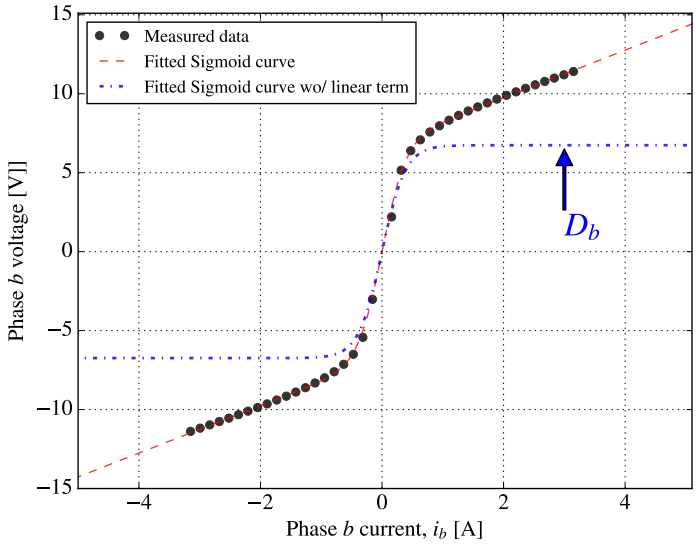

Figure 30. The measured voltage-current characteristics of an inverter when dc bus voltage is $U_{\text{dc}} = 180$ V.

5.12. Curve Fitting

Typical fitting function includes arctan, exponential function and sigmoid function.

5.12.1. Fitting for Standstill DC Test

We will use sigmoid function and SciPy for example. The Sigmoid function for curve fitting is implemented in Python as follows

```
# Given two iterables: xdata and ydata
def sigmoid(x, a1, a2, a3):
    return a1 * x + a2 / (1 + np.exp(-a3 * x)) - a2/2
from scipy.optimize import curve_fit
popt, pcov = curve_fit(sigmoid, xdata, ydata)
a1, a2, a3 = popt
```

where the three coefficients, $a_1, \frac{a_2}{2}, a_3$ are the straight line slope, the plateau voltage, and the exponent coefficient, respectively. Example fitting results are shown in Fig. 30.

In our case, a_1 is an estimate of the total resistance including inverter resistance and winding resistance, and we will only need a_2 and a_3 for compensating the distorted voltage, depending on the inverter model.

If Choi and Sul's model is adopted for compensation, based on (365), all we need is to solve for $V_{\text{dist}} = \frac{a_2}{2}/3$.

If look-up table or fitted curve is adopted for compensation, with the measured phase current i_x, the compensation voltage will be $\hat{D}_x(i_x) = \text{sigmoid}(i_x, a_1, a_2, a_3)$. In ideal situation, we would have $\hat{D}_x(i_x) - D_x(i_x) = -\sum_{x=a,b,c} \text{sign}(i_x)$.

5.12.2. Fitting for Blocked Rotor Rotating Field Test

By doing a rotating field test, we make sure the 3 phase currents are sinusoidal using PI regulator in dq frame. The voltage-current characteristics obtained in a blocked rotor rotating field test do not include the zero sequence voltage u_0.

One realizes there is mismatch between the result of the blocked rotor rotating field

test to that of standstill dc test, mainly during low current region. We tend to believe that the result from the blocked rotor rotating field test is more accurate, meaning the standstill dc test can be erroneous during low current region.

In practical situation, a blocked rotor is not usually available. This reveals the need of online correction of the a_3 coefficient that corresponds to the low current region.

5.13. Stray Capacitors

This section will briefly review the one parameter inverter model based on physics of power switches, where stray capacitors (or parasite capacitors, see C_{stray} in Fig. 26) are neglected. In order to account for the effect of stray capacitors, the experimentally measured U-I curve data points are fitted to modified sigmoid function, which results in a two parameter inverter model that will later be identified online.

5.13.1. One Parameter Inverter Model

The inverter is modelled using one unknown parameter V_{dist}

$$D_a = V_{\text{dist}} \left[2\text{sign}\left(i_a\right) - \text{sign}\left(i_b\right) - \text{sign}\left(i_c\right)\right] \tag{366}$$

which does not match our desired model in which $\hat{D}_x(i_x)$ is only a function of single phase current i_x. To remove D_a's dependency on other phases, a zero sequence voltage

$$u_0 = V_{\text{dist}} \left[\text{sign}\left(i_a\right) + \text{sign}\left(i_b\right) + \text{sign}\left(i_c\right)\right] \tag{367}$$

can be added to D_a, leading to the one parameter inverter model $\hat{D}_x(i_x)$:

$$\hat{D}_a = D_a + u_0 = 3V_{\text{dist}}\text{sign}\left(i_a\right) = V_{\text{plateau}}\text{sign}\left(i_a\right) \tag{368}$$

which gives the plateau voltage as $V_{\text{plateau}} = 3V_{\text{dist}}$.

The one parameter inverter model has taken dead-time, turn-on/off time, conduction voltage drop into account [29]. When the compensation voltage in (368) is put in action, excessive compensation occurs during zero-current crossing. This fact implies that there exists neglected effect that is contributing to the terminal voltage when current is low.

5.13.2. Effect of Stray Capacitors

Following [30], during dead-time, both upper and lower power switches are turned off. Consequently, the actual inverter terminal voltage u_{xg} is not controlled, and is determined by the load current i_x and the power switch's small yet non-negligible stray capacitor C_{stray}, as shown in Fig. 26. As per definition of capacitor, the rate of change of voltage across the stray capacitor is proportional to the load current i_x. When i_x is so large that the charging of stray capacitor finishes instantaneously during dead-time, the effect of C_{stray} can be neglected. On the other hand, the stray capacitor's effect becomes dominant during dead-time, when load current i_x is so low such that [31, (7.3)]

$$|i_x| < i_{\text{ZCC}} \triangleq C_{\text{stray}} \frac{V_{\text{dc}}}{T_{\text{dead}}} \tag{369}$$

where the threshold value i_{ZCC} depends on the dead time T_{dead}, dc bus voltage V_{dc} and stray capcitance C_{stray}. When the stray capacitor is slowly charged, the actual output terminal voltage u_{xg} would vary linearly, instead of a step change, leading to extra voltage gain (when $i_x > 0$) or loss (when $i_x < 0$).

In conclusion, the compensation in (368) must be reduced in low current region, e.g., when $|i_x| < i_{\text{ZCC}}$, but the extent of the reduction is a nonlinear function of load current i_x, and additional shape parameters are needed to describe this inverter model's dependency on load current i_x. In extreme case, when $i_x = 0$, the compensation voltage should be $\hat{D}_x(0) = 0$. It is suggested in [30] to experimentally measure the voltage distortion caused by stray capacitors.

5.14. Online Detection of Inverter Parameters

See [9].

5.15. Delay on Updating the PWM Comparison Register

See [31, Figure 7.15]. When the motor spins at higher speeds, at the time the calculated inverter compensation voltage is applied, the motor rotor would have rotated by a certain angle. To compensate the prorogation time from algorithm to update of gate signal, S. K. Sul suggested a 1.5 Ts compensation. The compensation is dependent on the synchronous speed and sampling time T_S.

5.16. Ortega's DTC Math

See [32].

6. Chapter 6: Motion Control

6.1. Command Tracking Performance

6.2. Disturbance Rejecting Performance

6.3. Noise Attenuating Performance

6.4. Two-Degree-Of-Freedom PI Regulator

6.5. Notch Filter

Notch filter can be added to the feedback path to remove flexible modes in the measured output. The notch filter can be understood as a pair of slightly damped stable zeros, and two poles are added to compensate for the 40 dB/dec gain for higher frequencies. [54]

6.6. Friction Model

LuGre Model. See "A New Model for Control of Systems with Friction"

[54] https://ww2.mathworks.cn/en/videos/control-systems-in-practice-part-5-a-better-way-to-think-about-a-nc
html

See also the book by John J.Craig - Introduction to Robotics Mechanics and Control 3rd edition-Pearson Education, Inc. (2005).pdf

Appendix A. List of Trigonometric Identities

For a complete list, see [1].

$$\sin(A \pm B) = \sin A \cos B \pm \cos A \sin B \tag{A1}$$

$$\cos(A \pm B) = \cos A \cos B \mp \sin A \sin B \tag{A2}$$

$$\sin A \cos B = \frac{1}{2}[\sin(A+B) + \sin(A-B)] \tag{A3}$$

$$\cos A \cos B = \frac{1}{2}[\cos(A+B) + \cos(A-B)] \tag{A4}$$

$$\sin A \sin B = \frac{1}{2}[\cos(A-B) - \cos(A+B)] \tag{A5}$$

$$\cos A + \cos\left(A - \frac{2\pi}{3}\right) + \cos\left(A + \frac{2\pi}{3}\right) = 0 \tag{A6}$$

$$\sin A + \sin\left(A - \frac{2\pi}{3}\right) + \sin\left(A + \frac{2\pi}{3}\right) = 0 \tag{A7}$$

$$\cos^2 A + \cos^2\left(A - \frac{2\pi}{3}\right) + \cos^2\left(A + \frac{2\pi}{3}\right) = \frac{3}{2} \tag{A8}$$

$$\sin^2 A + \sin^2\left(A - \frac{2\pi}{3}\right) + \sin^2\left(A + \frac{2\pi}{3}\right) = \frac{3}{2} \tag{A9}$$

$$\sin A \sin\left(A - \frac{2\pi}{3}\right) + \sin\left(A - \frac{2\pi}{3}\right) \sin\left(A + \frac{2\pi}{3}\right) + \sin\left(A + \frac{2\pi}{3}\right) \sin A = -\frac{3}{4} \tag{A10}$$

$$\cos A \cos\left(A - \frac{2\pi}{3}\right) + \cos\left(A - \frac{2\pi}{3}\right) \cos\left(A + \frac{2\pi}{3}\right) + \cos\left(A + \frac{2\pi}{3}\right) \cos A = -\frac{3}{4} \tag{A11}$$

$$\sin A \cos A + \sin\left(A - \frac{2\pi}{3}\right) \cos\left(A - \frac{2\pi}{3}\right) + \sin\left(A + \frac{2\pi}{3}\right) \cos\left(A + \frac{2\pi}{3}\right) = 0 \tag{A12}$$

$$\sin A \cos\left(A + \frac{2\pi}{3}\right) + \sin\left(A - \frac{2\pi}{3}\right) \cos A + \sin\left(A + \frac{2\pi}{3}\right) \cos\left(A - \frac{2\pi}{3}\right) = -\frac{3\sqrt{3}}{4} \tag{A13}$$

$$\sin A \cos\left(A - \frac{2\pi}{3}\right) + \sin\left(A - \frac{2\pi}{3}\right) \cos\left(A + \frac{2\pi}{3}\right) + \sin\left(A + \frac{2\pi}{3}\right) \cos A = \frac{3\sqrt{3}}{4} \tag{A14}$$

$$\cos A \cos B + \cos\left(A - \tfrac{2\pi}{3}\right) \cos\left(B - \tfrac{2\pi}{3}\right) + \cos\left(A + \tfrac{2\pi}{3}\right) \cos\left(B + \tfrac{2\pi}{3}\right) = \tfrac{3}{2} \cos(A - B) \tag{A15}$$

$$\sin A \sin B + \sin\left(A - \tfrac{2\pi}{3}\right) \sin\left(B - \tfrac{2\pi}{3}\right) + \sin\left(A + \tfrac{2\pi}{3}\right) \sin\left(B + \tfrac{2\pi}{3}\right) = \tfrac{3}{2} \cos(A - B) \tag{A16}$$

$$\sin A \cos B + \sin\left(A - \tfrac{2\pi}{3}\right) \cos\left(B - \tfrac{2\pi}{3}\right) + \sin\left(A + \tfrac{2\pi}{3}\right) \cos\left(B + \tfrac{2\pi}{3}\right) = \tfrac{3}{2} \sin(A - B) \tag{A17}$$

Appendix B. Multi-Phase Machine Theory

This theory studies electric machine that utilizes the reaction torque, and one consequence of this assumption is that the magnetomotive force $\mathcal{F}$ differs from the magnetic flux density B only by a scalar, and in other words, a uniform air gap is assumed.

Generally speaking, the winding function of a symmetrical m phase winding that has a phase band of π/m in its star of slots plot, can be written as a Fourier series at an angular location α in the air gap [33]:

$$N_j(\alpha) = \sum_{v=1}^{\infty} N_{(v)} \cos\left\{ v\left[\alpha - (j-1)\frac{2\pi}{m}\right]\right\},\ j = 1, 2, ..., m \tag{B1}$$

where $j = 1, 2, ..., m$ is phase index, $v = 1, 3, 5, ..., \infty$ is harmonic index, and α denotes an arbitrary electrical angular location along the air gap, meaning that α is n_{pp} times mechanical angular location along the air gap, with n_{pp} as the pole pair number of the fundamental component of the winding function of the multi-phase winding.

For a $m = 3$ phase winding, (B1) becomes:

$$\begin{aligned}
N_1(\alpha) &= N_{(1)}\cos(\alpha) + N_{(3)}\cos(3\alpha) + N_{(5)}\cos(5\alpha) + \cdots \\
N_2(\alpha) &= N_{(1)}\cos\left(\alpha - \frac{2\pi}{3}\right) + N_{(3)}\cos\left[3\left(\alpha - \frac{2\pi}{3}\right)\right] + N_{(5)}\cos\left[5\left(\alpha - \frac{2\pi}{3}\right)\right] + \cdots \\
N_3(\alpha) &= N_{(1)}\cos\left(\alpha - \frac{4\pi}{3}\right) + N_{(3)}\cos\left[3\left(\alpha - \frac{4\pi}{3}\right)\right] + N_{(5)}\cos\left[5\left(\alpha - \frac{4\pi}{3}\right)\right] + \cdots
\end{aligned} \tag{B2}$$

The coefficients of the Fourier series are known as *winding factors*, indicating the winding's capability to produce a v-th order harmonic magnetomotive force per ampere. The winding factors can be calculated with the aid of *star of slots plot*.

For (B1), the corresponding m phase current excitation with intentionally injected harmonic components is

$$i_j = \sum_{k=1}^{\infty} i_{j(k)} = \sum_{k=1}^{\infty} I_{(k)} \sin\left\{ k\left[\omega_{\text{syn}} t - (j-1)\frac{2\pi}{m}\right] + \phi_{(k)}\right\} \tag{B3}$$

where $j = 1, 2, ..., m$ is phase index, $k = 1, 3, 5, ..., \infty$ is current harmonic index, $\phi_{(k)}$ is initial phase angle, and ω_{syn} is the synchronous angular speed of the fundamental component. For a three phase winding, the excitation becomes:

$$\begin{aligned}
i_1 &= I_{(1)}\sin\left(\omega_{\text{syn}} t + \phi_{(1)}\right) + I_{(3)}\sin\left[3\left(\omega_{\text{syn}} t + \phi_{(3)}\right)\right] + I_{(5)}\sin\left[5\left(\omega_{\text{syn}} t + \phi_{(5)}\right)\right] + \ldots \\
i_2 &= I_{(1)}\sin\left(\omega_{\text{syn}} t - \frac{2\pi}{3} + \phi_{(1)}\right) + I_{(3)}\sin\left[3\left(\omega_{\text{syn}} t - \frac{2\pi}{3} + \phi_{(3)}\right)\right] + I_{(5)}\sin\left[5\left(\omega_{\text{syn}} t - \frac{2\pi}{3} + \phi_{(5)}\right)\right] + \ldots \\
i_3 &= I_{(1)}\sin\left(\omega_{\text{syn}} t - \frac{4\pi}{3} + \phi_{(1)}\right) + I_{(3)}\sin\left[3\left(\omega_{\text{syn}} t - \frac{4\pi}{3} + \phi_{(3)}\right)\right] + I_{(5)}\sin\left[5\left(\omega_{\text{syn}} t - \frac{4\pi}{3} + \phi_{(5)}\right)\right] + \ldots
\end{aligned} \tag{B4}$$

For each current harmonic, it produces a magnetomotive force waveform as

$$F_{(k)}(\alpha) = N_1(\alpha)\, i_{1(k)} + N_2(\alpha)\, i_{2(k)} + \cdots + N_m i_{m(k)} \tag{B5}$$

and the total resulting magnetomotive force in the air gap is

$$F(\alpha,t)=\sum_{k=1}^{\infty}F_{(k)}(\alpha,t)=\sum_{k=1}^{\infty}\left[N_1(\alpha)\,i_{1(k)}(t)+N_2(\alpha)\,i_{2(k)}(t)+\cdots+N_m(\alpha)\,i_{m(k)}(t)\right] \tag{B6}$$

which is rewritten using the m-phase winding's full magnetomotive force due to k-th order current harmonic defined as follows

$$\begin{aligned}
&F_{(k)}(\alpha)=\sum_{j=1}^{m}i_{j(k)}N_j\\
&=\sum_{j=1}^{m}\left\{I_{(k)}\sin\left[k\left(\omega_{\text{syn}}t-(j-1)\frac{2\pi}{m}\right)+\phi_{(k)}\right]\sum_{v=1}^{\infty}N_{(v)}\cos\left[v\left(\alpha-(j-1)\frac{2\pi}{m}\right)\right]\right\}\\
&=I_{(k)}\sum_{j=1}^{m}\left(\sin A\sum_{v=1}^{\infty}N_{(v)}\cos B\right)\\
&=\frac{I_{(k)}}{2}\sum_{j=1}^{m}\left\{\sum_{v=1}^{\infty}N_{(v)}\left[\sin(A+B)+\sin(A-B)\right]\right\}\\
&=\sum_{v=1}^{\infty}F_{(k,v)}
\end{aligned} \tag{B7}$$

The m-phase winding's v-th order magnetomotive force harmonic excited by the k-th order current harmonic is

$$\begin{aligned}
&F_{(k,v)}=\frac{I_{(k)}}{2}\sum_{j=1}^{m}\left\{N_{(v)}\left[\sin(A+B)+\sin(A-B)\right]\right\}\\
&A=k\left[\omega_{\text{syn}}t-(j-1)\frac{2\pi}{m}\right]+\phi_{(k)}\\
&B=v\left[\alpha-(j-1)\frac{2\pi}{m}\right]\\
&A+B=k\left[\omega_{\text{syn}}t-(j-1)\frac{2\pi}{m}\right]+\phi_{(k)}+v\left[\alpha-(j-1)\frac{2\pi}{m}\right]\\
&\Rightarrow A+B=\left(k\omega_{\text{syn}}t+\phi_{(k)}+v\alpha\right)-(v+k)(j-1)\frac{2\pi}{m}\\
&A-B=k\left[\omega_{\text{syn}}t-(j-1)\frac{2\pi}{m}\right]+\phi_{(k)}-v\left[\alpha-(j-1)\frac{2\pi}{m}\right]\\
&\Rightarrow A-B=\left(k\omega_{\text{syn}}t+\phi_{(k)}-v\alpha\right)+(v-k)(j-1)\frac{2\pi}{m}
\end{aligned} \tag{B8}$$

which equals 0 when $k\pm v$ does not equal 0 or multiple of m so that the trigonometry equality: $\sum_{j=1}^{m}\sin\left(x+j\frac{2\pi}{m}\right)=0$ can be applied.

Iterating through all k and v values, we have the following results:

$$F_{(k,v)}(\alpha,t)=\begin{cases}\frac{mN_{(v)}I_{(k)}}{2}\sin\left(k\omega_{\text{syn}}t+\phi_{(k)}\right)\cos\left(v\alpha\right) & ,\text{ if } k\pm v=0,\pm m,\pm 2m,\dots\\ \frac{mN_{(v)}I_{(k)}}{2}\sin\left(k\omega_{\text{syn}}t+\phi_{(k)}+v\alpha\right) & ,\text{ if } k+v=0,m,2m,\dots\\ \frac{mN_{(v)}I_{(k)}}{2}\sin\left(k\omega_{\text{syn}}t+\phi_{(k)}-v\alpha\right) & ,\text{ if } k-v=0,\pm m,\pm 2m,\dots\\ 0 & ,\text{ others}\end{cases} \tag{B9}$$

The electrical angular speed of $\mathcal{F}_{(k,v)}$ can be derived as follows (which imposes that $\mathcal{F}_{(k,v)}=\text{Const.}$ stays as a constant):

$$\frac{\mathrm{d}}{\mathrm{d}t}\left(k\omega_{\text{syn}}t+\phi_{(k)}\pm v\alpha\right)=0\;\Rightarrow\;k\omega_{\text{syn}}\pm v\frac{\mathrm{d}}{\mathrm{d}t}\alpha=0\;\Rightarrow\;\frac{\mathrm{d}}{\mathrm{d}t}\alpha=\mp\frac{k}{v}\omega_{\text{syn}} \tag{B10}$$

The desired magnetomotive force should have constant speed of $\frac{\mathrm{d}}{\mathrm{d}t}\alpha=\omega_{\text{syn}}$, that is, $k=v$, and note when $k=v$, the angular speed is always positive.

For a three phase machine, the inverter (especially with low switching to fundamental ratio) might inject 5th and 7th order current harmonics, and those current harmonics will generate harmonic magnetomotive force rotating at speed of $\frac{-5}{v}\omega_{\text{syn}}$ and $\frac{7}{v}\omega_{\text{syn}}$, respectively, which are responsible for torque ripple that has a frequency of 6 times the synchronous frequency, $6\frac{\omega_{\text{syn}}}{2\pi}$ [Hz].

For a three phase machine, the magnetomotive force harmonic of 5th and 7th has a speed of $\frac{-k}{5}\omega_{\text{syn}}$ and $\frac{k}{7}\omega_{\text{syn}}$, respectively. Let $k=1$, meaning only fundamental current is excited. In this case, according to Faraday's law of induction, the harmonic magnetic field induces an back electromotive force in the three phase winding that has an angular speed of ω_{syn}, and such electromotive force is often modeled as *harmonic leakage inductance* because it is a synchronous voltage. The harmonic magnetic field produces remarkable torque during direct starting of a grid-fed induction machine.

Appendix C. Field Modulation Principles

C.1. Magnetic Permeance

Constant Magnetic Conductance

Rotor Angle Dependent Magnetic Conductance

C.2. Magnetic Induction

Appendix D. Leakage Inductance

This course introduces a series of leakage inductance symbols: the phase self-leakage inductance L_σ, the phase mutual-leakage inductance M_σ, the stator leakage inductance: $L_{ls}=L_\sigma-M_\sigma$, the rotor leakage inductance: L_{lr}.

See Lipo (2012), Section 1.12. We have three main types of leakage inductance, including slot leakage, end winding leakage, and harmonic (or belt, differential) leakage.

Slot leakage, end winding leakage is self-inductance.

The harmonic leakage occurs between different phases.

Appendix E. The Magnetomotive Force of One Conductor

See "harmonic field effects in induction machines" (1977).

Appendix F. Numerical Simulation Basics

F.1. Euler Method

F.2. Runge-Kutta Method

Appendix G. Space Vector PWM

There are at least hundreds of references that explain SVPWM for you. So, let's do it from a differen perspective, by explaining the famous C codes for SVPWM provided by Texas Instruments.

```
1  @njit(nogil=True)
2  def SVGEN_DQ(v, one_over_Vdc):
3
4      # Normalization (which converts [Volt] into [s])
5      Talfa = v.Ualfa * one_over_Vdc # v.Ualfa is in sense of
           amplitude invariant Clarke transformation
6      Tbeta = v.Ubeta * one_over_Vdc # v.Ubeta is in sense of
           amplitude invariant Clarke transformation
7      Tz    = v.Unot  * one_over_Vdc # duration of the added zero
           sequence voltage
8
9      # Inverse clarke transformation??
10     A = Tbeta # 0 degree line pointing at 0 degree
11     C =  1.7320508*Talfa - Tbeta # C =  sin( 60/180*np.pi)*Talfa -
           sin(30/180*np.pi)*Tbeta
12     B = -1.7320508*Talfa - Tbeta # B = -sin( 60/180*np.pi)*Talfa -
           sin(30/180*np.pi)*Tbeta
13
14     # 60 degree Sector determination
15     Sector = 0
16     if (A > 0): Sector = 1
17     if (C > 0): Sector = Sector+2
18     if (B > 0): Sector = Sector+4
19
20     # X,Y,Z calculations (Note an additional factor of 1.7320508 is
           introduced to be equivalent to normalizing Ualfa and Ubeta
           to a base value of Vdc/sqrt(3))
21     XXX =             Tbeta*1.7320508
22     YYY =  1.5*Talfa + Tbeta*0.8660254
23     ZZZ = -1.5*Talfa + Tbeta*0.8660254
24
25     if Sector == 0: # Sector 0: this is special case for (Ualfa,
           Ubeta) = (0,0)*/
26         v.Ta = 0.5
27         v.Tb = 0.5
28         v.Tc = 0.5
29     if Sector == 1: #Sector 1: t1=Z and t2=Y (abc ---> Tb,Ta,Tc)*/
30         t1 = ZZZ
31         t2 = YYY
32         v.Tb=(1-t1-t2)*0.5 + Tz*0.5
33         v.Ta = v.Tb+t1              # taon = tbon+t1        */
```

```
34          v.Tc = v.Ta+t2                  # tcon = taon+t2         */
35      elif Sector == 2:      # Sector 2: t1=Y and t2=-X (abc ---> Ta,
            Tc,Tb)*/
36          t1 = YYY
37          t2 = -XXX
38          v.Ta=(1-t1-t2)*0.5 + Tz*0.5
39          v.Tc = v.Ta+t1                  #  tcon = taon+t1        */
40          v.Tb = v.Tc+t2                  #  tbon = tcon+t2        */
41      elif Sector == 3:      # Sector 3: t1=-Z and t2=X (abc ---> Ta,
            Tb,Tc)*/
42          t1 = -ZZZ
43          t2 = XXX
44          v.Ta=(1-t1-t2)*0.5 + Tz*0.5
45          v.Tb = v.Ta+t1                  #   tbon = taon+t1       */
46          v.Tc = v.Tb+t2                  #   tcon = tbon+t2       */
47      elif Sector == 4:      # Sector 4: t1=-X and t2=Z (abc ---> Tc,
            Tb,Ta)*/
48          t1 = -XXX
49          t2 = ZZZ
50          v.Tc=(1-t1-t2)*0.5 + Tz*0.5
51          v.Tb = v.Tc+t1                  #   tbon = tcon+t1       */
52          v.Ta = v.Tb+t2                  #   taon = tbon+t2       */
53      elif Sector ==  5:     # Sector 5: t1=X and t2=-Y (abc ---> Tb,
            Tc,Ta)*/
54          t1 = XXX
55          t2 = -YYY                       #   tbon = (1-t1-t2)*0.5    */
56          v.Tb=(1-t1-t2)*0.5 + Tz*0.5
57          v.Tc = v.Tb+t1                  #   taon = tcon+t2       */
58          v.Ta = v.Tc+t2
59      elif Sector == 6:      # Sector 6: t1=-Y and t2=-Z (abc ---> Tc,
            Ta,Tb)*/
60          t1 = -YYY
61          t2 = -ZZZ
62          v.Tc=(1-t1-t2)*0.5 + Tz*0.5
63          v.Ta = v.Tc+t1                  #   taon = tcon+t1       */
64          v.Tb = v.Ta+t2                  #   tbon = taon+t2       */
65
66      # Logic reversal
67      v.Ta = 1-v.Ta
68      v.Tb = 1-v.Tb
69      v.Tc = 1-v.Tc
70
71      # Set max allowed duty ratio
72      if (v.Ta>v.SYSTEM_MAX_PWM_DUTY_LIMATATION): v.Ta=v.
            SYSTEM_MAX_PWM_DUTY_LIMATATION
73      if (v.Tb>v.SYSTEM_MAX_PWM_DUTY_LIMATATION): v.Tb=v.
            SYSTEM_MAX_PWM_DUTY_LIMATATION
74      if (v.Tc>v.SYSTEM_MAX_PWM_DUTY_LIMATATION): v.Tc=v.
            SYSTEM_MAX_PWM_DUTY_LIMATATION
75      if (v.Ta<v.SYSTEM_MIN_PWM_DUTY_LIMATATION): v.Ta=v.
            SYSTEM_MIN_PWM_DUTY_LIMATATION
76      if (v.Tb<v.SYSTEM_MIN_PWM_DUTY_LIMATATION): v.Tb=v.
            SYSTEM_MIN_PWM_DUTY_LIMATATION
77      if (v.Tc<v.SYSTEM_MIN_PWM_DUTY_LIMATATION): v.Tc=v.
            SYSTEM_MIN_PWM_DUTY_LIMATATION
78
79      return v
```

G.1. The Amplitude Invariant Clarke Transformation

One should realize the transformation matrix in (363) is not $\boldsymbol{T}(0)$.

Later in this section when we are discussing space vector modulation, there is a need to treat the projected phase axes (let's denote them as $\vec{a}_p$, $\vec{b}_p$ and $\vec{c}_p$) in the DQ plane as the actual axes for the phase quantities. This can be equivalently achieved by scaling the transformation matrix $T(0)$ by a factor of $\sqrt{\frac{2}{3}}$, which equals $\cos(35.3°)$, the cosine of the angle between $\vec{a}$-axis and $\vec{a}_p$-axis (note $35.3° = 90° - 54.7$, cf. the direction cosine in (115)).

After the scale by a factor of $\cos(35.3°)$, the conservative of power or energy is lost after the transformation. In other words, the power or energy in $\alpha\beta\gamma$ frame is only two-thirds of that in *abc* frames. This transformation is known as the amplitude invariant transformation because now 1 V of voltage in a-axis now corresponds to exactly 1 V of voltage in a_p-axis or α-axis.

G.2. Pulse Width Modulation and Volt-Second Equivalence

The easy-to-ignore assumption that has been made in the development of the SVPWM technique is that the output terminal voltage is equal to duty ratio times dc bus voltage. In practice, this assumption is valid because of the volt-second equivalence property of inductive circuit.

G.3. Why Centered and Why Triangular Carrier Waveform

There is another hidden assumption about the PWM frequency. The PWM frequency is assumed to be high enough such that the modulation waveform seems to be a constant value in one cycle of carrier waveform.

References

[1] T. A. Lipo, *Analysis of synchronous machines*. CRC Press, 2012.

[2] D. W. Novotny and T. A. Lipo, *Vector control and dynamics of AC drives*. Oxford university press, 1996, vol. 41.

[3] D. Cline, *Variational principles in classical mechanics*. University of Rochester River Campus Librarie, 2017.

[4] S. D. Umans, *Fitzgerald and Kingsley's Electric machinery*, 7th ed. McGraw-hill, 2013.

[5] D. Li, R. Qu, J. Li, W. Xu, and L. Wu, "Synthesis of flux switching permanent magnet machines," *IEEE Transactions on Energy Conversion*, vol. 31, no. 1, pp. 106–117, 2015.

[6] F. Khorrami, P. Krishnamurthy, and H. Melkote, *Modeling and adaptive nonlinear control of electric motors*. Springer Science & Business Media, 2003.

[7] S. E. Rauch and L. J. Johnson, "Design principles of flux-switch alternators [includes discussion]," *Transactions of the American Institute of Electrical Engineers. Part III: Power Apparatus and Systems*, vol. 74, no. 3, pp. 1261–1268, 1955.

[8] J. Ou, Y. Liu, R. Qu, and M. Doppelbauer, "Experimental and theoretical research on cogging torque of pm synchronous motors considering manufacturing tolerances," *IEEE Transactions on Industrial Electronics*, vol. 65, no. 5, pp. 3772–3783, 2018.

[9] J. Chen, J. Mei, X. Yuan, Y. Zuo, J. Zhu, and C. H. T. Lee, "Online adaptation of two-parameter inverter model in sensorless motor drives," *IEEE Transactions on Industrial Electronics*, vol. 69, no. 10, pp. 9860–9871, 2022.

[10] Y. Tang, *Electric Machinery 5th Edition*. China Machine Press, 2014.

[11] J. Chen, "Adaptive observer design for speed sensorless induction motor drives (in chinese)," Ph.D. dissertation, Zhejiang University, 2019.

[12] Z. Chen, M. Tomita, S. Doki, and S. Okuma, "An extended electromotive force model for sensorless control of interior permanent-magnet synchronous motors," *IEEE Transactions on Industrial Electronics*, vol. 50, no. 2, pp. 288–295, Apr 2003.

[13] IEEE, "Ieee standard test procedure for polyphase induction motors and generators," *IEEE Std 112-2004 (Revision of IEEE Std 112-1996)*, 2004.

[14] G. R. Slemon, "Modelling of induction machines for electric drives," *IEEE Transactions on Industry Applications*, vol. 25, no. 6, pp. 1126–1131, Nov 1989.

[15] K. J. Åström and P. R. Kumar, "Control: A perspective," *Automatica*, vol. 50, no. 1, pp. 3–43, 2014. [Online]. Available: https://www.sciencedirect.com/science/article/pii/S0005109813005037

[16] J. Chen and J. Huang, "Online decoupled stator and rotor resistances adaptation for speed sensorless induction motor drives by a time-division approach," *IEEE Transactions on Power Electronics*, vol. 32, no. 6, pp. 4587–4599, June 2017.

[17] R. Marino, P. Tomei, and C. M. Verrelli, *Induction motor control design*. Springer London, 2010.

[18] S. Shao, S. McAleer, R. Yan, and P. Baldi, "Highly accurate machine fault diagnosis using deep transfer learning," *IEEE Transactions on Industrial Informatics*, vol. 15, no. 4, pp. 2446–2455, 2019.

[19] J. Chen, X. Yuan, F. Blaabjerg, and C. H. T. Lee, "Overview of fundamental frequency sensorless algorithms for ac motors: A unified perspective," *IEEE Journal of Emerging and Selected Topics in Power Electronics*, vol. 11, no. 1, pp. 915–931,

2023.

[20] R. Ortega, L. Praly, A. Astolfi, J. Lee, and K. Nam, "Estimation of rotor position and speed of permanent magnet synchronous motors with guaranteed stability," *IEEE Transactions on Control Systems Technology*, vol. 19, no. 3, pp. 601–614, 2011.

[21] C. Schauder, "Adaptive speed identification for vector control of induction motors without rotational transducers," *IEEE Transactions on Industry Applications*, vol. 28, no. 5, pp. 1054–1061, 1992.

[22] K. S. Narendra and A. M. Annaswamy, *Stable adaptive systems*. Massachusetts, U.S.A.: Courier Corporation, 1989.

[23] G. Besançon, J. D. León-Morales, and O. Huerta-Guevara, "On adaptive observers for state affine systems," *International Journal of Control*, vol. 79, no. 6, pp. 581–591, 2006. [Online]. Available: http://dx.doi.org/10.1080/00207170600552766

[24] J. Chen, J. Mei, X. Yuan, Y. Zuo, and C. H. T. Lee, "Natural speed observer for nonsalient ac motors," *IEEE Transactions on Power Electronics*, vol. 37, no. 1, pp. 14–20, Jan 2022.

[25] R. Marino, P. Tomei, and C. Verrelli, "Adaptive control for speed-sensorless induction motors with uncertain load torque and rotor resistance," *International Journal of Adaptive Control and Signal Processing*, vol. 19, no. 9, pp. 661–685, 2005.

[26] R. Marino, P. Tomei, and C. M. Verrelli, "An adaptive tracking control from current measurements for induction motors with uncertain load torque and rotor resistance," *Automatica*, vol. 44, no. 10, pp. 2593–2599, 2008.

[27] R. A. Torres, H. Dai, W. Lee, T. M. Jahns, and B. Sarlioglu, "Current-source inverters for integrated motor drives using wide-bandgap power switches," in *2018 IEEE Transportation Electrification Conference and Expo (ITEC)*, 2018, pp. 1002–1008.

[28] H. Dai, R. A. Torres, F. Chen, T. M. Jahns, and B. Sarlioglu, "An h8 current-source inverter using single-gate wbg bidirectional switches," *IEEE Transactions on Transportation Electrification*, vol. 9, no. 1, pp. 1311–1329, 2023.

[29] J.-W. Choi and S.-K. Sul, "Inverter output voltage synthesis using novel dead time compensation," *IEEE Transactions on Power Electronics*, vol. 11, no. 2, pp. 221–227, Mar 1996.

[30] J.-S. Kim, J.-W. Choi, and S.-K. Sul, "Analysis and compensation of voltage distortion by zero current clamping in voltage-fed pwm inverter," *IEEJ Transactions on Industry Applications*, vol. 117, no. 2, pp. 160–165, 1997.

[31] S.-K. Sul, *Control of electric machine drive systems*. John Wiley & Sons, 2011, vol. 88.

[32] R. Ortega, N. Barabanov, G. Escobar, and E. Valderrama, "Direct torque control of induction motors: stability analysis and performance improvement," *IEEE Transactions on Automatic Control*, vol. 46, no. 8, pp. 1209–1222, Aug 2001.

[33] M. Kang, "Research on multiphase bearingless motors (in chinese)," Ph.D. dissertation, Zhejiang University, 2008.